

ÉCOLE DOCTORALE DES SCIENCES CHIMIQUES

Institut de Chimie – UMR 7177

THÈSE présentée par :

Xiaohui DI

soutenue le : 10 avril 2024

pour obtenir le grade de : **Docteur de l'université de Strasbourg**

Discipline/ Spécialité : Chimie

**Zéolithes dopées au cuivre(I) comme
catalyseurs verts pour la synthèse
organique**

THÈSE dirigée par :

M. PALE Patrick
M. CHASSAING Stefan

Professeur, Université de Strasbourg
Maitre de conférences, Université de Strasbourg

RAPPORTEURS :

M. DJAKOVITCH Laurent
M. BELMONT Philippe

Directeur de recherche, IRCELyon, Université C. Bernard Lyon
Professeur, Université de Paris-Cité

AUTRE MEMBRE DU JURY :

Mme. HESSE Stéphanie

Professeure, Université de Lorraine

INVITÉE :

Mme. BENETEAU Valérie

Maitre de conférences, Université de Strasbourg

Try and fail, but don't fail to try!

Acknowledgements

Time flies, and three years have gone by in a flash. Acknowledgement is not only an end of my dissertation, but also marks the ending of my doctoral studies at the University of Strasbourg. Looking back on the past three years, I would like to express my sincere gratitude to all the people who helped me, because it was all quite tough for me, and I encountered all kinds of problems and difficulties in the course of my research, but because of your help, I did it. Thank you all.

Firstly, I would like to thank the members of the jury, Professor Stéphanie HESSE, Laurent DJAKOVITCH and Philippe BELMONT, for being the jurors of my PhD defense and the reviewers of my doctoral dissertation.

Secondly, I'd like to express my deepest gratitude to my distinguished and respectable supervisor, Professor Patrick PALE, for his constant encouragement, guidance, patience and most of all, his support during my writing of the thesis paper. He has spent a great deal of time reading and correcting my thesis. Without his advice, I would have been lost in organic chemistry.

Then, it is Professor Stefan CHASSAING. I will never forget your understanding and help when I had just arrived in France. You gave me the courage to persevere and overcome my illness. Furthermore, your approachability and humor also brought fun to my intense scientific research life. Because I changed my major during my Ph.D., I really want to share all my thoughts and efforts with you, and I appreciate your patience and understanding all the time. It was a pleasure to spend this period of study with you, which will be an unforgettable memory for the rest of my life.

Further, I am also grateful to Professor Valérie BENETEAU. She gave me a lot of guidance and help in both scientific research and personal life. She showed me how important a rigorous academic attitude is to scientific research, otherwise it is quite possible to miss the correct results. I have learned a lot from her during my study time here, which will benefit me for all my life.

I would also like to thank the other laboratory staff; Aurélien, Jean-Marc and Victor, for your kind help and guidance when I was stuck in experimental difficulties. You always patiently gave me a lot of constructive suggestions and helped me to solve problems together.

I would also like to express my thanks to the doctoral students in the laboratory, notably Andrés, Eliot, Loïc, Franck, Elliot, Robin, Pierre, Fabian and Mathieu, who made the lab into a lively and warm place to work, sharing knowledge, joy, stress and supports in general.

Special thanks to Andrés and Eliot, who always gave me insightful comments, whether on public occasions or in private talks.

Andrés, you are so kind and lovely, and always patiently tutored me in my professional knowledge. Despite your busy schedule, you still sacrificed a lot of your rest time to help me. I will never forget the days when we discussed together until late at night. You gave me the greatest support and encouragement, both in study and in life. I am very glad to meet you and become your friend. I wish you all the best in the future!

Eliot, you were the first friend I met in the lab. You always helped me, comforted me, and supported me when I was most uncomfortable and frustrated. I am so glad that I met you as a good friend in my life journey. I hope I will have the chance to see you again in the future!

The laboratory family always touches my heart. They all tried their best to help me despite the language barrier. I really appreciate to them.

Thanks also to Ludovik, Delphine and Marc, as well as to the various analysis services for their availability and helpfulness.

Finally, I would like to acknowledge my family and my boyfriend Dr. Qi for their endless support, encouragement, patience and understanding. They gave me the incentive to do this work and accommodated me without reservation during the final months of finalizing my dissertation. My special thanks to Qi for your emotional help and love. I would not complete my thesis without your attentive care and warm comfort. I will always remember the time you stayed up late with me to write my thesis, and the time you patiently helped me revise it. I also owe my sincere gratitude to my friends who took the time to listen to me and help me to solve my problems during the difficult course of writing my thesis. Thank you!

In addition, thanks to the doctoral scholarship provided by the China Scholarship Council for financial support.

Contents

Abbreviations.....	1
Preface	5
<i>Part one. State of the art.</i>	9
Thesis objectives: Cu^I-zeolites as new heterogeneous and green catalysts for organic synthesis.....	11
Chapter I. Zeolites.....	15
1. Generalities.....	17
1.1. Structure of zeolites	17
1.2. Physicochemical properties of zeolites.....	18
1.2.1. Physical properties	18
1.2.2. Shape-selective properties of zeolites for chemical catalysis	20
1.2.3. Chemical properties	22
2. From natural zeolites to tailor-made zeolites	25
2.1. Natural zeolites	25
2.2. Synthesis of zeolites	26
2.2.1. History of synthetic zeolites.....	26
2.2.2. <i>De novo</i> synthesis of zeolites	27
2.2.3. Synthesis of acidic zeolites	28
2.2.4. Synthesis of metal-doped zeolites.....	29
2.2.4.1. <i>Via</i> isomorphous substitution of zeolite framework composition.....	30
2.2.4.2. <i>Via</i> ion exchange of zeolite extra-framework cations and related strategies	31
2.2.4.2.1. Aqueous and solid-state ion exchange of zeolites.....	31
2.2.4.2.2. Chemical vapor deposition (CVD) and ligand exchange	34
2.2.4.3. <i>Via</i> chemical encapsulation techniques in zeolite topologies	35
2.2.4.4. <i>Via</i> the ship-in a-bottle synthesis strategy.....	37
2.3. Applications of zeolites	39
2.3.1. The applications of zeolites in industry	40

2.3.1.1. Zeolites as ion-exchangers	40
2.3.1.2. Zeolites for adsorption and separation processes.....	41
2.3.1.3. Zeolites as heterogeneous catalysts in industry	42
2.3.2. The applications of zeolites in organic synthesis.....	42
2.3.2.1. Acidic zeolites in organic synthesis	42
2.3.2.1.1. Acidic zeolites in protecting groups chemistry	43
2.3.2.1.2. Acidic zeolites in carbonylation reactions.....	47
2.3.2.2. Metal-doped zeolites in organic synthesis	48
2.3.2.2.1. Scandium-doped zeolites.....	49
2.3.2.2.2. Iron-doped zeolites	49
2.3.2.2.3. Silver-doped zeolites	51
2.3.2.2.4. Gold-doped zeolites.....	52
2.3.2.2.5. Palladium-doped zeolites	53
2.3.2.2.6. Copper-doped zeolites	60

Part two. The formation of aromatic C-C and C-X bonds for the synthesis of aromatic motifs by copper(I)-zeolite-catalyzed coupling reactions. 71

Chapter II. C_{aryl}-C_{aryl} bond formations via copper(I)-zeolite-catalyzed homocoupling-type reactions 73

1. Introduction	75
2. How to produce biaryl via homocoupling reactions?.....	76
2.1. The historical Ullmann reaction	76
2.2. Homocoupling of aryl halides	78
2.2.1. Palladium-catalyzed homocoupling reactions of aryl halides	78
2.2.1.1. Palladium-catalyzed homogeneous homocoupling reactions	78
2.2.1.2. Palladium-catalyzed heterogeneous homocoupling reactions	81
2.2.2. Copper-catalyzed homocoupling reactions of aryl halides.....	84
2.2.2.1. Copper-catalyzed homogeneous homocoupling reactions.....	84
2.2.2.2. Copper-catalyzed heterogeneous homocoupling reactions	85
2.2.3. Other metal-catalyzed homocoupling of aryl halides	87
2.2.3.1. Au-catalyzed heterogeneous homocoupling of aryl halides	87
2.2.3.2. Mn-catalyzed homocoupling of aryl halides.....	89
2.2.3.3. Ni-catalyzed homocoupling of aryl halides	89

2.2.3.4. Co-catalyzed homocoupling of aryl halides.....	91
2.2.3.5. Fe-catalyzed homocoupling of aryl halides	92
2.3. Homocoupling of arylboronic acids	92
2.3.1. Pd-catalyzed homocoupling of arylboronic acids.....	93
2.3.1.1. Pd-catalyzed homogeneous homocoupling reactions	93
2.3.1.2. Pd-catalyzed heterogeneous homocoupling reactions	93
2.3.2. Cu-catalyzed homocoupling of arylboronic acids	94
2.3.2.1. Cu-catalyzed homogeneous homocoupling reactions	94
2.3.2.2. Cu-catalyzed heterogeneous homocoupling reactions	95
2.4. Homocoupling of aryldiazonium salts.....	96
2.4.1. Homogeneous homocoupling reactions of aryldiazonium salts	97
3. Our current research progresses	104
3.1. Preparation of Cu ^I -USY.....	104
3.2. Current research themes	105
4. Biaryl synthesis <i>via</i> copper(I)-zeolite-catalyzed homocoupling reaction of arylboronic acids.....	107
4.1. The optimization of reaction conditions	107
4.2. Scope and limitations.....	112
4.3. Recyclability studies of catalyst and gram-scale experiments	114
4.4. Cascade/one-pot synthesis based on homocoupling reaction.....	116
4.5. Mechanism proposal.....	119
5. Biaryl synthesis <i>via</i> copper(I)-zeolite-catalyzed homocoupling reaction of aryldiazonium salts.....	123
5.1. The optimization of reaction conditions	123
5.2. Scope and limitations.....	129
6. Conclusion.....	131
Chapter III. C_{aryl}-heteroatom bond formation towards phenols <i>via</i> copper(I)-zeolite-catalyzed Chan-Lam-Evans coupling reactions	133
1. Introduction	135
1.1. C _{aryl} -heteroatom bond formation	135

1.2. Phenol synthesis.....	137
2. The history of Ullmann-type reactions to Chan-Lam-type reactions.....	138
2.1. From Ullmann reactions....	138
2.1.1. Palladium-catalyzed Ullmann coupling reactions	140
2.1.1.1. Palladium-catalyzed homogeneous Buchwald–Hartwig reactions	141
2.1.1.2. Palladium-catalyzed heterogeneous Buchwald–Hartwig reactions	143
2.1.2. Palladium-catalyzed hydroxylation of aryl halides towards phenols	146
2.1.2.1. Palladium-catalyzed homogeneous hydroxylation of aryl halides.....	146
2.1.3. Copper-catalyzed Ullmann coupling reactions.....	149
2.1.3.1. Copper-catalyzed homogeneous reactions	150
2.1.3.2. Copper-catalyzed heterogeneous reactions	150
2.1.4. Copper-catalyzed hydroxylation of aryl halides towards phenols	151
2.1.4.1. Copper-catalyzed homogeneous hydroxylation of aryl halides	151
2.1.4.2. Copper-catalyzed heterogeneous hydroxylation of aryl halides	155
2.2. ... to Chan-Lam-type reactions	156
2.2.1. Homogeneous and heterogeneous Chan-Lam-type reactions.....	157
2.2.1.1. Homogeneous Chan-Lam-type reactions	158
2.2.1.2. Heterogeneous Chan-Lam-type reactions	159
2.2.2. Hydroxylation of arylboronic acids towards phenols <i>via</i> Chan-Evans-type reactions	161
2.2.2.1. Hydroxylation of arylboronic acids towards phenols under homogeneous conditions	162
2.2.2.2. Hydroxylation of arylboronic acids towards phenols under heterogeneous conditions	163
3. Our current research progresses and theme.....	166
4. Chan-Lam-Evans coupling reactions for C-O bond formation towards phenols.....	168
4.1. The optimization of reaction conditions	168
4.2. Reaction scope and limitation.....	172
4.3. Recyclability study of catalyst and gram-scale experiment	174
4.4. Mechanism.....	175
5. Conclusion.....	177

Chapter IV. Copper(I)-zeolite-catalyzed cross-dehydrogenative coupling (CDC) reaction to form C-C bonds and their applications on the synthesis of THIQ derivatives	179
1. Introduction	181
2. THIQ derivatives through CDC reactions-State of the art	185
3. Promising research themes	191
4. Our research progresses.....	193
4.1. Preliminary results	193
4.2. The synthesis of THIQ derivative.....	194
4.2.1. C-N bond cross-coupling	195
4.2.1.1. The protection of <i>ortho</i> -iodophenol (S.13)	197
4.2.1.2. The arylation of S.8.....	198
4.2.2. CDC reaction of 2-aryl-substituted THIQs (S.10a and S.10b) with terminal alkyne (S.7).....	200
5. Conclusion.....	201
General conclusions and perspectives	203
1. General conclusions.....	205
2. Perspectives	205
Résumé en français.....	209
<i>Part three. Experimental part.</i>	211
General information and general procedures	213
Analytical data of compounds from Chapter II.....	221
Analytical data of compounds from Chapter III.....	231
Analytical data of compounds from Chapter IV	238
References	241

Abbreviations

AAS	atomic absorption spectroscopy	DES	deep eutectic solvent
ABAs	arylboronic acids	DFT	density-functional theory
Ac	acetyl	DIPEA	<i>N,N</i> -diisopropylethylamine
acac	acetylacetonate	DMA	<i>N,N</i> -dimethylacetamide
AIE	aqueous ion-exchange	DME	dimethoxyethane
BDC	benzene-1,4-dicarboxylate	DMF	<i>N,N</i> -dimethylformamide
BHMPO	<i>N,N'</i> -bis(4-hydroxy-2,6-dimethylphenyl)oxalamide	DMM	dimethoxymethane
BINAP	2,2'-bis(diphenylphosphino)-1,1'-binaphthyl	DMSO	dimethyl sulfoxide
BPY	4,4'-bipyridine	dppf	bis(diphenylphosphino)ferrocene
BTX	benzene, toluene, xylene	DTBB	4,4'-di- <i>tert</i> -butylbiphenyl
(BzO) ₂	benzoyl peroxide	EDG	electron-donating group
CDC	cross-dehydrogenative-coupling	EFAI	extra-framework aluminium
CEL	Chan-Evans-Lam	EWG	electron-withdrawing group
CFP	catalytic fast pyrolysis	FAP	fluorapatite
CNT-Chit	carbon nanotube-chitosan	FCC	fluid catalytic cracking
cod	1,5-cyclooctadienyl	FTC	framework type code
COF	covalent organic framework	GO	graphene oxide
CRF	controlled release fertilizer	HE	Hantzsch ester
CuAAC	copper-catalyzed azide-alkyne cycloaddition	ICP-AES	inductively coupled plasma-atomic emission spectroscopy
CVD	chemical vapor deposition	ICP-OES	inductively coupled plasma-optical emission spectroscopy
Cy	cyclohexyl	IE	ion-exchange
DCM	dichloromethane	IL	ionic liquid

IZA-SC	International Zeolites Association Structure Commission	PSS	product shape selectivity
IUPAC	International Union of Pure and Applied Chemistry	PT	proton-transfer
LDH	layered double hydroxide	RSS	reactant shape selectivity
MeCN	acetonitrile	Salen	<i>N,N'</i> - bis(salicylidene)ethylenediamine
MIDA	<i>N</i> -methyliminodiacetic acid	Salophen	<i>N,N'</i> -disalicylidene-1,2- phenylenediamine
MMT	montmorillonite	SAR	silicon-to-aluminium ratio
MOF	metal-organic framework	scCO ₂	supercritical carbon dioxide
MOM	methoxymethyl	SCIE	supercritical ion-exchange
MOR	Mordenite	SCR	selective catalytic reduction
MTG	methanol-to-gasoline	SDAs	structure-directing agents
MTO	methanol-to-olefins	SDMTM	stepwise direct methane to methanol
MW	microwave	SDS	sodium dodecyl sulfate
MWCNTs	multi-walled carbon nanotubes	SET	single-electron transfer
NaAsc	sodium ascorbate	SSA	specific surface area
NCs	nanoclusters	SSIE	solid-state ion-exchange
NHC	<i>N</i> -heterocyclic carbene	TBHP	<i>tert</i> -butyl hydroperoxide
NMP	<i>N</i> -methyl-2-pyrrolidone	TFA	trifluoroacetic acid
NMR	nuclear magnetic resonance spectroscopy	THF	tetrahydrofuran
NP	nanoparticle	THIQ	tetrahydroisoquinoline
NSC	neural stem cell	THP	tetrahydropyranyl
PEG	polyethylene glycol	TLC	thin layer chromatography
PFG	phosphine functionalized graphene	TMOF	trimethyl orthoformate
PhI=NTs	[<i>N</i> -(<i>p</i> -tolylsulfonyl)imino] phenyliodinane	TMS	trimethylsilyl

PMO	periodic mesoporous organosilica
PVP	poly(<i>N</i> -vinylpyrrolidone)
Tris-HCl	[tris(hydroxymethyl)aminoethane]- HCl
TS	titanosilicate
TSS	transition state shape selectivity
US	ultrasound
USY	Ultra-Stable Y Zeolite
WHO	World Health Organization
XPS	X-ray photoelectron spectroscopy
ZSM-5	Zeolite Socony Mobil-5
1,10-phen	1,10-phenanthroline

Preface

Since 1828, when the German chemist Friedrich Wöhler synthesized urea for the first time using inorganic substances such as ammonium cyanate and ammonium sulfate, the prelude to the artificial synthesis of organic compounds, including bioactive ones, has been opened. From that time and mostly since the beginning of the XXth century, chemists began to synthesize more and more complex molecules, as well as valuable scaffolds or bioactive compounds. For that, chemists developed and are still developing new reactions to conveniently and efficiently form carbon-carbon (C-C) and carbon-heteroatom (C-X) bonds, which constitute the backbone and the functional groups of organic compounds.

Among them, the construction of aryl-aryl bonds, was highly desirable since the resulting biaryl motifs are often encountered in natural products and in a large number of biologically active parts of pharmaceuticals. In the last decades, transition metal-catalyzed coupling reactions, such as Ullmann¹, Suzuki-Miyaura cross-coupling², Glaser homocoupling³, as well as cross-dehydrogenative-coupling (CDC)⁴ reactions, have occupied a pivotal position to form aryl-aryl bonds for the synthesis of important compounds or moieties in organic synthesis. Meanwhile, the formation of C_{aryl}-X bonds creates molecular diversities, and the function of many organic compounds containing C-C bonds-based backbone is often derived from the presence of heteroatoms, such as nitrogen, oxygen and sulphur.⁵ For instance, pharmaceuticals and conductive polymers⁶ often contain C-N bonds, and almost all natural products contain ether, ketone or ester functions featuring C-O bonds. The formation of C_{aryl}-X bonds have been achieved in various transformations, such as Ullmann-type reactions^{7,8} Chan-Lam-type reactions⁹⁻¹¹ and Huisgen cycloaddition reactions.¹²

However, organic synthesis, especially multi-step synthesis, often relies on the use of numerous stoichiometric toxic and/or hazardous reagents, unrecoverable catalysts and harsh reaction conditions, resulting in serious environmental concerns. Among these, the negative impact of metal catalysts on the environment and economy should not be neglected. To solve these problems, the concept of 'Green Chemistry' has emerged in the late 1990s. Green Chemistry aims at achieving sustainable and safer chemical processes while minimizing waste production and energy consumption,¹³ gaining the attention of most academia as well as industries, not only the petrochemical and bulk industries but also the fine chemicals and organic synthesis industries. Within this context, designing heterogeneous catalysts by immobilizing metals on solid supports has aroused great interest, as they possess several intrinsic advantages compared

to their homogeneous counterparts in terms of recovering and recycling, thus making the products easy to separate and purify.¹⁴ As a result, several materials have been evaluated, among which zeolites as environmentally friendly natural or synthetic minerals. Due to their low cost, excellent stability and easy preparation, zeolites became popular in chemical industries, where they are worldwide applied to petroleum transformations into numerous chemicals.

However, only 13% zeolites are actually used for catalysis, mainly in petrochemical and bulk chemical industries.¹⁵ Most of zeolites are indeed used for water treatment depollution and as adsorbents. Furthermore, their applications in organic synthesis are still rare, although zeolites doped with metal ions are well known for their catalytic activity.

Compared to noble metals, such as palladium (Pd), rhodium (Rh), iridium (Ir), and ruthenium (Ru), first row 3d-block transition metals, mostly iron (Fe), cobalt (Co), nickel (Ni), copper (Cu), are now favored due to their lower cost and higher abundance in nature.¹⁶ Among these metals, Cu salts and complexes are able to promote a large number of organic reactions.^{1,3,9-11,17,18}

On this basis, our research group has made great contributions to the chemistry of copper-doped zeolites, with for example the development of the first heterogeneous copper-catalyzed azide-alkyne cycloaddition (CuAAC).^{19,20} Nevertheless, the catalytic potential of zeolite-based copper catalysts in organic synthesis still needs to be explored and exploited in further depth given that their applications in organic transformations remain limited.

Therefore, the objective of this thesis is to evaluate the potential of Cu^I-doped zeolites to form C-C bonds for the synthesis of valuable compounds or motifs in a variety of organic transformations and to prioritize the development of more environmentally friendly and mild reaction procedures based on the principles of Green Chemistry. The construction of C-X bonds has also been studied to expand the application scope of the catalyst. Recyclability of the zeolite-based catalytic solids has been scrutinized for each developed protocol.

Accordingly, this manuscript is divided into three parts.

Part One. State of the art.

Chapter I introduces zeolites and their emerging role as heterogeneous catalysts in organic synthesis. Zeolite origins, structures, acidities and preparation methods will be briefly described.

The known applications of zeolites to organic chemistry will then be surveyed in more details. In addition to Brønsted acidic zeolites, a particular emphasis will be focused on (transition) metal-loaded zeolites, especially copper-doped zeolites, because they are the type of catalyst applied to the methodologies developed in this thesis.

Part Two. The formation of aromatic C-C and C-X bonds for the synthesis of aromatic motifs by copper(I)-zeolite-catalyzed coupling reactions.

Chapter II is devoted to the formation of biaryl C-C bonds *via* copper(I)-zeolite-catalyzed homocoupling reactions. The development of several homocoupling reactions using different coupling partners, such as aryl halides, arylboronic acids (ABAs) and aryldiazonium salts, will be introduced in detail. In particular, catalysts and reaction conditions employed in these reactions will be discussed to highlight the importance of designing and developing novel efficient heterogeneous catalysts for the homocoupling of aryl halides, ABAs and aryldiazonium salts, respectively.

Chapter III focuses on the formation of C_{aryl}-X bonds towards phenols *via* copper(I)-zeolite-catalyzed Chan-Lam-type coupling reactions. We will show that arylboronic acids could be interesting alternatives to aryl halides to form C_{aryl}-X bonds. The reaction conditions for the construction of C-O bonds to synthesize phenols will be scrutinized within the “green chemistry” context.

Chapter IV is dedicated to the copper(I)-zeolite-catalyzed cross dehydrogenative coupling (CDC) reaction to form C_{sp3}-C_{sp} bonds and their applications to the synthesis of tetrahydroisoquinoline (THIQ) derivatives.

Part Three. Experimental part.

Chapter V described all experimental results.

Part one. State of the art.

On the structures, properties, syntheses and applications of zeolites.

Thesis objectives: Cu^I-zeolites as new heterogeneous and green catalysts for organic synthesis

The benzene ring structure is a predominant feature in numerous biologically active compounds. Most of them occur as biaryl, phenol and isoquinoline scaffolds or compounds (**Figure 1**), which are encountered in many natural products and some important synthetic intermediates. For instance, biaryl moiety composed of a C_{aryl}-C_{aryl} bond can be found as valuable secondary metabolites in various organisms.²¹ The most typical of these metabolites is the vancomycin family of antibiotics.²² Furthermore, the biaryl motif is also a useful building block for pharmaceuticals, such as the sartan family of blood pressure regulators (**Figure 1A**) and agrochemicals.^{23,24} Phenols (**Figure 1B**) are an important class of antioxidants, which can inhibit the oxidative degradation of a large number of biological aerobic organisms, *e.g.* α -tocopherol, a well-known vitamin E component, proved to be the most efficient phenol derivative to trap the damaging peroxy radicals in human blood plasma. Besides, salicylic acid bearing a phenol moiety can be used to relieve pain and fever.²⁵ Isoquinoline derivatives (**Figure 1C**) widely exist in nature²⁶ and in many drugs. For instance, the famous papaverine is an important antispasmodic drug, and 1-benzyl-1,2,3,4-tetrahydroisoquinolines (THIQs) are dopamine receptor antagonists.²⁷

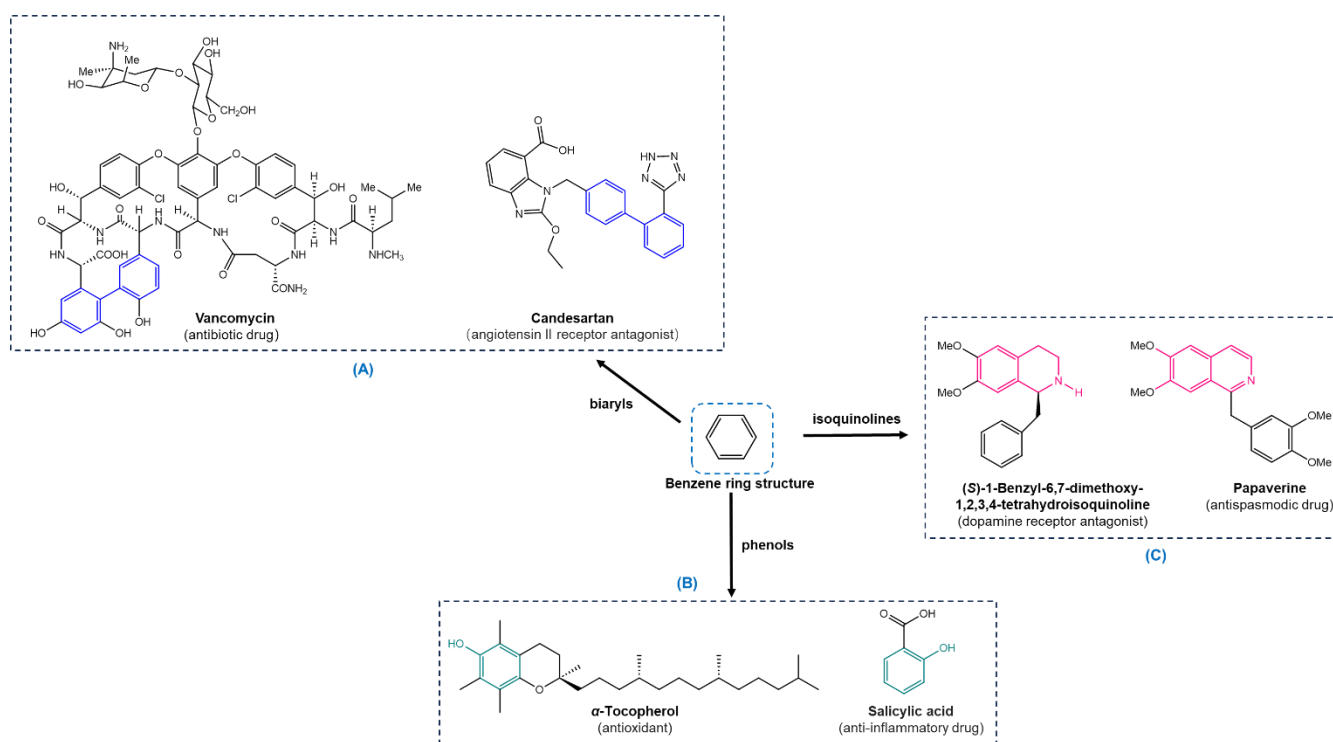
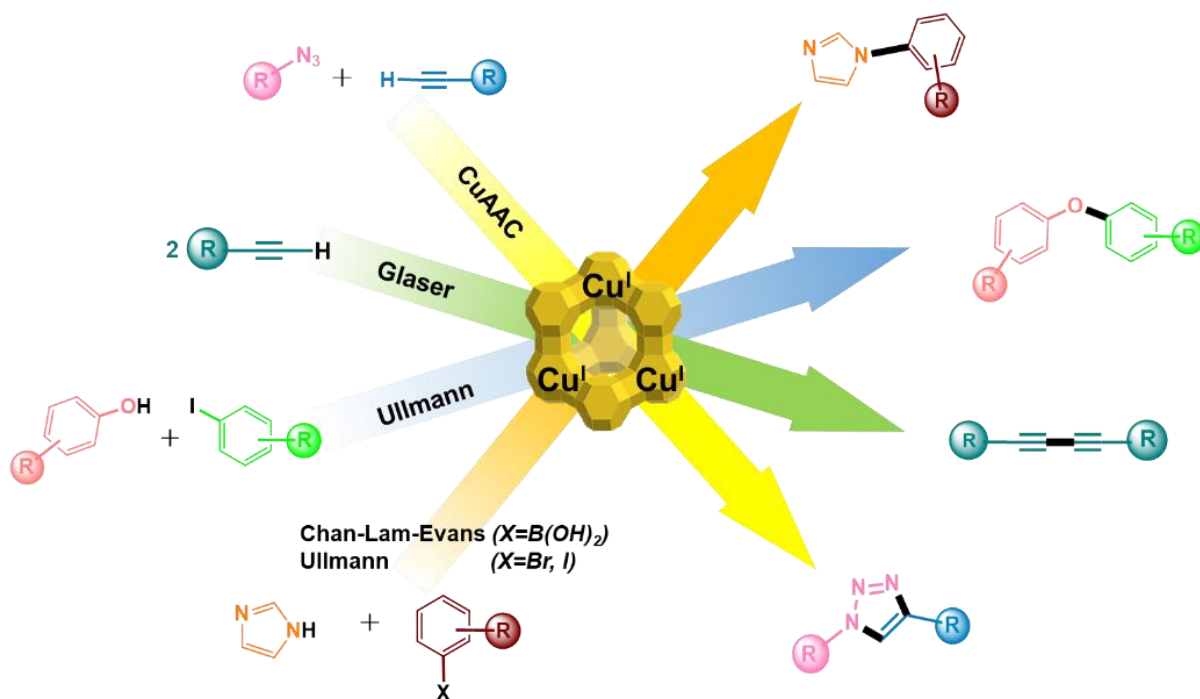


Figure 1. Representative examples of bioactive compounds exhibiting the biaryls (A), phenols (B) and isoquinoline motifs (C).²¹⁻²⁷

As a result, the formation of C_{aryl}-C_{aryl} and C_{aryl}-X bonds have become important for the synthesis of such valuable scaffolds or molecules. Over more than a century since the emergence of the Ullmann reaction¹ and its derived Ullmann-type reactions^{7,8}, the first copper-mediated C_{aryl}-C_{aryl} bond and C_{aryl}-X bond formation reactions, a variety of routes have been disclosed for forming aromatic C-C and C-X bonds, and arguably transition metal-mediated coupling reactions are still the most common methods.²⁸⁻³⁰ However, initial reactions were commonly mediated by a stoichiometric amount of transition metal under harsh conditions such as high temperature and long reaction time, which were unsatisfactory from an economic and environmental point of view. Based on the eco-environmental concept of Green Chemistry, organic chemists have been seeking to develop new and more benign methods to construct C_{aryl}-C_{aryl} and C_{aryl}-X bonds. Besides, the improvement of existing chemical method conditions is also an important topic, especially the design of new and high-efficiency metal catalysts.

Considering the negative impacts of environmental pollution, energy consumption, and high costs caused by the use of metal species, replacing metal or standard homogeneous catalysts with heterogeneous catalysts (to improve the utilization of catalytic metal ions) has become a growing field of interest in the last decade, but it is still a challenging task in organic synthesis. One of the preparation methods of heterogeneous catalysts is immobilizing metal ions on inorganic solid materials. Among them, natural or synthetic zeolites have been favored due to their low cost, stability, and high selectivity^{13,31}. However, the application of zeolites, especially transition metal-doped zeolites, in organic synthesis surprisingly remains underestimated and mainly focused on the Friedel-Crafts reactions^{32,33} and oxidation processes^{34,35}, as will be exemplified in Chapter I.

The fact that copper is relatively abundant in nature, inexpensive, and widely employed in various organic transformations makes it highly attractive in organic synthesis. Our research group^{36,37} has been devoted to the preparation of Cu^I-zeolites and their applications for organic synthesis. A representative and efficient example is Cu^I-USY (Ultra-Stable Y zeolite), which has been widely applied to a variety of organic transformations, including copper-catalyzed Azide-Alkyne Cycloaddition (CuAAC)^{19,20}, Glaser homocoupling³⁸, and Ullmann^{39,40}/ Chan-Lam-Evans^{41,42} coupling reactions (**Scheme 1**).



Scheme 1. Cu^I-USY toolbox in organic synthesis.^{19,20,38-42}

This thesis aims to develop more sustainable synthetic methodologies to form C_{aryl}-C_{aryl} and C_{aryl}-O bonds towards valuable molecules or motifs with the help of the heterogeneous Cu^I-USY catalyst (**Chapter II** and **Chapter III**). Furthermore, this catalyst will also be employed to the economical cross dehydrogenative coupling reactions for the formation of C_{sp3}-C_{sp} bonds (**Chapter IV**). Green solvents will be used preferentially as most common organic solvents are toxic and unsafe.

The next chapter will introduce the origin and development of zeolites. Their important physicochemical properties, preparation methods, and applications to organic synthesis are illustrated in detail. Regarding the latter, the potential of Cu^I-USY as green and heterogeneous catalyst in organic synthesis will be highlighted.

Chapter I. Zeolites

1. Generalities

Zeolites are natural minerals derived from the tectosilicate family represented by the general formula: $(M^{n+})_{x/n}[(AlO_2)_x (SiO_2)_y]^{x-} \cdot wH_2O$ ($M^{n+} = H^+, NH_4^+$, metal ions...). These minerals were first discovered in 1756 by A. F. Cronstedt, who named them zeo from the Greek zein (boiling) and lithos (stone) due to the strange boiling behaviors occurring on their surface when heated.⁴³ Since their discovery, the zeolite family has been growing constantly. Besides 40 reported natural zeolites, the International Zeolites Association Structure Commission (IZA-SC) has reported 240 kinds of zeolites. IUPAC references these different zeolites through a three-letter code derived from their original name and based on the so-called “Framework Type Code” (FTC) (e.g., FAU represents faujasite framework zeolites, including USY (Ultra-Stable Y zeolite); MFI represents Mobil-type five framework zeolites, including ZSM-5 (Zeolite Socony Mobil-5), etc.)

1.1. Structure of zeolites

From the chemical composition and structure perspective, zeolites are a category of crystalline inorganic microporous polymers that are composed mainly of silicon oxide tetrahedra $[SiO_4]$ and aluminium oxide tetrahedra $[AlO_4]^-$ units (also known as T-members) linked together by shared oxygen atoms. According to differences in zeolite origin, some silicon atoms in the tetrahedra are replaced by aluminium atoms, leading to extra-negative charges in the system. Such substitution therefore induces the presence of some cations to counterbalance the negative charges (**Figure 2**). In natural zeolites, abundant alkali or alkaline earth cations like Na^+ , K^+ , Mg^{2+} , and Ca^{2+} are the most common charge-compensating ions. These cations can also be easily exchanged by acidic protons and (transition) metal cations in synthetic zeolites, and the former can also exist in ammonium-loaded zeolites. These show that the more aluminium in zeolites, the more acidic they are or the more cations they content.

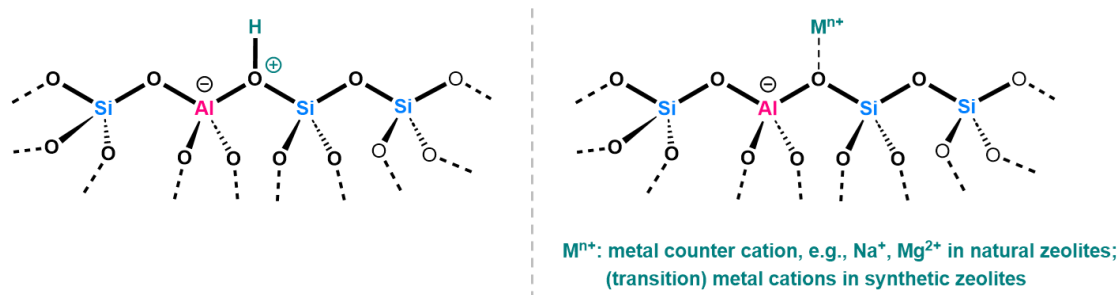


Figure 2. Chemical composition and structure of zeolites.

Furthermore, these $[\text{SiO}_4]$ and $[\text{AlO}_4]^-$ secondary building units are able to form different zeolite 3D structures with specific topologies due to their different assembling methods during the crystallization process of zeolite synthesis. Therefore, each zeolite possesses cage or channel internal shape with different sizes. Typical examples are USY (Ultra-Stable Y zeolite) (**Figure 3, top**) and ZSM-5 (Zeolite Socony Mobil-5) (**Figure 3, bottom**), respectively.

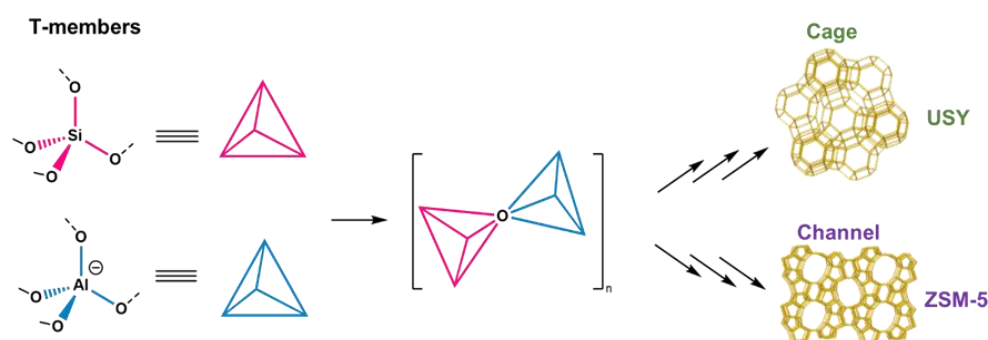


Figure 3. 3D structures of the USY (top) and the ZSM-5 (bottom).³⁷

1.2. Physicochemical properties of zeolites

1.2.1. Physical properties

Besides the pore shape, zeolites still possess a series of important physical characteristics such as the pore size, the ratio of silicon (Si) to aluminium (Al) (Si/Al ratio, SAR), and the specific surface area (SSA). Interestingly, SAR directly determines the number and density of negative charges in the zeolite framework. The properties of the most studied H-zeolites are shown in **Table 1**. Obvious distinctions can be made between cage-type and channel-type zeolites with different pore sizes, different SAR and acidic site loadings. According to Loewenstein rule⁴⁴, zeolites with good performance and thermal stability must have a $\text{SAR} > 1$. The greater the Al-content, the more (Brønsted or Lewis) acidic sites are generated on the zeolite unit. Therefore,

many scientists have controlled the SAR to obtain zeolites with specific crystal structures and designed porosity and number of anionic sites, directly impacting the acidity and the reactivity of these modified zeolites. Generally, zeolites are classified into three categories: a) low silica zeolites with SAR ≈ 1 , b) moderate silica zeolites with SAR $\approx 1.5\sim 5$, and c) high silica zeolites with SAR ≥ 10 .

Table 1. Main characteristics of typical H-zeolites.

H-Zeolite	Source	Topology	Pore Diameter (Å)	Si/Al Ratio (SAR)	Acidic site loading (mmol/g)	Specific surface area (m ² /g)
H-Y	Aldrich (334413)	Cage-type	7.4 × 7.4	1.5	6.67	-
H-USY	Zeolyst International (CBV 500)	Cage-type	7.4 × 7.4	2.9	3.8	620
H-MOR	Zeolyst International (CBV 20A)	Channel-type	6.5 × 7.0 3.4 × 3.8	10.3	1.48	400
H-ZSM5	Zeolyst International (CBV 5020)	Channel-type	5.1 × 5.5 5.3 × 5.6	25	0.86	425
H-β	Zeochem International (ZEOCAT PB/H)	Channel-type	7.6 × 6.4 5.5 × 5.5	12.5 - 17.5	0.90-1.23	700

Another unique property of zeolite is microporosity (pore size $\emptyset < 20 \text{ \AA}$), which distinguishes the pore dimensions of different zeolites. The intramolecular micropore environment provides the shape selectivity to discriminate different molecular sizes only those whose size fit within the zeolite can enter or leave the zeolite. However, a crowd of molecules can lead to severe pore blocking or coking, thus deactivating the active sites of the zeolite.⁴⁵ In specific applications, the microporous structures of zeolites could cause significant inconvenience, great efforts have been made to address these problems by introducing high-order porosities into zeolites, such as meso- ($20 \text{ \AA} < \emptyset < 500 \text{ \AA}$) and macro-porosity ($\emptyset > 500 \text{ \AA}$).⁴⁶ Hierarchical porosity is a more recent term that describes porous topologies with varying pore diameters, combining at least two levels of pore size. For instance, the intrinsic micropores of zeolites coupled with complementary mesoporous or macroporous network offer the opportunity to accommodate larger molecules, and could mainly shorten the diffusion path length. Such hierarchical porosity minimize the diffusion limitation and thus facilitate the mass transfer of reactants/products related to their access and exit from the catalytic active centers.⁴⁵ The

residence time of reactants/products on the catalytic active sites is greatly shortened due to the weakened shape selectivity constraints, thereby suppressing possible undesirable side reaction/by-products. Another distinct superiority is that the molecule-surface interactions in larger pores can be neglected since the surface curvature becomes flatter.

Considering the above advantages, zeolites with hierarchical porosity are considered as one of the most promising industrial catalytic materials.⁴⁵ Various approaches have been achieved to synthesize hierarchical zeolites; they are mainly divided into “*in situ*” and “post-synthesis” methods. The former creates hierarchical zeolites by assembling microporous and mesoporous materials during the first synthesis of zeolite, while the latter post-treated the pre-synthesized zeolites to introduce hierarchical porosity into them.⁴⁵ More specifically, the post-synthesis treatments of previously formed zeolites involve demetallation (extraction of framework atoms), which can be realized by steam,⁴⁷⁻⁵⁰ acid,⁵¹⁻⁵⁴ base,⁵⁵⁻⁶⁰ or fluoride treatments⁶¹⁻⁶⁴. USY (ultra-stable Y) zeolite is a typical hierarchical zeolite bearing micro-/meso- porous architectures. The mesoporosity is commonly introduced by heating NH₄-Y zeolite with water vapor at high temperature (nearly 500 °C) (**Figure 4**). This operation partially dealuminates the zeolite framework to form mesoporous structures without significantly disrupting the zeolite’s faujasite topologies and crystal structure. Such treatment also increases the (hydro)thermal stability of zeolite. As a result, USY zeolite with a higher Si/Al ratio has improved catalytic performance than the parent Y zeolite and has been widely used in industrial applications, especially in petroleum refining processes (cracking, isomerization).⁶⁵

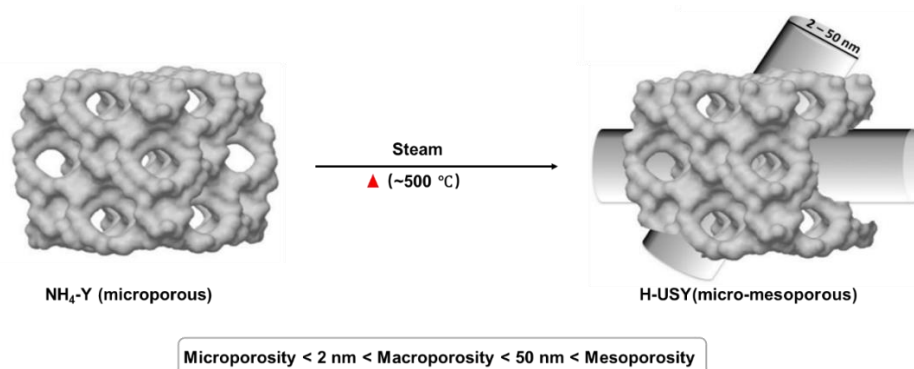


Figure 4. An example of preparation of H-zeolite via dealumination strategy: the H-USY case.

1.2.2. Shape-selective properties of zeolites for chemical catalysis

Zeolites can serve as reliable catalysts not only depending on their acidic properties but also on their capacity to discriminate molecule dimensions.⁶⁶ Indeed, zeolites exhibits an important

shape selectivity, that allows sieving molecules according to their dimensions, such as bulky and small molecules as well as linear and branched molecules. Such selectivity of zeolites affects reaction substrates but also the occurrence of reactions and the distribution of products. More precisely, the shape selectivity can cause mass transfer limitations and internal diffusion restrictions when the guest molecular size excessively increases.

There are three generally accepted types of shape selectivity in zeolites (**Figure 5, top**):

Reactant Shape Selectivity (RSS): In a reactant mixture, only those with appropriate molecular size can penetrate into the micropores of the zeolite and access active sites. The critical parameters of the selectivity are the geometry of the pore-entrance and the intra-pore diffusional properties of the starting materials. Practical applications are reflected in the selective cracking of linear alkanes and alkenes, but not their branched isomers, achieved with small pore zeolites.⁶⁷

Transition State Shape Selectivity (TSS): When compatible reactants enter and reach to the acidic sites, they have to be converted first into transition states before forming the final products. However, the confinement effects of zeolite (channels or cages) might affect the procedure and alter the final product distribution, *i.e.*, the so-called ‘transition state shape selectivity’. In this case, products can only be formed from reactions with transition states/intermediates of the appropriate shape and size according to zeolite type. Undesired reactants (products) cannot diffuse into (or out of) the zeolite crystal due to restricted TSS.⁶⁶ This selectivity has been widely applied in methanol-to-hydrocarbon (MTH) process catalyzed by different H-ZSM-5 zeolites.⁶⁶

Product Shape Selectivity (PSS): When differently sized and shaped products can be formed from a reaction occurring within the zeolite, only those having the appropriate size for the zeolite characteristics can overcome the diffusion limitations of zeolite and be readily desorbed from the zeolite. This phenomenon obviously impacts the final product distribution. A representative example is the alkylation of toluene with methanol over H-ZSM-5 zeolite, forming predominantly *para*-xylene (**Figure 5, bottom**).⁶⁸

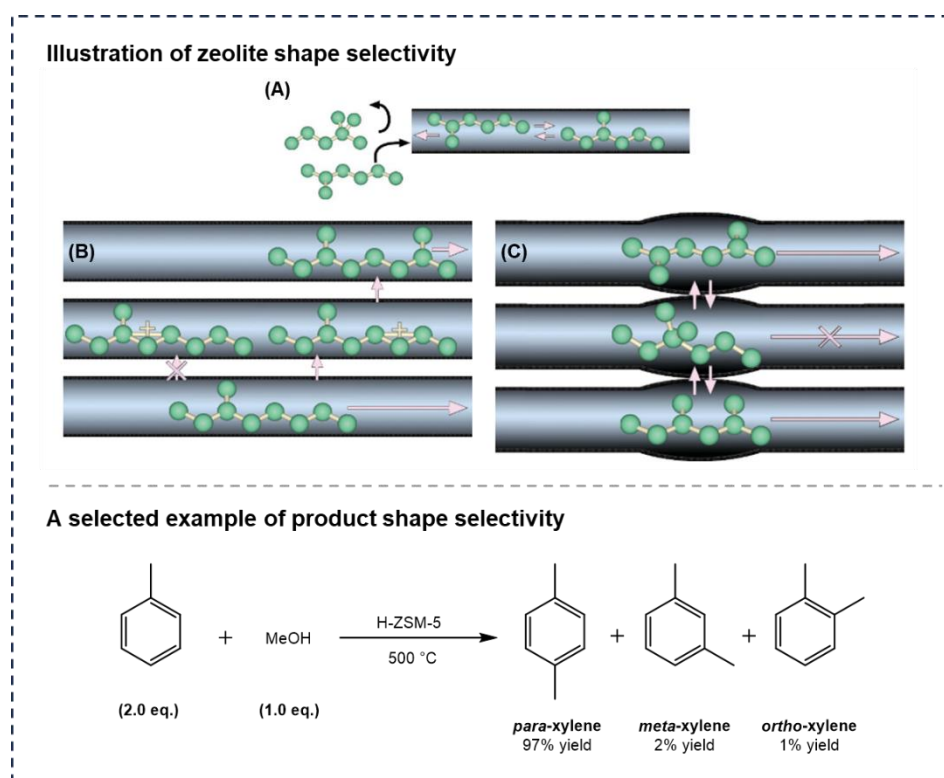


Figure 5. Illustration of zeolite shape selectivity (top): (A) Reactant shape selectivity; (B) Transition state selectivity and (C) Product shape selectivity,⁶⁹ and a selected example of product shape selectivity (bottom)⁶⁸.

In brief, the overall shape selectivity of zeolites may contribute to limiting the formation of by-products, making the processes more environmentally friendly and more cost-effective.⁷⁰ Furthermore, hierarchical zeolites with additional meso- or macropores can considerably improve the catalyst activity and lifespan, which appears to be more promising than catalysts only with microporosity. Although some challenges and limitations still exist, for instance, deciphering of catalyst deactivation mechanisms, zeolite robustness, and mass transfer limitation of the zeolite, their application potential, together with excellent catalytic performance in numerous chemical transformations, should not be underestimated. Examples of protic and metal-loaded zeolite catalysts will be given in section I-2.3.

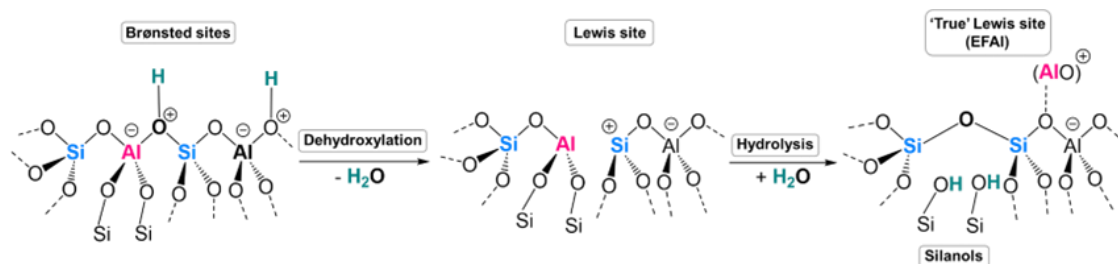
1.2.3. Chemical properties

When those molecules screened by shape selectivity enter the zeolite, the type and strength of acidity exhibited by the zeolite, will become the predominant factors affecting their catalytic performance for organic transformations.

As a kind of acidic mineral, zeolites have been regarded as solid acid catalysts for important chemical processes in many practical industrial applications, such as petroleum cracking⁷¹, methanol-to-gasoline (MTG) and methanol-to-olefins (MTO)⁷². However, as with other mineral acids, not all zeolites have the same acidity and acid strength. It is of great significance to distinguish the acid type of zeolite (Lewis acid or Brønsted acid) and the number, density and locations of the acidic active sites within the zeolite material as those directly influencing the zeolite acid strength.⁷³

Firstly, we must have a clear understanding of Lewis acid and Brønsted acid sites. Taking H-zeolites as an example, it can be regarded as Brønsted acid if focusing on the chemical composition of zeolites (**Scheme 2, left**). In a H-zeolite framework, protons are connected to the oxygen atoms of the zeolite to form Si-(OH)-Al bridging hydroxyl groups. However, the proton has a weaker affinity in a Si-(OH)-Al group. Since each zeolite topology bears a characteristic Si-O-Al bond angle, the latter can affect the labile H-zeolite bond in the Si-(OH)-Al constellation, making the proton easily transferable. As a result, the partial charges of the zeolite structure are affected, leading to an increase in its acidic strength. In addition, the acid site density, which is explicitly related to the framework aluminium content, *i.e.*, the Si/Al ratio, also controls the acidity of zeolite. Therefore, zeolites with the same topology but different SAR can display different degrees of acidity. Generally, the higher the SAR in the framework, the more acidic the zeolite would be. From that point on, Mortier⁷⁴ claimed that the relationship between aluminium content on the zeolite and acidity could be explained using Sanderson's electronegativity scale. He believed that the acid strength of a Si-(OH)-Al unit was judged by the overall electronegativity of the zeolite framework.⁷⁴ Since the electronegativity of the Si atom is higher than that of the Al atom (2.14 *vs* 1.71, on Sanderson's electronegativity scale), the H-zeolite bond is more easily polarized and has lower deprotonation energy in a silica-rich zeolite, resulting in a higher zeolite acidity. However, in addition to the important electronegativity, the stability of the conjugate base also controls the acid strength. Representative examples are hydrogen halides. Compared to other halides (fluoride, chloride), iodide anion possesses a larger ionic radius and a relatively dispersed negative charge, making the corresponding acid more prone to donate protons, resulting in higher acidity and more stable conjugate anions. In analogy to weakly coordinating anions (WCA's) principle,⁷⁵ the high dispersion of aluminium in silicon-rich zeolites contributes to improving the charge delocalization effect, allowing high-silica zeolites acting as the relatively stable conjugate

anions or bases derived from the corresponding strong acids. This also proves that there is a negative correlation between zeolite's acid strength and aluminium content.



Scheme 2. The generation of ‘true’ Lewis site.

It is also worth mentioning that the confinement effects also affect the acidity of zeolites.⁷⁶ The uneven spatial environment surrounding the Brønsted acid sites can also greatly enhance the acidity⁷⁷, as the channels or cages of zeolites can maximize the interaction of reactants at specific acidic sites.

Apart from Brønsted acid sites, zeolites can potentially possess Lewis acid sites, which depend on the initial preparation conditions or the post-treatment conditions/methods. Generally, Brønsted acid sites in zeolites can be converted to Lewis acid sites at increased temperatures. In H-zeolites, for instance, the Si-(OH)-Al bridging hydroxyl groups will lose water (dehydroxylation) at elevated temperatures to generate a three-fold coordinated aluminium and a silylium cation, both of which containing empty orbital for coordination (**Scheme 2**). These so-called ‘Lewis sites’ further produce ‘true’ Lewis sites, also known as extra-framework aluminiums (EFAl), through the ejection of Al species from the framework in the continued presence of water.⁷⁸ The EFAl is defined as $(\text{AlO})^+$ species acting as compensating cations of zeolite framework. Simultaneously, the defect-Si-OH, described as Brønsted acidic silanol (SiOH), is generated at the aluminium extraction site. In the presence of water, ‘true’ Lewis sites can further evolve to different octahedral aluminium hydroxide species $(\text{Al}(\text{OH})_x, (x=4 \text{ or } 6))$, producing an additional Brønsted acidity. In brief, a zeolite can cover three different Brønsted acid groups, among which Si-OH-Al bridging hydroxyl groups exhibit the highest acidity, and defect-Si-OH groups show the weakest acidity.

Although zeolites were almost universally regarded as superacids from 1994, the definition is still debated now.⁷⁹ In the light of new evidence from Haw⁷², it might be more reasonable to refer to zeolites as “solid acids” or “solid acid catalysts” rather than specifying a particular degree of their acidity.⁸⁰ It is hard to define the acidic strength of zeolites because they contain a mixture of Brønsted (proton) acid sites and Lewis acid sites, as well as polyvalent cations

(EFAI) and the defect sites (-Si-OH), that can also function in an acid manner. However, so-called ‘superacid’ behavior has been observed under special temperatures, indicating that the acid strength of zeolite is highly dependent on temperature.⁷²

Furthermore, all these acid units of Brønsted and Lewis acids can be replaced by other active cations (especially metal ions) *via* ion exchange (IE) reactions. However, they have different reactivity due to their distinct acidity. Especially, the defect-Si-OH groups with the weakest acidity can only be ion-exchanged at relatively high temperatures compared with the stronger acidic sites.⁸¹ The formation of transition metal-doped zeolites through IE reactions will be discussed in section I-2.2.4.2.

2. From natural zeolites to tailor-made zeolites

2.1. Natural zeolites

As is well known, from their discovery by Cronstedt, zeolite minerals (or natural zeolites) are often found as minor constituents in cavities of basaltic and volcanic rocks.⁴³ Later, major geological discoveries have revealed that they could be formed during the transformation of volcanic ash sediments with groundwater or alkaline/saline lakes in various geological environments and variable chemical temperature conditions. The soil composition, temperature, and pressure greatly play decisive roles in the formation of zeolites. When the pyroclastic sediments deposit in a basic aqueous solution, the ratio of dissolved Si/Al, the alkaline cations, and the pH of the solution are the primary determinants of the type of zeolite formed. The synthesis of zeolites begins at a low temperature of 4 °C and gradually forms different zeolites as the temperature increases. Furthermore, zeolites can only stabilize at pressures below 3-5 kbar due to their porous structure.

Natural zeolites are rarely pure since they are usually contaminated by other minerals, metals, quartz, or other zeolites to varying degrees during formation. Consequently, they are virtually excluded from many valuable commercial applications requiring high uniformity and purity.⁸⁰ Moreover, the sole microporous dimension of zeolites also greatly limits their applications (for details, see Chapter I-1.2.1.). Within this context, novel techniques for developing the synthesis of modified zeolites with higher purity and precisely designed structure emerged.

2.2. Synthesis of zeolites

2.2.1. History of synthetic zeolites

Synthetic zeolites possess several merits compared to their corresponding natural analogs. The improved uniform structure and high purity allow them to be widely applied in various industries. In addition, desirable zeolite structures that do not exist in nature can be fabricated.⁴³ Currently, 240 kinds of zeolites have been discovered, including approximately 40 types of natural zeolites and more than 150 types of synthetic zeolites.⁸⁰

Zeolites are commonly synthesized through a hydrothermal process, which imitates the hydrothermal conditions at elevated temperatures and pressures required for natural occurring zeolites.⁸² The history of artificial zeolites can be traced to 1862 when St Claire Deville⁸³ prepared levynite in the laboratory. However, the first attempt at the laboratory scale lacks reproducibility. Later, in the late 1940s, Richard Barrer theoretically studied the relationship between the preparation conditions and conversion of known mineral phases at high temperatures (170-270 °C) and proposed the first reliable hydrothermal synthesis conditions of minerals.⁸⁴ Shortly after, various attempts have been made by the academic community to improve the conditions of zeolite synthesis. In 1949, Robert Milton discovered that milder reaction conditions could be achieved using more reactive starting materials, such as freshly precipitated aluminosilicate gels. In the next few years, several zeolites were synthesized, like A, B, and X zeolites.⁸⁵ By 1953, Milton and his colleagues had synthesized 20 kinds of zeolites, including 14 types of natural zeolite structures that have not been disclosed yet.⁸⁶ Following the foundations laid in the 1950s, many significant developments regarding the synthesis of zeolites had been realized in the ensuing decade. Of note was Barrer's seminal discovery that the ratio of Si/Al and the size of pore and particle could be tuned using organic ammonium cations as structure-directing agents (SDAs).⁸⁷ It must be mentioned that most zeolites synthesized in laboratories prior to this period were low-silica zeolites with known structure. Compared to their natural analogs, an obvious distinction was that the formation of natural zeolites did not require organic structure-directing agents (SDAs).¹⁵ However, it has been proved that using organic SDAs can not only synthesize new zeolitic frameworks with higher Si/Al ratios, like ZSM-5 (MFI) and zeolite Beta (BEA), but also facilitates the formation of other zeolites which have been previously prepared without organic SDAs (e.g. FAU and LTA frameworks).⁸⁸ Owing to Barrer's significant contribution to the preparation of zeolites, numerous zeolites with different physicochemical properties, such as higher ratio of Si/Al or nano-size zeolites^{89,90},

have been prepared using diverse SDAs,⁹¹ of which the synthesized Beta⁹² and ZSM-5⁹³ zeolites are one of the most used today.

2.2.2. *De novo* synthesis of zeolites

Theoretically, several million zeolite structures are predicted to be feasible and stable,⁹⁴ stressing the huge potential of zeolites as tailor-made materials for numerous applications. However, the number of zeolites actually reported (240 kinds of zeolites) is far below the predicated value. This fact is closely related to the existing zeolite synthesis conditions that still need to be improved. Since zeolites are crystallization products, the lattice energy of their crystal structure plays a decisive role in their relative stability. During the crystallization process of zeolite synthesis, several necessary elements are highly combined, resulting in abundant possible zeolite structures, but only those relatively stable structures will remain.

Zeolites are usually synthesized by a typical hydrothermal synthetic process, which includes several common elements: 1) two types of starting substrates, namely silica source (sodium silicate, tetraalkylorthosilicate (alkyl = methyl, ethyl), precipitated, colloidal, or fumed silica, certain mineral silicates like clays and kaolins, ...) and alumina sources (sodium aluminate, aluminium sulfate, aluminium hydroxide, ...); 2) reaction media (water); 3) a mineralizing agent to dissolve silicates and aluminates, (most commonly alkali metal hydroxides or halide salts, ...) and 4) a structuring directing agent (SDA) that is a crystallization template (usually organic amines and/or alkylammonium species). The procedure is shown schematically in **Figure 6** and is briefly described as follows:

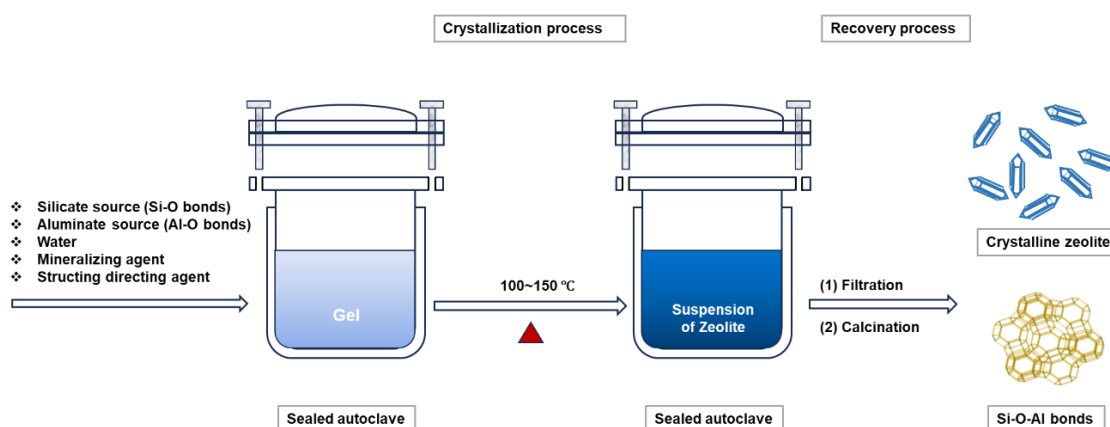


Figure 6. *De novo* synthesis process of zeolites.

a. Both starting materials containing Si-O and Al-O bonds are mixed in an alkaline medium.

b. The aqueous reaction mixture is heated (to 100-150 °C) and pressurized (if needed) in a sealed autoclave.

c. The substrates remain in an amorphous gel state for a period after raising to the synthesis temperature.

d. After the above “induction period”, the crystalline zeolite containing Si-O-Al bonding is gradually generated from the amorphous hydrogel in the absence or presence of SDAs (e.g., tetrapropylammonium species) in some cases.

e. The synthesized zeolite crystals are then recovered after filtration, washing and drying. The SDAs, if used, are removed by calcination.

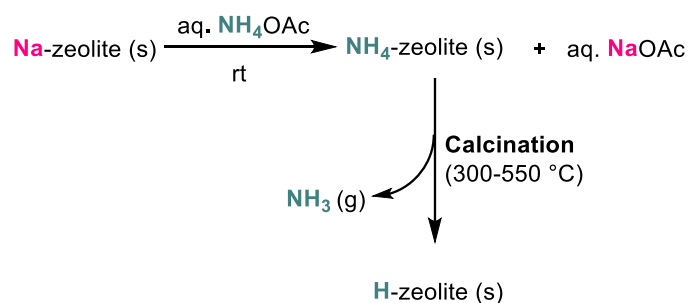
It is possible to create different crystal morphologies of zeolite by adjusting the order and quantity of adding starting materials, the temperature, and the time in the autoclave. Of course, different sources of substrates and SDAs, as well as the type and concentration of the mineralizing agent, will also generate diverse zeolite crystalline structures.⁹¹

Furthermore, of the two different mineralizers shown above, alkali metal hydroxides are the most frequently used mineralizing reagents, which are similar to the alkaline conditions required for the synthesis of natural zeolites and have been widely applied in the zeolite manufacturing industry. However, the required high pH condition will cause environmental and economic problems. In 1978, Flanigen and Patton⁹⁵ reported the use of fluoride salts, enabling the synthesis process to be performed at lower pH conditions and the formation of larger zeolite crystals.⁹⁶ Nevertheless, this strategy is less attractive for large-scale applications due to the high toxicity and corrosivity of fluoride ions.⁹⁷

2.2.3. Synthesis of acidic zeolites

During the crystallization of the zeolite framework, different alkali or alkali earth cations will be incorporated due to the employed varying silicate, aluminate, and mineralizing reagents. Sodium ions are frequently present in commercially available zeolites. These zeolites can generate the corresponding ammonium form NH₄-zeolites *via* ion exchange (IE). A typical procedure is to perform multiple consecutive aqueous ion exchange (AIE) reactions (see Chapter I-2.2.4.2.1.) in aqueous solutions of ammonium acetate or ammonium nitrate of defined concentrations (**Scheme 3**).

It is easier to obtain acidic zeolites (H-zeolites) from the corresponding NH₄-zeolites by thermally removing the ammonia by calcination (**Scheme 3**). Considering the predominant hydrothermal and chemical stability of zeolites, the calcination can be carried out under air at high temperatures (typically more than 500 °C), with complete deamination after several hours. A few examples are also performed under inert atmosphere. Moon and co-workers⁹⁸ optimized the deamination stage of NH₄-Y zeolite in flowing helium. It was found that the material calcinated at 400 °C for 24 h had a larger SSA and higher crystallinity than the zeolite calcinated at 500 °C or 600 °C. Besides, prolonged heating time at increased temperatures would lead to the collapse of the crystalline structure of zeolite. Moreover, most of the ammonia was removed even at the calcination temperature of 300 °C. These experimental data varied significantly according to the specific zeolite structure.



Scheme 3. The synthesis of NH₄- and H-zeolites *via* cation-exchange.

2.2.4. Synthesis of metal-doped zeolites

Metal catalysts are extensively used in research laboratories and industrial/manufacturing processes due to their excellent catalytic performance. As homogeneous catalysts, most metal cations suffer from non-recoverable/non-recyclable issues, which have motivated the incorporation/immobilization of metal cations into solid materials. Thus, “metal-doped” zeolites have been developed, and many metal components with specific structural and chemical properties have been incorporated/immobilized in/on the zeolites *via* different methods. It is intricate to predict the optimal method to synthesize a specific metal-doped zeolite. It cannot be assumed that the same starting material employed in different preparation methods will generate comparable materials. Furthermore, each method is significantly influenced by the chosen synthesis parameters, such as the amount and properties of precursors, the temperature, and the applied solvent, as well as the SDA. According to the specific synthetic method, other experimental factors may also be critical.

Moreover, different salts/complexes of the same cation are not always suitable for each method. Further improvements are also required when switching from one cation to another. Therefore, the multi-step optimization process of a metal-doped zeolite involves many parameters. Once the prepared zeolite is identified, it may not be applicable in all conceivable fields. Thus, it is desirable to build an arsenal of identified metal-doped zeolites and exploit their performance in all applications.

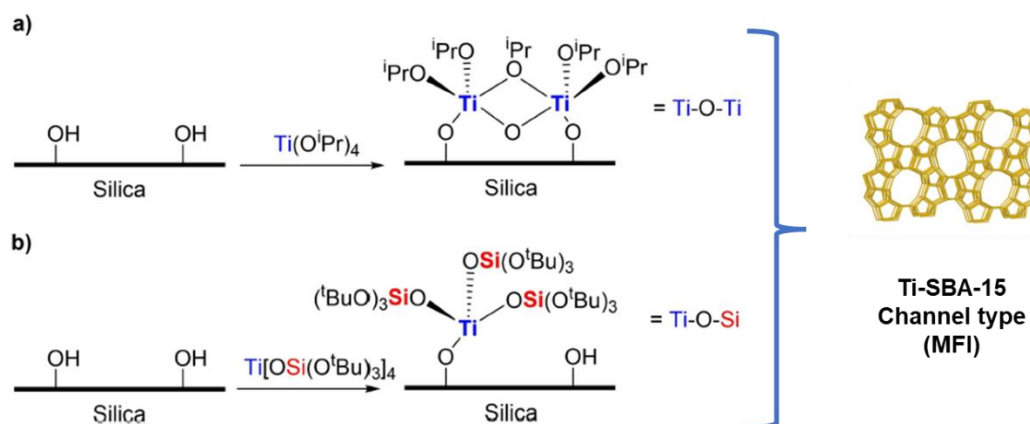
The following part will introduce three main methods for synthesizing metal-doped zeolites and discuss their structural and reactivity properties.

2.2.4.1. Via isomorphous substitution of zeolite framework composition

Zeolites are formed when aluminium atoms replaced some silicon atoms in pure silicates. This process has become an inspiration for the design of new zeolite-type materials with improved properties. This could be achieved by further replacing silicon or aluminium atoms in a zeolite framework by other components to obtain zeolite-like structures. This concept is known as isomorphic substitution. Through this method, chemists envisage incorporating catalytically active metal cations into the zeolite framework to solve the problems of metal leaching and create single metal sites (Lewis acid sites) with catalytic activity. For instance, it has been proved that the introduced tetravalent titanium and tin can generate strong Lewis acid sites for catalysis. Two major families of zeolite-type materials are metallosilicate materials and (metallo)aluminophosphate materials. The early metallosilicate materials were reviewed in detail by Szostak.⁹⁹ A large number of metallosilicate materials containing incorporated tetrahedral iron, chromium, gallium, germanium, and titanium have been reported.⁴³ Wilson *et al.*¹⁰⁰ reported the discovery of a new class of aluminophosphate molecular sieves. Shortly after, some metal cations were also incorporated into the aluminophosphate frameworks, such as lithium, magnesium, titanium, manganese, iron, cobalt, zinc, Ga, Ge, and arsenic.¹⁰⁰

It is generally believed that Ga atoms can easily substitute aluminium atoms, and silicon atoms are easily replaced by Ge atoms in aluminosilicate systems since these metals belong to the same family in the periodic table.¹⁰¹ In addition, titanosilicates (TS) are prepared using titanium alkoxide precursors *via* a bottom-up approach, while tin-containing silicates are produced from the reaction of a dealuminated zeolite with SnCl₄ in a top-down approach. An example of titanosilicate was given in **Scheme 4**. A kind of Ti-SBA15 which was prepared by grafting a tri(alkoxy)siloxy complex of Ti(IV) (Ti[OSi(O^tBu)₃]₄) on the SBA-15 (a kind of mesoporous zeolite), exhibited excellent catalytic activity for olefin epoxidation due to its high dispersion

of Ti species,¹⁰² compared to that prepared by impregnation with titanium alkoxides $\text{Ti}(\text{O}^i\text{Pr})_4$ on the SBA-15¹⁰³.



Scheme 4. Ti species in (uncalcinated) Ti-SBA-15 catalysts prepared by post-synthesis grafting of a) $\text{Ti}(\text{O}^i\text{Pr})_4$ and b) $\text{Ti}[\text{OSi}(\text{O}^t\text{Bu})_3]_4$.¹⁰²⁻¹⁰⁴

A comprehensive summary of such zeolite-type materials and their applications in sustainable chemistry has been reviewed recently.¹⁰⁵ In this manuscript, we will thus not further discuss the isomorphous substitution of zeolite framework composition.

2.2.4.2. Via ion exchange of zeolite extra-framework cations and related strategies

Ion exchange is one of the most widely used strategies to form metal-doped zeolites, which exchanges the extra-framework cations of zeolites for catalytically active metal ions. It can be broadly categorized into two types, ‘wet’ or ‘aqueous’ (AIE) and “solid-state” ion-exchange (SSIE). The merits and demerits of each method are shown in **Table 2**. Furthermore, the relevant updated strategies are also described in this section.

2.2.4.2.1. Aqueous and solid-state ion exchange of zeolites

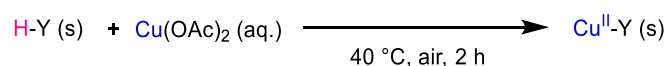
In aqueous ion exchanges (AIEs) or ‘wet exchanges’, the metal cations contained in the corresponding salts or metal oxides will be released in a pH-controlled solution. The solutions that are too acidic or too basic will damage the zeolite framework. Such a solution-mediated method enables the insoluble zeolite to be tightly surrounded by numerous exchange cations in suspension and allows the resulting material to be easily separated from the mixture by filtration. More beneficially, this approach is feasible to manufacture large quantities on a multigram lab scale. However, the drawback is that AIE cannot achieve 100% quantitative exchange from original cations to the expected cations in a one-time performance since the IE process is dynamically reversible. It is inevitable to repeat the AIE process several times if materials with

high loading in the desired metal cations are needed. This results in a more cumbersome process, with high costs and waste of chemical resources since most utilized cations will be directly discarded after filtration. In addition, the material obtained after filtration must be washed and dried, so preparing a zeolite-based catalyst through this method may take several days or weeks. Unfortunately, AIE is unsuitable for metal salts that are sparingly soluble or insoluble in water or other solvents. Some cations with intense hydration effects cannot penetrate the micropores of zeolites due to their large volume, resulting in a limited number of metal cations accessing to the zeolite available exchange sites by AIE.

Table 2. Comparison of aqueous (AIE) and solid-state ion-exchange (SSIE).

AIE	VS	SSIE
Easily	Scalable	Easily
Milder (rt ~ 100 °C)	Temperature	Higher (mostly > 300 °C)
Common	Equipment	Specific
Multiple consecutive operations (days to week)	Operation	Often single operation
Low (uncontrollable) exchange degrees per time	Exchange degrees	High (adjustable) exchange degrees per time
Yes	pH control	No
Hydrated zeolite product recoverd by filtration	Work-up	Usually soxhlet extratcion after exchange
Excessive metal used (waste increase)	Waste	Moderate metal used (Waste reduction)
Lower	Efficiency	Higher (faster)
Limited to soluble salts with small hydration shell	Limitation	Usually under vaccum or inert atmosphere

Due to the excellent stability and solubility of copper(II) ions in aqueous solution, zeolites containing copper(II) could be easily prepared through such exchange. For instance, Ipaktschi *et al.*¹⁰⁶ used an acidified sodium Y zeolite to exchange with Cu(OAc)₂ *via* multiple AIE processes to obtain a Cu^{II}-Y zeolite as the important precursor for the desired Cu^I-Y (**Scheme 5**).



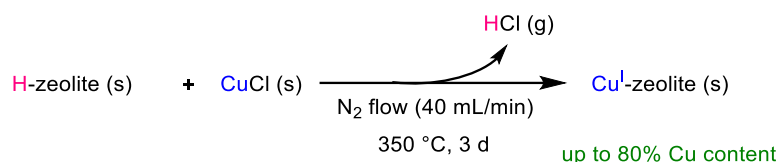
Scheme 5. Preparation of Cu^{II}-Y *via* multiple AIE process.

In contrast, the solid-state ion exchange (SSIE) involves the exchange of ions between two solids with little or no water present. The first reports of SSIE in zeolites appeared in the early 1970s.^{107,108} Now, it has become a valuable route to prepare zeolite catalysts, and many transition and noble metal cations have been successfully introduced into zeolite *via* this method.¹⁰⁹

The common method of preparing catalysts by SSIE is to heat an intimate mixture of the zeolite and metal salt containing the entering ion at a defined temperature (typically 300 ~ 400 °C) under high vacuum or inert atmosphere (in air in some cases). The mixtures are prepared by vigorous mechanical mixing (in a mortar or *via* ball milling) or by suspending the two precursors in a volatile solvent and mixing thoroughly, then by evaporating the solvent.¹¹⁰

The protective atmosphere during thermal treatment strongly influences the nature of metal species obtained. Metal oxides can be observed if the IE is run under oxygen (air), some of which aggregate into nanoparticles. Reduction reactions may occur between the metal and the corresponding oxidation state under anaerobic conditions. Different metal oxidation states will probably exist after the SSIE process, but they can be easily detected by various spectroscopic methods.

The SSIE method has some advantages over the previously mentioned AIE method (**Table 2**). For instance, the SSIE method can effectively avoid the restrictive cations hydration effects in the AIE method, thus making the cations more accessible to the channels and cages of zeolites. Obviously, the SSIE method would be desirable for insoluble salts in the solution. From a practical point of view, the SSIE approach largely avoids the handling and disposal of excess electrolyte solution, reducing the costs of wasted chemical resources and environmental damage. Interestingly, there are significant differences in the catalytic activity of the obtained zeolite by SSIE and AIE using the same starting materials. The SSIE method usually produces a higher-efficiency catalyst, even with relatively low metal charge cations. Consequently, the exchange approach and chosen parameters will largely determine the distribution and localization of the entering cations into the catalyst. For instance, Cu^I-zeolites are frequently prepared by SSIE method due to the sensitivity of copper(I) species to redox processes and the low solubility of Cu(I) salts in water. Our research group¹¹¹ has synthesized five different copper(I)-doped zeolites (USY, Y, ZSM-5, MOR, β) through this method. These catalysts were prepared *via* SSIE reaction between their H-forms and CuCl (**Scheme 6**), and Cu^I-USY proved to be an efficient catalyst in many organic transformations.



Scheme 6. Preparation of Cu^I-doped zeolites *via* SSIE.

It is necessary to provide an accurate protocol for the SSIE procedure and characterization of metal-doped zeolites to allow their reproducible preparation and identification.

Armor¹¹² has disclosed a proposal on this subject, including 1) the source and composition of the original zeolite and the incoming cation, 2) the diagram of the extra time-temperature, 3) the pH value before and after IE, 4) the stirring rate for AIE, 5) elemental analysis of the final metal-doped zeolite, 6) the loading amount of desired metal cations, etc.

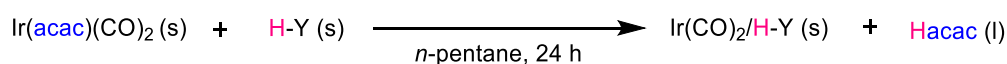
Last year, Erkey and coworkers¹¹³ reported a new IE process for the preparation of copper-mordenite (Cu-MOR) catalysts by Cu^{II} cation exchange of copper trifluoroacetylacetonate (Cu(C₅H₄F₃O₂)₂) with H-MOR in supercritical CO₂. The supercritical IE (SCIE) was performed at 80 °C for three days, which was significantly lower than the usual temperature of SSIE (between 300 °C~550 °C). However, a special pressure-resistant apparatus (up to 27.58 MPa) was required in SCIE. In addition, they also investigated the catalytic performance of the obtained Cu^{II}-MOR for the stepwise direct methane to methanol (sDMTM) process and found that the Cu^{II}-MOR prepared by SCIE showed higher methanol productivity (>16%) compared to the Cu^{II}-MOR obtained *via* AIE with the same Cu loading (2.3 wt%). These results indicated that the ion-exchange sites selected in zeolites using SCIE differ significantly from those selected by AIE.

2.2.4.2.2. Chemical vapor deposition (CVD) and ligand exchange

Chemical vapor deposition (CVD) is a technique closely related to SSIE for the preparation of metal-doped zeolites, where the metal cations from a volatile metal precursor (chloride, organometallic compounds, etc.) react with the zeolite precursor under anhydrous conditions at high temperature. This process leads to a selective and stoichiometric metathesis reaction between the Brønsted acid sites of the zeolite and the metal precursor, producing the defined single-atom catalysts. CVD has been used to prepare various zeolites doped with tin (SnCl₄)¹¹⁴, nickel (Ni(C₅H₅)₂)¹¹⁵, and refractory metals like rhenium (CH₃ReO₃)¹¹⁶. The main distinction between CVD and SSIE is that the IE process is performed in a vapor-solid rather than a solid-solid reaction. The volatile component containing metal cations is heated in another reactor and

directly deposited onto the zeolite surface with the help of a carrier inert gas or under vacuum condition. In other words, there is no physical contact between the two precursors at the beginning of the CVD process.

In addition to CVD, another term, “ligand exchange,” can also be found in the literature to describe the IE process. Well-defined metal complexes, used as the metal ion precursors, are assumed to exchange their ligands with the cations on the zeolite’s Brønsted acid sites in a chemical reaction. Based on this, Gates and co-workers have prepared a series of noble transition metal-doped zeolite catalysts (Rh¹¹⁷, Ir¹¹⁸, Pt¹¹⁹) from commercially available organometallic compounds (alkyl, carbonyl, and acetoacetate metal complexes) precursors. With such technique a single-atom and well-defined cluster catalysts with specific metal contents could also be prepared in some cases. Besides, Gates’ group¹²⁰ found that the zeolite crystal framework had a significant effect on the stabilization of the metal complex unit and was superior to other amorphous supports. Such performance might be the main reason for the higher sintering resistance of the resulting metal-doped zeolites. A related example (**Scheme 7**) has been published in which Ir[(*acac*)(CO)₂] produced a highly stable Ir(CO)₂/H-Y complex *via* “ligand-exchange”.



Scheme 7. A ligand-exchange example to prepare a highly stable Ir(CO)₂/H-Y catalyst.

The metal-doped zeolite catalyst obtained by the above-mentioned methods can be directly applied to the catalysis of specific chemical transformations. Furthermore, the nature of the introduced metal species can be further modified by post-treatment procedures, for instance, reducing the metal cations to metal nanoparticles or single metal atoms. Notably, nanoparticles in/on zeolite can also be prepared by other methods without the IE process.

2.2.4.3. *Via* chemical encapsulation techniques in zeolite topologies

Zeolites are commonly used as solid supports to immobilize metal nanoparticles (NPs). Here are two categories: metal@zeolite and metal/zeolite (**Figure 7**). The former (**Figure 7a**) is a directionally designed material where metal nanoparticles are only encapsulated in the zeolite microporous pores (channels or cages).¹²¹ In contrast, NPs are deposited on the surface of metal/zeolite (**Figure 7b**).

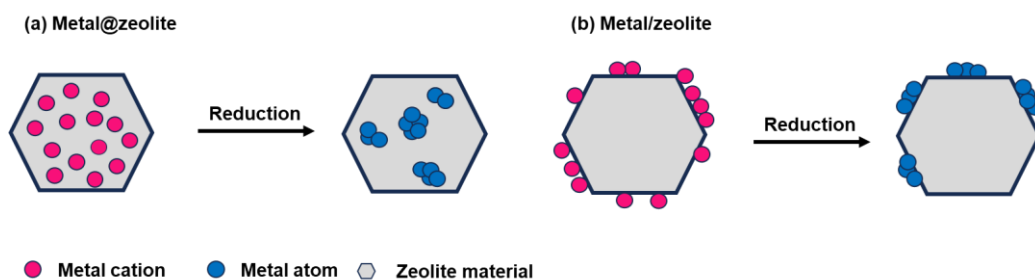


Figure 7. Comparison of Metal@zeolite and metal/zeolite.

The metal nanoparticles formed within the pores are better controlled by the size of the micropores.^{122,123} Besides, the zeolite topology also partially contributes to this shape selectivity of NPs in metal@zeolite, but it cannot control the size of metal on metal/zeolite materials.¹²⁴ Furthermore, NPs inside the pores are tightly immobilized in the zeolite framework, making them more resistant to sintering and leaching due to the lack of mobility.¹²⁵ This feature allows them to be used at relatively high temperatures without catalyst deactivation due to sintering.

Many strategies have been recently employed to encapsulate NPs into zeolite channels and cages, such as post-synthesis,^{126,127} co-crystallization^{123,126}, and 2D to 3D transformation¹²⁸ methods. The first two methods will be briefly described below.

The post-synthesis approach is the most frequently used strategy and relies on reducing metal cations, as shown in **Figure 7**. Generally, the metal species are introduced by impregnation or IE of the charge-balancing cations.¹²⁹ The subsequent reduction process is usually carried out in a flowing hydrogen atmosphere at the lowest permissible temperature to prevent sintering.

As for co-crystallization, it is more suitable for small-pore zeolites.¹³⁰ The limitation of small pore size makes it tough to perform an IE process when the incoming cation is a bulky counterion or carries an important hydration shell. When performing the co-crystallization process, nanoparticle precursors need to be formed and included within the zeolite during the crystallization of the zeolite matrix. In the last step, NPs are generated by calcinating metal precursors in a defined atmosphere (e.g., air or H₂). The resulting catalysts are rarely used in organic synthesis since it does not allow normal-sized chemical molecules to enter the zeolite. Nevertheless, these catalysts still display great potential for other applications. A representative example is Pd@S-1 (MFI), which exhibited outstanding activity in the hydrogen production process from formic acid under mild conditions and whose attractive recyclability has also been verified.¹³¹

It is worth mentioning that some of the above strategies for preparing metal-doped zeolites can simultaneously generate Brønsted and Lewis acid sites in/on zeolites, thus making it possible to design multifunctional zeolites for certain catalytic domino reactions based on strong metal-acid synergistic effects.¹³²

2.2.4.4. *Via the ship-in a-bottle synthesis strategy*

Ship-in-a-bottle (SIB) synthesis strategy is commonly applied for the synthesis of new nanoporous hybrid particles by encapsulating a molecule of interest into a microporous zeolite. This strategy incarcerates larger functional guests within the zeolite cavities (cages or channels), making them impossible to diffuse outside the particle.¹³³ Therefore, the enclosed large molecules in the cavities of zeolite resemble a ship in a bottle (**Figure 8, top**), which is typically referred to as ship-in-a-bottle catalysts.¹³⁴

The term "ship in a bottle" (SIB) was most likely coined by Herron in 1986, while working at Dupont's Wilmington Research and Development Center, who reported the synthesis of several metallic complexes encapsulated in zeolites.¹³⁵ So far, there are many examples reported in the literature related to encapsulated zeolites by introducing nickel(II)-Schiff base complex¹³⁶, Co(bpy)₃²⁺ and Ru(bpy)₃¹³⁴⁻¹³⁷, and cobalt(II)-salen complexes¹³⁸. Several attempts have also been made to confine nanostructures such as clusters, metal oxides, polymers, and catalysts within nanoscale zeolites.¹³⁹⁻¹⁴²

There are two possible strategies for the preparation of zeolite ship-in-a-bottle complexes, including the utilization of flexible ligands (FL) and the synthesis of zeolite around the complexes.¹⁴³ The former is the typically SIB method to encapsulate large complexes (guests) into zeolites.¹³⁴ The large guests inside the zeolite cavities are derived from smaller precursors that can diffuse through the zeolite pores and then react inside the cavities of zeolite to form the target guest.¹³³ In this method, a FL, as a precursor with suitable size, can freely penetrate into the zeolite cavities and form a complex with the metal ions that have been previously introduced by an ion exchange method. The complexes formed are sufficiently larger and harder that they do not diffuse out of the zeolite pores. The method allowed the size of the metal complexes to be controlled by the shape selectivity of zeolite, and the excess flexible ligand could be recycled if the synthesis reaction was performed in solution, since they can penetrate out of the zeolite pores and into the liquid phase.¹⁴⁴ For instance, Amooghin and co-workers¹³⁴ encapsulated a cobalt-organic complex in zeolite Y cavities through the ship-in-a-bottle (SIB) synthesis method for highly selective membrane gas separation. As is shown in **Figure 8**, Co²⁺ was

introduced in the zeolite (Co-1) through an AIE process involving cobalt(II) acetate salt and NaY. Then the polyaza Co–ligand complexes (Co-2 and Co-3) were formed with the diamine and diketone (flexible ligands) *via* the ship-in-a-bottle (SIB) synthesis method in the nanoreactors of modified zeolite Y. And the so-obtained macrocyclic [Co(tetra-aza)]²⁺ complex (Co-3) was encapsulated in the zeolite due to its larger size than the zeolite pores.

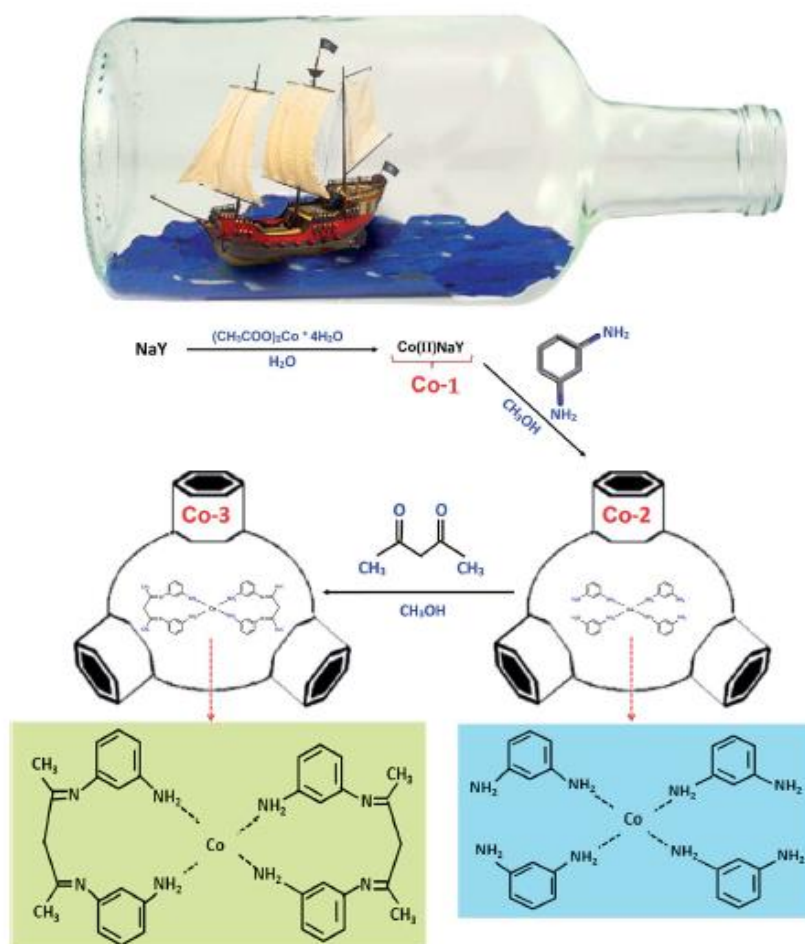


Figure 8. The encapsulation of Co-ligand complexes in zeolite Y *via* two SIB synthesis processes.¹³⁴

Another complementary SIB method for encapsulating complexes into the zeolite is to build the bottle around the ship.¹⁴³ This approach requires performing the crystallization procedure of the zeolite from a gel that contains the preformed guest. In this method, metal complexes (preformed guest) are simultaneously added to a synthetic mixture of zeolite under the synthetic conditions of zeolite framework (specific pH and high temperature), then are encapsulated in zeolite cavities. However, there are two obvious limitations in this methodology: 1) the preformed complexes should be stable enough to survive the relatively harsh pH and temperature conditions during the zeolite synthesis procedure for a long period; and 2) the zeolite crystal structure should still be able to form in the presence of the guest. The latter

explains why this build-the-bottle-around-the-ship approach has been employed almost exclusively for faujasites X and Y since the ease of crystallization of their structure.¹³⁴

Since the seminal work of Herron on the ship-in-a-bottle synthesis of metal complexes encapsulated in zeolites, a vast number of examples of this and other types of guests have been reported. These reports have continuously explored the application of zeolites containing encapsulated guests as chemical catalysts for different fields (traditional catalysis, electrocatalysis,¹⁴⁵ photocatalysis¹⁴⁶), sensors, and the development of functional materials also benefited from ship-in-a-bottle methodologies.¹³³ These ship-in-a-bottle catalysts have been widely used in various industrial processes such as oxidation^{147,148}, isomerization and catalytic cracking due to their good environmental compatibility and increased economic efficiency.¹³⁴ Furthermore, the “ship-in-a-bottle” strategy has also been utilized in the pharmaceutical industry to advance cancer treatment.¹⁴⁹ Various studies have demonstrated the effectiveness of these functionalized nanoparticles synthesized by the SIB method in co-delivering drugs, and achieving targeted delivery, as well as responding to multiple stimuli to control drug release. For instance, Douhal and co-workers¹⁵⁰ used the “ship-in-a-bottle” strategy to load a hydrophilic anticancer drug in porous metal-organic framework nanoparticles. This nanomaterial effectively controls drug encapsulation and release, and highly efficient results have been observed in the human pancreatic cell line PANC1.

A comprehensive summary of such “ship-in-a-bottle” synthesis strategy and their applications in a variety of fields has been reviewed.¹³³ In this manuscript, we will not further discuss the method given the core of the thesis.

2.3. Applications of zeolites

As versatile inorganic materials, zeolites exhibit a wide range of applications owing to their tremendously attractive physicochemical properties. e.g., the high specific surface (300~1000 m²/g), great ion-exchange (IE) capacities, and adsorption. These features allow zeolites to be mainly used as industrial detergents, adsorption, and drying agents. Besides, the abundant acidic catalytic active sites, unique shape selectivity, and excellent hydrothermal stability also contribute to their promising applications for catalysis. However, the majority of zeolites (72%) have been developed as detergents, and only 13% are used as heterogeneous catalysts, mainly in petrochemical and bulk industries (**Figure 9**).⁶⁵ Furthermore, the development of zeolites used as catalysts in fine chemistry and organic synthesis remain limited. Zeolites doped by

metal ions, especially transition metal ions, are still scarce regarding applications in organic synthesis, making it highly desirable to explore their catalytic potential in organic synthesis and fine chemistry.

This section will demonstrate current applications of zeolites in industries and organic synthesis, and the applications of metal-doped zeolites in organic synthesis will be emphasized since it is closely to this subject of this thesis.

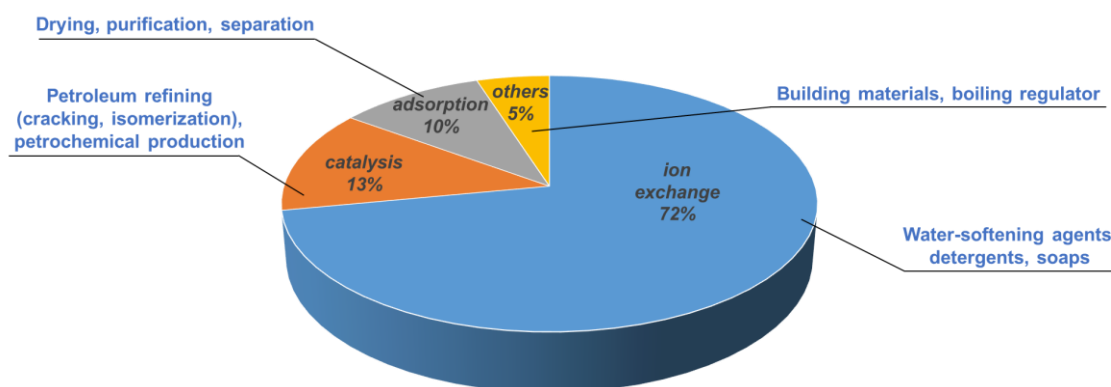


Figure 9. The main applications of zeolites in industries.

2.3.1. The applications of zeolites in industry

As shown in **Figure** , three main applications of zeolites in industry are ion exchangers, adsorption/drying agents, and heterogeneous catalysts, which are briefly described as follows.

2.3.1.1. Zeolites as ion-exchangers

Zeolite has a negatively charged framework that induce some cations to neutralize their negative charges. These cations are bound to the zeolite through reversible electrostatic interactions, which imparts a remarkable ion exchange capacity to zeolite.

This feature allows zeolites to be used as water softeners, absorbing Ca^{2+} ions and Mg^{2+} ions in water, and as detergents to efficiently remove phosphates which are recognized facilitators of eutrophication, e.g. zeolite A, zeolite P and zeolite X.¹⁵¹

Furthermore, zeolites are also used in agriculture to improve plant growth and soil quality¹⁵² due to their great affinity for NH_4^+ and ammonia gas (NH_3) which could be derived or leached from N fertilizer. They can adsorb and release nutrients *via* ion exchange process between

2potassium (or calcium) species required for plants and ammonium ions. Nutrient-loaded zeolites can act as controlled release fertilizers (CRFs) to improve the efficiency of fertilizer use and reduce the negative environmental impact due to the loss of nitrogen from N fertilizer in air, soil and groundwater.

Besides, such a feature also allows them to be used as feed additives, litters and excreta amendments in livestock industry.¹⁵³ Karamanlis *et al.*¹⁵⁴ reported that adding 0.2% zeolite in the diet or/and 2.0 kg/m² into the litter of broilers results in greater weight gain in broilers without affecting feed conversion. Poultry house ammonia levels could be reduced from 21.15 ppm to 17.25 ppm when inclusion of 15 g zeolite /kg feed additive were added into the diet of broilers.¹⁵⁵ Similarly, zeolites can be utilized as cat litter deodorizer in household purpose. For instance, Imerys (clinoptilolite) acts as a natural odor eliminator owing to its excellent ion exchange ability to absorb ammonia from cat excreta, meaning that litter tray stays fresher for longer.

Additionally, zeolites also exhibit the potential as effective capture materials for hazardous, radioactive isotopes,¹⁵⁶ e.g., ¹³⁷Cs⁺, which is commonly released in nuclear disasters. Therefore, zeolites were extensively employed for this aspect after the disasters in Chernobyl in 1986 and Fukushima in 2011.

2.3.1.2. Zeolites for adsorption and separation processes

Zeolites are extensively applied in adsorption and separation processes since the 1950s, and are commonly referred to molecular sieves. The most prominent application market in this aspect is to dry various gases or organic solvents by absorbing water molecules¹⁵⁷. For instance, a range of gases including formaldehyde and hydrogen sulfide has been shown to be adsorbed by zeolites, which can be added to small air filters in order to adsorb such toxic gases and reduce allergy problems in domestic uses. Furthermore, zeolites show outstanding performance as adsorbents in water cleaning and treatment.¹⁵⁸ Various natural zeolite clinoptilolites as effective adsorbents exhibit excellent performance in water and wastewater treatment.¹⁵⁸

Zeolite adsorption and separation properties are closely related to their structural characteristics. Specifically, the pore size, shape, and hydrophobicity (with a high Si/Al ratio), as well as the nature of the cations that compensate for the charges, play a decisive role in zeolite adsorption property. All these key factors can be modified to design more highly selective materials for a variety of applications.

2.3.1.3. Zeolites as heterogeneous catalysts in industry

Among the 240 structures of zeolites, only 17 types of zeolites have been widely used in industry, most of which are used in petroleum cracking as H-form acidic catalysts.⁶⁵ Zeolites with larger pores are of great value in petroleum catalytic cracking, hydrocracking, and hydroisomerization. Compared with silica-alumina catalysts commonly used in this process, zeolites as catalysts in the petroleum industry can increase gasoline yield by more than 20% and handling capacity can be increased by about 30%. In the hydroisomerization reaction of *n*-hexane, the conversion rate can also be raised by over 30%. Interestingly, more than 95% synthetic zeolites are applied in the Fluid Catalytic Cracking (FCC).⁶⁵

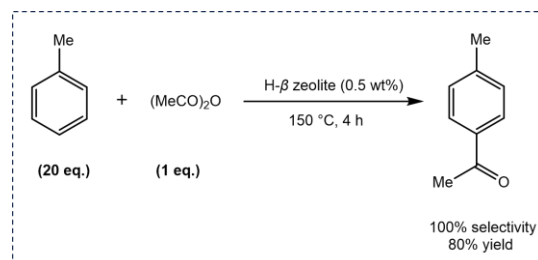
In addition to the application of zeolites in cracking, they also show great potential in converting renewable bio-based materials into valuable chemicals. Hierarchical zeolites have exhibited remarkable performance in catalytic fast pyrolysis (CFP) of biomass due to their high thermal/hydrothermal stability. For instance, zeolites have been gradually used for the CFP of lignocellulosic biomass to produce various precursors of transportation fuels such as aromatic hydrocarbons and olefins.¹⁵⁹ CFP using ZSM-5 zeolite as a catalyst produces BTX (benzene, toluene, xylene) and naphthalene, which are known as building blocks for the chemical industry.¹⁶⁰

2.3.2. The applications of zeolites in organic synthesis

2.3.2.1. Acidic zeolites in organic synthesis

Zeolites bearing a proton as a charge-compensating cation (H-zeolites) are frequently used as protic acidic zeolites. These protons are mostly linked to the oxygen atom in the zeolite framework. Therefore, they are used as strong acids since they have at least the same acidity as protonated ethers or alcohols ($-5 < \text{pK}_a < -10$), and can even behave as superacids. Due to their inherent safe and reusable properties, these zeolites have replaced traditional liquid mineral acids in some transformations, leading to more sustainable and eco-friendly chemical processes, while minimizing waste production. Furthermore, the low price and the possibility of regenerating their activity by re-calcination decrease the production cost in specific industry processes. Hence, such zeolites have been widely used as recoverable heterogeneous stoichiometric reagents or catalysts in various organic transformations. Apart from the famous Friedel-Crafts reactions detailed by Giovanni *et al.* (**Scheme 8**),³³ another well-known application of H-zeolites is in protecting groups chemistry. Additionally, they are also highly

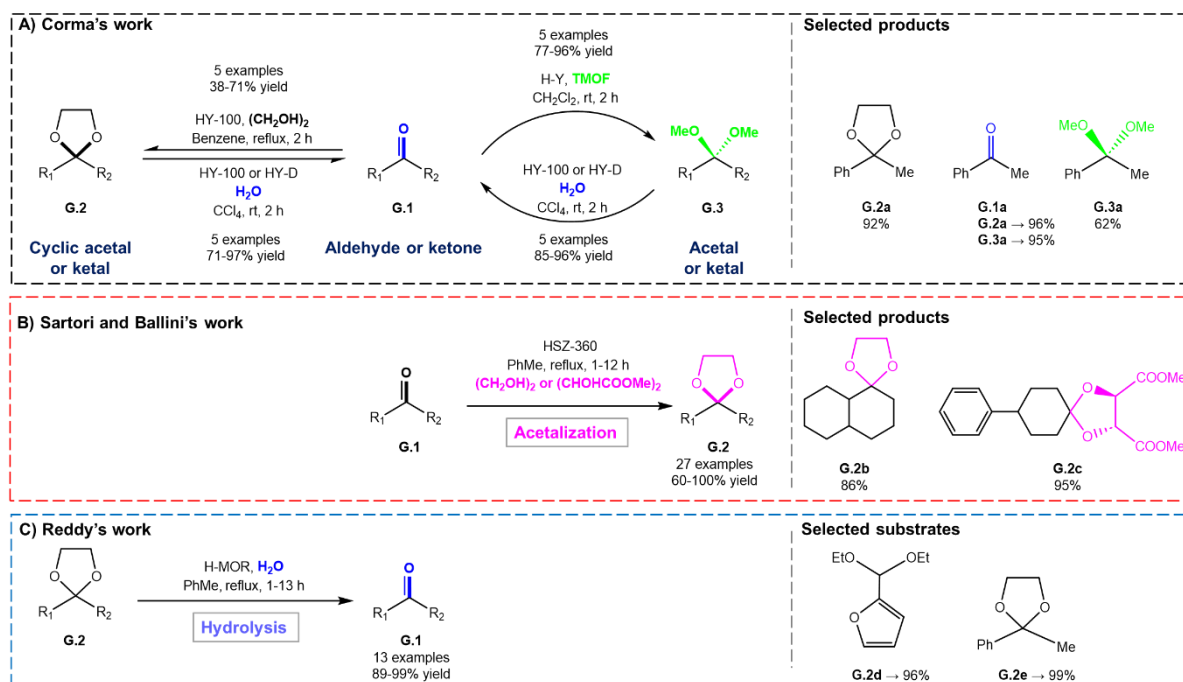
efficient in carbonylation reactions. The following section will briefly overview examples of acidic zeolites in the (de)protections of common functional groups. An atom-economical carbonylation reaction catalyzed by acidic zeolite will also be presented.



Scheme 8. An example of H- β zeolite-promoted Friedel–Crafts acylation reaction.^{33,161}

2.3.2.1.1. Acidic zeolites in protecting groups chemistry

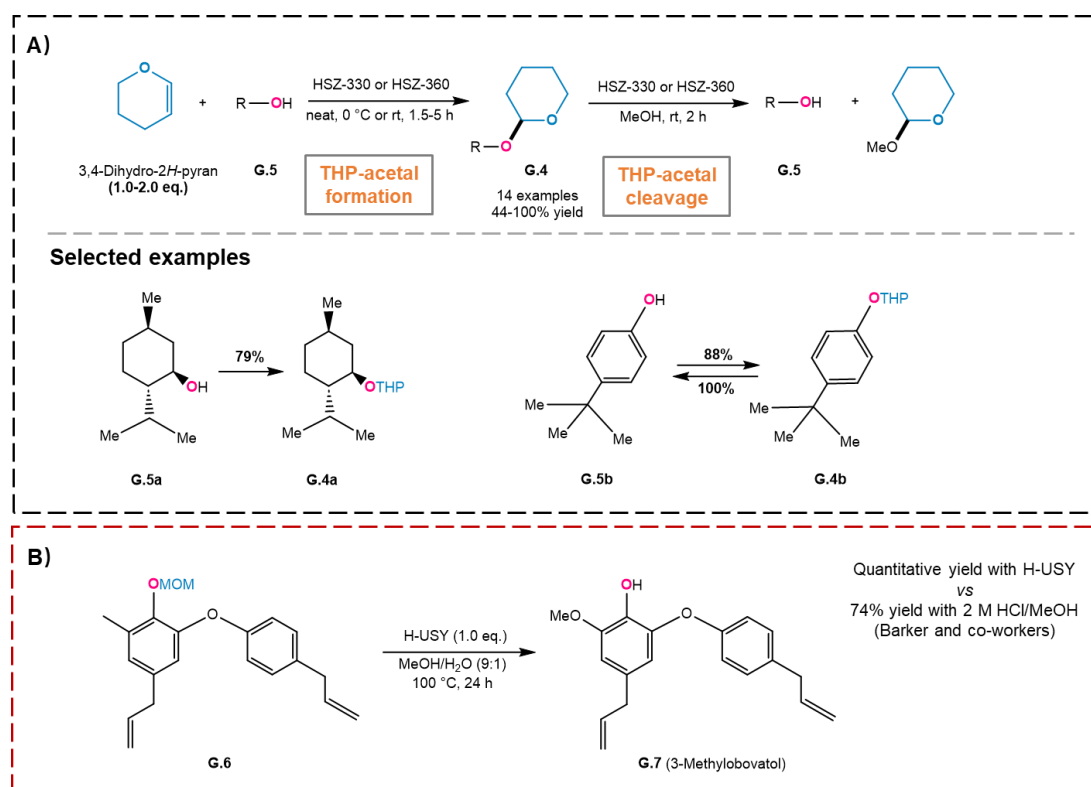
The carbonyl group is a common functional group, which sometimes requires protection during a synthetic sequence. H-zeolites have shown excellent performance in protecting and deprotecting various carbonyl-derived functional groups. For instance, Corma *et al.*¹⁶² successfully used several H-zeolites for the acetalization of various carbonyl compounds (aldehydes or ketones) (e.g. **G.1a** \rightarrow **G.2a** and **G.1a** \rightarrow **G.3a**) and for the hydrolytic cleavage of the corresponding acetals or ketals with excellent yields (e.g. **G.2a** \rightarrow **G.1a** and **G.3a** \rightarrow **G.1a**) (**Scheme 9A**). They found that H-Y zeolites were the most efficient catalysts to promote the formation and hydrolysis of different dimethyl and cyclic ethylene acetals or ketals in the presence of trimethyl orthoformate (TMOF) or 1,2-ethanediol ((CH₂OH)₂).¹⁶² However, the latter was less efficient than the former in yield reactions. Another reported H-Y zeolite, HSZ-360 from Tosoh Corporation, could efficiently form the cyclic ketals from the corresponding carbonyl derivatives with 1,2-ethanediol (e.g. \rightarrow **G.2b**).¹⁶³ Interestingly, *R,R*-dimethyltartrate ((CHOHCOOMe)₂) could also be used to synthesize chiral acetals in a reaction catalyzed by HSZ-360 (e.g. \rightarrow **G.2c**). Under the same conditions, high yields were obtained (60-100%) (**Scheme 9B**). The zeolite could be regenerated and reused at least five times in these reactions. In addition, Reddy *et al.*¹⁶⁴ found that H-MOR could hydrolyze various acetals and ketals to the corresponding aldehydes or ketones with excellent yields, from 89% to 99% (**Scheme 9C**).



Scheme 9. The formation and hydrolysis of acetals or ketals with protic zeolites.¹⁶²⁻¹⁶⁴

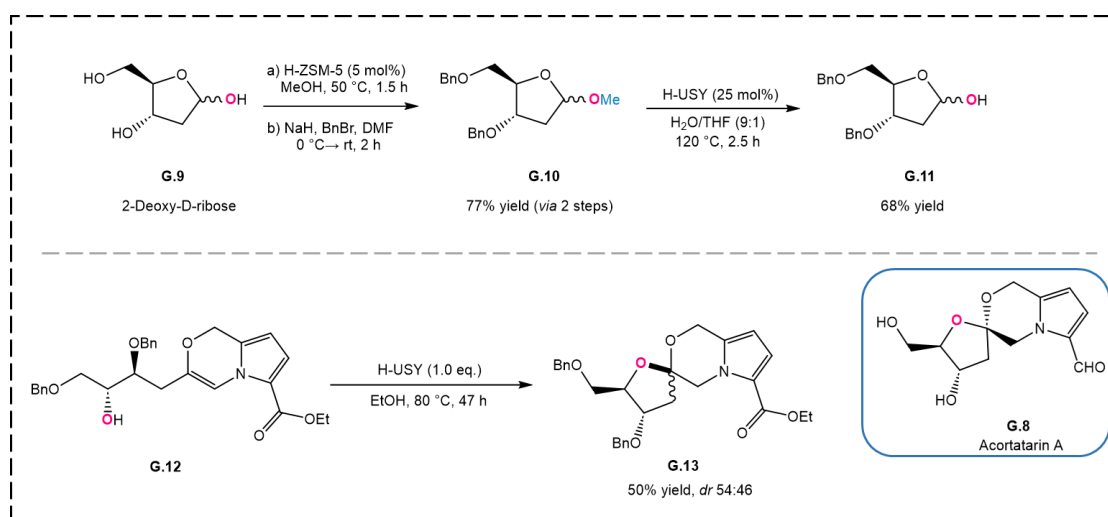
Furthermore, acidic zeolites are also commonly applied to protect hydroxy groups, another essential function group encountered in most organic compounds. Many protecting groups have emerged to selectively protect the hydroxy functions temporarily or for long-term. For instance, a well-known method to protect the hydroxy groups of alcohols and phenols is converting them to their corresponding ethers or acetals/ketals. Tetrahydropyranyl (THP) acetal is one of the most helpful protective groups due to its stability and low cost. Several acidic-zeolites like H-beta¹⁶⁵, HSZ-330, or HSZ-360¹⁶⁶ have proved to be efficient catalysts for the formation or cleavage of THP acetals **G.4** from/to alcohols **G.5** (**Scheme 10**). The mild conditions without solvent disclosed by Ballini and coworkers¹⁶⁶ were highly attractive.

Similarly, Chassaing and co-workers⁴⁰ published a highly chemoselective deprotection of methoxymethyl (MOM) acetal (in **G.6**) with stoichiometric amounts of H-USY in the final step of the synthesis of the natural product (**G.7**), *i.e.*, 3-methylbovatol (**Scheme 10**). Compared to the known method¹⁶⁷ using 2 M HCl in MeOH, which led to the corresponding phenol with a 74% yield, this procedure significantly improved the yield of the product **G.7** (quantitative yield) and simplified the process since the solid acid (H-USY) could be easily removed by filtration after the reaction without further treatment.



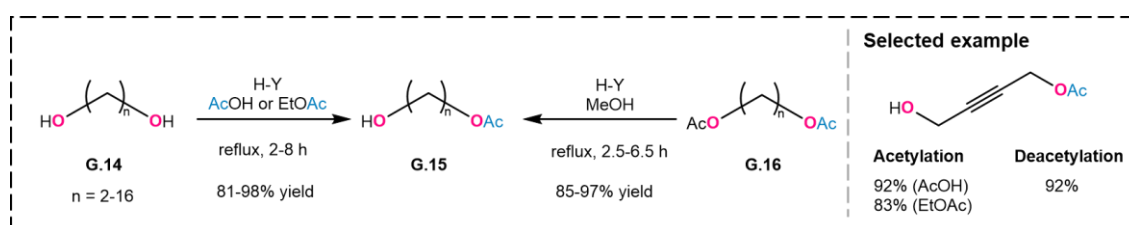
Scheme 10. A) Formation and cleavage of THP acetals with protic zeolites¹⁶⁶; B) H-USY-mediated MOM deprotection for 3-methylobovitol synthesis⁴⁰.

Furthermore, our research group¹⁶⁸ performed the total synthesis of acortatarin A (**G.8**) using acidic-zeolites in different (de-)protection steps. As shown in **Scheme 11**, H-ZSM-5 catalyzed the complete transformation of 2-deoxy-D-ribose (**G.9**) to the corresponding methyl acetal (**G.10**) in MeOH under anhydrous conditions. When the remaining hydroxyl groups were benzylated, H-USY selectively catalyzed the hydrolysis of **G.10** at the anomeric position to produce **G.11**. Also, a stoichiometric amount of H-USY was subsequently used in the spiroketalization of the enamine **G.12** to form **G.13**, which was the key intermediate for the synthesis of target **G.8**.



Scheme 11. The multi-step synthesis of acortatarin A with the help of protic zeolites.¹⁶⁸

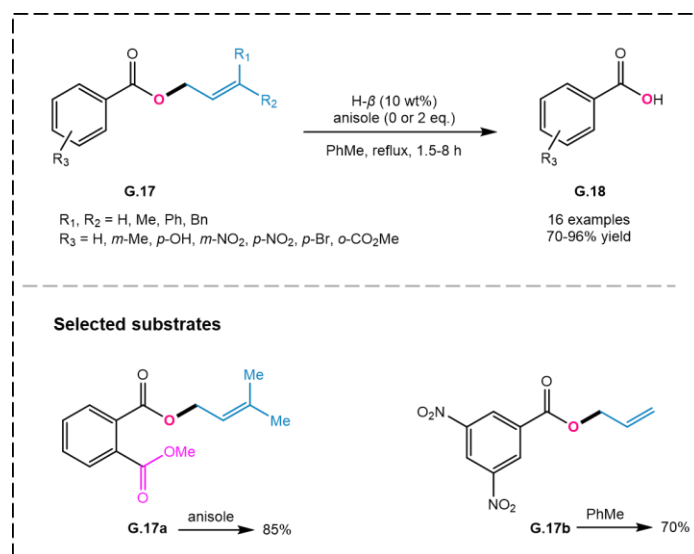
Acetylation is another valuable method to protect the hydroxy group. Das *et al.*¹⁶⁹ reported that H-Y zeolite could selectively catalyze the monoacetylation of symmetric diols **G.14** to **G.15**, and the monoacetylation of symmetric diacetates **G.16** in MeOH (**Scheme 12**). They used acetic acid (AcOH) or the more environmentally friendly ethyl acetate (EtOAc) as the acetylating agents instead of the frequently used acetic anhydride, leading to a greener procedure, which has been applied to a variety of saturated and unsaturated diols **G.14** as well as diacetates **G.16**. It was worth noting that the zeolite could be reused at least three times.



Scheme 12. Protic zeolite-catalyzed monoacetylation of alcohols and monodeacetylation of diacetates.^{169,170}

Protic zeolite-catalyzed cleavage of acetates is not the only method for deprotection of hydroxyl groups. Allylic esters are also considered excellent protecting groups due to their easy preparation and high stability under diverse reaction conditions. Kumar and co-workers¹⁷¹ reported the highly selective H- β zeolite-catalyzed deprotection of allyl (-like) ester **G.17** for the preparation of the corresponding aromatic carboxylic acids **G.18** with excellent yields (**Scheme 13**). Various substituted aromatic allyl esters, including prenyl, allyl, cinnamyl, and benzyl esters, were successfully deprotected, while the allyl esters derived from aliphatic acids were unreactive. Furthermore, these reactions have to be performed under anhydrous conditions

with toluene acting as the nucleophile. In some cases, more electron-rich anisole was also required to facilitate the reactions. The zeolite could be reused without losing activity.



Scheme 13. H- β -mediated selective deprotection of allylic and benzylic esters.¹⁷¹

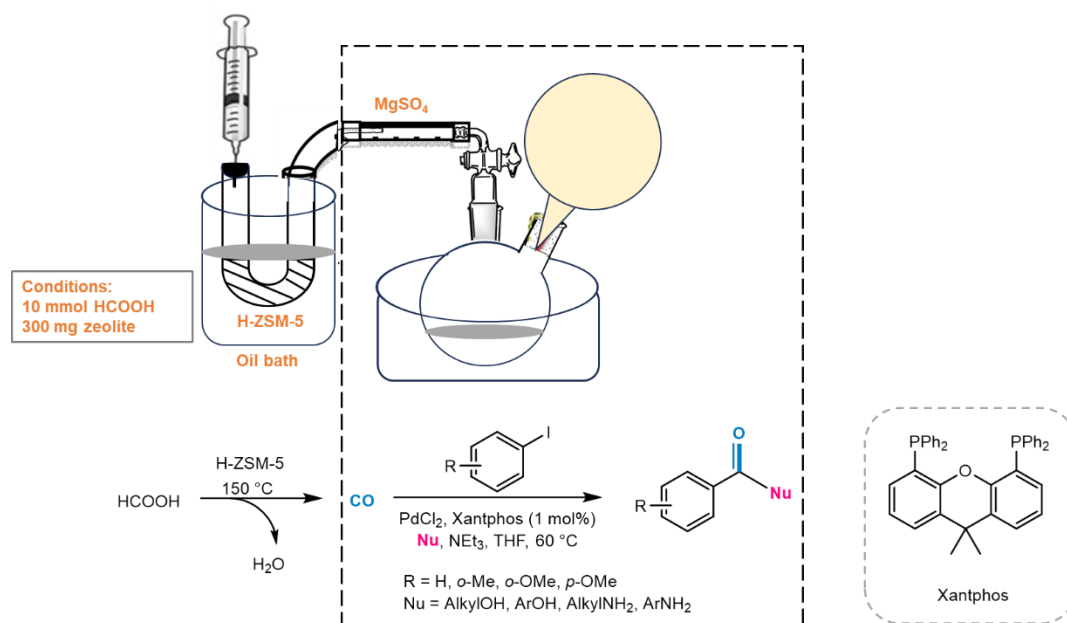
Overall, there are two noteworthy advantages of all these procedures. Firstly, the zeolites used in the above reactions are commercially available, thereby saving time in catalyst preparation. Secondly, most zeolites could be reused at least 2 or 3 times without losing activity and provided consistent excellent yields. However, zeolites should be activated *via* calcination and stored under anhydrous conditions before use since the amount of adsorbed water dramatically influences the zeolite activities. Hence, a relatively short calcination procedure is also essential to restore the zeolite reactivity before reusing the recovered materials.

2.3.2.1.2. Acidic zeolites in carbonylation reactions

One of the most atom-economical methods to produce carbonyl derivatives is the carbonylation reaction, which is also an important industrial reaction with the hydroformylation process to synthesize aldehydes on a scale of millions of tons per year.³⁶ However, performing this reaction on a laboratory scale remains challenging due to the difficulty of handling toxic and unsafe gases, *i.e.*, carbon monoxide. To solve these problems, a variety of precursors have been explored for the generation of CO *in situ*. Unfortunately, some metal carbonyl precursors (such as HCo(CO)₄ and Co₂(CO)₈) were more toxic than CO, while others needed to be catalyzed by metal complexes (Pd or Rh) in more complex processes.

Recently, acidic zeolites have established a facile alternative (**Scheme 14**) in the so-called Morgan reaction¹⁷², in which the formic acid was decomposed to CO and water at high

temperatures in the presence of sulfuric acid. H-ZSM-5 was proved to be the most efficient catalyst to promote the release of CO from formic acid at 150 °C. A simple and inexpensive apparatus was designed to generate CO *in situ* and directly transfer it to a flask for palladium-catalyzed coupling reactions, thus providing an efficient and economical approach to synthesize esters and amides. Moreover, the zeolite could be reused without losing activity.



Scheme 14. Green and safe carbonylation reactions *via* H-zeolite-catalyzed CO production from formic acid.¹⁷²

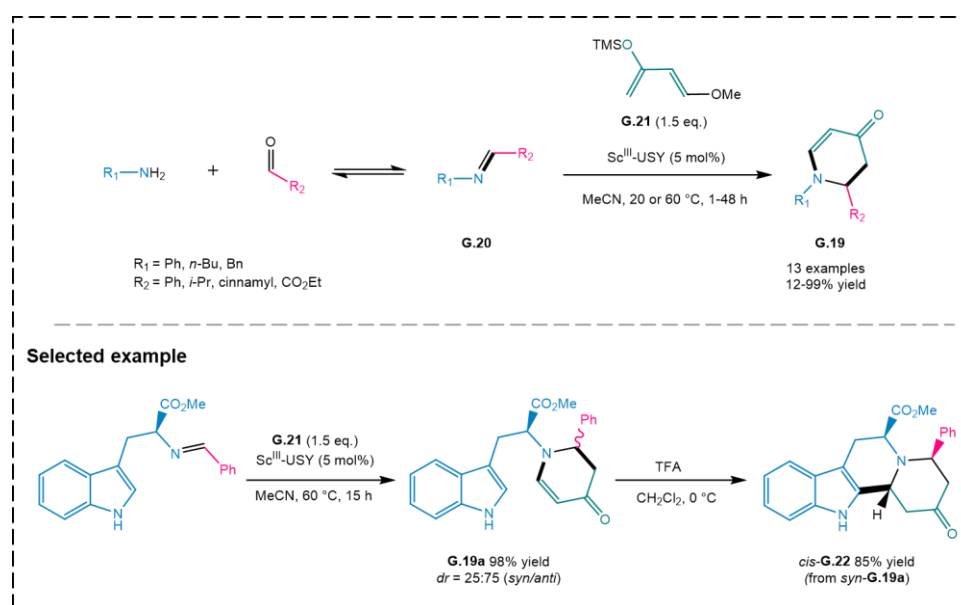
2.3.2.2. Metal-doped zeolites in organic synthesis

Initially, metal-doped zeolites were commonly applied in industrial applications to produce liquid long-chain hydrocarbons from syngas (a mixture of CO and H₂) *via* the Fischer-Tropsch process or the selective catalytic reduction (SCR), *i.e.*, converting NO_x into N₂ and H₂O. These catalysts are usually made of specific metals such as Fe, Co, and Cu.¹⁶⁰ Co^{II}-doped zeolites are also recognized as efficient catalysts for the oxidation of alkenes, such as styrene and α -pinene.¹⁷³ Among the metal-doped zeolites applied in organic synthesis, copper species-loaded zeolites are the most frequently used due to their abundant resources, low cost, and easy preparation. This section will primarily emphasize the application of copper-doped zeolites in organic synthesis since it is the core of this thesis. Several examples of zeolite catalysts doped with other (transition) metals (such as Sc, Fe, Ag, Au and Pd) will also be presented. The catalysts' properties and potential applications as recyclable heterogeneous catalysts will be discussed.

2.3.2.2.1. Scandium-doped zeolites

As the first d-block metal ([Ar] 3d¹ 4s²), scandium (Sc) has been used in several organic transformations due to its Lewis acid properties. Sc^{III} salts are relatively expensive because of the scarcity of scandium resources on Earth. Therefore, exploiting heterogenized scandium catalysts is highly desirable from economic and ecological perspectives. Within this context, our group¹⁷⁴ synthesized a Sc^{III}-USY from H-USY and Sc(OTf)₃ by SSIE technique at 450 °C. The zeolite successfully catalyzed a Mukaiyama aldol condensation¹⁷⁵ and two hetero-Diels-Alder-reactions^{176,177}.

An aza-Diels-Alder-reaction was catalyzed by Sc^{III}-zeolites to produce piperidinones **G.19**, in which imines **G.20** acted as aza-dienophiles to react with the electron-rich Danishefsky diene **G.21** (Scheme 15).¹⁷⁷ This approach allows the generation of imines *in situ*, providing a more convenient and efficient domino reaction route to synthesize piperidinones **G.19** but at the expense of reduced product yields. Beneficially, the heterogeneous version reaction has been extended to optically pure aromatic amino acids to synthesize the analogs of natural alkaloids containing piperidinone moieties, e.g., **G.22**. Rewardingly, this Sc-zeolite could be reused ten times with consistently high product yields.

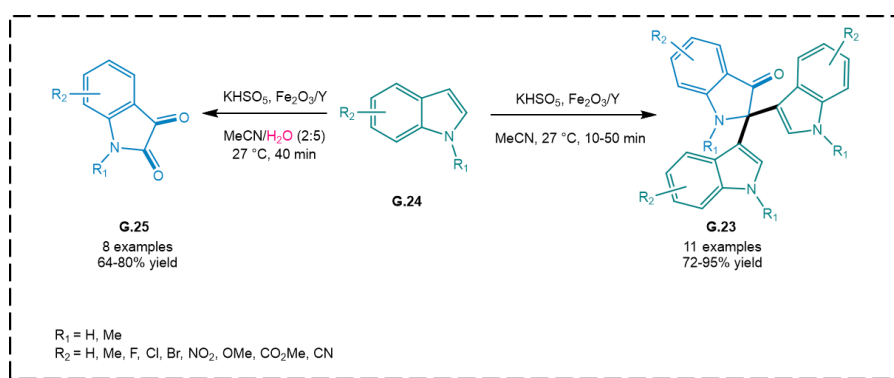


Scheme 15. Sc^{III}-USY-catalyzed aza-Diels-Alder reaction to piperidinones.¹⁷⁷

2.3.2.2.2. Iron-doped zeolites

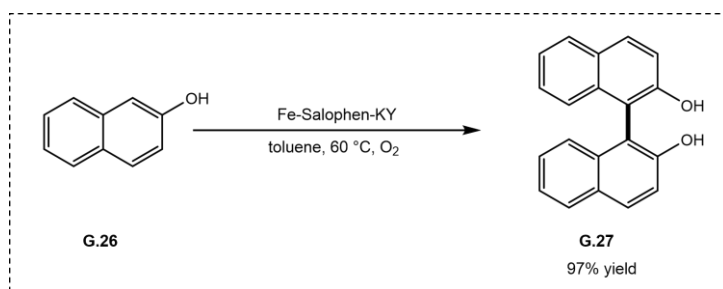
A cheap and recyclable iron(III) oxide nanocatalyst supported on Y-zeolite successfully catalyzed the synthesis of C2 di-indolyl indolones **G.23** under mild conditions (Scheme 16).¹⁷⁸ The catalyst was synthesized *via* precipitation on the Y-zeolite surface in basic Fe(NO₃)₃·9H₂O

solution (pH = 8~9). Subsequently, Fe₂O₃ nanoparticles (average 2.36 nm) were formed on the Y-zeolite surface after heating the washed zeolite precursor at 327 °C for 12 h. C2-selective trimerization reactions of various indoles **G.24** synthesized the products **G.23** in yields ranging from 72% to 95% in less than one hour (10-50 min). Screening of various aluminosilicate supports showed that materials with a lower Si/Al ratio afforded higher yields of the C2 trimerized products **G.23**. Notably, the catalyst could be separated and reused at least five times without loss of activity when re-calcinated after each run. The significant decrease in product yield at the sixth run might be caused by the sharp reduction in the specific surface area of the zeolite (about 70 m²·g⁻¹). Furthermore, indoles **G.24** were selectively oxidated into isatins **G.25** at room temperature in a short reaction time by adjusting the ratio of H₂O and oxidant.



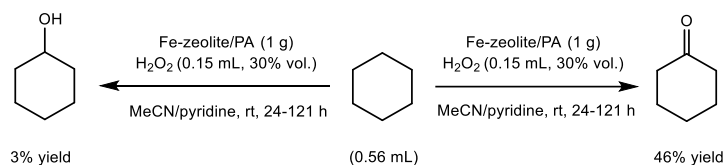
Scheme 16. Synthesis of C2 di-indolyl indolones **G.23 and isatins **G.25** from indoles **G.24**.**¹⁷⁸

Deka and co-workers¹⁷⁹ prepared several Fe(III)-Schiff-base-complexes-doped zeolites for the oxidative coupling of 2-naphthol (**G.26**) to directly synthesize 1,1'-binaphthol (BINOL) (**G.27**). These catalysts were prepared *via* a flexible ligand method, in which prepared Fe(III)-exchanged zeolites (Fe-LiY, Fe-NaY, and Fe-KY) were treated with stoichiometric excess ligands (*N,N'*-bis(salicylidene)ethylenediamine (Salen) or *N,N'*-disalicylidene-1,2-phenylenediamine (Salophen)) at 250-270 °C for 48 h under constant stirring. After filtering, washing and drying, the resultant products were further purified by Soxhlet extraction to remove all unreacted species or species on the surface of the zeolite. These encapsulated catalysts successfully promoted the highly selective conversion of β -naphthol to BINOL under aerobic conditions in toluene at 60 °C in the absence of any additive. Fe-Salophen-KY provided excellent conversion and yield of the expected product (**G.27**) among all the complex catalysts (**Scheme 17**).



Scheme 17. Fe-Salophen-KY-catalyzed oxidative coupling of 2-naphthol.¹⁷⁹

Garcia and co-workers¹⁴⁸ successfully encapsulated Fe^{III}-picolinate (Fe-PA) complex into a series of zeolites (zeolite Y and mordenite) for the Gif oxidation of cyclohexane (**Scheme 18**). The zeolite ship-in-a-bottle complexes were synthesized by treating pre-exchanged Fe(III)-zeolites with picolinic acid in dichloromethane. The formation of the Fe-PA complex was demonstrated by diffuse-reflectance UV-vis, FT-IR and luminescence spectroscopies. These solids were found to be efficient and reusable heterogeneous catalysts for the oxidation of cyclohexane with H₂O₂ in a mixture solvent of MeCN and pyridine. Compared to the corresponding Fe(III) complex-catalyzed the same process¹⁸⁰, these zeolites containing encapsulated Fe^{III}-picolinate complex provided a similar selectivity and much higher conversion. In all reactions, cyclohexanol and cyclohexanone were the only products observed, and the latter was always the major product. Mordenite was found to be the best host for this purpose.

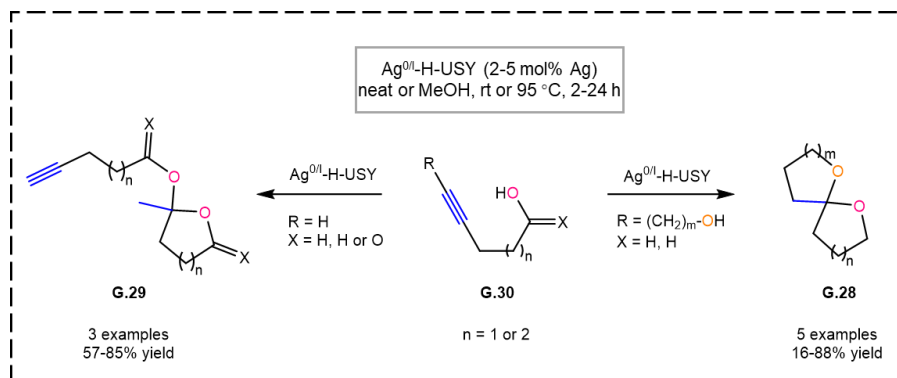


Scheme 18. zeolites containing encapsulated Fe^{III}-picolinate complex-catalyzed the Gif oxidation of cyclohexane.¹⁴⁸

2.3.2.2.3. Silver-doped zeolites

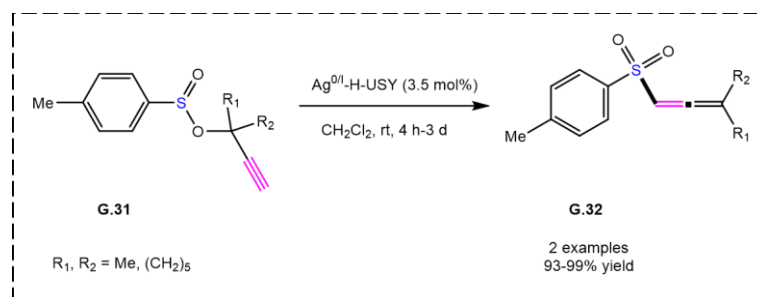
Pale and co-workers¹⁸¹ synthesized a bifunctional Ag^{0/1}-H-USY zeolite *via* AIE reaction for the intramolecular spiroketalisation (\rightarrow **G.28**) and intermolecular ketalisation (\rightarrow **G.29**) of the alkyne(di)ols **G.30** (**Scheme 19**). The spiroketal moiety is extensively present as an important structure scaffold in many natural products and bioactive molecules.¹⁸² Many noble transition metals have been applied to synthesize this reaction under homogeneous conditions, such as Pd¹⁸³, Ir¹⁸⁴, Rh^{185,186}, Hg¹⁸⁷, and Au¹⁸⁸⁻¹⁹⁰. This study developed the first Ag^I-based

heterogeneous version to achieve this transformation. Beneficially, this novel approach was performed without solvent or in MeOH under milder conditions. The catalyst with low silver loadings (2-5 mol%) could be reused at least five times after reactivation (calcination) between each run, affording comparable high product yields for each run.



Scheme 19. $\text{Ag}^{0/\text{I}}$ -H-USY-catalyzed (spiro)ketalisation of alkyne(di)ols **G.30**.¹⁸¹

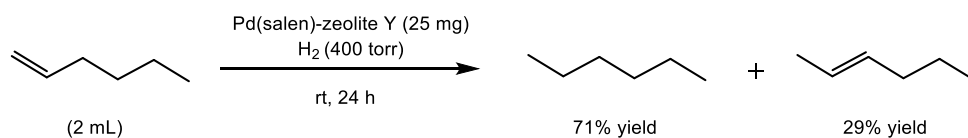
In addition, Hampton and Harmata successfully used the same $\text{Ag}^{0/\text{I}}$ -H-USY zeolite for catalyzing the [2,3]-sigmatropic rearrangement of propargylic sulfinates **G.31** to allenic sulfones **G.32** (Scheme 20).¹⁹¹ Compared to their previously reported homogeneous conditions¹⁹², the zeolite only provided similar reaction outcomes at the expense of a longer reaction time and higher silver loadings (3.5 mol% vs 2.0 mol%). Furthermore, the zeolite in this reaction could be reused up to three times without any decrease in efficiency.



Scheme 20. [2,3]-sigmatropic rearrangement of propargyl sulphinates **G.31** for the synthesis of allenic sulphones **G.32**.¹⁹¹

2.3.2.2.4. Gold-doped zeolites

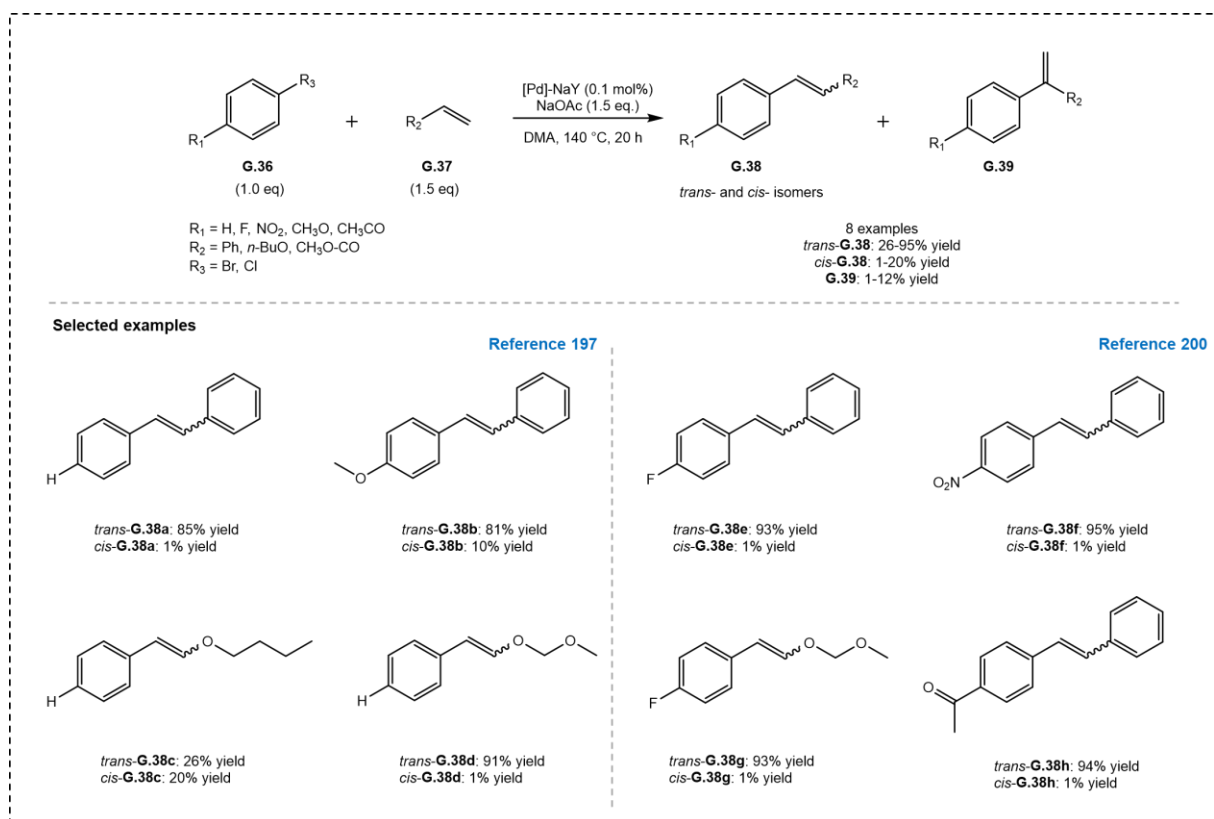
Dharmaraj and co-workers¹⁹³ synthesized *N*-arylated indazoles (**G.34** and **G.35**) from 1*H*-indazole (**G.33**) with diverse aryl halides *via* a gold-modified Y zeolite-catalyzed *N*-arylation reaction (Au-zeolites) in 2016 (Scheme 21). Such *N*-aryl-indazoles are found in a variety of natural products and exhibit prominent medicinal properties.¹⁹⁴ However, the direct arylation of **G.33** towards these products (**G.34** and **G.35**) is still challenging since this transformation



Scheme 22. zeolites containing encapsulated Pd(salen) complex-catalyzed the hydrogenation of hex-1-ene.¹⁹⁶

Heck coupling reactions

In 1999, Djakovitch and co-workers¹⁹⁷ first published the heterogeneous Heck reaction of aryl halides (**G.36**) with olefins (**G.37**) with palladium-doped zeolites in order to synthesize styrene derivatives (**G.38**) (**Scheme 23**). Four types of Pd-complexes ($[\text{Pd}(\text{NH}_3)_4]^{2+}$, $\text{Pd}(\text{OAc})_2$, $[\text{Pd}(\text{C}_3\text{H}_5)\text{Cl}]_2$ and palladacycle) were immobilized in the NaY zeolite *via* a reported AIE process^{198,199}, in which the corresponding palladium salt solution was added dropwise to a suspension of NaY zeolite in THF, the mixture was then stirred at room temperature for defined times. These heterogeneous catalysts (except for the palladacycle-doped zeolite) were successfully applied to the reaction of aryl bromide and styrene with NaOAc as the base and dimethylacetamide (DMA) as the solvent at different temperatures (100 °C or 140 °C), providing comparable yields and selectivity compared to those obtained with the corresponding Pd-complex in bulk solution respectively (58-95% yields for *trans*-isomer). In particular, $[\text{Pd}(\text{NH}_3)_4]^{2+}$ complex-doped zeolite (0.1 mol% Pd) proved to be the best catalyst, providing *ca.* 93% yield of the *trans*-isomer product and traces of the *cis*-isomer as well as 7% side-product (**G.39**). A series of aryl halides and olefins were screened with the optimized catalyst (0.1 mol%) at 140 °C for 20 h, producing the expected *trans*-isomer yields in 26-95% (**Scheme 23, with examples bottom left**). Recyclability studies of these materials indicated that the reaction temperature had a significant impact on the activities of catalysts, as these Pd-doped zeolites directly reused at 140 °C still provided comparable yields to those of the first run, while a markedly decrease in yield was observed when catalysts were reused at 100 °C. Interestingly, catalysts inactivated at 100 °C could be regenerated at 140 °C for 1 h in air under the reaction conditions. Sheldon test indicated that no significant leaching was observed for the Pd-complex-loaded zeolites (except for the $[\text{Pd}(\text{C}_3\text{H}_5)\text{Cl}]_2$ -loaded NaY used at 140 °C).

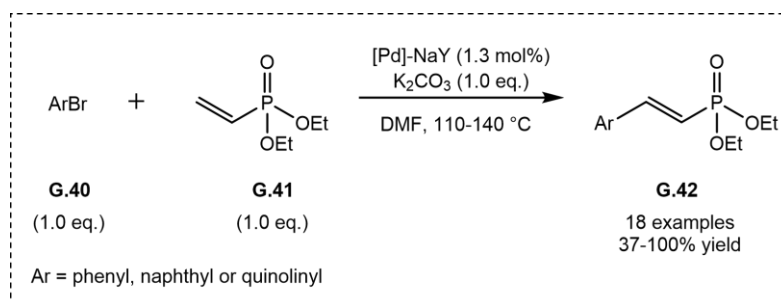


Scheme 23. Pd-loaded NaY-catalyzed Heck reaction.^{197,200}

Shortly after, Djakovitch's group²⁰⁰ further studied the influence of preparation and treatment of the catalysts, and the catalytic performances of several Pd-exchanged zeolites with different dispersion (Pd particles, ionic species Pd(II) and $[\text{Pd}(\text{NH}_3)_4]^{2+}$, and neutral complexes $\text{Pd}(\text{OAc})_2$ and $[\text{Pd}(\text{C}_3\text{H}_5)\text{Cl}]_2$) in Heck reactions (**Scheme 23, with examples bottom right**). These catalysts were prepared by a similar AIE reaction as mentioned above^{198,199}, but a calcination at 500 °C in O_2 atmosphere of the exchanged $[\text{Pd}(\text{NH}_3)_4]^{2+}$ zeolite was required to give the $[\text{Pd}(\text{II})]\text{-NaY}$ zeolite, and subsequent treatment at 350 °C with flow H_2 gas was needed to provide $[\text{Pd}(0)]\text{-NaY}$. $[\text{Pd}(0)]\text{-}$ and $[\text{Pd}(\text{II})]\text{-NaY}$ were recognized as the models in low Pd dispersion, exhibiting comparable activities to the fresh catalysts. Both catalysts could be reused up to five times, and only slightly decrease in yields were observed for each run (< 5%). Generally, the zeolites modified by ionic Pd species gave higher activities in the reaction of aryl bromide and olefins, and $[\text{Pd}(\text{NH}_3)_4]^{2+}\text{-NaY}$ again proved to be the best catalyst, providing 95% yields of the *trans*-isomer product (**G.38**). The kinetic studies indicated that Pd(0) species were the active species as they are for the homogeneous systems. The protocol was successfully extended to cyclic alkenes, producing 60% yields of the desired product (**G.38**). Compared with other Pd-loaded support materials (MgO , TiO_2 , SiO_2 , ZnO , Al_2O_3 , ZrO_2 , C, mordenite and zeolite Y), the Pd-doped zeolites (mordenite or Y-type) exhibited the highest activities in the

model reaction of bromobenzene (1.0 equiv.) with styrene (1.5 equiv.) under the same conditions (in DMA at 140 °C for 20 h), providing excellent conversions (83-100%) and yields (72-85%).²⁰¹ In particular, $[\text{Pd}(\text{NH}_3)_4]^{2+}\text{-NaY}$ afforded full conversion and the highest yield. Interestingly, the Pd loading (4-7 wt.%), the zeolite structure (mordenite or Y-type) and the zeolite counter ion (H- or Na-form) had a minor influence on the conversion and selectivity in the investigated Heck model reactions²⁰².

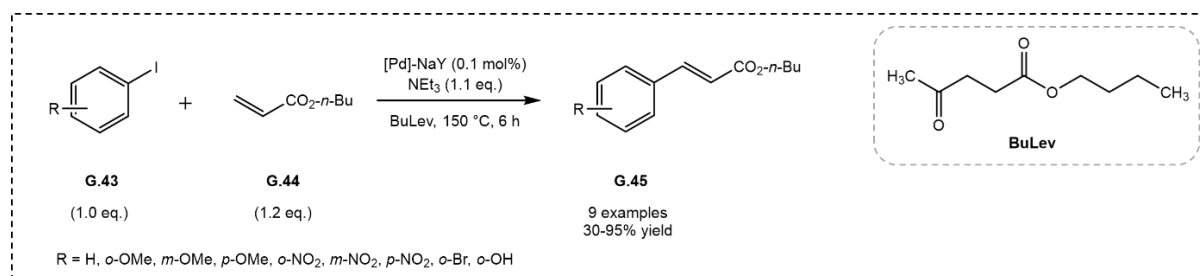
In 2010, the $[\text{Pd}(\text{NH}_3)_4]^{2+}\text{-NaY}$ -catalyzed Heck reaction was successfully applied to the synthesis of diethyl 2-arylvinylphosphonate **G.42** (**Scheme 24**)²⁰³, which is a significant starting material for synthesizing pharmaceutically relevant molecules, such as anticancer, antiviral drugs, insecticides and antibacterial, etc²⁰⁴. Various aryl and heteroaryl halides (**G.40**) were engaged in this reaction under the optimal conditions ($[\text{Pd}]/\text{NaY}$ (1.3 mmol%) in DMF at 110-140 °C in the presence of K_2CO_3), resulting in most cases in high yields (80-100%). Recyclability studies of this catalyst were performed with the coupling reaction of 2-bromonaphthalene and diethylvinylphosphonate (**G.41**). When the reaction proceeded in DMF, the catalyst could not be reused while it could be reused for three times when *N*-methyl-2-pyrrolidone (NMP) was the solvent with a progressive decrease in yields (from 100% to 20%). Sheldon test (by hot filtration) indicated that active palladium species were dissolved into the solvent during the reaction, as an increase in yield was observed after removing the catalyst (from 20% to 60%).



Scheme 24. Heterogeneous Heck arylation of the diethyl vinylphosphonate by various aryl and heteroaryl bromides.²⁰³

More recently, Djakovitch and co-workers²⁰⁵ first used bio-sourced alkyl levulinates as the solvents for the $[\text{Pd}(\text{NH}_3)_4]^{2+}\text{-NaY}$ -catalyzed Heck reactions of aryl halides (**G.43**) and *n*-butyl acrylate (**G.44**), providing an environmental and green method for the synthesis of various fine chemicals (e.g. → **G.45**) (**Scheme 25**). Pd@NaY (0.1 mol% Pd) with Et_3N as the base and *n*-butyl levulinate (BuLev) as the solvent at 150 °C proved to be the optimal conditions, affording quantitative conversions of aryl halides in short reaction time (6 h), and good to high isolated

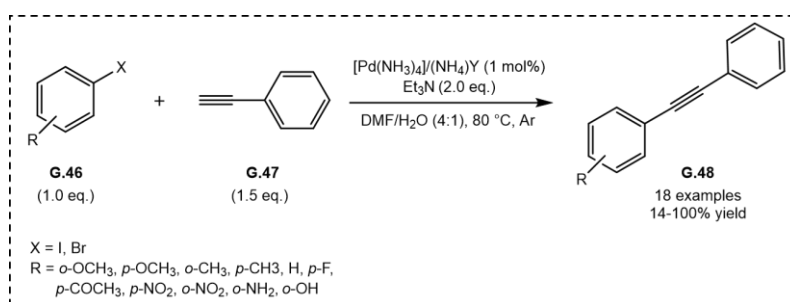
yields of the product (30-95%) in most cases (**Scheme 25**). Furthermore, the solvent could be recovered by simple distillation and reused in the same reaction, providing a comparable conversion (*ca.* 85%). The catalyst could be reused for three times with a progressive decrease in conversion (from 85% to 60%). The Sheldon test indicated that the reaction was due to the leached Pd species. XPS analyses showed that less active Pd-aggregates^{206,207} were formed by the reduction of Pd species during the reaction, which could explain the limited reusability of this catalyst.



Scheme 25. Heck coupling in BuLev with the help of Pd@NaY.²⁰⁵

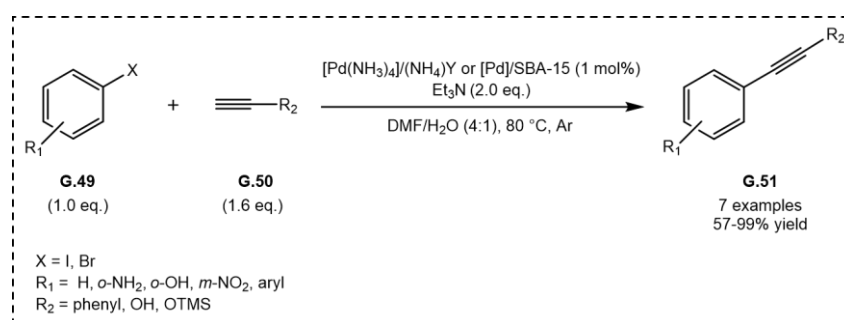
Sonogashira coupling reactions

In 2004, Djakovitch's group^{208,209} developed a new Pd-loaded zeolite catalyst for the Sonogashira coupling reaction of aryl halides (**G.46**) with phenylacetylene (**G.47**) (**Scheme 26**). 1 mol% [Pd(NH₃)₄](NH₄)Y in a mixture of solvents (DMF/H₂O (4:1)) at 80 °C under argon proved to be the best conditions. Copper which was regarded as a necessary cocatalyst for the standard Sonogashira coupling reactions²¹⁰, did not improve the reactivity of the reactions under current reaction conditions, but significantly deactivated the Pd-doped zeolite catalyst. The catalyst was prepared *via* an AIE process in which an ammonia solution of [Pd(NH₃)₄]Cl₂ was exchanged with a suspension of the zeolite (NH₄)Y in bidistilled water at room temperature for 24 h. A series of substituted aryl bromides and iodides (**G.46**) were screened under the optimal conditions, providing the corresponding products (**G.48**) in 14-100% yields. The catalyst could be reused five times and only a decrease in yield was observed after the first run (from 100% to 87% for the coupling of *para*-iodoanisole with phenylacetylene (**G.47**), the yield remained then stable over the 5th run and high product yields (*ca.* 87%) could be obtained. A Sheldon test indicated that the catalyst exhibited an excellent stability towards leaching, as the clear filtrate obtained was little active. Furthermore, the determination of palladium content was performed in most cases using atomic absorption spectroscopy (AAS) and showed that only tiny amount of palladium species leached in the solution (<10 ppm), which could be negligible.



Scheme 26. Pd-doped zeolite-catalyzed Sonogashira coupling reaction with phenylacetylene as terminal alkyne.^{208,209}

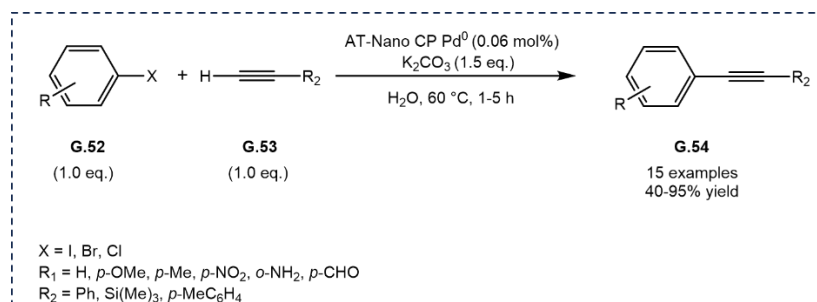
The next year, Djakovitch's group²¹¹ compared the catalytic performance of microporous $[\text{Pd}(\text{NH}_3)_4]^{2+}/\text{NaY}$ and mesoporous materials ($[\text{Pd}]/\text{SBA-15}$) in the Sonogashira coupling reaction of aryl halides (**G.49**) with **G.50** (Scheme 27). Generally, these catalysts all exhibited high activity and selectivity in several Sonogashira coupling reactions of aryl halides with acetylenes, resulting in complete conversion and good yields of various target organic molecules (**G.51**) (57-99% yield) within short reaction times (3–6 h). However, when using large aryl halides such as 2-bromonaphthalene and 9-bromoanthracene as the starting materials, the $[\text{Pd}(\text{NH}_3)_4]^{2+}/\text{NaY}$ was inactive due to the relatively small apertures of zeolite ($\phi = 7.4 \text{ \AA}$).



Scheme 27. Sonogashira coupling reaction catalyzed by $[\text{Pd}(\text{NH}_3)_4]^{2+}/\text{NaY}$ or $[\text{Pd}]/\text{SBA-15}$ applied to the synthesis of target organic molecules.²¹¹

In 2014, a novel palladium nanoparticles-doped zeolite was synthesized by Baghbanian and co-workers²¹² for Sonogashira coupling reactions of aryl halides (**G.52**) with terminal alkynes (**G.53**) (Scheme 28). The catalyst $[\text{Pd}(0)@\text{AT-Nano CP}]$ was prepared in three steps. First, the commercial nanozeolite clinoptilolite (Nano CP) was converted to Na^+ -exchanged zeolite *via* a AIE process, then the latter was treated by $\text{H}_2\text{SO}_4(\text{aq.})$ to obtain the activated Nano CP (AT-Nano CP). A subsequent ligand exchange with $\text{K}_2\text{PdCl}_4(\text{aq.})$ under stirring for 6 h at room temperature allowed obtaining AT-Nano CP- $[\text{PdCl}_4]^{2-}$. Finally, the latter was reduced with hydrazine to provide the desired Pd nanoparticles-loaded zeolite. Various internal aryl alkynes (**G.54**) were synthesized with this nanocatalyst (0.06 mmol% Pd) in the presence of K_2CO_3 in

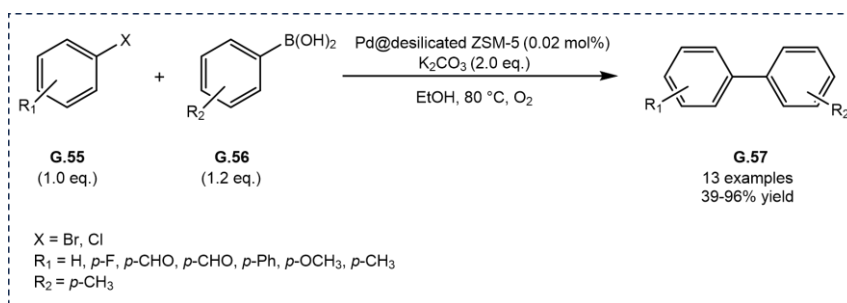
water at 60 °C, with yields ranging from 40% to 95%. Aryl halides substituted with electron-withdrawing groups led to better conversions in shorter reaction times in comparison with electron-donating substituents. Furthermore, the catalyst could be reused and recycled for eight times without significant loss of catalytic activity. A Sheldon test indicated that no Pd⁰ species leached to the solvent and the result was further supported by ICP-AES analysis.



Scheme 28. AT-Nano CP-Pd⁰-catalyzed Sonogashira coupling reaction.²¹²

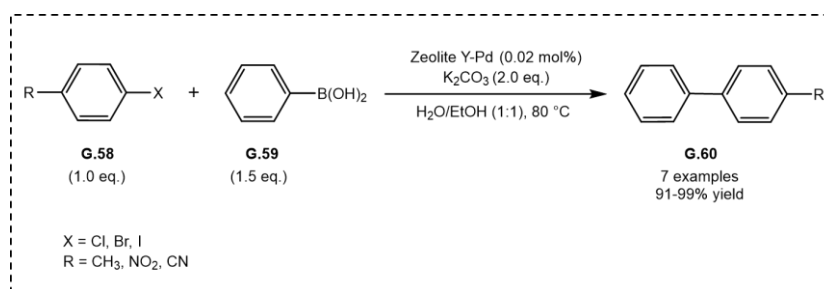
Suzuki-Miyaura coupling reactions

In 2013, Kumbhar and co-workers²¹³ reported a Pd@desilicated ZSM-5 catalyst to promote Suzuki-Miyaura couplings in the absence of ligand (**Scheme 29**). The catalyst was prepared *via* a AIE process between prepared desilicated ZSM-5 in dry THF and Pd(OAc)₂ solution at room temperature for 48 h. Interestingly, the Pd@desilicated ZSM-5 exhibited enhanced catalytic activity in the model reaction of bromobenzene and phenylboronic acid, providing higher yields in shorter reaction times compared to the results obtained with the Pd@ZSM-5 as the catalyst (96% yield in 2 h vs 80% yield in 3 h). Pd@desilicated ZSM-5 catalyst (0.02 mmol% Pd) with K₂CO₃ (2 equiv.) in ethanol at 80 °C under aerobic conditions proved to be the best conditions (**Scheme 29**). Various aryl halides (**G.55**) and arylboronic acids (**G.56**) were screened under the optimal conditions, providing the desired products (**G.57**) with yields in 39-96%. A hot filtration test was performed in the model reaction and the result indicated that no Pd species leached into the solvent. The catalyst could be reused at least four times with a progressive decrease in yields (from 96% to 82%), which could be due to the difficulty in separating the small amounts of the catalyst employed from the reaction mixture.



Scheme 29. Pd@desilicated ZSM-5-catalyzed Suzuki-Miyaura coupling reactions.²¹³

In 2018, Tadjarodi and co-workers²¹⁴ developed a new Pd nanoparticles-supported zeolite Y catalyst (Z-Y-Pd NPs) for the Suzuki-Miyaura (S-M) coupling of aryl halides (**G.58**) with phenylboronic acid (**G.59**) (**Scheme 30**). The Pd-loaded zeolite was prepared through a AIE reaction of H-Y zeolite with a basic solution of PdCl₂ in ethylene glycol under ultrasonic treatment for 1 h. Z-Y-Pd NPs (0.02 mol%) and K₂CO₃ (1.0 mmol) in a mixture of water/ethanol (1:1, v/v) at 80 °C turned out to be the optimal conditions for the coupling reactions. Various aryl halides, and even aryl fluorides, could react with phenylboronic acid with this catalyst, affording the expected products (**G.60**) in 63-99% yields (**Scheme 30**). Reusability study of the Z-Y-Pd NPs catalyst was evaluated in the reaction of bromobenzene and phenylboronic acid. The catalyst was separated from the reaction mixture by centrifugation, washed with ethyl acetate and dried at room temperature before being directly used for the next run. It was found that the catalyst could be recycled over ten times without losing activity.



Scheme 30. Pd-doped zeolite Y-catalyzed Suzuki-Miyaura coupling reaction.²¹⁴

2.3.2.2.6. Copper-doped zeolites

As already mentioned, copper-doped zeolites were initially applied for depollution processes, especially in the selective catalytic reduction (SCR) of NO_x.²¹⁵ Shortly after, they gained wide attention as heterogeneous catalysts for organic synthesis since both copper salts or complexes can serve as oxidation agents, coupling agents, and Lewis acids in diverse homogeneous organic transformations.²¹⁶⁻²¹⁸ With the development of organic synthesis or organometallic chemistry, new reactions promoted by stoichiometric or catalytic amounts of copper are

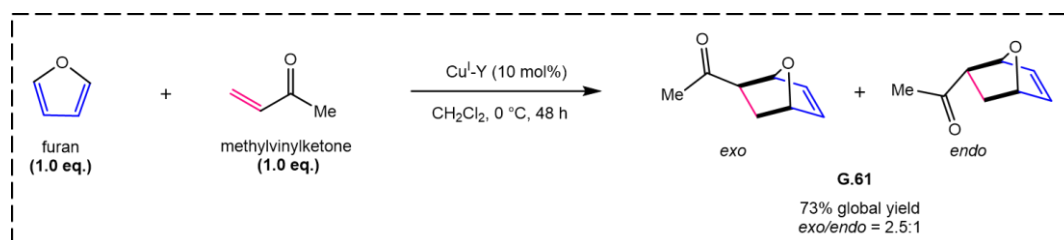
continuously discovered.²¹⁹⁻²²¹ Compared to other metals, e.g. palladium, platinum or the other coinage metals silver and gold, copper is an interesting alternative for its low cost, availability, and lower toxicity.

Because copper compounds exhibit strong Lewis acidity, in particular alkyno- and alkenophilicity,²²² it could be useful to load copper(I) or copper(II) species into zeolites, but only a few examples have so far been reported. They mostly correspond to cycloaddition and coupling reactions. The following sections are categorized by reaction type and provide several examples promoted by different copper-doped zeolites.

2.3.2.2.6.1. Copper-doped zeolites in cycloaddition reactions

Diels-Alder reactions

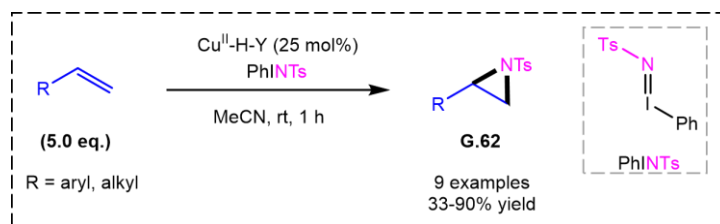
Ipaktschi *et al.*¹⁰⁶ were the first to use copper-doped zeolites in organic synthesis. They prepared a Cu(I) exchanged Y-zeolite to catalyze Diels-Alder reactions (**Scheme 31**). The catalyst was synthesized in two steps. First, an acidified sodium Y zeolite was exchanged with Cu(OAc)₂ *via* multiple AIE processes to obtain a Cu^{II}-Y zeolite, which was then reduced by CO at 300 °C to form the desired Cu^I-Y zeolite. Several dienes and oxygen-containing dienophiles were screened with yields of **G.61** up to 98%. When furan was used as the diene and methylvinylketone as the dienophile, this catalyst provided an additional 30% yields of the product **G.61** at ambient pressure compared to standard conditions, which required high pressure (15000 atm) to promote Diels-Alder reactions with furans.²²³ Furthermore, the shape selectivity of this Cu^I-Y zeolite induced a preferred *exo*-selectivity, as it provided a higher yield of the *exo*-isomer product (*exo/endo* = 2.5:1), while high-pressure conditions led to equivalent amounts of both isomers (*exo/endo* = *ca.* 1). However, it is regrettable that no information on the recyclability of the zeolite in this reaction was provided.



Scheme 31. Cu^I-Y-catalyzed Diels-Alder reaction of methylvinylketone and furan.¹⁰⁶

In 1999, Hutchings *et al.*²²⁴ disclosed a Cu^{II}-H-Y zeolite for the aziridination of alkenes (**Scheme 32**) based on the previously Cu(OTf)₂-catalyzed homogeneous conditions developed

by Evans and co-workers²²⁵. Various aziridine compounds (**G.62**) were synthesized from different terminal alkenes catalyzed by Cu^{II}-H-Y at room temperature using [*N*-(*p*-tolylsulfonyl)imino] phenyliodinane (PhI=NTs) as the superior nitrogen source.



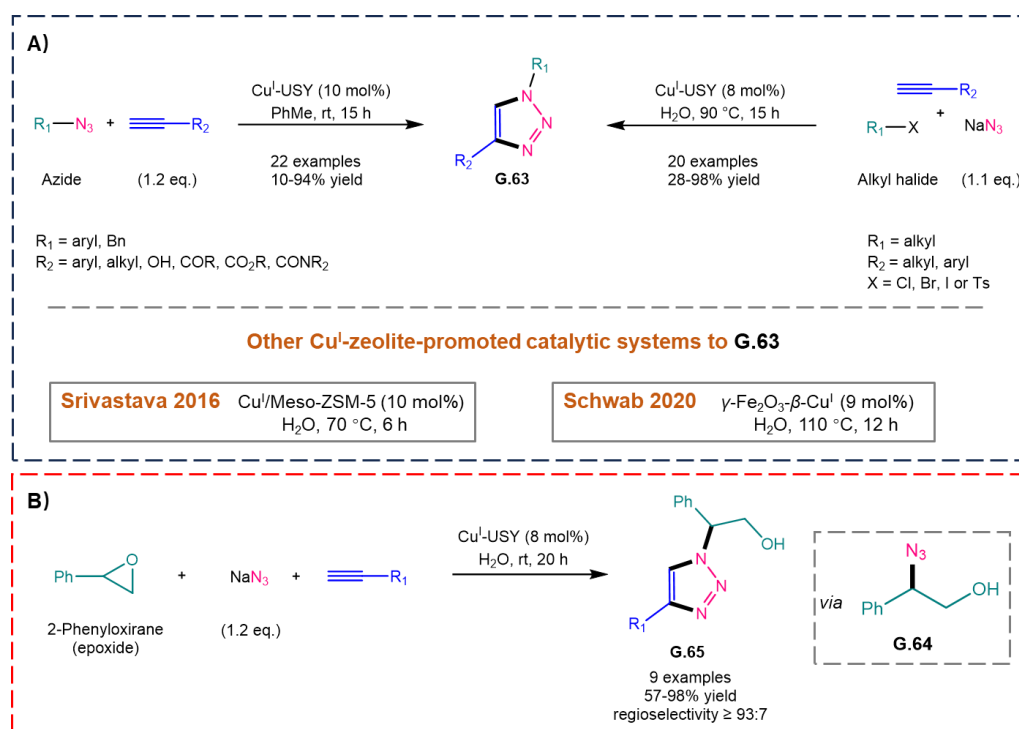
Scheme 32. Cu^{II}-H-Y-catalyzed aziridination of alkenes.²²⁴

The catalyst was prepared *via* AIE reaction in Cu(OAc)₂ solutions and then calcination at 550 °C under air. The nature of the copper species on the zeolite was unknown since analytical data on the catalyst characteristics were not provided. During the recyclability studies, a progressive decrease in yield was observed, indicating that the catalytic activity of zeolite was stepwise lost. However, the Sheldon test result showed that less than 0.5% Cu²⁺ was leached from the zeolite after each run, indicating that clogging of zeolite pores may be the reason for catalyst deactivation. This inference was further confirmed as the inherent activity of the catalyst was recovered *via* recalcination after each run.

Shortly after, Hutchings's group²²⁶ further studied the assessment of this catalyst stability in the presence of a chiral bis(oxazoline) ligand with different nitrogen sources (PhI=NTs and PhI=NNs). They found that the yield and enantioselection could be significantly improved from 29% to 76% by using a slight excess of the nitrene donor relative to styrene (1:1.5), compared to the initial conditions using an excess of styrene (5:1). The Sheldon test indicated that when using PhI=NNs as the nitrogen donor, a significantly enhanced copper leaching was observed with or without the additional chiral ligand (334-369 ppm), while only 0.16% of the copper was leached into solution with PhI=NTs as the nitrene donor in the absence or presence of the chiral modifiers (6-72 ppm). Interestingly, the leached copper(II) species did not play a significant role in the formation of the aziridine as PhI had an enhanced poisoning effect on Cu²⁺ in solution and the slow time-dependent Cu-leaching observed. Nevertheless, the leaching of copper ions will eventually limit the re-use of the catalyst, which is uneconomical from a practical point of view.

CuAAC reactions

Besides the Diels-Alder cycloaddition, another cycloaddition promoted by copper-doped zeolites is the modified Huisgen cycloaddition¹², *i.e.*, copper-catalyzed azide-alkyne cycloaddition (CuAAC) which was developed by Sharpless¹⁸ and Meldal¹⁷. In 2007, our group^{19,20} explored the potential of five typical Cu^I-doped zeolites (USY, Y, ZSM-5, MOR, β) to synthesize 1,2,3-triazoles **G.63** for CuAAC reaction (**Scheme 33A, left**). These catalysts were prepared *via* SSIE reaction between their H-forms and CuCl. Cu^I-USY proved to be the most efficient heterogeneous catalyst with high regioselectivity since only one regioisomer product was produced. This methodology was expanded to carbohydrates and aminoacid derivatives for the synthesis of valuable glycoconjugates. Carbohydrates as azides reacted with different terminal alkynes catalyzed by Cu^I-USY, various glycopeptides and oligosaccharide mimics could thus be efficiently obtained.²²⁷



Scheme 33. Cu^I-USY-catalyzed CuAAC for the synthesis of 1,2,3-triazoles.^{19,20,227-231}

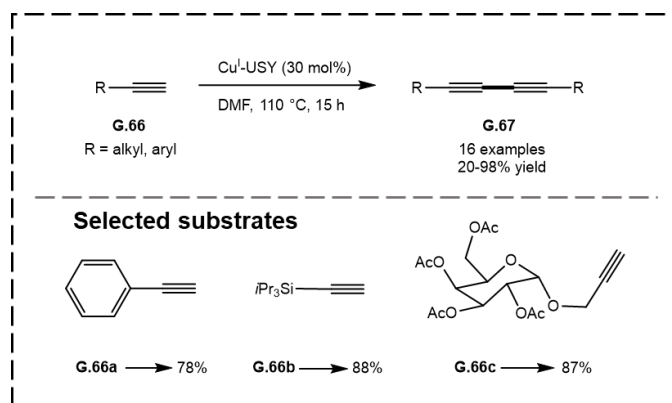
Shortly after, our research group²²⁸ further developed a one-pot two-step method for the synthesis of triazoles in 2010 (**Scheme 33A, right**). This method allowed the synthesis of organic azides *in situ* between organic halides (or tosylates) and easy-to-handle sodium azide (NaN₃) before the CuAAC reaction. Catalyzed by a recyclable heterogeneous catalyst with water as the solvent, this method leads to a green protocol for the synthesis of triazoles. Similarly, in another Cu^I-USY-catalyzed cascade process²²⁹, the catalyst first promoted the

formation of 2-azidoethanol **G.64** through a regioselective ring-opening reaction of epoxides, then catalyzed the CuAAC reaction between **G.64** with terminal alkynes, which produce β -hydroxytriazoles **G.65** in water at room temperature (**Scheme 33B**). In 2016, a mesoporous zeolite ZSM-5 doped with copper nanoparticles was employed to catalyze the analogous cascade reaction in water under N₂ atmosphere.²³⁰ The copper nanoparticles were prepared by a chemical reduction method in which Cu(NO₃)₂·3H₂O aqueous solution was added dropwise into a mixed solution of sodium dodecyl sulfate (SDS) and NaBH₄ in an ice bath for 0.5 h. The pre-prepared suspension of mesoporous ZSM-5 was then added to the above-prepared Cu nanoparticles solution to synthesize the modified catalyst. To more conveniently recover the zeolite catalyst, Schwab *et al.*²³¹ developed a Cu^I- β zeolite supported on magnetic γ -Fe₂O₃ microspheres (γ -Fe₂O₃- β -Cu(I)). This catalyst could be recovered quickly from the reaction mixture using an external magnet. Such a method provides the basis for further preparation of easily recyclable heterogeneous catalysts.

2.3.2.2.6.2. Copper-doped zeolites in coupling reactions

Homocoupling reactions

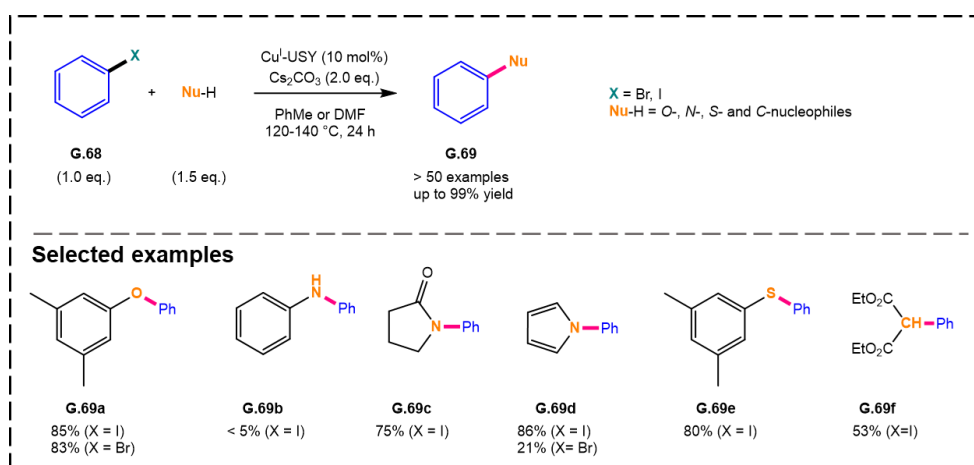
One of the oldest known copper-mediated homocoupling reactions can date back to the Glaser homocoupling reaction³, in which terminal alkynes (**G.66**) were dimerized based on forming intermolecular C-C bonds. Various copper catalysts have been applied to the homocoupling reactions, but all were carried out under homogeneous conditions. In 2009, Pale and co-workers³⁸ developed the first copper-based-catalyzed heterogeneous version. They investigated a series of copper(I)-modified zeolites with different morphologies (USY, Y, ZSM-5, β , MOR) for the synthesis of diynes (**G.67**). Zeolites possessing large internal cages, e.g., Cu^I-Y and Cu^I-USY, proved to be the most efficient catalysts, providing high (quantitative) yields of products (**Scheme 34**). This reaction was performed in DMF at 110 °C without additional bases and ligands. In such a convenient and efficient method, a variety of diynes, including carbohydrate derivatives, were prepared with yields ranging from 20% to 98%.



Scheme 34. Cu^{I} -USY-catalyzed diyne synthesis.³⁸

Cross-coupling reactions

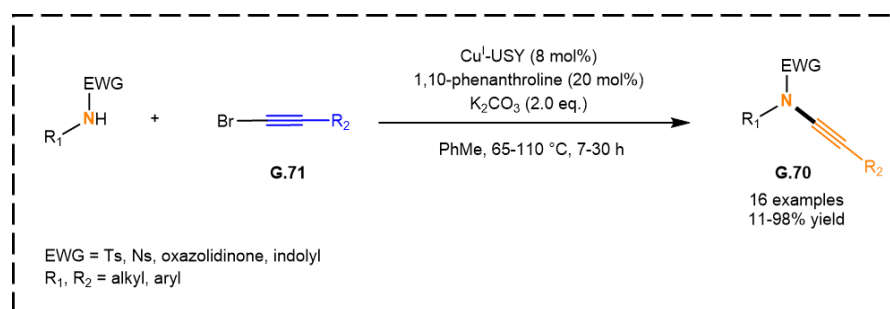
Ullmann-Goldberg coupling reactions^{7,8,232} were the earliest copper-mediated cross-coupling reactions for the synthesis of biaryls and aryl ethers by forming C-C, C-O, C-S, and C-N bonds between an aryl electrophile **G.68** and a nucleophile (Nu-H). Chassaing and co-workers^{39,40} reported a copper(I)-zeolite-catalyzed heterogeneous version of this coupling reaction with several *O*-, *S*-, *N*-, and *C*-nucleophiles (**Scheme 35**). They synthesized more than 50 coupling products (**G.69**) with yields up to 99% using 10 mol% Cu^{I} -USY in toluene or DMF in the presence of Cs_2CO_3 and without additional ligands. Unfortunately, more environmentally friendly solvents such as EtOH or water did not produce satisfactory results under the same conditions. It is noteworthy that the catalyst could be reused five times without losing activity.



Scheme 35. Cu^{I} -USY-catalyzed Ullmann-type coupling reactions.^{39,40}

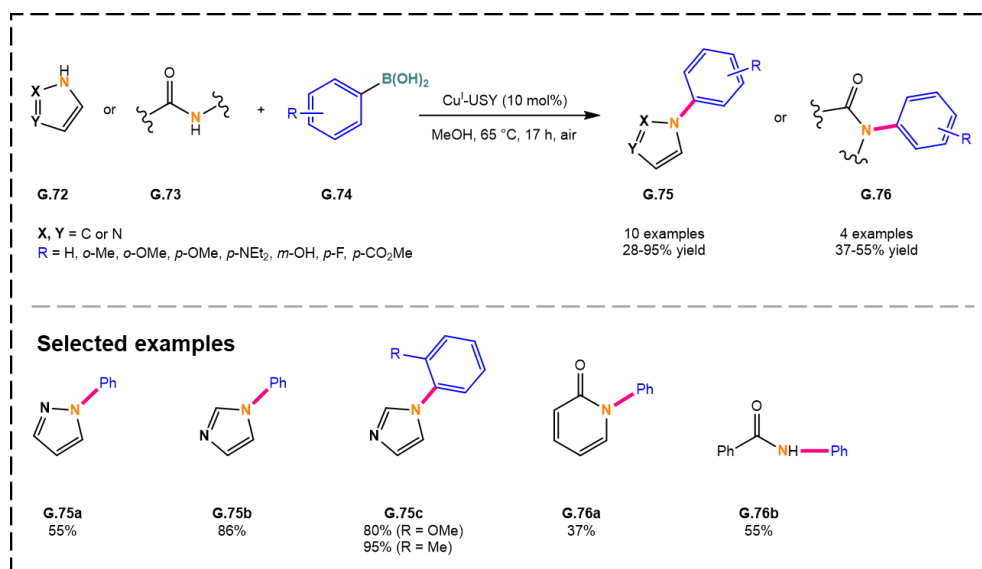
In 2014, our group²³³ disclosed the Cu^{I} -USY-catalyzed preparation of various ynamides **G.70** (**Scheme 36**). A series of bromoalkynes **G.71** were coupled to *N*-nucleophiles (deactivated amines and nitrogen heterocycles) with 1,10-phenanthroline as a ligand with yields up to 98%.

This approach was also tolerant to a wide range of functional groups compared to the previous homogeneous conditions using $\text{CuSO}_4 \cdot 5\text{H}_2\text{O}$ ^{234,235}. Besides, the catalyst could be recycled up to five times without dramatic loss of activity.



Scheme 36. Cu^I-USY-catalyzed Hsung coupling reaction to ynamides.²³³

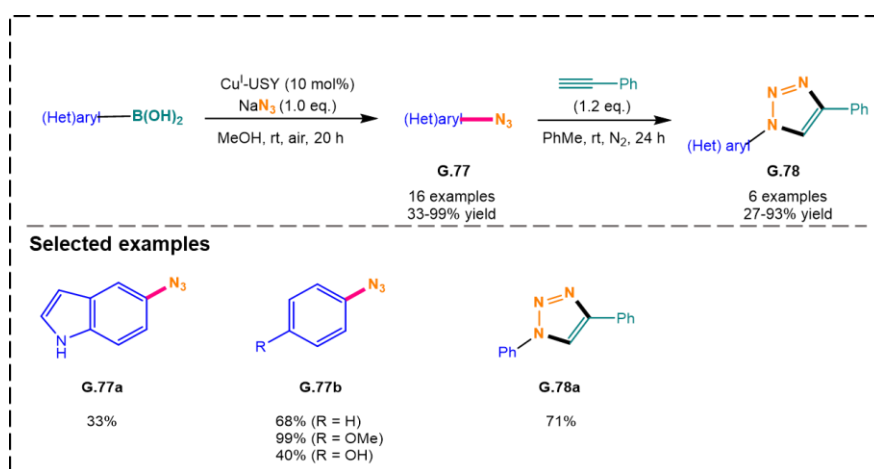
In 2017, our research group⁴² published a Cu^I-USY-catalyzed Chan-Lam-type C-N cross-coupling reaction between azoles **G.72** or amides **G.73** and a variety of aromatic boronic acids **G.74** (Scheme 37). This reaction was performed using 10 mol% Cu^I-USY in refluxing methanol under air without any base and ligand. Under such attractive and simple conditions, a series of *N*-arylation products **G.75** and **G.76** were synthesized with yields ranging from 28% to 95%. However, the developed Cu^I-zeolite could only be recycled two times, with a significant decrease in yield at the third run. A Sheldon test showed that copper species partially leached into the solvent, which might explain the poor recyclable performance of the catalyst.



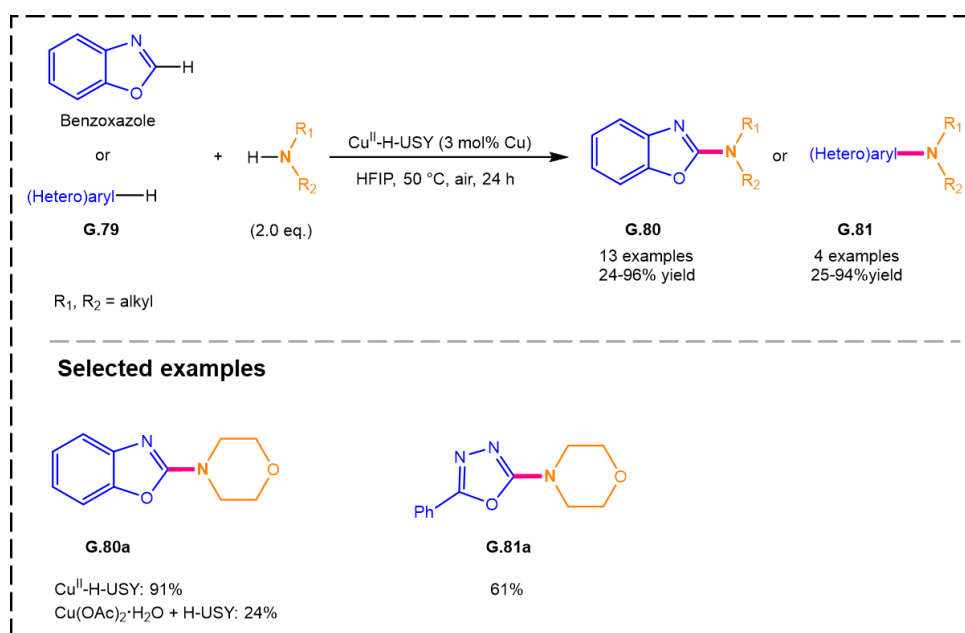
Scheme 37. Cu^I-USY-catalyzed Chan-Lam-type coupling reaction for C-N bond formation.⁴²

Shortly after, our group⁴¹ disclosed a modified Chan-Lam-type azidation reaction of (hetero)aryl or (*E*)-cinnamyl boronic acids with NaN_3 to produce **G.77** (Scheme 38, left). Cu^I-

USY again proved to be the best catalyst to promote the reaction in MeOH at room temperature in air without additional bases or ligands. In the previous Cu^I-USY-catalyzed Chan-Lam-type protocol⁴², some copper species leached into the solvent. In this azidation, the Cu^I-USY catalyst could be recycled five times without losing activity, indicating that the lower temperature may reduce the leaching effect of copper ions. Furthermore, this protocol was successfully applied to a one-pot azidation-CuAAC procedure, allowing azides to be synthesized *in situ* and directly used in the next Cu^I-USY-catalyzed CuAAC reaction (Scheme 38, right). The catalyst efficiently promoted the synthesis of six triazoles **G.78** with yields ranging from 27% to 93%. Interestingly, the isolated yield of the corresponding triazoles was higher than that of the azidation product **G.77** in some cases.



In 2020, De Vos *et al.*²³⁶ prepared a Cu^{II}-H-Y zeolite for the cross-dehydrogenative coupling reaction (CDC) of azoles **G.79** and secondary amines to synthesize 2-amino-azoles **G.80** and **G.81** (Scheme 39). The direct C-H bond activation reaction was performed under air without additional ligands and additives, making it more attractive and convenient. A range of azoles and amines were employed based on the model CDC reaction of benzoxazole and morpholine. The results showed that the scope of azoles covered diverse substituted benzoxazoles, while the amine scope was only compatible with secondary aliphatic and benzylic derivatives. Additionally, 5-phenyl-1,3,4-oxadiazole was also reactive, providing a 61% yield of the expected coupling product **G.81a**.



Scheme 39. Cu^{II}-H-USY-catalyzed aerobic CDC reaction between azoles Z.49 and secondary amines.²³⁶

Furthermore, the authors²³⁶ compared the catalytic performance of several zeolites with different topologies or the same topology with different SAR. They found that the strongly dealuminated Y zeolites (USY) with higher SAR ratios were more hydrophobic and reactive, producing preferable product yields. This might be due to the fact that these zeolites have a good removal effect on the water generated from the catalytic sites, thus protecting the catalytic activity of zeolites. In addition, the residual unexchanged protons on the zeolite played a key role, as they served as Brønsted acid to pre-activate the benzoxazole ring. Furthermore, Sheldon tests showed that copper species were heavily leached from the zeolite, and only 42% product yield was provided when reusing the zeolite for the second run (91% yield in the first run). It should be mentioned that the yield of the reaction catalyzed by Cu^{II}-H-USY was much higher than that promoted by a mixture of Cu(OAc)₂·H₂O and H-USY (91% vs 24%).

In summary, it can be found that most examples above are catalyzed by metal-doped Y or USY zeolite. This is not only because they are easily available and cheap but also because of their superior performance frequently exhibited in organic reactions. Indeed, the large pore sizes and internal cages frames inherent to these zeolites contribute significantly to their catalytic performance in organic synthesis. The hierarchical USY zeolite has large mesopores of 40 Å in addition to the microporous cavities of 12 Å, making it particularly attractive in organic applications. These characteristics allow larger molecules to conveniently enter the zeolite and access to the catalytic sites, thereby enhancing chemical diffusion for faster conversion in

organic transformations. For these reasons, USY zeolites have become among the most popular materials for supporting a series of catalytic active metal species.

Part two. The formation of aromatic C-C and C-X bonds for the synthesis of aromatic motifs by copper(I)-zeolite-catalyzed coupling reactions.

Chapter II. C_{aryl}-C_{aryl} bond formations *via* copper(I)-zeolite-catalyzed homocoupling-type reactions

1. Introduction

Aryl-aryl (C-C) bond formations represent an important challenge in organic synthesis. Such pivotal bonds are mostly constructed by (transition) metal-catalyzed homo- and cross-coupling reactions.²⁹ These bonds are encountered in various natural product scaffolds, such as biaryls and biphenols, as well as in many synthetic bioactive compounds used in pharmaceutical and agrochemical fields.²⁹ For example, these motifs can be found as a pharmacophore in medicinally important compounds²⁴, such as anti-inflammatory (felbinac), anti-hypertensive (micardis and irbesartan) and anticancer (riccardin C) drugs, as well as in the pesticide boscalide (Figure 10). Furthermore, biaryl moieties constitute a large family of compounds, which can be found as secondary metabolites in various organisms. The most typical of these metabolites are the vancomycin family of antibiotics,²² well known for their ability to treat infections caused by bacteria that are resistant to other drugs. Of note is that vancomycin has been listed on the World Health Organizations (WHO) list of essential medicines since 2017.

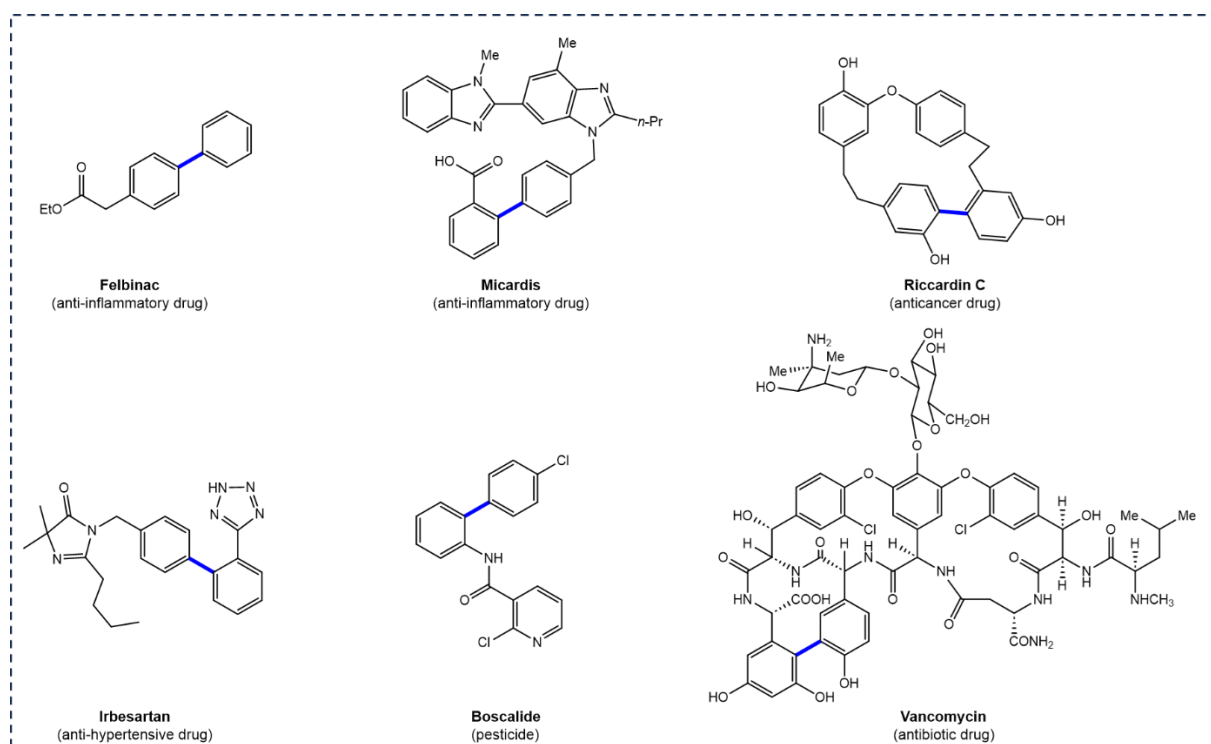


Figure 10. C_{aryl}-C_{aryl} bonds in medicinally and agriculturally important compounds.^{24,29}

The known syntheses of biaryls in organic synthesis mostly rely on metal-catalyzed cross-² or homocoupling reactions¹. Compared to cross-coupling reactions, only a few publications described the formation of symmetrical biaryls through homocoupling reactions. Homocoupling was often seen as a side-reaction in various organic transformations. However,

such homocoupling could provide a rapid and convenient access to symmetrical biaryls *via* the formation of C_{aryl}-C_{aryl} bonds.

2. How to produce biaryl *via* homocoupling reactions?

2.1. The historical Ullmann reaction

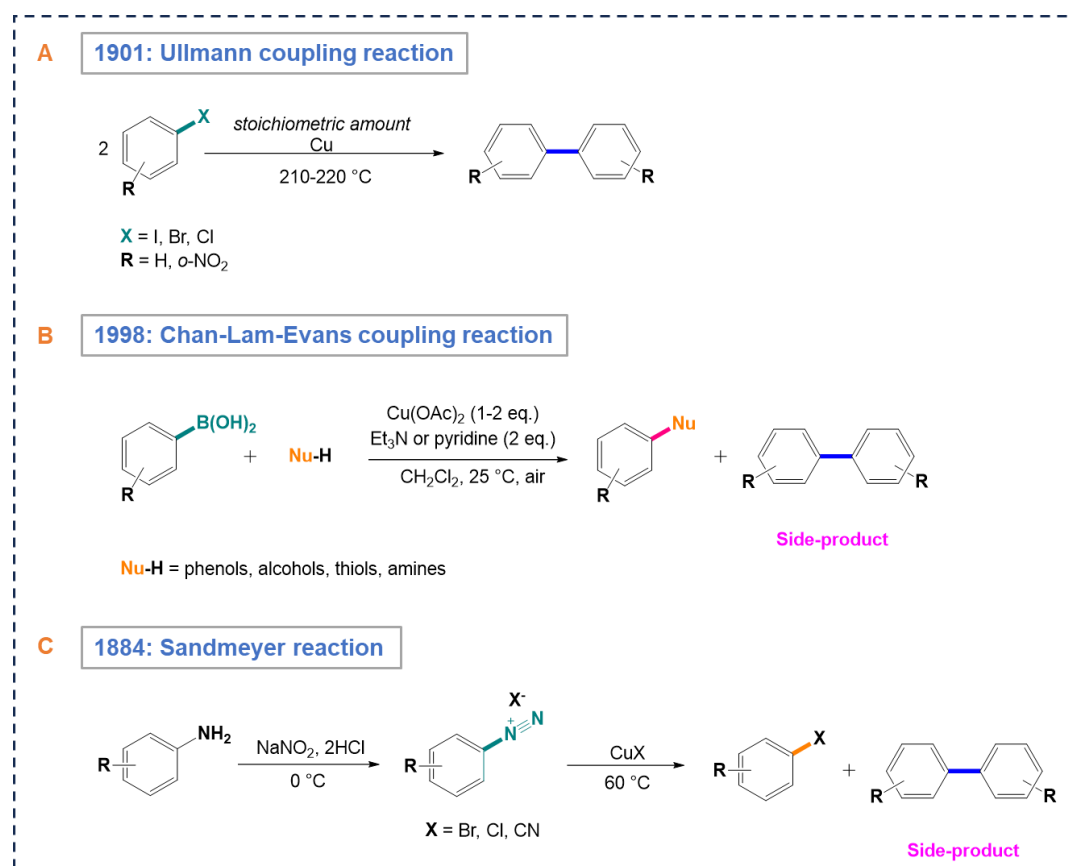
The formation of the first C_{aryl}-C_{aryl} bonds can be traced back to the Ullmann reactions (**Scheme 40, A**) in 1901¹. Ullmann reported the coupling of two molecules of the same aryl halide in the presence of stoichiometric amounts of copper. These reactions correspond to what it is nowadays called a homocoupling reaction of aryl halides. However, the Ullmann reactions had various limitations, such as very high temperature (200-220 °C), long reaction time (1 or 2 days), and limited applications due to such harsh conditions.

Inspired by these seminal works, chemists have been looking for new synthetic methods to improve the reaction conditions for the formation of biaryl C-C bonds, but still mostly focused on metal-catalyzed cross-coupling reactions.

Among the developed versions, the palladium-catalyzed Suzuki–Miyaura (S-M) cross-coupling between arylboronic acids and aryl halides has become a powerful and effective method for the formation of aryl–aryl bonds.²³⁷ In 1979, N. Miyaura and A. Suzuki discovered that alkenyl, alkynyl and arylboronic acids could be engaged in palladium-catalyzed cross-coupling reactions.^{238,239} This finding started a burst in cross-coupling reactions of arylboronic acids and their applications in aryl-aryl bond formations, but also induced the seminal work on copper-promoted Chan-Lam-Evans coupling reactions⁹⁻¹¹ to form C_{aryl}-O and C_{aryl}-N bonds (**Scheme 40, B**). Homocoupling was regarded as a side-reaction in these reactions. However, such homocoupling of arylboronic acids allowed the synthesis of symmetrical biaryls by forming aryl-aryl bonds at mild temperature under air, making it highly attractive compared to the original Ullmann reaction conditions.

Meanwhile, aryldiazonium salts, which could be conveniently prepared from the corresponding anilines with sodium nitrite (NaNO₂) in cold acidic solution or with nitrous acid (HNO₂) (**Scheme 40, C**), are also attractive alternatives to the common electrophiles, such as aryl halides or triflates²⁴⁰⁻²⁴⁴ for the aromatic C-C bond formation coupling reactions. The copper(I)-mediated homocoupling of aryldiazonium salts was also initially discovered as a side reaction during studies on the Gattermann synthesis of aryl halides from aryldiazonium salts and copper(I) halides, also named the Sandmeyer reaction (**Scheme 40**). This seminal work also

opens an opportunity to rapidly synthesize symmetrical biaryls based on homocoupling reaction of aryldiazonium salts.



Scheme 40. Cu-mediated coupling reactions of aryl halides (top), arylboronic acids (medium) and aryldiazonium salts (bottom), which provide access to biaryls.^{1,9-11,240-244}

However, most of these homocoupling reactions were carried out under homogeneous palladium or copper conditions in the presence of bases and ligands, resulting in serious environmental problems and waste of resources. Heterogeneous catalysts were expected to be developed aiming to minimize these negative effects. Unfortunately, not many heterogeneous versions have been disclosed to date, despite the inherent advantages including easy separation, better handling characteristics and recyclability heterogeneous catalysts exhibit. In particular, an extremely limited quantities of copper-based catalysts^{245,246} have been developed for homocoupling reactions of aryl halides and arylboronic acids (ABAs), as well as aryldiazonium salts, despite of their low costs and abundance on Earth compared to other metal-based catalysts. Moreover, none of them relied on the use of zeolites as catalysts, although the potential of zeolites as inexpensive and stable support materials should not be underestimated.

Considering that Cu^I-zeolite has frequently exhibited excellent catalytic activity in various organic transformations (see Chapter I-2.3.2.2.6.), the interests of the present study are mainly focused on the Cu^I-USY-catalyzed homocoupling of ABAs and aryldiazonium salts.

As mentioned above, the introductory section will introduce several methods for the synthesis of symmetrical biaryls *via* different metal-catalyzed homocoupling reactions with selected but non-exhaustive examples, aiming to highlight the importance of designing and developing novel efficient heterogeneous catalyst for the homocoupling of ABAs and aryldiazonium salts, respectively.

2.2. Homocoupling of aryl halides

As the first transition metal-mediated homocoupling reaction, Ullmann reaction was one of the main methods for the formation of C_{aryl}-C_{aryl} bonds during the first 60 years of the last century, arousing a surge of scientific interest in this area to improve reaction conditions and expand their applications. With the further understanding of the Ullmann reaction mechanism, and the development of novel ligands, the improvements of catalytic systems and the application of different green technologies, Ullmann reactions could be conducted under milder conditions with desirable yields and excellent functional group tolerance.²⁴⁷⁻²⁵⁴

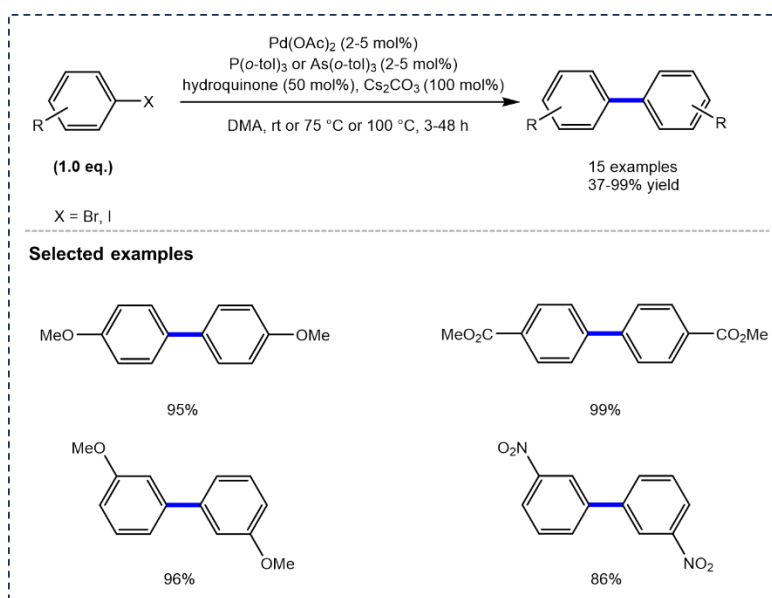
Palladium-promoted homocoupling of aryl halides under homogeneous conditions in the presence of special ligands and bases are still predominant in this field, with only limited examples related to other metals.²⁵⁵ Copper was the original catalyst in the Ullmann reaction, but only one Cu-based catalyst has been further developed for the homogeneous homocoupling of aryl halides. Furthermore, only a handful of metal-promoted reactions had been reported under heterogeneous conditions. Most of them relied on palladium deposited on carbon or palladium nanoparticles deposited on graphene, and only five examples used copper. For the latter, only cuprous oxide as nanocrystals deposited on graphene or copper deposited on hydrotalcite or silica or glucose have been described. In the following section, we will describe several examples of Ullmann homocoupling reactions catalyzed by different metals.

2.2.1. Palladium-catalyzed homocoupling reactions of aryl halides

2.2.1.1. Palladium-catalyzed homogeneous homocoupling reactions

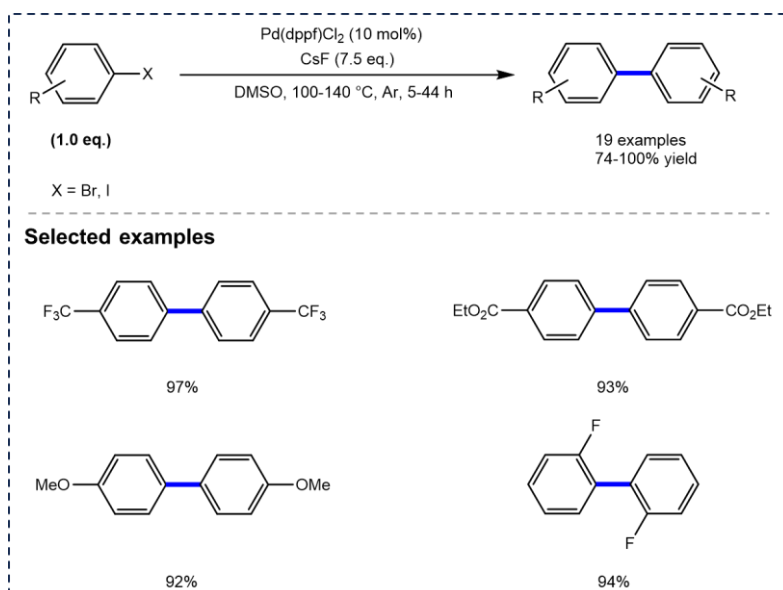
Rawal and co-workers²⁵⁶ developed homocoupling reactions of aryl halides catalyzed by a Pd(OAc)₂/P(*o*-tol)₃ catalytic system in the presence of hydroquinone (**Scheme 41**). The order

of addition of reagents and the hydroquinone were essential for the reaction effectiveness. The coupling reaction proceeded faster when $P(o\text{-tol})_3$ was replaced by $As(o\text{-tol})_3$. A variety of aryl halides was employed under the present reaction conditions; it was observed that aryl iodides containing either electron-withdrawing or electron-donating groups worked well and afforded the biaryls in high yields. However, a high amount of hydroquinone and base Cs_2CO_3 , as well as a toxic solvent dimethylacetamide (DMA) were required.



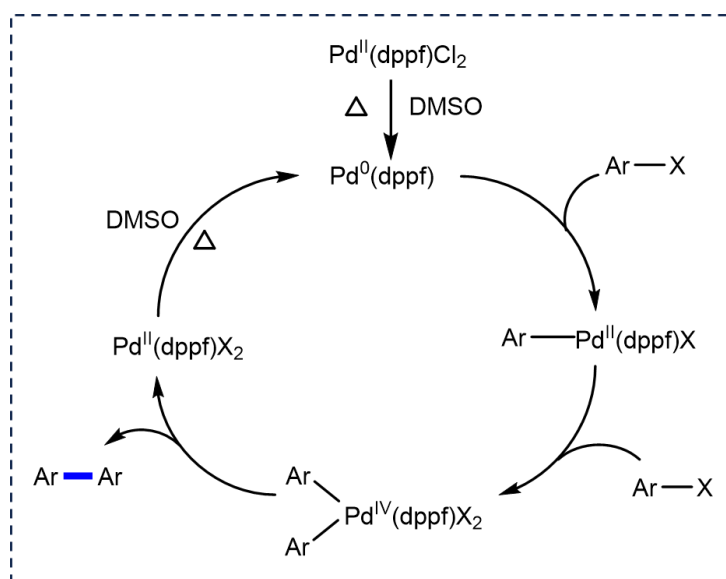
Scheme 41. Palladium/hydroquinone-catalyzed homocoupling of aryl halides.²⁵⁶

Qi *et al.*²⁵⁷ developed a palladium-catalyzed reductive homocoupling reaction of aryl halides using DMSO as solvent and CsF as base without additional reducing agents. Among the palladium species explored, $Pd(dppf)Cl_2$ ($dppf = 1,1'$ -bis(diphenylphosphino)ferrocene) was the most efficient catalyst, providing the desired product in almost quantitative yield (**Scheme 42**). However, relative high temperature and an inconvenient solvent (DMSO) were required. Under these conditions, a variety of aryl and heteroaryl iodides and bromides were employed. It seemed that neither electronic effects nor steric hindrance affected the coupling performance.



Scheme 42. Palladium-catalyzed homocoupling of aryl halides in DMSO.²⁵⁷

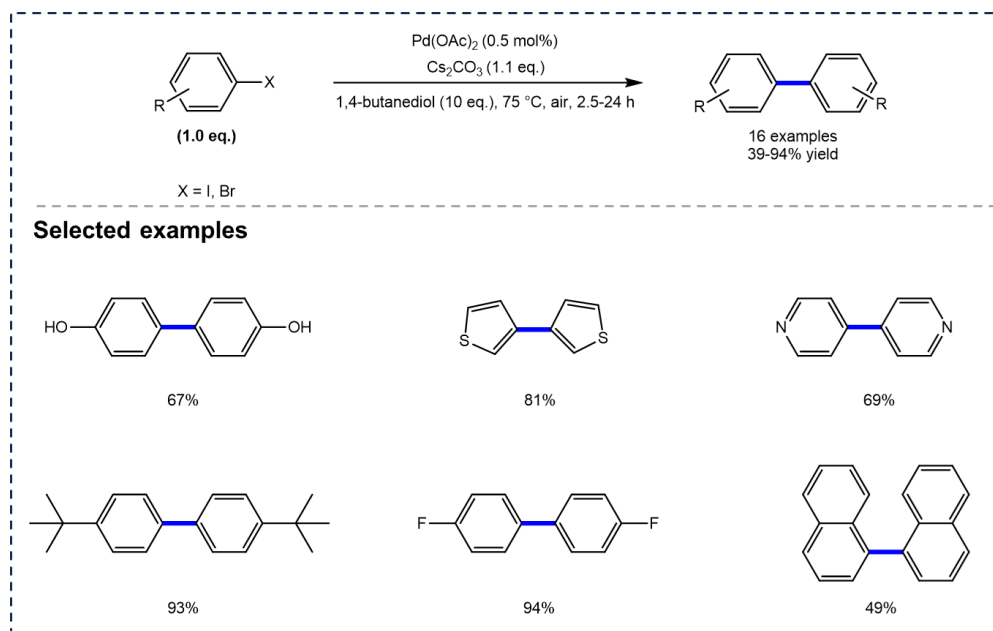
The author proposed a possible mechanism based on the reaction analysis by X-ray photoelectron spectroscopy (XPS)²⁵⁷ (**Scheme 43**). Pd^{II} complex would be reduced to the Pd⁰ active complex by DMSO under heating, indicating that DMSO had the dual role of acting as a solvent and a reducing agent. Furthermore, two steps of oxidative addition and a reductive elimination were required in the reaction to complete the catalytic cycle.



Scheme 43. A proposed mechanism of Pd-catalyzed homocoupling in DMSO.²⁵⁷

Feng *et al.*²⁵⁸ reported an efficient method for the preparation of symmetrical biaryls by palladium-catalyzed reductive homocoupling of aryl halides (**Scheme 44**). 0.5 mol% Pd(OAc)₂ in the presence of Cs₂CO₃ at 75 °C for 2 h were the optimal conditions when iodobenzene was

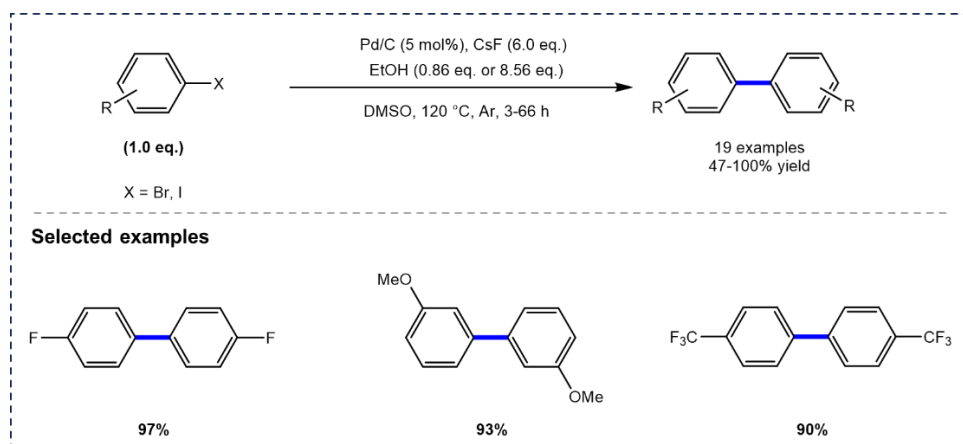
selected as the model substrate. 1,4-butanediol played a dual role as both a reductant and a ligand for the synthesis of the desired homocoupling product. Various aryl halides bearing electron-donating or electron withdrawing groups could be converted to the desired homocoupling products under these catalytic conditions, although long reaction time or high palladium catalyst loading were required in some cases.



Scheme 44. Pd-catalyzed homocoupling of aryl halides with 1,4-butanediol as ligand.²⁵⁸

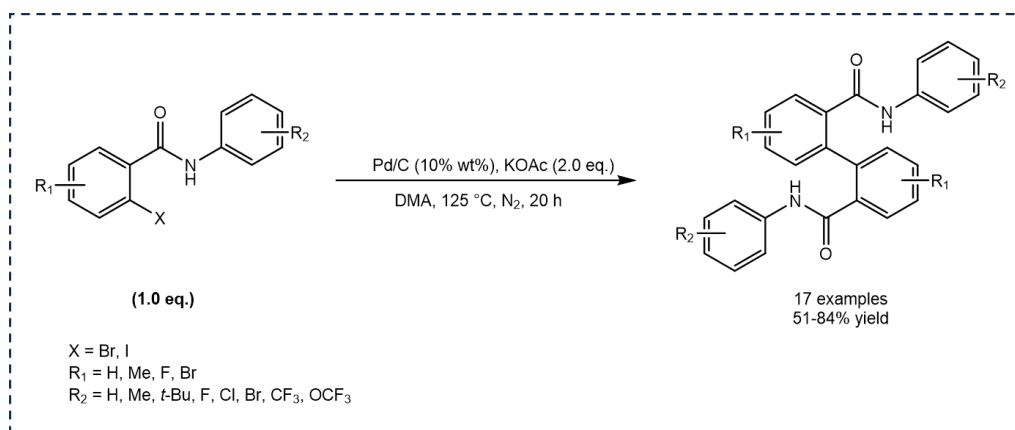
2.2.1.2. Palladium-catalyzed heterogeneous homocoupling reactions

In 2010, Qi *et al.*²⁵⁹ first reported a palladium on carbon (Pd/C)-catalyzed reductive homocoupling of aryl halides using ethanol as the reducing reagent, although DMSO was used as solvent at high temperature (**Scheme 45**). It was found that a small amount of ethanol (0.86 mmol) could increase the yield of the expected dimer product, but further addition of ethanol promoted the formation of the reduction product. Furthermore, a base screening demonstrated that cesium salts were superior to potassium salts in the reaction. The former provided higher yields than the latter (86% vs 20% (CsF:KF) and 85% vs 78% (Cs₂CO₃:K₂CO₃)). High temperatures were also beneficial for the transformation of aryl halides and the yields of the homocoupling products. A variety of aryl halides were employed under the present conditions, providing the homocoupling products in good to excellent yields.



Scheme 45. Pd/C-catalyzed homocoupling of aryl halides.²⁵⁹

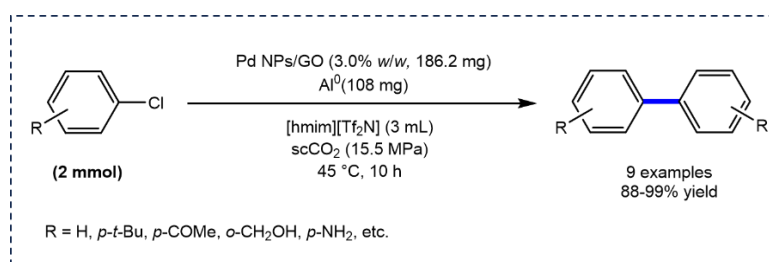
In 2017, Yang *et al.*²⁶⁰ developed a Pd/C-catalyzed homocoupling to synthesize symmetrical biaryl diamides. The reaction was conducted in dimethylacetamide (DMA) in the presence of KOAc under a nitrogen atmosphere without any ligand (**Scheme 46**). The catalytic system Pd/C–KOAc exhibited high reactivity, allowing various 2-halo-*N*-phenylbenzamides being conveniently converted to the corresponding biaryl diamides with moderate to good yields. The Pd/C catalyst could be easily recovered by a simple filtration given the insolubility of Pd/C in water. Recyclability of the catalyst was studied with the homocoupling of 2-iodo-*N*-phenylbenzamide. The results indicated that the catalyst could be reused at least for four times, but with the yield of the product dropping to 51% at the fourth run.



Scheme 46. Pd/C-catalyzed homocoupling reactions of 2-halo-*N*-phenylbenzamides.²⁶⁰

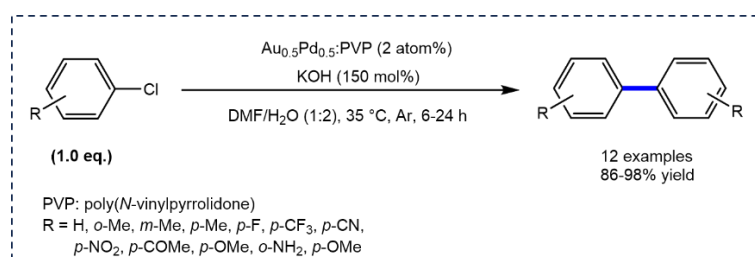
In 2011, Cheng and co-workers²⁶¹ reported a reductive homocoupling reaction of aryl chlorides catalyzed by palladium nanoparticles (Pd NPs) supported on graphene oxide (GO) (**Scheme 47**). The reaction was conducted in an environmentally benign ionic liquid (IL)/supercritical carbon dioxide (scCO₂) system with high product yields. The combination of IL and scCO₂

showed superior advantages over traditional organic solvents in product separation, catalyst recovery, and reuse of reaction media. The utilization of IL ([hmim][Tf₂N]) significantly improved the stability of the Pd NPs, making the catalyst easier to recycle. It was found that carbon dioxide, a naturally abundant, relatively nontoxic, economical but ‘green housing’ gas, significantly enhanced the selectivity of the GO supported Pd NPs-catalyzed reductive homocoupling of aryl chlorides. The Pd NPs catalyst and IL could be recycled at least 5 times without obvious loss of activity.



Scheme 47. Pd NPs-catalyzed homocoupling of aryl chlorides in supercritical carbon dioxide.²⁶¹

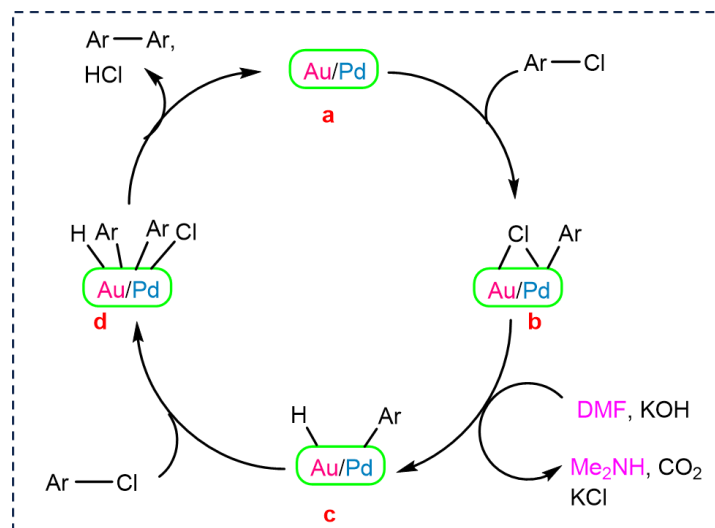
In 2012, Sakurai *et al.*²⁶² developed a poly(*N*-vinylpyrrolidone) (PVP) stabilized bimetallic gold–palladium alloy nanoclusters (NCs) catalyst for the homocoupling reaction of aryl chlorides (**Scheme 48**). The reaction could be conducted at low temperature in a mixed reaction media of *N,N*-dimethylformamide (DMF) and water in the presence of base since the support material PVP was a hydrophilic polymer. It was found that DMF played a dual role as both a co-solvent and reducing agent in the reaction. The corresponding reaction did not occur using monometallic gold and palladium nanoclusters, or the physical mixture of the two metals. More interestingly, the heterogeneous bimetallic Au/Pd alloy NCs catalyst (Au_{0.5}Pd_{0.5}:PVP) exhibited a higher catalytic activity for chloroarenes than for bromoarenes.



Scheme 48. Bimetallic Au-Pd alloy nanoclusters-catalyzed homocoupling of aryl chlorides.²⁶²

The author proposed a possible mechanism for the homocoupling of aryl chlorides catalyzed by bimetallic Au_{0.5}Pd_{0.5}:PVP (**Scheme 49**).²⁶² During the catalytic cycle, an oxidative addition of aryl chloride with the bimetallic catalyst **a** produced the intermediate **b**. Then, the latter **b**

was reduced by DMF in the presence of KOH to form the intermediate **c**. Subsequently, a second oxidative addition reaction occurred between ArCl with **c** to generate intermediate **d**. Finally, a reductive elimination reaction produced the expected product Ar-Ar, and the catalyst **a** was regenerated.

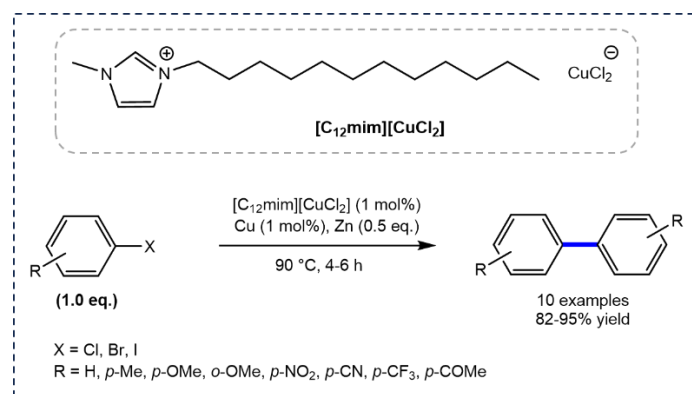


Scheme 49. Possible pathway for bimetallic Au_{0.5}Pd_{0.5}:PVP-catalyzed homocoupling of aryl chlorides.²⁶²

2.2.2. Copper-catalyzed homocoupling reactions of aryl halides

2.2.2.1. Copper-catalyzed homogeneous homocoupling reactions

In 2011, Hu and co-workers²⁶³ reported a novel reductive homocoupling reaction of aryl halides for the synthesis of biaryls using the ionic liquid 1-dodecyl-3-methylimidazolium cuprous chloride ([C₁₂mim][CuCl₂]) as a catalyst and a reaction medium with metallic zinc and copper powder (**Scheme 50**). The reaction proceeded faster in this ionic liquid than other traditional organic solvents, and provided the expected product in higher yield. The metallic zinc and copper were also necessary for the reaction, and only lower yields were obtained without either component. Various aryl halides bearing electron-donating or electron-withdrawing groups were employed under the present conditions, affording the biaryl products in good to excellent yields (82-95%).

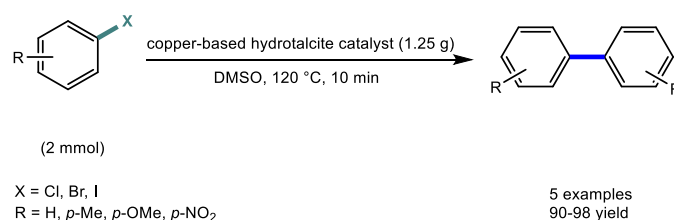


Scheme 50. [C₁₂mim][CuCl₂]-catalyzed homocoupling of aryl halides.²⁶³

2.2.2.2. Copper-catalyzed heterogeneous homocoupling reactions

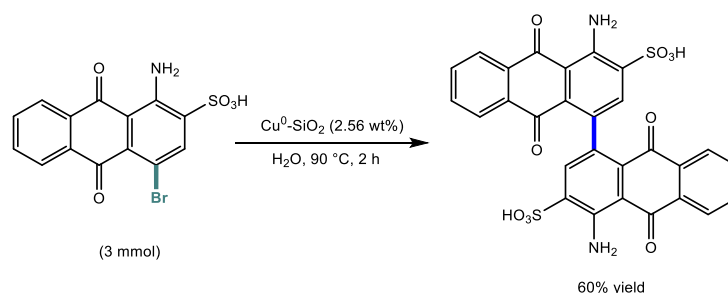
To the best of our knowledge, only five publications have reported the establishment of C-C bonds *via* copper-catalyzed homocoupling reaction of aryl halides.

In 2013, Mokhtar *et al.*²⁶⁴ developed a copper-based hydrotalcite catalyst for the reaction (**Scheme 51**). The catalyst could be reused at least three times without loss of activity. However, the application of this reaction was limited due to the poor product scope.



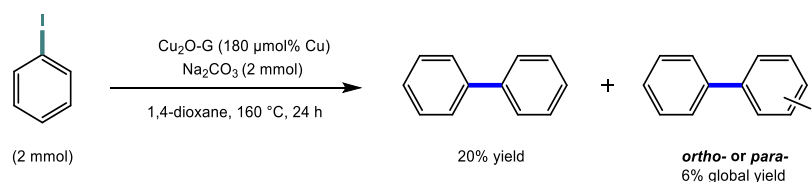
Scheme 51. Ullmann homocoupling of aryl halides using Cu-based hydrotalcite.²⁶⁴

In 2017, Xie *et al.*²⁶⁵ prepared ligand-free silica-supported Cu nanoparticles for the homocoupling reaction of bromamine acid (**Scheme 52**). The catalyst could be used five times under the same reaction conditions with a low loss of activity, providing comparable yields for each run.



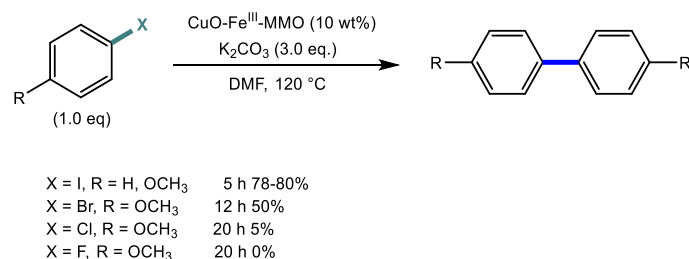
Scheme 52. Cu⁰-SiO₂-catalyzed Ullmann homocoupling reaction of bromamine acid.²⁶⁵

García *et al.*²⁶⁶ synthesized a graphene-supported Cu₂O species (Cu₂O-G) for the homocoupling of iodobenzene (**Scheme 53**). The conversion was low (26%) and the selectivity for the resulting biphenyl product was 78%. However, the catalyst could only be recycled once (for the second run, the conversion and the selectivity were 27% and 78%, respectively) as the graphene film exfoliated during the reaction. Furthermore, high temperature and basic conditions were necessary in the reaction.



Scheme 53. Ullmann homocoupling of aryl halides using graphene-supported Cu₂O species.²⁶⁶

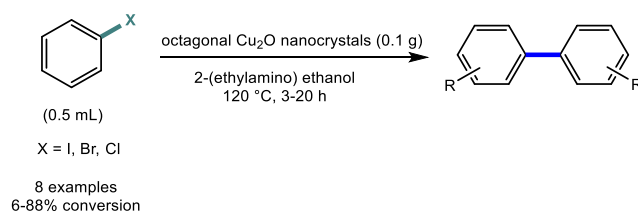
In 2016, Selvakannan and co-workers²⁶⁷ reported a novel copper-based bimetallic catalyst for the ligand-free homocoupling reactions of aryl halides (**Scheme 54**). The Cu-Fe mixed metal oxide (CuO-Fe^{III}-MMO) derived from a Cu-Fe layered double hydroxide (LDH) through thermal decomposition at 600 °C for 4 h. A limited scope of reactants has been explored under the optimal conditions, which required an excess of base and DMF as solvent at high temperature. The results showed that moderate and high yields of the biphenyl products could be obtained in the transformations of aryl iodides and bromides, whereas the reactions of chlorides and fluorides did not occur even after prolonged reaction times. Recycling studies were performed for the homocoupling reaction of *para*-iodoanisole. The result indicated that the catalyst could be reused for five times with a negligible decrease in activity (from 80% to 78% yield).



Scheme 54. CuO-Fe^{III}-MMO-catalyzed homocoupling of aryl halides.²⁶⁷

Sarkar *et al.*²⁶⁸ recently developed a series of Cu₂O nanocrystals supported on glucose with well-defined sizes and shapes (**Scheme 55**). The morphology-controlled Cu₂O nanocrystals exhibited high activity for the base-free Ullmann homocoupling reactions of aryl halides, but

high temperature was required (120 °C). For chlorobenzene, a 62% conversion was observed over octagonal Cu₂O nanocrystals, indicating that the size and shape-dependent properties of Cu₂O nanocrystals were critical for the activity of the aryl halide. The catalyst could be reused for several times and hot filtration test indicated that no further transformation occurred after removing the catalyst from the reaction mixture. ICP analysis showed that only a negligible amount of Cu was detected, which indicated that the reaction was promoted under heterogeneous conditions.



Scheme 55. Cu₂O nanocrystals-catalyzed homocoupling of aryl halides.²⁶⁸

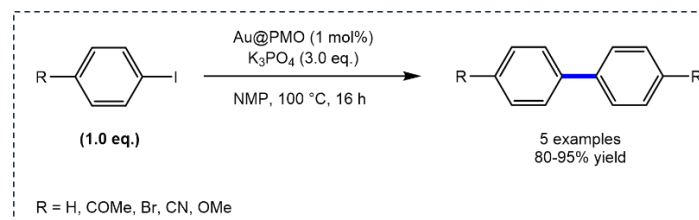
2.2.3. Other metal-catalyzed homocoupling of aryl halides

In addition to palladium and copper as catalysts for the homocoupling reaction of aryl halides, some other metals, such as Au-, Ni-, Co-, Mn- and Fe-based catalysts, have also successfully catalyzed the reaction and provided good yields. Several examples have been reported in a recent review published by Stefani *et al.*²⁵⁵ Interestingly, no Au-catalyzed homogeneous homocoupling of aryl halides has been reported but three gold-based heterogeneous catalysts were developed for this reaction. Some examples of homocoupling of aryl halides catalyzed by different metals will be presented in this work, respectively.

2.2.3.1. Au-catalyzed heterogeneous homocoupling of aryl halides

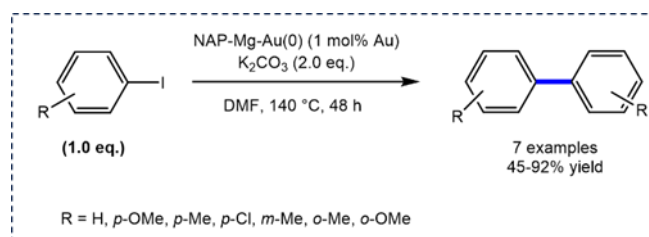
In 2011, Karimi and co-workers²⁶⁹ first developed Au nanoparticles supported on a bifunctional periodic mesoporous organosilica (Au@PMO) for homocoupling of aryl iodides. Au@PMO, as an efficient and reusable heterogeneous catalyst, could promote the reaction in the presence of K₃PO₄ in *N*-methyl-2-pyrrolidone (NMP) at 100 °C, providing good to excellent yields (80-95%) of the expected dimer products (**Scheme 56**). It was worth noting that this novel gold catalyst exhibited high reactivity and selectivity for the formation of biaryls from aryl iodides, and no reduction products were observed. However, this protocol was not applicable for the coupling of aryl bromides even upon increased temperature, up to 130 °C, increased catalyst loading to 2 mol% and with a prolonged reaction time (36 h). Recyclability of Au@PMO was

studied with the homocoupling of iodobenzene, and the results showed that the catalyst could be reused for five times without obviously catalytic activity loss. The amount of Au species leached into the solution after each run was negligible (< 1 ppm) as measured by atomic absorption spectroscopy (AAS).



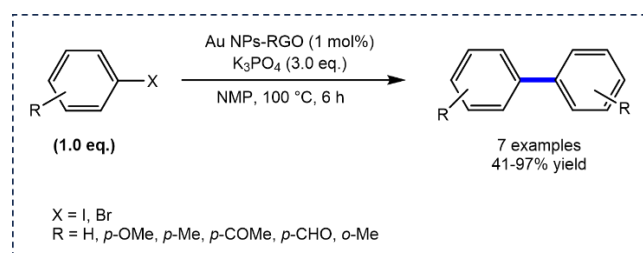
Scheme 56. Au@PMO-catalyzed homocoupling of aryl iodides.²⁶⁹

Shortly after, Maheswaran's group²⁷⁰ reported a nanocrystalline magnesium oxide-supported catalyst made of gold nanoparticles (NAP-Mg-Au(0)) for the Ullmann homocoupling of aryl iodides (**Scheme 57**). This efficient heterogeneous catalyst (1 mol%) exhibited high activity in the model homocoupling of 4-iodoanisole with excess K_2CO_3 as base and DMF as solvent at high temperature, providing 78% yield of the expected biaryl. Several aryl iodides substituted with different functional groups were employed under the optimal conditions, but aryl iodides bearing electron-donating groups at the *ortho* position led to lower yields than the *para*-substituted analogs. The recyclability of NAP-Mg-Au(0) was examined in the model reaction. It was observed that the yield of the biaryl compound stepwise dropped (from 78% to 66%) when the catalyst was recovered by simple centrifugation and directly reused in the next three runs. The Au content in the NAP-Mg-Au(0) recovered after three reaction cycles was determined by ICP-OES. The result revealed that approximately 9.5% of Au content was lost from the fresh catalyst. This might be the underlying reason for the gradual decrease of yield after each run. Interestingly, the solution containing the leached gold species after removing the catalyst was not active for the reaction, indicating that the reaction was a truly heterogeneous process.



Scheme 57. NAP-Mg-Au(0)-catalyzed homocoupling of aryl iodides.²⁷⁰

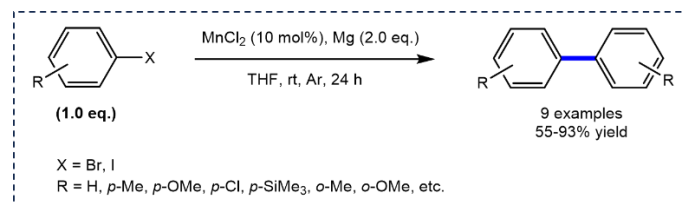
In 2013, Dabiri and co-workers²⁷¹ also published a gold nanoparticle stabilized on reduced graphene oxide (Au NPs-RGO) as an efficient and reusable heterogeneous catalyst for the homocoupling of aryl iodides. Aryl bromides containing electron-withdrawing groups (*para*-CHO and *para*-COCH₃) were coupled for the first time in the presence of this catalyst with 41-68% yields of the dimers (**Scheme 58**). Another advantage of this catalyst over the other two Au-catalysts discussed above was that lower reaction times were required in the reaction to afford good yields of biaryls. Recyclability of the Au-based catalyst was explored with the homocoupling of iodobenzene. The results showed that this catalyst could be recovered by simple filtration and reused for over six times without obvious loss of activity.



Scheme 58. Au NPs-RGO-catalyzed homocoupling of aryl halides.²⁷¹

2.2.3.2. Mn-catalyzed homocoupling of aryl halides

Yuan and co-workers²⁷² reported an efficient one-pot Ullmann-type coupling reaction using a stoichiometric amount of metallic magnesium and catalytic amount of MnCl₂. This reaction was carried out in THF at room temperature without external base and ligand, providing an economical and environmentally friendly method for the synthesis of biaryls (**Scheme 59**). Several aromatic halides were employed under these conditions, affording the expected dimers in yields up to 93%. To the best of our knowledge, this was the only manganese-catalyzed homocoupling of aryl halides to date. Unfortunately, the mechanism is not clear yet.

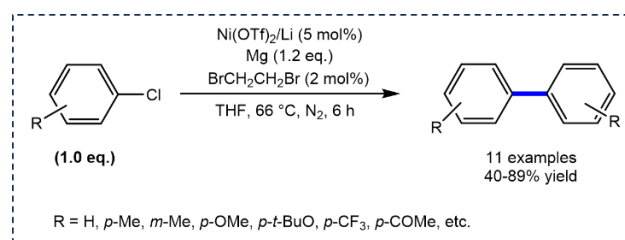


Scheme 59. MnCl₂-catalyzed homocoupling of aryl halides.²⁷²

2.2.3.3. Ni-catalyzed homocoupling of aryl halides

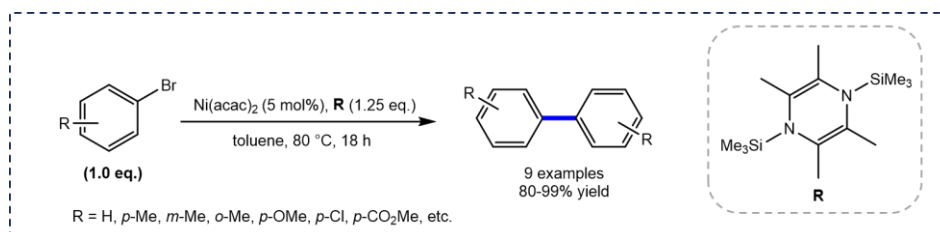
Li *et al.*²⁷³ reported a one-pot homocoupling of aryl chlorides catalyzed by nickel triflate (Ni(OTf)₂) with metallic Mg and Li in 2009 (**Scheme 60**). A variety of aryl chlorides provided

the desired biaryl products in moderate to good yields under the reaction conditions. When aryl chlorides contained electron-donating groups, only *meta*- and *para*-substituted aryl chlorides could be converted to the expected dimers. Furthermore, aryl chlorides bearing electron-withdrawing groups have a strong tolerance to the reaction conditions but with low yields. The nickel triflate catalyst could be easily recovered from the aqueous layer during the work-up and could be reused effectively without significant loss of activity.



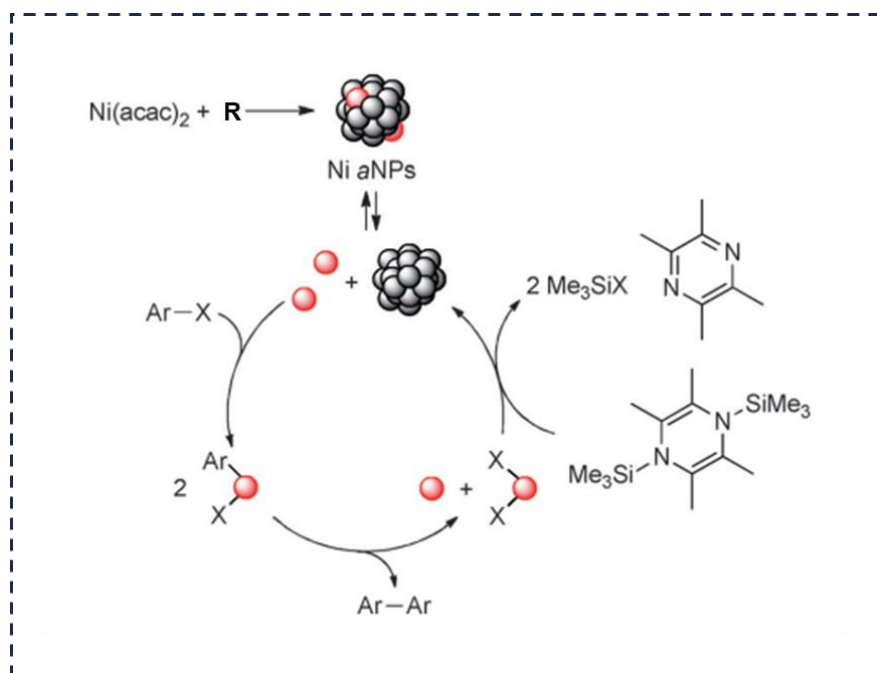
Scheme 60. Ni(OTf)₂-catalyzed homocoupling of aryl chlorides.²⁷³

Recently, Sato and co-workers²⁷⁴ developed amorphous nickel(0) nanoparticles (Ni *a*NPs) to promote the reductive Ullmann coupling reactions. This effective catalyst was obtained *via* a reduction reaction of [Ni(acac)₂] with 2,3,5,6-tetramethyl-1,4-bis(trimethylsilyl)-1,4-diaza-2,5-cyclohexadiene (**R**) as reductant. Various aryl bromides bearing electron-donating and electron-withdrawing groups were tolerated in the Ni(acac)₂/**R** catalytic system. Only aryl bromides bearing a substituent at *meta*- or *para*-position could be applied as substrates (**Scheme 61**).



Scheme 61. Ni nanoparticles-catalyzed homocoupling of aryl bromides.²⁷⁴

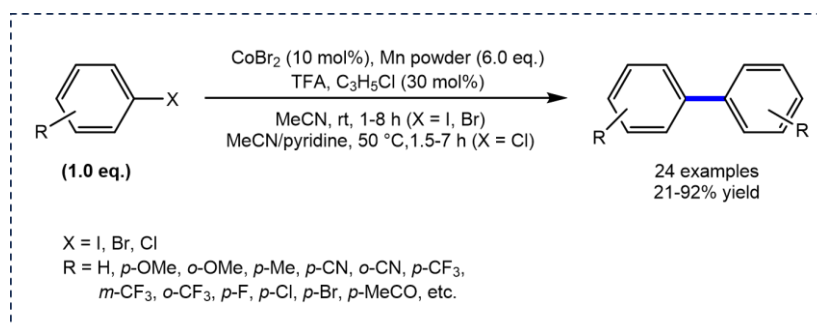
The authors proposed a mechanism for the reaction (**Scheme 62**). Ni(acac)₂ and **R** generated the Ni *a*NPs *in situ*, then some Ni⁰ species leached from the Ni *a*NPs. Subsequently, these Ni⁰ species were oxidized by the aryl halide to produce NiX(Ar), and the latter was later converted to the expected homocoupling product, NiX₂ and Ni. Finally, NiX₂ was reduced by the heterocycle **R** to furnish Ni⁰ again as active catalytic species. During this cycle, Ni *a*NPs played a pivotal role in providing Ni⁰ to the reaction system.



Scheme 62. Proposed mechanism for Ni aNPs-catalyzed reductive homocoupling of aryl halides.²⁷⁴

2.2.3.4. Co-catalyzed homocoupling of aryl halides

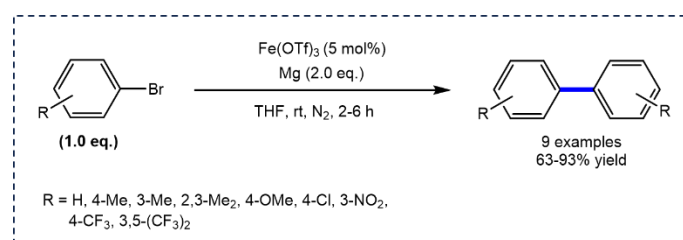
Gosmini and co-workers²⁷⁵ reported a cobalt-catalyzed homocoupling reaction of aryl halides. The homocoupling was initiated using CoBr_2 as the catalyst in the presence of manganese powder and traces amounts of trifluoroacetic acid (TFA) (**Scheme 63**). The use of allyl chloride could decrease the amount of the reduction products without affecting the reaction kinetics, as allyl chloride did not react with the active catalytic species²⁷⁶. Solvent screening showed that the reaction did not occur at room temperature when THF, DMF, and toluene were used as reaction solvents, respectively, even with pyridine as a co-solvent. The fact that reaction could be conducted in MeCN indicated that MeCN probably acted as a ligand for the cobalt active species.



Scheme 63. CoBr_2 -catalyzed homocoupling of aryl halides.^{275,276}

2.2.3.5. Fe-catalyzed homocoupling of aryl halides

Zhang and co-workers²⁷⁷ reported a Fe(OTf)₃-catalyzed homocoupling reaction of aryl bromides in the presence of magnesium strips in anhydrous THF (**Scheme 64**). The catalyst could be recovered from the aqueous layer during the work-up and reused in subsequent run with a consistently high product yield of 81%. Aryl bromides substituted with electron-donating groups at the *meta*- or *para*-positions provided the homocoupling products in high yields. Aryl bromides substituted with strong electron-withdrawing groups, such as trifluoromethyl and nitro group, were well tolerated under the reaction conditions.



Scheme 64. Fe(OTf)₃-catalyzed homocoupling of aryl bromides.²⁷⁷

2.3. Homocoupling of arylboronic acids

Homocoupling reaction of arylboronic acids (ABAs) is a frequently occurring side-reaction in cross-couplings, such as Suzuki-Miyaura^{278,279} and Chan-Lam^{280,281} reactions, but only a limited number of reports have been published on the development of synthetic protocols of this reaction. The dominant strategies for these reactions are still using stoichiometric or catalytic amounts of palladium complexes or copper salts with additional base and ligands.^{221,255} There are also some reports using other metals like Au²⁸²⁻²⁸⁵, Fe²⁸⁶ and Rh²⁸⁷-based catalysts with specific reaction conditions (e.g. the necessity of high temperature, hazardous solvents, oxidant, base and complex ligand).

As far as we know, only a few examples regarding the palladium-catalyzed and copper-based heterogeneous versions have been published. Here we will present the current development of this reaction catalyzed by palladium and copper catalysts under homogeneous and heterogeneous conditions, respectively.

2.3.1. Pd-catalyzed homocoupling of arylboronic acids

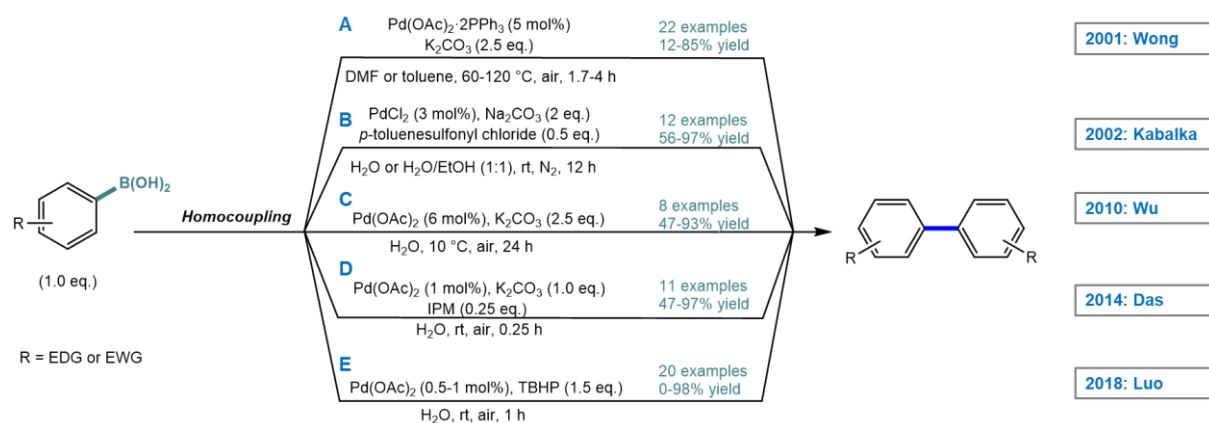
2.3.1.1. Pd-catalyzed homogeneous homocoupling reactions

In 2001, Wong and co-workers²⁸⁸ reported a Pd salt-catalyzed homocoupling of ABAs in the presence of base (K_2CO_3) and phosphine ligand (PPh_3) (**Scheme 65, A**). However, toxic solvents, DMF or toluene, and high temperature were necessary to promote the reaction.

Kabalka *et al.*²⁸⁹ also subsequently developed a catalytic Pd salt-mediated homocoupling of ABAs, which similarly required the presence of a base, specific additive as well as an inert atmosphere (**Scheme 65, B**).

Wu's²⁹⁰ and Das's groups²⁹¹ improved the $Pd(OAc)_2$ -catalyzed homocoupling conditions of ABAs, allowing the reaction to be performed under mild condition in water under air, respectively. Nevertheless, a base was still necessary (**Scheme 65, C and D**).

More recently, Luo and co-workers²⁹² reported a palladium-catalyzed oxidative homocoupling of ABAs in water at ambient conditions in the absence of base. However, a specific oxidant *tert*-butyl hydroperoxide (TBHP) was employed, and this reagent was unsafe from a practical perspective (**Scheme 65, E**).



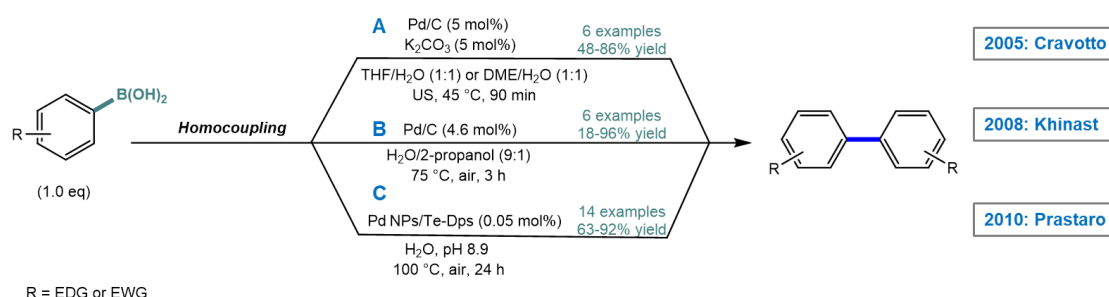
Scheme 65. Pd-promoted homogeneous homocoupling of ABAs.²⁸⁸⁻²⁹²

As described above, these methods are associated with various limitations, such as the need for hazardous solvent, base, additive, long reaction times and limited substrate scope, which are unsatisfactory from an economic and ecological point of view.

2.3.1.2. Pd-catalyzed heterogeneous homocoupling reactions

To the best of our knowledge, there are only three reports related to the Pd-catalyzed heterogeneous homocoupling of ABAs.

Cravotto *et al.*²⁹³ reported a Pd/C-catalyzed ligand-free homocoupling of ABAs in aqueous media under high-intensity ultrasound (US) (**Scheme 66, A**). This approach provided biaryls in moderate to good yields within 90 min. Moreover, the same products could be obtained in DME with comparable yields under microwave (MW) irradiation conditions.



Scheme 66. Pd-catalyzed homocoupling of ABAs under heterogeneous conditions.²⁹³⁻²⁹⁵

In 2008, Khinast *et al.*²⁹⁴ reported a Pd/C-catalyzed homocoupling reaction of ABAs in a mixture solvent of H₂O/2-propanol (9:1 volume ratio) at 75 °C under air (**Scheme 66, B**). No base and ligand were required for promoting the reaction, and the heterogeneous nature of the catalysts made the process operationally simple. Several arylboronic acids have been employed under these conditions, affording the expected biaryls in good to excellent yields. However, the incorporation of the methylthio group resulted in a low yield (18%), indicating that the presence of sulfur negatively impacts the catalytic activity of this catalyst.

Prastaro *et al.*²⁹⁵ synthesized palladium nanoparticles immobilized on a thermostable DNA binding protein from starved cells (Dps) derived from the bacterium *Thermosynechoccus elongates* (Te-Dps) for the homocoupling of ABAs in 2010. This Pd-based catalytic system provided an efficient method for the synthesis of biaryls in water under air using only 0.05 mol% catalyst loading in the presence of a 0.1M Tris-HCl buffer (pH 8.9) (**Scheme 66, C**).

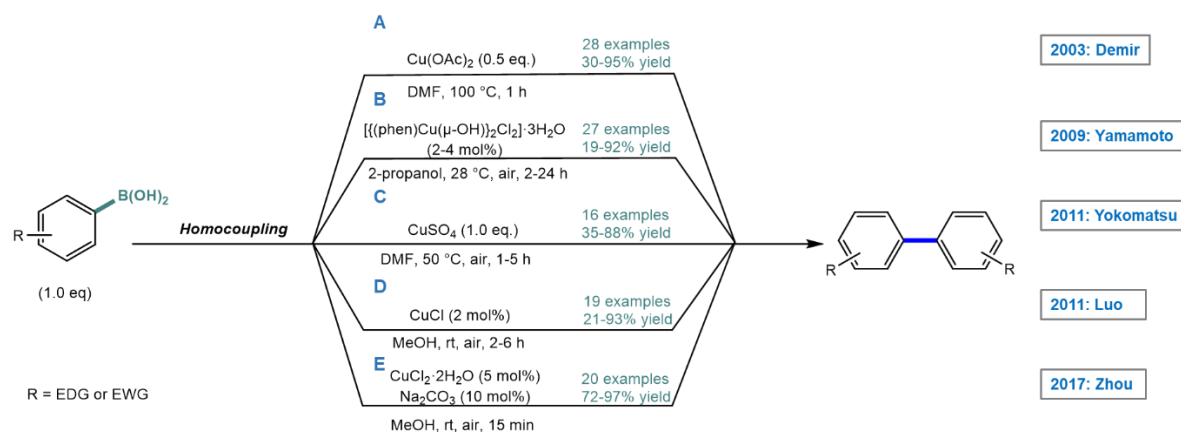
2.3.2. Cu-catalyzed homocoupling of arylboronic acids

2.3.2.1. Cu-catalyzed homogeneous homocoupling reactions

Although some palladium-catalyzed methods for the synthesis of symmetrical biaryls through homocoupling reactions of ABAs have been reported, using cheap and readily available Cu catalysts is still highly desirable.

Demir *et al.*²⁹⁶ first reported the synthesis of symmetrical biaryls by Cu-mediated homocoupling of ABAs in 2003. They found that both Cu(I) and Cu(II) species could promote

the reaction without any additive in DMF to provide the expected products in moderate to high yields (**Scheme 67, A**). However, a high reaction temperature and high amounts of $\text{Cu}(\text{OAc})_2$ as well as an O_2 atmosphere were required.



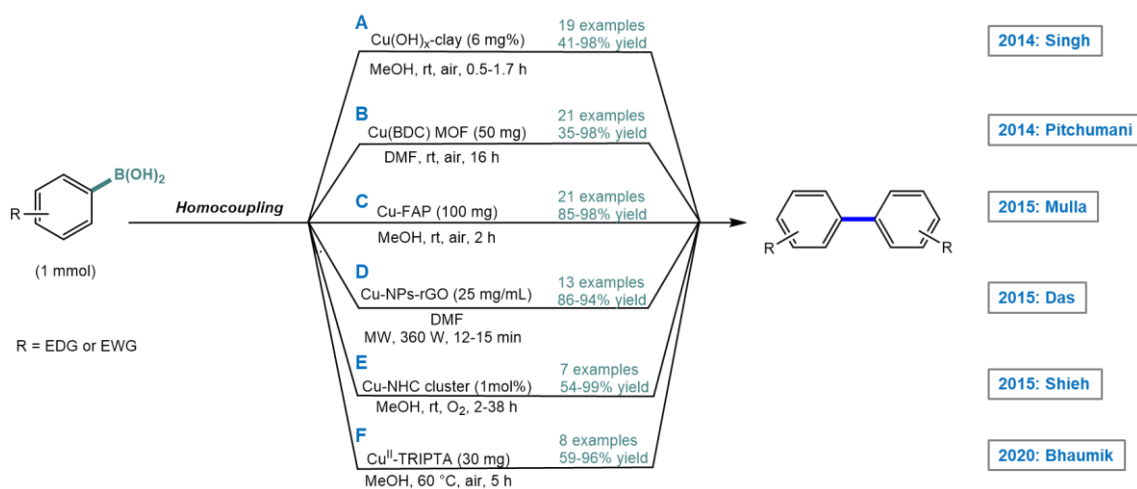
Scheme 67. Copper-promoted homogeneous homocoupling of ABAs.²⁹⁶⁻³⁰⁰

In 2009, Yamamoto and co-workers²⁹⁷ successfully performed the homocoupling of ABAs with a $\text{Cu}(\text{II})/1,10\text{-phenanthroline}$ (phen) complex catalytic system. These novel copper-catalyzed conditions allowed the reaction to proceed with a 2–4 mol% catalyst loading at milder temperature under air (**Scheme 67, B**). In addition to the Cu complexes, simple Cu salts such as CuSO_4 ²⁹⁸, CuCl ²⁹⁹, and $\text{CuCl}_2 \cdot 2\text{H}_2\text{O}$ ³⁰⁰ were also fruitfully utilized (**Scheme 67, C-E**).

2.3.2.2. Cu-catalyzed heterogeneous homocoupling reactions

As far as we know, there are less than ten copper-based heterogeneous versions that have been published.

In 2014, Singh and coworkers³⁰¹ reported a clay (montmorillonite-KSF) encapsulated $\text{Cu}(\text{OH})_x$ as heterogeneous catalytic system for the homocoupling of arylboronic acids in the absence of base and ligands at room temperature under air (**Scheme 68, A**).



Scheme 68. Homocoupling of ABAs promoted by different copper-based heterogeneous catalysts.³⁰¹⁻³⁰⁶

Metal–organic frameworks (MOFs) have become a hot topic in the field of heterogeneous catalysis in recent years. In 2014, Pitchumani and co-workers³⁰² prepared a copper terephthalate Cu(BDC) MOF as an efficient and reusable heterogeneous catalyst for the homocoupling of ABAs to yield symmetrical biaryls under mild reaction conditions (**Scheme 68, B**).

Furthermore, Mulla *et al.*³⁰³ reported a base- and ligand-free copper fluorapatite (Cu-FAP) as an environmentally benign and efficient heterogeneous catalyst for the homocoupling of ABAs under ambient reaction conditions (**Scheme 68, C**).

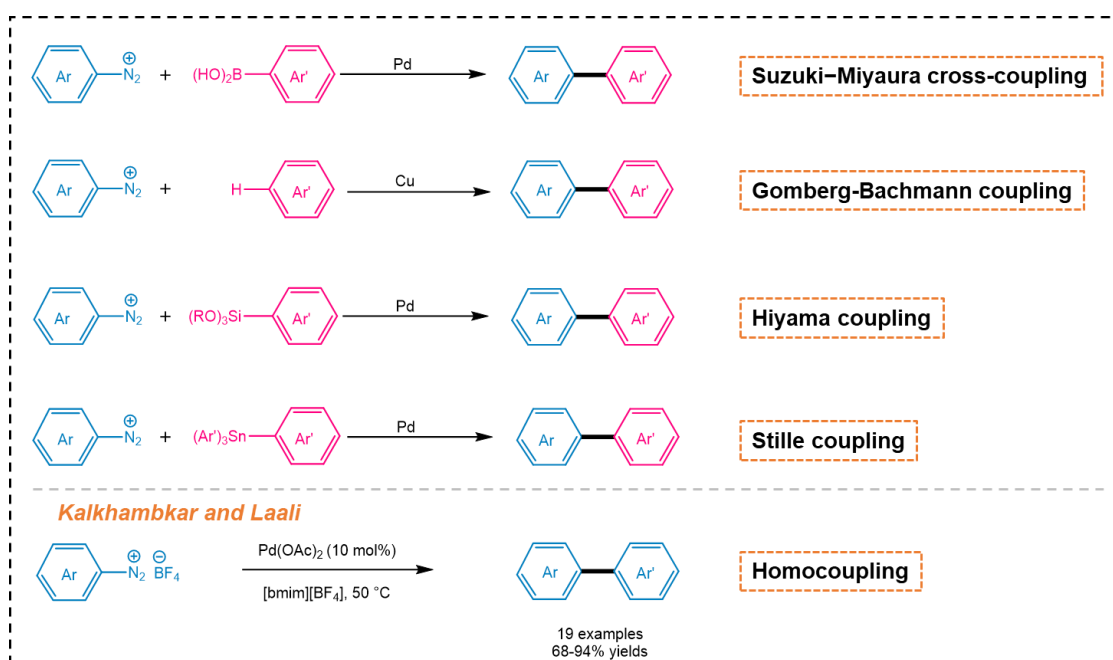
Das and co-workers³⁰⁴ synthesized copper nanoparticles (Cu-NPs) (**Scheme 68, D**) and Shieh *et al.*³⁰⁵ prepared a copper *N*-heterocyclic carbene (Cu-NHC) cluster (**Scheme 68, E**) for the synthesis of biaryl compounds *via* homocoupling reaction of ABAs.

Bhaumik's group³⁰⁶ recently performed the homocoupling of ABAs with a novel copper oxide immobilized covalent organic framework (COF) material (Cu^{II}-TRIPTA) under mild and eco-friendly conditions (60 °C, methanol as solvent) (**Scheme 68, F**).

2.4. Homocoupling of aryldiazonium salts

Aryldiazonium salts have been extensively used as building blocks in organic synthesis³⁰⁷ due to their readily availability from inexpensive anilines, and their superior reactivity.³⁰⁸ As surrogates of aryl halides, aryldiazonium salts have also been applied in coupling reactions catalyzed by transition metals for C_{aryl}-C_{aryl} bond formations (**Scheme 69, top**). In most cases, palladium and copper complexes have been used as outstanding catalysts in these coupling reactions to synthesize versatile functional molecules. These related reactions have been

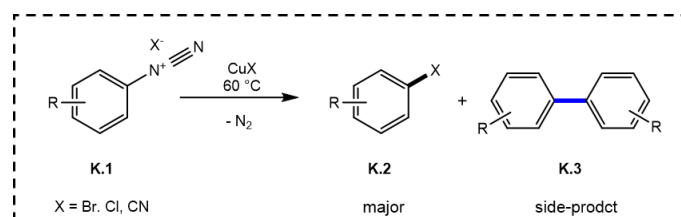
thoroughly reported in Wang and co-workers' review³⁰⁷. It should be pointed out that only one example of palladium salt-catalyzed homocoupling of aryldiazonium salts was mentioned in the literature (**Scheme 69, bottom**).³⁰⁹ To the best of our knowledge, only a few examples of homocoupling reactions of aryldiazonium salts catalyzed by transition metals have been published over the past few decades. Furthermore, there is no heterogeneous version reported so far in the literature.



Scheme 69. Transition-metal-catalyzed coupling reactions of aryldiazonium salts to form $C_{\text{aryl}}-C_{\text{aryl}}$ bonds.³⁰⁷⁻³⁰⁹

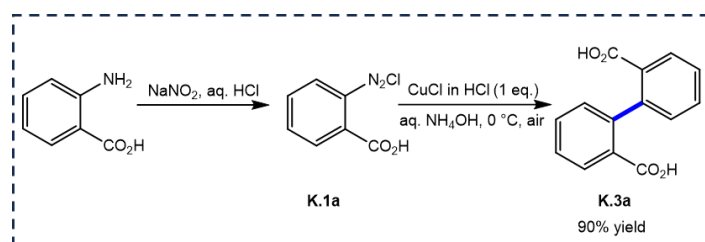
2.4.1. Homogeneous homocoupling reactions of aryldiazonium salts

As mentioned before (see Chapter II-2.1.), the copper(I)-mediated reductive homocoupling of aryldiazonium salts was initially discovered as a side reaction during studies on the Sandmeyer reaction (**Scheme 70**). This seminal work provided a new method for the synthesis of symmetrical biaryl compounds through homocoupling reactions of aryldiazonium salts.



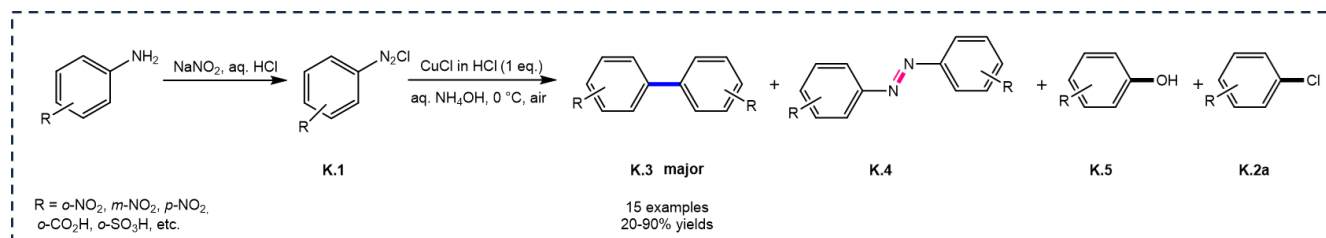
Scheme 70. Sandmeyer reaction.

In 1941, Atkinson and co-workers³¹⁰ first published the preparation of diphenic acid (**K.3a**) from the diazotized anthranilic acid *via* a reductive homocoupling reaction with yields up to 90% (**Scheme 71**). The reaction was performed in an ice bath with Cu^I species as the reduction reagent. The aqueous solution of copper(I) ions was prepared *via* a reduction reaction of an ammoniacal copper(II) sulfate solution with hydroxylamine. They found that the solution of the cupro-ammonia ion acted as an excellent reducing agent in the reaction, whereas the cupric-ammonia solutions could not convert the reaction substrate. Nevertheless, an excess of Cu^I species was necessary to reduce substrate **K.1a**. This method is thus not atom-economical nor environmentally friendly.



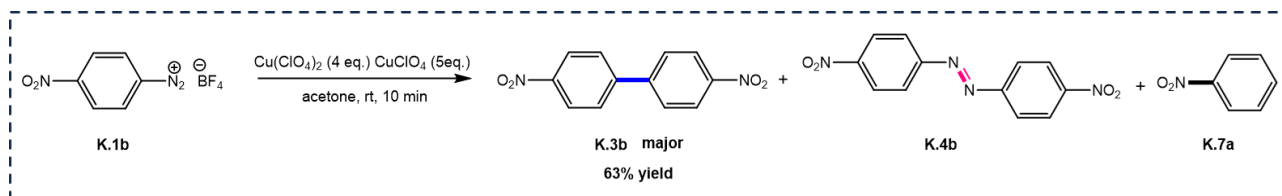
Scheme 71. Homocoupling of diazotized anthranilic acid for the synthesis of diphenic acid.³¹⁰

In 1945, based on his preliminary work, Atkinson extended the reaction scope with diverse diazotized amines.³¹¹ The same solution of copper(I)-ammonia ion was used as the reductive reagent to synthesize various symmetrical biaryls (**K.3**) with 20-90% yields from the corresponding nitro-anilines, nitro-toluidines, anthranilic acid, a variety of halogeno- and nitro-anthranilic acids, several amino naphthalene carboxylic acids, as well as *ortho*-amino benzene sulfonic acid (**Scheme 72**). A few amounts of by-products, such as phenol (**K.5**) and chlorobenzene (**K.2a**), were also observed in the reaction. However, the product scope mainly covered the biaryls substituted with special electron-withdrawing groups. The poor yields of biaryl products from substrates lacking suitable coordination groups in the *ortho*-position of the diazonium group made this method not widely applicable.



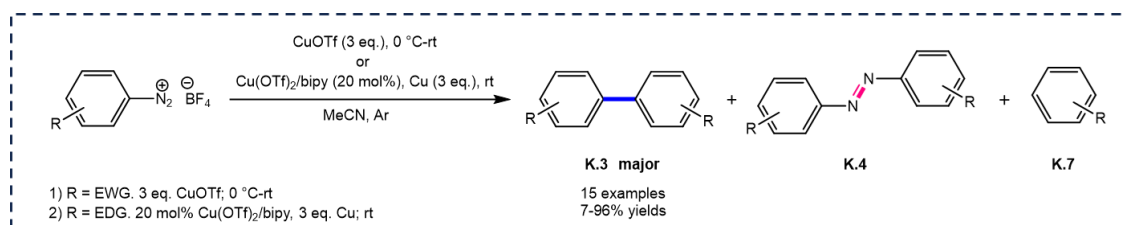
Scheme 72. The synthesis of symmetrical biaryls from various diazotized amines.³¹¹

In 1974, Cohen and co-workers³¹² found that in the presence of copper(II) perchlorate $\text{Cu}(\text{ClO}_4)_2$ (4 equiv.), copper(I) perchlorate (5 equiv.) could efficiently couple *para*-nitrophenyldiazonium tetrafluoroborate (**K.1b**) in a large volume of acetone, affording 63% yield of 4,4'-dinitrobiphenyl (**K.3b**) and few amounts of **K.4b** and nitrobenzene (**K.7a**) (**Scheme 73**).



Scheme 73. Homocoupling of *para*-nitrophenyldiazonium tetrafluoroborate.³¹²

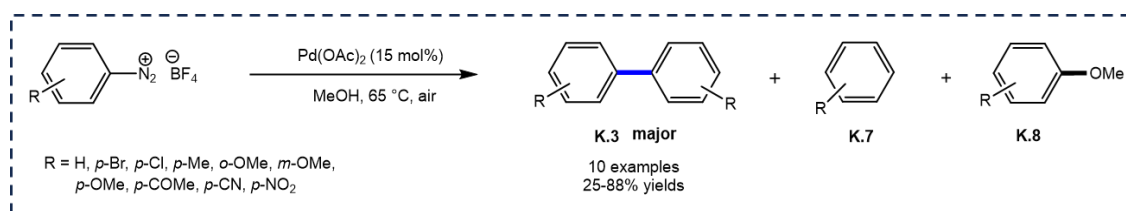
These results suggested that the homocoupling of aryldiazonium salts catalyzed by copper(I) species could proceed through an aryl-copper intermediate, but a more precise mechanism was not clarified. At that time, the development of a practical method for coupling aryldiazonium salts to symmetrical biaryls did not attract much attention, and thus research in this area has been dormant for a long time since then. It is only in 2007 that Cepanec and co-workers³¹³ published the first practical method for synthesizing symmetrical biaryls from aryldiazonium salts. The reaction was promoted by copper(I) triflate (CuOTf) in acetonitrile (MeCN) at room temperature under anaerobic and anhydrous conditions (**Scheme 74**). A series of aryldiazonium tetrafluoroborates were investigated, affording the expected products in high yields (**K.3**) and trace amounts of by-products **K.4** and benzene (**K.7**). The reaction strongly depended on the electronic nature of the aryldiazonium salts. Electron-rich substrates were converted to biaryl compounds in good yields under these conditions, whilst electron-poor substrates reacted more effectively with stoichiometric amounts of copper(I) triflate (3 equiv.).



Scheme 74. Copper salts-catalyzed homocoupling of aryldiazonium salts to symmetrical biaryls.³¹³

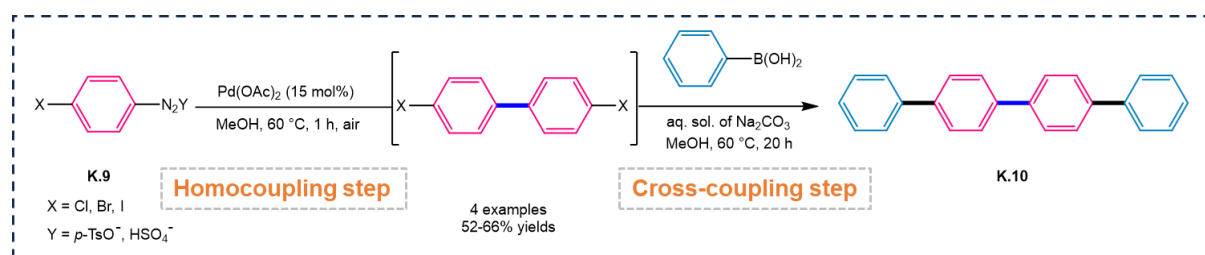
In the same year, Hanna and co-workers³¹⁴ reported a palladium-catalyzed intermolecular homocoupling of arenediazonium salts to prepare symmetrical biaryls. The reaction was carried

out in refluxing MeOH, employing catalytic amounts of palladium acetate ($\text{Pd}(\text{OAc})_2$) (15 mol%) under air without additional terminal reducing agent. The products (**K.3**) were obtained in yields ranging from 25% to 88% (**Scheme 75**). However, significant amounts of by-products, benzene (**K.7**) and anisole (**K.8**), were formed during the reaction, and the former was supposed to be generated from the reaction of arenediazonium salts with methanol. This represented the first palladium-catalyzed homocoupling of aryldiazonium tetrafluoroborates towards symmetrical biaryls, although the underlying mechanism and broader product scope are still under study.



Scheme 75. Pd(OAc)₂-catalyzed homocoupling of aryldiazonium salts.³¹⁴

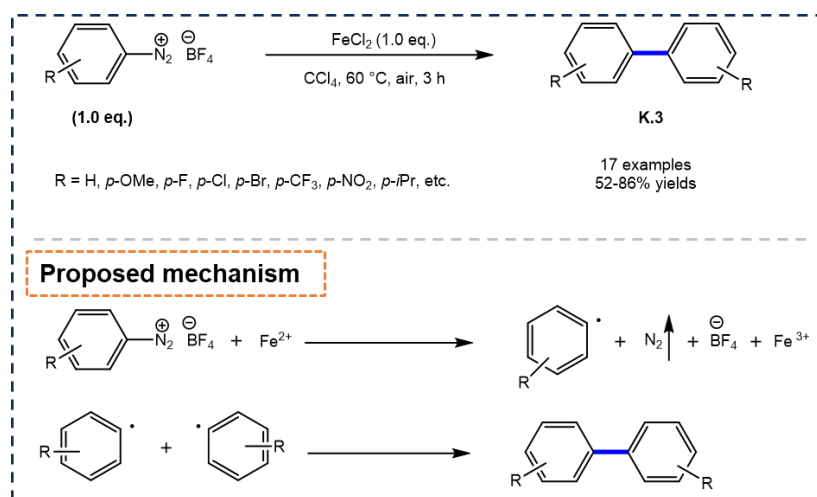
In 2011, Chi and co-workers³¹⁵ developed the palladium-catalyzed homocoupling of arenediazonium tosylate salts (**K.9**) in a one-pot process (**Scheme 76**). $\text{Pd}(\text{OAc})_2$ proved to be an efficient dual catalyst during the synthesis of *para*-quaterphenyl (**K.10**) with the homocoupling reaction as one key step. The reactivity of the arenediazonium salts (**K.9**) proved to be greater than that of the corresponding halides. This difference in reactivity was beneficial to develop an effective and practical method for the synthesis of polyaryls in a single reaction vessel.



Scheme 76. One-pot homo- and cross-coupling reactions of arenediazonium salts.³¹⁵

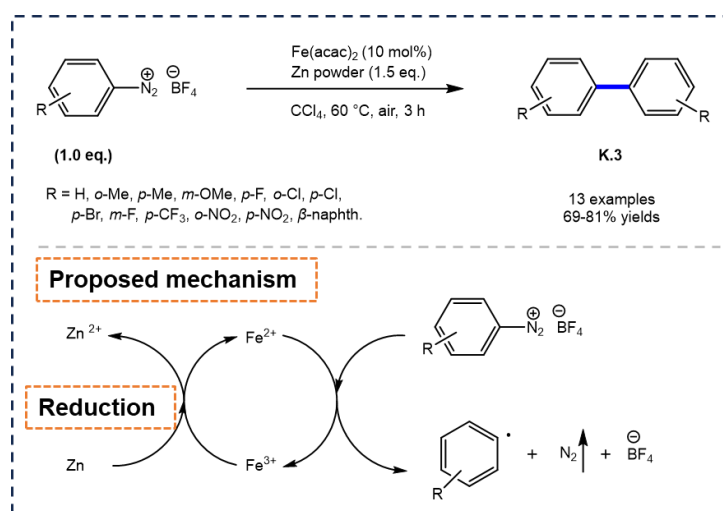
Shortly after, Cheng's group³⁰⁸ discovered a novel approach for converting arenediazonium tetrafluoroborates to their homocoupling compounds using stoichiometric ferrous salts. A solution of ferrous chloride (FeCl_2) in carbon tetrachloride (CCl_4) enabled the intermolecular homocoupling reaction to occur under mild conditions (**Scheme 77, top**). A series of substituted arenediazonium salts were successfully employed to afford biaryl compounds in 52-86% yields. Furthermore, the addition of a radical scavenger, e. g., hydroquinone or 2,6-di-*tert*-butylphenol

could terminate the ferrous chloride-promoted homocoupling of arenediazonium salts, indicating that free radicals were formed in the reaction system and that the process might undergo a single-electron transfer pathway (**Scheme 77, bottom**). Fe^{2+} induced the reduction of arenediazonium cation, resulting in the cleavage of the C–N bond and the release of N_2 gas, as well as the formation of the aryl radical and Fe^{3+} . Then, two equiv. of this aryl radical recombined, leading to the desired homocoupling biaryl product. A quantitative analysis with $[\text{K}_3\text{Fe}(\text{CN})_6]$ solution by forming a turnbull's blue precipitation ($\text{KFe}[\text{Fe}(\text{CN})_6]$) showed that more than 95% Fe^{2+} has been oxidized into Fe^{3+} during the procedure. This result suggested that the reductive homocoupling of arenediazonium salt and the oxidation of ferrous ion were stoichiometrically coupled. This new method avoided the generation of by-products due to coupling of substrate and solvent, but it was undesirable given the high toxicity of CCl_4 used as solvent and a stoichiometric amount of Fe salts was required.



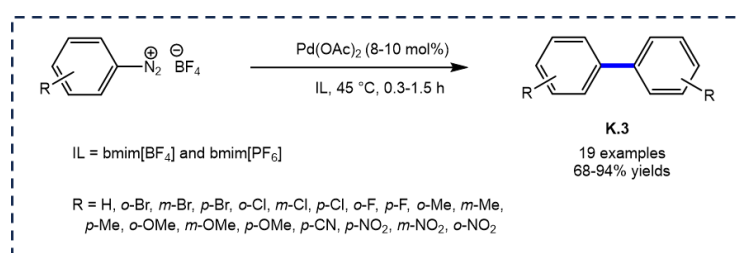
Scheme 77. FeCl_2 -catalyzed homocoupling of arenediazonium salts and proposed mechanism.³⁰⁸

Based on the proposed mechanism mentioned above, Cheng's group³¹⁶ again optimized the homocoupling conditions of arenediazonium tetrafluoroborates by regenerating Fe(II) ions from the formed Fe(III) ions with a suitable reducing agent. This allowed making this reaction efficient with catalytic amounts of ferrous ions (**Scheme 78**). The optimal conditions used 10 mol% of iron(II) acetylacetonate ($\text{Fe}(\text{acac})_2$) with Zn powder (3 equiv.) as the reductant and CCl_4 as solvent at 60 °C under air. These conditions allowed obtaining 78% of the product. A broad substrate scope, with various substituents on the phenyl ring (e.g., methyl, trifluoromethyl, halogen, nitro, methoxyl), was demonstrated with products yields from 69% to 81%.



Scheme 78. $\text{Fe}(\text{acac})_2$ -catalyzed homocoupling of arenediazonium salts and proposed mechanism.³¹⁶

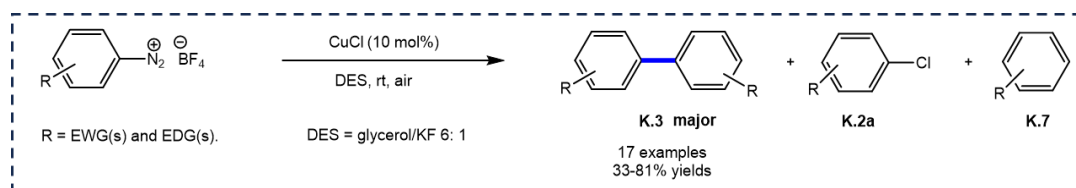
Laali and co-workers³⁰⁹ disclosed in 2016 a palladium-catalyzed intermolecular homocoupling reaction of arenediazonium salts in imidazolium ionic liquids (ILs) (**Scheme 79**). Imidazolium ILs represented ideal media since both ArN_2^+ salts and $\text{Pd}(\text{OAc})_2$ could be dissolved in the ionic liquid. A library of symmetrical biaryls was obtained with yields up to 94% under mild conditions in the absence of oxidant, ligand and additive. Notably, the ILs could be recovered and recycled at least three times with a slight decrease in product yield from 87% to 80%, making the method more economical and environmentally friendly. This approach offered the added advantage of recycling and reusing the ILs.



Scheme 79. $\text{Pd}(\text{OAc})_2$ -catalyzed homocoupling of arenediazonium salts in ILs.³⁰⁹

Based on the previous work of Capanec *et al.*³¹³, Dughera's group³¹⁷ developed a CuCl-catalyzed Ullmann homocoupling of arenediazonium salts in a deep eutectic solvent (DES). The reactions were promoted by 10 mol% CuCl under mild conditions without additive and ligand, affording various target products with yields up to 81% (**Scheme 80**). Several DESs, produced by mixing glycerol with different salts (K_2CO_3 , Cs_2CO_3 or KF), were exploited, among which the one composed of glycerol and KF in a ratio of 6:1 proved to be the optimal solvent. Furthermore, they found that the synthesis of the desired product was strongly

dependent on the order of adding reagents. The targeted homocoupling product (**K.3**) was obtained with good yields when CuCl was first added to the solvent and then adding diazonium salt; in contrast, a reduction product (**K.7**) could be formed when CuCl and aryldiazonium salts were added simultaneously. This was the first time that deep eutectic solvents were used as solvents for the homocoupling of arenediazonium salts, whose outstanding performance in the reaction provided a greener and more sustainable protocol for the synthesis of symmetrical biaryls.



Scheme 80. CuCl-catalyzed homocoupling of arenediazonium salts in DES.^{313,317}

Generally, all the above works mainly focused on palladium-, iron- and copper-catalyzed homocoupling reactions of aryldiazonium salts. Copper species should gain more attention in these reactions considering the high cost of palladium-catalyzed reactions, and the highly toxic solvent (CCl₄) required for iron-catalyzed reactions. Several novel green solvents have been used in the reaction with stoichiometric or catalytic amounts of copper(I) species, providing more sustainable and environmentally friendly protocols for the synthesis of symmetrical biaryls from arenediazonium salts, especially arenediazonium tetrafluoroborates. However, all the reactions proceed under homogeneous conditions, making it difficult to separate the product and catalyst, resulting in a waste of resources.

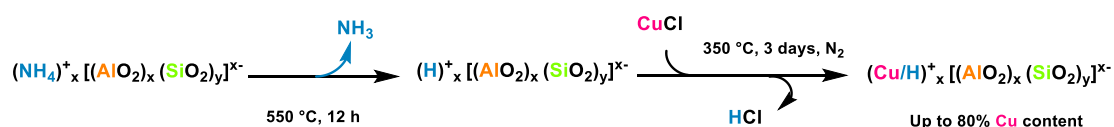
3. Our current research progresses

Before discussing my experimental results, a brief introduction to the preparation method and characterization of Cu^I-USY are provided.

3.1. Preparation of Cu^I-USY

In 2001, Slade and co-workers first prepared a Cu^I-Y zeolite *via* SSIE technique between H-Y and CuCl.⁸¹ Inspired by this work, our group³¹⁸ developed a similar protocol for the synthesis of Cu^I-USY and characterized it in details in 2009. Since then, this catalyst has been continuously employed in various organic transformations to evaluate its catalytic performance as a cheap, easy-to-prepare heterogeneous catalyst. Current research is to further expand the application scope of this home-made catalyst in organic synthesis. Therefore, I prepared the catalyst before all my experiments according to the preparation approach we developed.

The catalyst was easily prepared *via* a simple two-step ‘solid-solid calcination-ion exchange’ method (SSIE, for details, see Chapter I-2.2.4.2.1.) (**Scheme 81**). The hierarchical USY (ultra-stable Y) zeolite was obtained from the dealuminated Y zeolite (for more information, see Chapter I-1.2.1.). The catalyst was prepared from the parent H-USY and CuCl through a SSIE reaction, in which the solid mixture was heated in a furnace at 350 °C under a N₂ flux for three days. ICP-AES analysis showed that the final copper loading of the material is approximately 2.5 ± 0.5 mmol/g, indicating that about 80% of the native protons were exchanged by copper(I) ions. Although the nature and locations of residual Brønsted acidic sites need to be further investigated, the obtained Cu⁺/H⁺-USY catalyst could act as a bifunctional catalyst that already proceeded efficiently in several organic transformations.



Scheme 81. Preparation of the Cu^I-USY.

All the copper(I)-doped zeolites involved in this manuscript were prepared following the same procedure, unless otherwise stated.

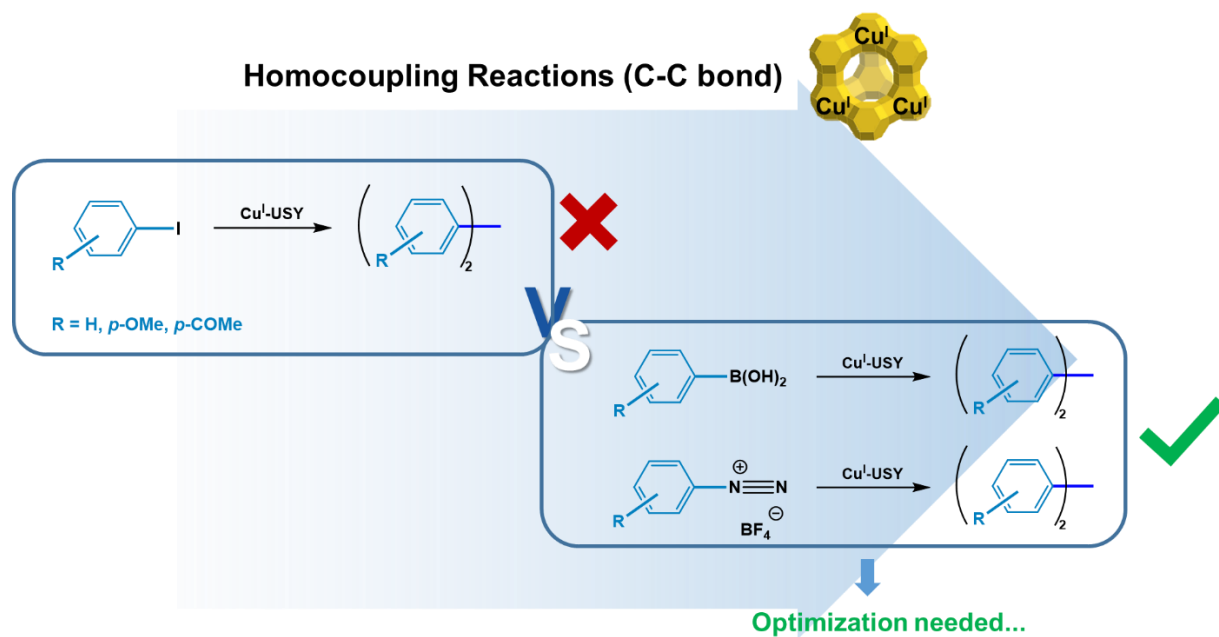
3.2. Current research themes

As described in the previous sections (see Chapter II-2.2.-2.4.), only a few publications described the formation of symmetrical biaryls through homocoupling reactions of aryl halides, arylboronic acids and aryldiazonium salts. Furthermore, most of these reactions were catalyzed by palladium or copper with bases and ligands under homogeneous conditions, resulting in various ecological problems.

In contrast to these reactions promoted by the precious metal palladium, only a minority of examples have been reported under heterogeneous conditions using cheap and abundant metal copper as a catalyst. It should be noted that none of them used stable and environmentally benign zeolites as support or catalyst to date. Therefore, it is of great significance to evaluate the catalytic potential of Cu^I-USY in these homocoupling reactions for the synthesis of symmetrical biaryls.

The formation of C_{aryl}-C_{aryl} bonds towards biaryls using different Cu^I-USY-catalyzed homocoupling reactions will be investigated in the following section.

In previous studies from our group, we have showed that Cu^I-USY was unable to catalyze Ullmann homocoupling reaction (**Scheme 82**). However, preliminary experimental results indicated that Cu^I-USY could successfully catalyze the homocoupling of *para*-methoxybenzeneboronic acid and the homocoupling of *para*-nitrobenzenediazonium tetrafluoroborate towards symmetrical biaryls. Therefore, it seemed worth investigating further the latter reactions. In this part, we focused on the optimization, reaction scope and applications of Cu^I-zeolite-catalyzed homocoupling reactions of arylboronic acids and aryldiazonium salts, respectively.



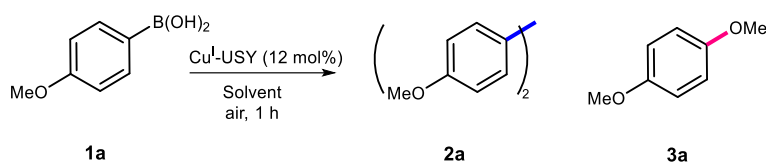
Scheme 82. Comparison of different Cu^I-USY-catalyzed homocoupling reactions towards biaryls.

4. Biaryl synthesis *via* copper(I)-zeolite-catalyzed homocoupling reaction of arylboronic acids

4.1. The optimization of reaction conditions

The *para*-methoxyphenyl boronic acid **1a** was selected as the model substrate due to its good reactivity in Chan-Evans-Lam (CEL) reactions.³¹⁹ The initial reaction was performed under conditions similar to those set up for the Chan-Lam-type C-N cross-coupling reactions we developed with Cu^I-USY as catalyst.²³¹ Different solvents and reaction temperature were first examined (Table 3).

Table 3. Screening of solvent conditions and temperature.^[a]



Entry	Solvent	Temperature (°C)	Conversion (%) ^[b]	Yield (%) ^[b]
1	CH ₂ Cl ₂	40	45	Traces
2	Toluene	65	42	Traces
3	EtOAc	65	17	Traces
4	Me ₂ CO	56	39	Traces
5	MeCN	65	40	Traces
6	<i>i</i> PrOH	65	17	Traces
7	CF ₃ CH ₂ OH	65	28	Traces
8	EtOH	65	90	25 ^[c]
9	MeOH	65	100	51^[c]; 14^[d]
10	H ₂ O	65	94	28 ^[c]
11	MeOH	25	100	38 ^[c] ; 10 ^[d]
12	MeOH	45	100	45 ^[c] ; 14 ^[d]
13 ^[e]	MeOH	65	66	13 ^[c] ; 1 ^[d]

^[a] Reactions run with *para*-methoxyphenylboronic acid (1.0 equiv. with a 0.25 M concentration) and Cu^I-USY (12 mol%) in the mentioned solvent for 1 h under air, unless otherwise stated.

^[b] Conversion and yield estimated by ¹H NMR using dimethyl terephthalate as internal standard.

^[c] Yield of 4,4'-dimethoxybiphenyl **2a**.

^[d] Yield of 1,4-dimethoxybenzene **3a**.

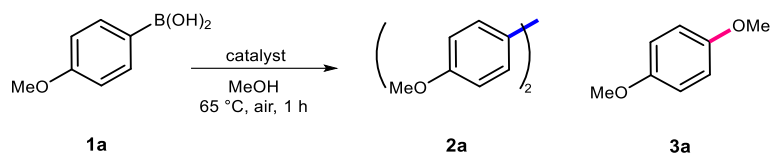
^[e] Reaction under Ar atmosphere.

The classical solvent for CEL reactions, *i.e.* dichloromethane (CH_2Cl_2), surprisingly did not allow full conversion of the substrate and only produced trace amounts of the desired product **2a** (entry 1). Toluene, which usually proved to be an outstanding solvent for zeolite-catalyzed organic transformations in our previous studies³⁹, provided reaction outcomes similar to those in CH_2Cl_2 (entry 2). Subsequently, several more polar solvents were explored, but they also afforded low to moderate conversion and **2a** was only barely detected (entries 3-5). Despite it was possible that competitive CEL coupling could occur, the reaction was performed in some protic organic solvents. Interestingly, such solvents allowed high and even full conversion in one hour (entries 6-9). As an ideal green solvent, water (H_2O) was also studied (entry 10). Among them, only methanol (MeOH) provided satisfying yield of the expected biphenyl compound **2a** (entry 9). However, and as suspected, the amount of the competitive by-products **3a** was non-negligible. Considering the possible role of H-bond, the strong H-bond donor trifluoroethanol ($\text{CF}_3\text{CH}_2\text{OH}$) was also examined, but low conversion and yield were still obtained (entry 7). Furthermore, heating was necessary in this reaction as low yield occurred at room temperature. Unfortunately, the increased reaction temperature also promoted the formation of undesired CEL product **3a** (entries 11-12 *vs* 9). In addition, running the reaction under inert atmosphere also led to lower conversion and yield (entry 13 *vs* 9).

These results proved that refluxing methanol is the best solvent for the reaction, although it has been reported as deleterious in the classical CEL reaction,¹¹ and that air is essential in the reaction.

Under the so-obtained conditions, several Cu-based catalysts were screened in the same model reaction (**Table 4**).

Table 4. Screening of catalysts and copper loading for the homocoupling of *para*-methoxyphenylboronic acid.^[a]



Entry	Catalyst	Loading (mol%)	Loading (mg)	Conversion (%) ^[b]	Yield (%) ^[b]
1	Cu ^{II} -USY	12	20	89	46 ^[c] ; 9 ^[d]
2	CuCl	12	6	100	51 ^[c] ; 17 ^[d]
3	Cu ^I -Beta	12	20	100	51 ^[c] ; 19 ^[d]
4	Cu ^I -MOR	12	20	100	47 ^[c] ; 20 ^[d]
5	Cu ^I -ZSM5	12	20	100	46 ^[c] ; 23 ^[d]
6	Cu ^I -USY	12	20	100	51 ^[c] ; 14 ^[d]
7	Cu^I-USY	6	10	100	53^[c]; 18^[d]
8	Cu ^I -USY	3	5	100	47 ^[c] ; 16 ^[d]
9	Cu ^I -USY	0.6	1	100	31 ^[c] ; 13 ^[d]
10	H-USY	12	15.4	0	0
11	NH ₄ -USY	12	20	43	Traces
12	No catalyst	0	0	42	7 ^[c] ; 2 ^[d]

^[a] Reactions run with *para*-methoxyphenylboronic acid (1.0 equiv. with a 0.25 M concentration) and catalyst in MeOH at 65 °C under air, unless otherwise stated.

^[b] Yield and conversion estimated by ¹H NMR using dimethyl terephthalate as internal standard.

^[c] Yield of 4,4'-dimethoxybiphenyl.

^[d] Yield of 1,4-dimethoxybenzene.

Since the Cu^I-USY-catalyzed model reaction was performed in air, the oxidation of Cu^I to Cu^{II} within the zeolite could be envisaged. In addition, Cu^{II} salts are the standard catalyst in the original CEL reactions⁹⁻¹¹. It was thus important to first evaluate Cu^{II}-USY as catalyst in order to clarify which copper species played a role in the reaction, since the Cu^I-USY-catalyzed model reaction was performed under air. Under the optimal conditions, the former was indeed active but less than Cu^I-USY, as both conversion and yield were lower (entry 1 vs 6). With the same copper species loading, CuCl was also evaluated; this salt provided similar results to Cu^I-

USY (entry 2 vs 6). Nevertheless, Cu^I-USY was preferred due to its simple separation and recyclability.

Due to the overall rod shape of the expected dimers **2a**, zeolites with linear internal pores would also be appropriate to host such kind of compounds. To check this possibility, a series of common zeolites with different pore sizes and shapes were loaded with copper(I) ions, characterized and applied as catalysts to the present homocoupling reaction (entries 3-5). Quite expectedly, Cu^I-Beta which exhibits two sets of channels with a rather large one (6.4 × 7.6 Å), gave results close to those achieved with Cu^I-USY and its largest pores (7.4 × 12 Å; entry 3 vs 6). Mordenite (MOR) and ZSM-5 with their smaller-sized channels (3-4 Å and 5-6 Å, respectively) provided similar results, but with a slightly lower amount of biaryl product **2a** and an increased amount of the CEL coupling product **3a** (entries 4-5 vs 3 vs 6). In contrast to what was expected, smaller-sized channel zeolites were more favorable for the coupling reaction rather than for the homocoupling reaction. Further control experiments showed that nearly no reaction took place with native zeolite or without any catalyst (entries 10-12). The latter results clearly highlighted the role of copper(I) ions in this reaction.

Cu^I-USY with large internal cage shape provided the best results in terms of conversion and yield, which was in agreement with our previous results^{19,20,38,39,181,227-229,233,318,320,321}. The catalyst loading was thus further investigated (entries 6-9), and the results showed that the yields was almost unchanged when the amount of Cu^I-USY was decreased by half (from 12% to 6%, entry 7 vs 6). However, the yields of both homocoupling product and coupling product progressively decreased when the catalyst loading was further reduced (entries 8-9 vs 6).

Based on these results and for practical and comparative reasons, we decided to set the catalyst loading for the following studies to 6 mol% to apply standardized conditions.

In addition, as is well-known, boronic acids are in equilibrium with their cyclic trimer boroxines, which can alter their reactivity. Furthermore, boronic acids in methanol could also be in equilibrium with the corresponding methyl boronate. As the latter could be the reactive species, it was worth to investigate their reactivity. Therefore, we briefly explored the reactivity of the corresponding methyl boronate and pinacol boronic ester (**Table 5**).

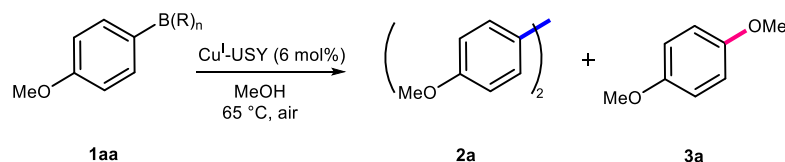
The methyl boronate exhibited good conversion and yield similar to those obtained when using boronic acid as the starting material (entry 2 vs 1). Interestingly, the formation of CEL product was significantly reduced, from 18% to 6%. However, methyl boronate is sensitive to water and is easily hydrolyzed into the corresponding boronic acid, making its preparation and

purification difficult. Furthermore, we could not exclude the possibility that it had been converted to boronic acid as our reaction was performed under air in open flask.

The pinacol boronic ester could directly couple with methanol to produce the CEL product **3a**, but also could be alcoholized to the corresponding methyl boronate in methanol. The latter subsequently produced the dimer product **2a** *via* homocoupling with the help of copper catalyst. However, the low conversion and yield of the expected biaryl product **2a** indicated that the alcoholysis rate of pinacol boronic ester was rather slow (entry 3). There was no significant change in yield of the dimer **2a** even when the reaction time was increased from 1 to 5 h (entry 4 *vs* 3). Furthermore, an increased yield of **3a** was observed when using the pinacol boronic ester as the starting material (entry 4 *vs* 1 and 2).

These results mentioned above could not reflect the hydrolysis rate of the starting boronate. Therefore, it was very hard to demonstrate which one was the real reagent in the present Cu^I-USY-catalyzed homocoupling reaction (entry 1 *vs* 2). Although similar results were obtained using boronic acid and the corresponding methyl boronate as the starting material, boronic acid was chosen for the following experiments from a practical point of view. Indeed, numerous boronic acids are commercially available.

Table 5. Cu^I-USY-catalyzed homocoupling of different boron reagents.



Entry	Boron reagent	Time (h)	Conversion (%) ^[a]	Yield (%) ^[b]
1		1	100	53 ^[c] ; 18 ^[d]
2		1	100	53 ^[c] ; 6 ^[d]
3		1	26	4 ^[c] ; 13 ^[d]
4		5	55	10 ^[c] ; 32 ^[d]

^[a] Reaction conditions: **boron reagent** (0.5 mmol, 1 eq.) and Cu^I-USY (6 mol%) in methanol at 65 °C under air unless otherwise stated.

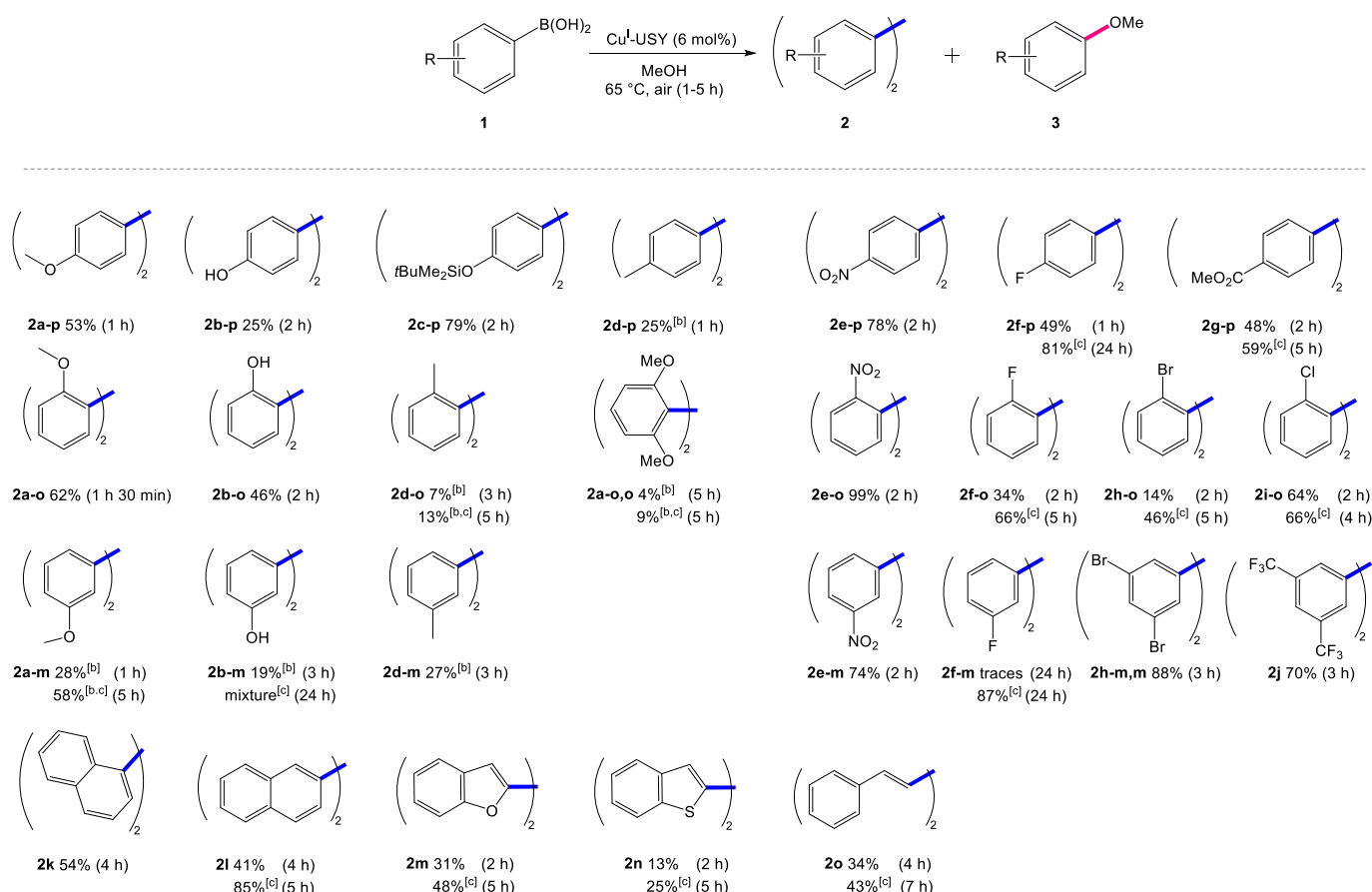
^[b] Yields estimated by ¹H NMR using dimethyl terephthalate as internal standard.

^[c] Yield of 4,4'-dimethoxybiphenyl.

^[d] Yield of 1,4-dimethoxybenzene.

4.2. Scope and limitations

Based on the above screening conditions and the suited boronic derivative, the possibilities and limitations of this Cu^I-USY-catalyzed homocoupling were further investigated, mostly with arylboronic acids substituted by different functional groups inducing various electronic or steric effects to explore their possible roles in the reaction (**Scheme 83**).



Scheme 83. Cu^I-USY-catalyzed homocoupling of various substituted arylboronic acids.^[a]

^[a] All reactions run with boronic acid **1** (0.5 mmol, 1.0 equiv.) and Cu^I-USY (6 mol%) in MeOH (2 mL) at 65 °C during 1-5 h under air until starting material is fully converted, unless otherwise stated.

^[b] Yields estimated by ¹H NMR using dimethyl terephthalate as internal standard.

^[c] Reactions performed at room temperature for 1 to 5 h until the starting material is fully converted, depending on the substrate.

As shown in **Scheme 83**, when *para*-methoxyphenyl boronic acid was used as the model substrate, it was fully converted after 1h and provided 53% yields of the isolated expected biphenyl compound **2a-p** with some coupling product **3a-p**. The hydroxy analog reacted similarly but afforded the corresponding biphenyl **2b-p** in a lower yield along with diverse side-products, which might be caused by catalytic oxidative degradation.³²² As expected, the

protection of this hydroxy group restored the formation of the homocoupling product and even increased its yield. A higher yield of the silylated derivative **2c-p** was indeed obtained, with only 4% of the CEL coupling product **3c-p**. The tolyl boronic acid also provided the desired product **2d-p** in low yields, with various side-products, probably again due to catalytic oxidative degradation.

The *ortho*-analogs of these boronic acids produced slightly higher yields of the corresponding dimers **2a-o** and **2b-o** (62-53% vs 46-25%), except again for the *ortho*-tolyl derivative **2d-o**. However, the sterically hindered *ortho-ortho*-dimethoxy-substituted analog only provided very low yields (4%) of the dimer **2a-o,o**, with 42% of the protodeboronation product and 10% of the CEL coupling product **3a-o,o**. This result indicated that the unfavorable steric effect from the crowded methoxy groups significantly reduced the homocoupling reaction of **1a-o,o**.

Comparatively, *para*- or *ortho*-substituted arylboronic acids with electron-withdrawing groups (EWG) provided higher yields of the expected dimers, even quantitative yields in some cases, than those obtained with electron-donating groups (EDG) (25% vs 78% or 99%). These results might be due to electronic effect. The EDG-substituted arylboronic acids exhibited stronger C-B bond compared to EWG-substituted derivatives, making them relatively hard to cleave and to form new intermolecular C-C bonds, resulting in lower yields of the homocoupling products.

Furthermore, in some cases, performing the reaction at room temperature proved advantageous, since higher yields could be observed (e.g. **2f-p** (49% vs 81%) and **2f-o** (34% vs 66%), as well as **2h-o** (14% vs 46%), at 65 °C and 25 °C, respectively). The latter results proved that such compounds are quite sensitive to the reaction conditions.

To further understand this discrepancy between *ortho*- and *para*-substituted arylboronic acids, the *meta*-substituted analogs, in which only inductive effects would be effective, were engaged under the same conditions. In the EDG series, the *meta*-methoxy-, -hydroxy- or -methylphenyl boronic acids afforded similar yields of the corresponding homocoupling products **2a-m**, **2b-m**, **2d-m** to those obtained for the *para*-derivatives. The results seemed to be more scattered in the EWG series. The *ortho*-nitro derivative provided the highest yields compared to its *para*- and *ortho*-analogs (99% vs 78% vs 74%, respectively). However, only traces of the homocoupling product **2f-m** were observed when the *meta*-fluorophenylboronic acid was used as the substrate under standard conditions, but satisfying yields could be obtained when the reaction was performed at room temperature (87%). Furthermore, its *para*-analog showed the same trend with a higher yield of the expected product **2f-p** produced at room temperature (81% vs 49%). Interestingly, the *meta*-dibromo- and 3,5-bis(trifluoromethyl)phenylboronic acid

afforded the corresponding homocoupling products **2h-m,m** and **2j** in excellent yields (88% and 70%, respectively).

Submitted to the standard conditions, the related but larger α - and β -naphthyl boronic acids also gave the corresponding expected products **2k**, **2l**, and a high yield of **2l** could be achieved if the reaction was run at room temperature (85% vs 41% at 25 °C and 65 °C, respectively). This could be explained from a thermodynamic point of view with undesired reactions prevented when the temperature decreased.

In addition, heteroaryl compounds were also briefly screened. 2,2'-bibenzofuran **2m** and 2,2'-bibenzo[*b*]thiophene **2n** were isolated at two different temperatures, and higher yields were again obtained when the reaction was performed at room temperature (48% vs 31%, 25% vs 13%, at 25 °C and 65 °C, respectively) Interestingly, styryl boronic acid could also be transformed to its dimer with moderate yield (see **2o**).

4.3. Recyclability studies of catalyst and gram-scale experiments

In addition to their low price, hydrothermal stability, and ease of preparation and handling, zeolites are environmentally benign support materials. The recoverability and recyclability of metal-doped zeolites, as with other excellent heterogeneous catalysts, should also be scrutinized to assess their heterogeneity for each new process. Therefore, the recycling of Cu^I-USY was examined in two 2.5 mmol scale experiments with the model reaction substrate **1a** (**Figure 11, A**) and one of the most reactive boronic acid **1e** (**Figure 11, B**), respectively. After each run, the catalyst was filtered, washed with solvent, and dried under vacuum, and then directly used for the next run without calcination. As is shown in **Figure 11**, the first two runs provided constant results in both cases, but the next runs surprisingly led to different results: a net decrease in yields occurred for substrate **1a**, while only a slow and classical decrease was observed for substrate **1e**, with still a good 61% yield after the 5th run. It is inevitable to lose some amounts of material due to the mechanical recovery of the catalyst at each cycle. Thus, the amount of starting material has been adapted to the recovered catalyst mass in each run. However, the progressive loss of catalyst activity was observed in both cases from the third to the fifth run, suggesting that multiple solvent washes might erode the catalyst activity.

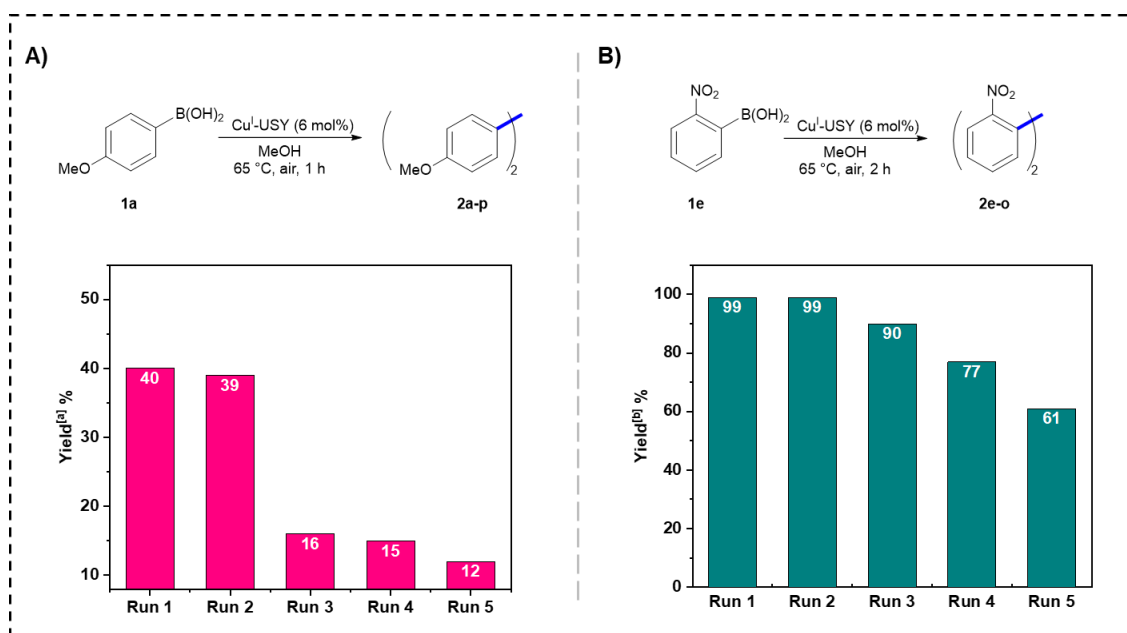


Figure 11. Recycling studies of Cu^I-USY in the successive homocoupling reaction.

^[a] Yields estimated by ¹H NMR using dimethyl terephthalate as internal standard.

^[b] Isolated yield.

To further identify the reason for such catalytic activity erosion, a Sheldon test was performed using *ortho*-nitrophenylboronic acid under the same reaction conditions (**Figure 12**). Preliminary results revealed that small amounts of active copper species leached from Cu^I-USY to the MeOH solution, since the reaction keeps running under the same reaction conditions after removing the Cu^I-USY catalyst. Although the yield of the product increased from 29% to 55% after filtration (green bar), it is by far different from the quantitative yield achieved in the presence of Cu^I-USY during the same time (blue bar). The leaching of copper species was probably another reason for the gradual decreased yield in the recyclability study, although this still needs to be confirmed by titrating the Cu content in the crude mixture by ICP analysis.

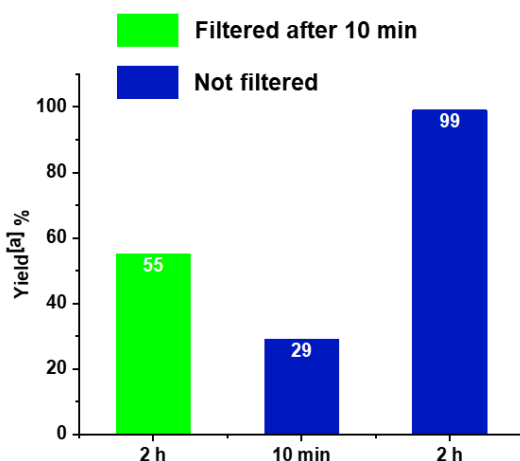
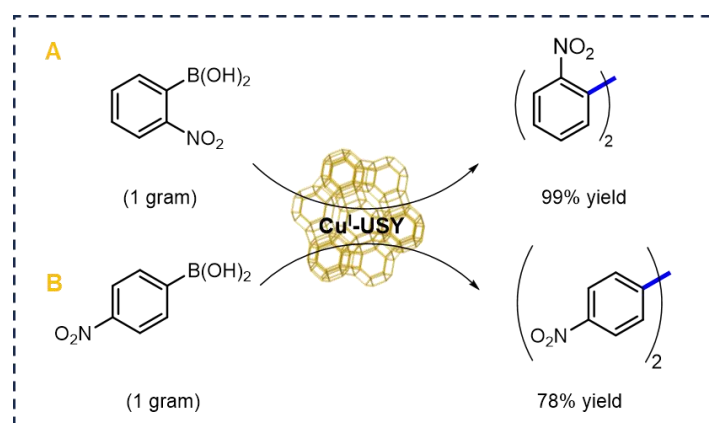


Figure 12. Sheldon test for the Cu^I-USY-catalyzed homocoupling of *ortho*-nitrophenylboronic acid.

^[a] Yields estimated by ¹H NMR using dimethyl terephthalate as internal standard.

Moreover, the possibility of scale-up of our protocol with 1-gram (6 mmol) *ortho*-nitrophenyl boronic acid was investigated, given the fact that this arylboronic acid provided excellent yields during the recycling study. As expected, 99% yield of the expected dimer **2e-o** was still observed in the gram-scale reaction (**Scheme 84, A**). Interestingly, its *para*-analog, *i.e.*, the *para*-nitrophenylboronic acid **1e**, also provided the expected homocoupling product **2e-p** in the same yield (78%) as the one obtained at 0.5 mmol scale (**Scheme 84, B**).



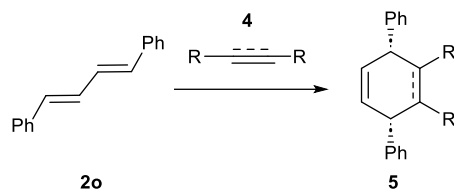
Scheme 84. Gram-scale experiments with nitrophenylboronic acids as homocoupling partners.

4.4. Cascade/one-pot synthesis based on homocoupling reaction

As the homocoupling reaction provided an efficient access to substituted diene **2o**, we envisaged combining this transformation with a Diels-Alder reaction (**Scheme 85**) to set up a cascade reaction. Therefore, *N*-phenyl maleimide and acetylene dicarboxylate were selected as

reactive dienophiles, and combined with the already obtained (*E,E*)-1,4-diphenylbuta-1,3-diene **2o** (Table 6) to evaluate the possibility of a one-pot two steps reaction.

Table 6. The optimization of Cu^I-USY-catalyzed Diels-Alder reaction.^[a]



Entry	Dienophile	Ratio (2o/4)	Catalyst loading (mol%)	Conditions ^[a]	Yield (%) ^[b]
1 ^[c]		1.2:1	0	Toluene	0
2		1.2:1	0	Toluene	84
3		1.2:1	12	Toluene	80
4 ^[d]	 4a	1.2:1	12	MeOH	18
5		1.2:1	12	MeOH	50
6		1:1	6	MeOH	34
7		1:2	6	MeOH	62
8		1:4	6	MeOH	84
9 ^[c]		1:2	6	MeOH	0
10		1:2	0	MeOH	84
11	 4b	1:2	0	Toluene	89
12		1:2	6	Toluene	85
13		1:2	0	MeOH	88
14		1:2	6	MeOH	23

^[a] Reaction conditions: 0.5 mmol (*E,E*)-1,4-diphenyl-1,3-butadiene, x mol% Cu^I-USY, in the mentioned solvent for 24 h at 110 °C under argon, unless otherwise stated.

^[b] Isolated yield unless otherwise stated.

^[c] Reaction performed under air.

^[d] Reaction performed at 90 °C.

To check its reactivity, the diene **2o** was first reacted with *N*-phenyl maleimide **4a** in refluxing toluene, a classical solvent for Diels-Alder reaction. The expected adduct **5a** was readily observed under inert atmosphere, while oxidative degradation occurred when the reaction was performed under air (entry 2 vs 1). The presence or absence of Cu^I-USY did not affect the reactivity, since nearly the same yields of **5a** were observed in both cases (entry 3 vs 2). The latter results suggest that the Cu^I-doped zeolite is probably not involved in this Diels-Alder

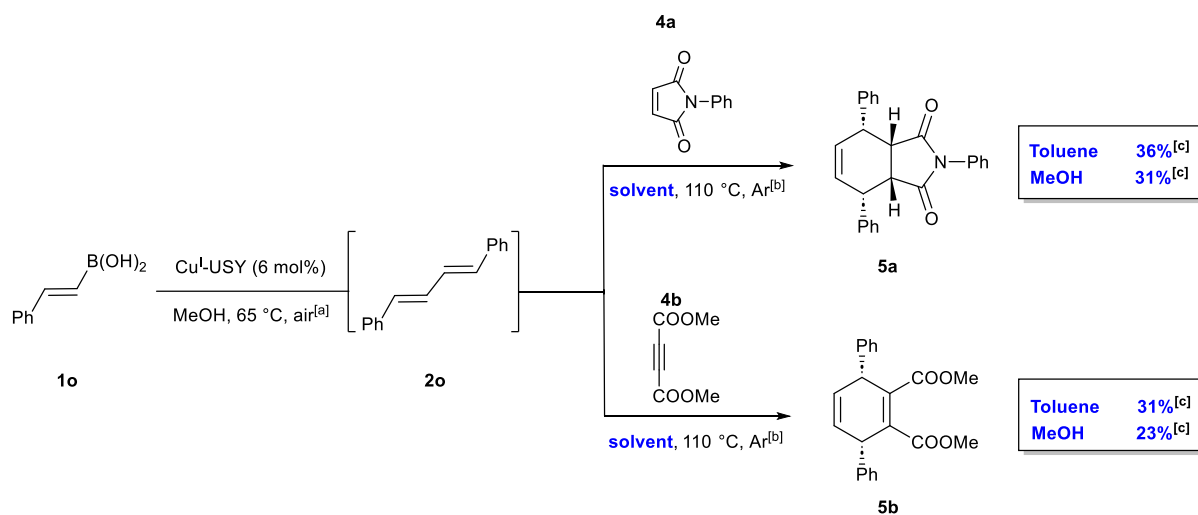
reaction. Therefore, this Diels-Alder reaction was performed in methanol for matching the Cu^I-USY-catalyzed homocoupling reaction conditions.

Interestingly, the reaction provided the desired product **5a** in useful but lower yield in this solvent (50% *vs* 80%; entry 5 *vs* 3). Varying the temperature revealed that the reaction was more efficient at elevated temperature under the same conditions (entry 4 *vs* 5). Decreasing the catalyst loading apparently decreased the product yield (entry 6 *vs* 5), but the diene-dienophile ratio turned out to be the more important factor. Indeed, high yield of the desired product **5a** was obtained when the reaction proceeded with excess of *N*-phenyl maleimide (entries 6-8). Here again, it was proved that running the reaction under air was deleterious (entry 9 *vs* 7) and Cu^I-USY did not seem to have an impact on the reactivity of the diene **2o** in methanol (entry 10 *vs* 7).

Subsequently, we switched the dienophile to the acetylene dicarboxylate **4b**. It was found that the desired product **5b** was provided in excellent yield when using toluene as the solvent with or without Cu^I-USY (entries 11-12). In contrast, similar yields were achieved in methanol only without zeolite catalyst (entry 13), while a moderate yield of product **5b** was observed in methanol in the presence of catalyst (entry 14 *vs* 13).

With these promising results in hands, we transposed the above-mentioned results into the one-pot sequence. The combination of both homocoupling and Diels-Alder indeed afforded the Diels-Alder adducts **5a** and **5b**, but the overall yields remained modest (**Scheme 85**). The yields of the desired adduct **5a** observed in toluene with *N*-phenyl maleimide **4a** as the dienophile were slightly higher than those observed in MeOH under the same conditions (36% *vs* 31%). However, the desired product **5b** was obviously provided in lower yield in MeOH than that in toluene (23% *vs* 31%) using acetylene dicarboxylate **4b** as the dienophile.

Nevertheless, the Cu^I-USY-catalyzed sequential one-pot process provided a simple and efficient method to synthesize the bicyclic products **5a** and **5b**, respectively, in an atom-economical synthetic procedure.



Scheme 85. $\text{Cu}^{\text{I}}\text{-USY}$ -catalyzed one-pot two steps processes.

^[a] Reaction run with (*E*)-2-phenylvinylboronic acid **1o** (0.5 mmol, 1 equiv.), and 6 mol% $\text{Cu}^{\text{I}}\text{-USY}$ in MeOH (2 mL) at 65 °C in air for 3 h until starting material is fully conversion.

^[b] Reaction run with (*E*)-2-phenylvinylboronic acid **1o** (0.5 mmol, 1 equiv.), and 6 mol% $\text{Cu}^{\text{I}}\text{-USY}$ in MeOH (2 mL) at 65 °C in air for 3 h, then addition of the corresponding dienophile (0.5 mmol, 1equiv.), followed by stirring in the mentioned solvent at 110 °C for 24 h under argon, unless otherwise stated.

^[c] Yields estimated by ¹H NMR using dimethyl terephthalate as internal standard.

4.5. Mechanism proposal

In our experiments, $\text{Cu}^{\text{I}}\text{-USY}$ successfully catalyzed the homocoupling reaction of boronic acids in MeOH without additional ligand and base, providing a simple and effective method for the synthesis of biaryl compounds. Such a simple protocol motivated us to get some insights about the reaction mechanism. Various mechanisms were proposed since copper species (I and II) have been applied to the homocoupling of boronic acids with base and/or ligands.^{297,300,323,324} However, some of them seem to be contradictory, and there was still no conclusion about the role of the monovalent or divalent copper ions in the catalytic cycle, ... until very recently. Indeed, the actual mechanism has been deciphered in 2022 by Grimaud and co-workers.³²⁵ After a series of NMR, experimental and theoretical studies, these authors disclosed the formation of dimeric $\text{Cu}^{\text{II}}\text{-Cu}^{\text{II}}$ complexes, which evolve into a mixed-valence $\text{Cu}^{\text{III}}\text{-Cu}^{\text{I}}$ dimer, allowing the synthesis of the biaryl compound through Cu-Cu transmetalation and reductive elimination procedures (**Figure 13**). Furthermore, they confirmed that the base plays a key role in bridging two copper species to construct these so-called dimeric complexes.

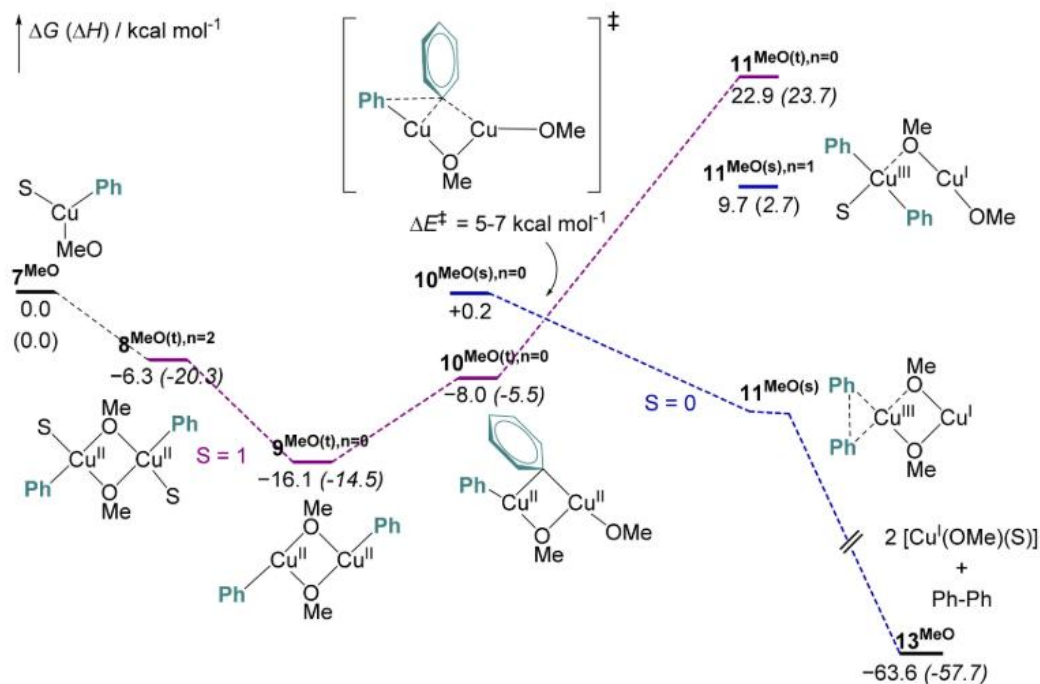


Figure 13. Gibbs energy profile of the Cu-to-Cu transmetalation and subsequent reductive elimination computed at the DFT level.³²⁵

Although it has not been ascertained yet, the presence of dimeric copper species within some zeolites has been proposed for nitrogen oxides decomposition.^{326,327} Therefore, it is extremely possible that dimeric copper complexes similar to those deduced from the above mechanistic study could occur in the so-called supercage in Y (Faujasite)-type zeolites. Indeed, it is well-known that the USY-doped Cu^I cations are located in the so-called site I', II and III' positions within the faujasite structure of zeolite (**Figure 14, left**).³²⁸ The Cu^I cations at site II and III' positions at the supercage border would be close enough to independently react with boronic acids and then be bridged by the solvent as described in the literature¹¹.

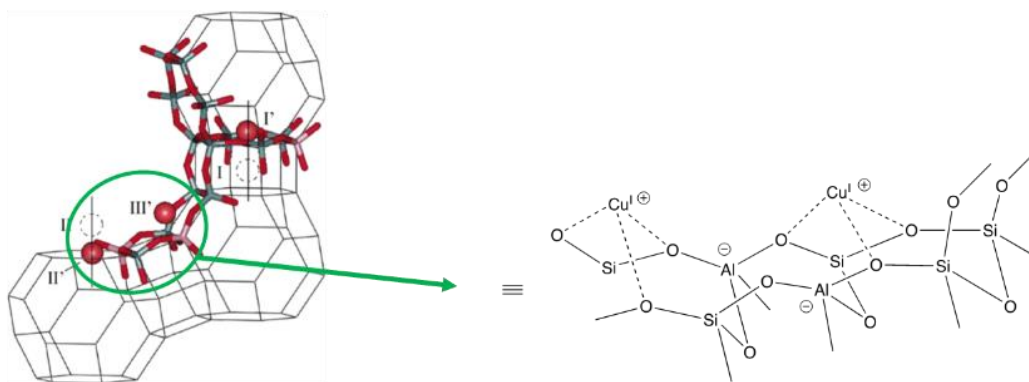
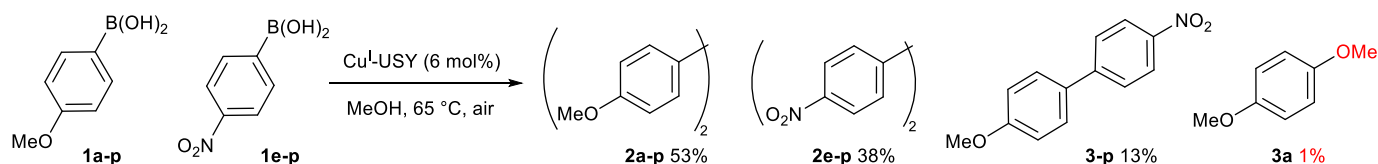


Figure 14. the location of Cu(I) species in USY zeolite.³²⁸

To evaluate such possibility, we thus performed a competition experiment as a way to test the feasibility of dimeric complexes as key intermediates in current heterogeneous homocoupling conditions (**Scheme 86**). Hypothetically, the reaction with two different boronic acids under the set-up conditions should lead to two homocoupling products with no cross-coupling product if each adduct is provided by a dimeric complex in a single zeolite cage. Indeed, when the *para*-methoxy (**1a-p**) and the *para*-nitro derivatives (**1e-p**) were mixed in a 1:1 mole ratio, the corresponding dimers **2a-p** was produced in yield similar to the independent reaction for the *para*-methoxy derivative (**1a-o**), but the yield of **2e-p** was lower than the one obtained with the *para*-nitro derivative as the sole reactant. Nevertheless, the cross-coupling product could also be detected in low yield (**Scheme 86**).



Scheme 86. $\text{Cu}^{\text{I}}\text{-USY}$ -catalyzed competition reaction between *para*-methoxyphenyl boronic acid and *para*-nitrophenyl boronic acid.^[a]

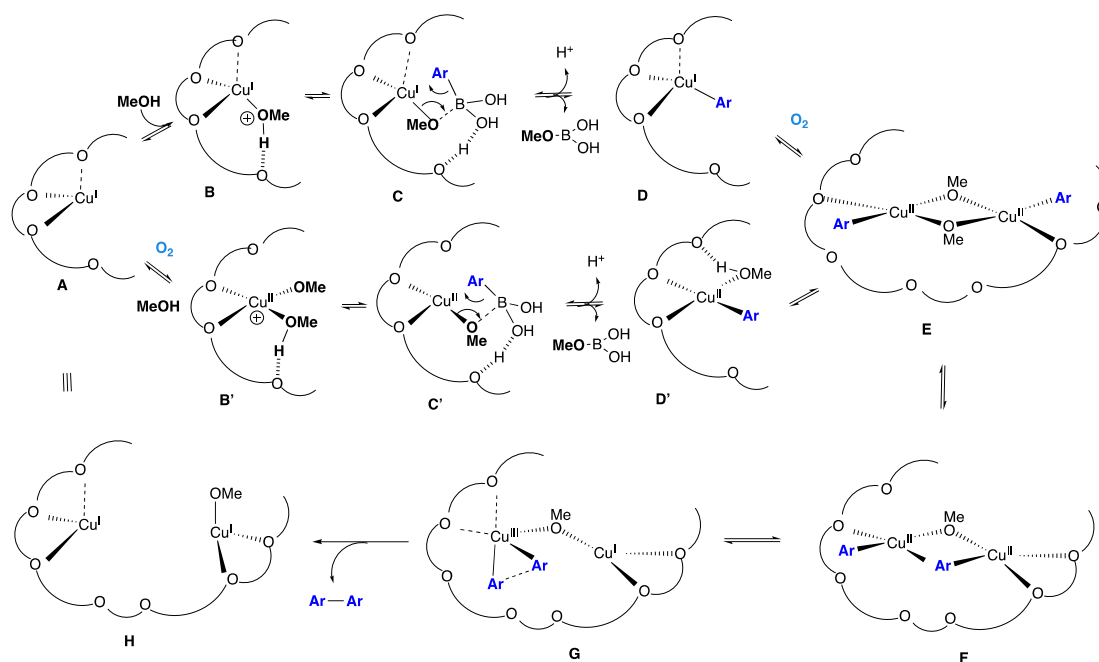
^[a] Reaction run with *para*-methoxyphenyl boronic acid **1a** (0.25 mmol, 1.0 equiv.), *para*-nitrophenylboronic acid, and $\text{Cu}^{\text{I}}\text{-USY}$ (6 mol%) in MeOH (2 mL) at 65 °C in air for 3 h until starting material is fully converted, unless otherwise stated.

^[b] Yields estimated by ^1H NMR using dimethyl terephthalate as internal standard.

As mentioned above, the presence of base, especially hydroxide, is usually mandatory for homocoupling reaction, and the recent mechanistic investigation showed its key role in the B-Cu transmetalation step. Therefore, in the absence of the base, the mechanism of this activation in the present work would be well worth exploring. As shown in **Table 3** (entries 1-9), solvents, especially hydroxylated solvents, proved to be essential for $\text{Cu}^{\text{I}}\text{-USY}$ -catalyzed homocoupling reaction. Furthermore, it could be found that the reactivity order observed in protic solvents corresponds to the Mayr nucleophilicity scale ($\text{MeOH} > \text{EtOH} > \text{CF}_3\text{CH}_2\text{OH} > \text{CH}_2\text{Cl}_2$)³²⁹. Such correlation indicates that the solvent nucleophilicity played a role in the reaction, most probably in the activating step mentioned above.

These results tend to support a mechanism in which methanol serves as a ligand to complete the copper coordination sphere within the zeolite framework and assist the transmetalation step between boronic acid and copper (see **B-C-D** and/or **B'-C'-D'** in **Scheme 87**), as well as contribute to the formation of dimeric complexes (**E**). Subsequently, the latter could allow Cu-Cu transmetalation (**F**) and reductive elimination (**G**) as reported, and lead to the formation of

desired biaryl compound. The oxygenated framework of the zeolite would act as a huge cooperative ligand in the whole procedure, stabilizing the copper intermediates and assisting in proton transfers at various stages.



Scheme 87. Mechanistic proposal for the Cu^I-zeolite-catalyzed homocoupling reaction of arylboronic acid.

5. Biaryl synthesis *via* copper(I)-zeolite-catalyzed homocoupling reaction of aryldiazonium salts

As mentioned in the bibliographic section (see Chapter II-2.4.), only a few examples of homocoupling of aryldiazonium salts have been reported. For such reactions, palladium and copper complexes have been used as catalysts under homogenous conditions, and none of them relied on heterogeneous catalyst. It was thus worth looking at such heterogeneous catalysts, and especially Cu^I-USY.

5.1. The optimization of reaction conditions

Due to its high activity in previous works, *para*-nitrobenzenediazonium tetrafluoroborate **K.1b** was selected as the substrate for the model reaction. It was thus submitted to various conditions, either the reported ones or adapted conditions (**Table 7**).

To evaluate the potential of Cu^I-USY as catalyst in the homocoupling of aryldiazonium salt, experiments were performed under some of the reported conditions mentioned above, but with Cu^I-USY instead of the reported catalyst. This would allow us to directly compare the Cu^I-USY performance to those of known copper catalysts.

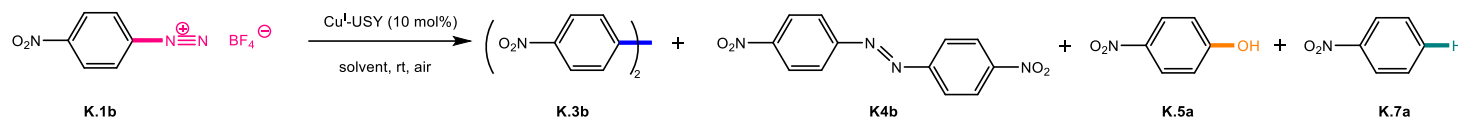
An efficient and really catalytic homocoupling of arenediazonium salts is the one described by Dughera³¹⁷ and co-workers. They used copper(I) chloride (10 mol%) but their best conditions were achieved with a deep eutectic solvent (DES) containing potassium fluoride (glycerol: KF 6:1) (entries 1-2). Unfortunately, a zeolite is not suitable for use with such solvent, due to the sensitivity of the silicoaluminate framework to fluoride. Nevertheless, we still performed a Cu^I-USY-catalyzed version in this solvent as a control reaction to compare with the developed results. As suspected, only trace amounts of the expected products were detected, regardless of whether the reaction was performed under air or an inert atmosphere (entries 3-4). The reduced product nitrobenzene (**K.7a**) could be observed as the main product in both reactions (entries 3-4). After a series of experimental and theoretical studies, these authors proposed a mechanism for the reduction reaction of aryldiazonium salts in DES (glycerol: KF 6:1), and proved that the reaction could be initiated by a formed glycerolate-like species without catalyst.³³⁰ This could be the reason for the high yield of **K.7a** in the Cu^I-USY-catalyzed homocoupling reaction of **K.1b**.

Meanwhile, another DES, safer and greener, was selected to avoid zeolite degradation. It was prepared by mixing urea and choline chloride in 2:1 ratio, and then applied to the homocoupling

of **K.1b** with Cu^I-USY as catalyst. However, only trace amounts of the expected product **K.3b** could be detected and only 30% of the reduced product **K.7a** was obtained when the reaction was performed under air (entry 5). Interestingly, an azo-compound, the 4,4'-dinitroazobenzene **K.4b**, was obtained in moderate yield (40%) during the reaction (entry 5). This compound was never found in Dughera *et al.*'s works³¹⁷. Furthermore, it was demonstrated that anoxic condition could provide slightly more **K.7a** product than **K.4b** (40% vs 30%) without significantly changing the product distribution compared to the results obtained under air conditions (entry 5 vs 6).

Dughera and co-workers³¹⁷ also mentioned that DMSO was an effective solvent for the homocoupling of arenediazonium salts. When the reaction was carried out at room temperature under air with CuCl as catalyst (10 mol%) in DMSO during 4 h, a mixture was obtained from which the homodimer was isolated with a modest 15% yield (entry 7). The de-diazotation product **K.7a** and the Sandmeyer product, *i.e.* 1-chloro-4-nitrobenzene, were also detected (entry 7). Under such conditions, but with Cu^I-USY as catalyst at the same loading, the targeted 4,4'-dinitrobiphenyl **K.3b** was isolated with a modest 22% yield. This result was slightly better than the one gained with Dughera conditions³¹⁷ (22% vs 15%; entry 8 vs 7). However, the reaction was slow and required at least 24 h. The major products were the corresponding azo-compound **K.4b** and de-diazotation product **K.7a** (35% and 30% respectively, entry 8). In contrast to the Dughera's conditions³¹⁷, *para*-nitrophenol **K.5a** was also observed, although in low yields (15%). Based on these results, a control experiment was performed in which the reaction was performed under an inert atmosphere to check whether the yield of product **K.3b** could be increased. Unfortunately, the result showed that almost no reaction occurred in this solvent in the absence of air (entry 9). For further comparison, the Dughera's work³¹⁷ using CuCl as catalyst was repeated but with a longer time, the results were similar to those with Cu^I-USY as catalyst (entry 10 vs 8). In this case, the same amount of homodimer (20% vs 22%, entry 9 vs 8), the same phenol side-product (17% vs 15%, entry 10 vs 8) and the de-diazotation product **K.7a** (27% vs 30%, entry 10 vs 8) were obtained. However, these results were different from those obtained by Dughera *et al.*³¹⁷ (entry 10 vs 7). The Sandmeyer product 1-chloro-4-nitrobenzene was surprisingly not obtained under our repeated reaction conditions (entry 10 vs 7), but the corresponding azo-compound **K.4b** and *para*-nitrophenol **K.5a** were observed (entry 10 vs 7).

Table 7. Trial reactions for the Cu^I-USY-catalyzed homocoupling of *para*-nitrobenzenediazonium tetrafluoroborate.^[a]



Entry	Catalyst (10 mol%)	Solvent	Atm.	T (°C)	Time (h)	Yields of K.3b ^[b] (%)	Yields of K.4b ^[b] (%)	Yields of K.5a ^[b] (%)	Yields of K.7a ^[b] (%)
1 ^[c]	CuCl	DES (Glycerol: KF = 6:1)	air	40	1	73	0	0	not isolated
2 ^[c]	CuCl	DES (Glycerol: KF = 6:1)	N ₂	40	2	62	0	0	not isolated
3	Cu ^I -USY	DES (Glycerol: KF = 6:1)	air	40	24	6	2	1	67
4	Cu ^I -USY	DES (Glycerol: KF = 6:1)	Ar	40	24	6	3	1	68
5	Cu ^I -USY	DES (Urea: choline chloride = 2:1)	air	50	24	0	40	1	30
6	Cu ^I -USY	DES (Urea: choline chloride = 2:1)	Ar	50	24	no	35	1	40
7 ^[c]	CuCl	DMSO	air	rt	4	15	0	0	not isolated
8	Cu ^I -USY	DMSO	air	rt	24	22	35	15	30
9	Cu ^I -USY	DMSO	Ar	rt	24	1	2	3	3
10	CuCl	DMSO	air	rt	24	20	32	17	27
11	Cu ^I -USY	DMF	air	rt	24	0	30	3	66
12	Cu ^I -USY	DMF	Ar	rt	24	0	42	1	68
13	Cu ^I -USY	MeCN	air	rt	24	0	4	13	9
14	Cu ^I -USY	Acetone	air	rt	24	0	0	8	0
15	Cu ^I -USY	EtOAc	air	rt	24	0	0	2	0
16	Cu ^I -USY	THF	air	rt	24	1	2	1	3
17	Cu ^I -USY	Toluene	air	rt	24	traces	traces	traces	traces
18	Cu ^I -USY	MeOH	air	rt	24	0	6	12	19
19	Cu ^I -USY	H ₂ O	air	rt	24	0	3	3	6

^[a] Reactions run with *para*-nitrobenzenediazonium tetrafluoroborate (0.5 mmol, 1.0 equiv. with a 0.25 M concentration) and Cu^I-USY (15 mg, 10 mol%) in the mentioned solvent for 24 h under air, unless otherwise stated.

^[b] Yields estimated from the crude mixture ¹H NMR using 1,3,5-trimethoxybenzene as internal standard, unless otherwise stated.

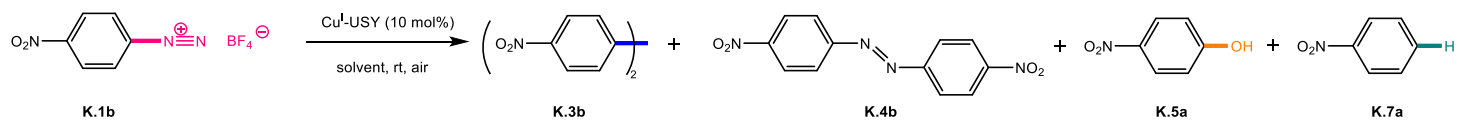
^[c] Isolated yields of **K.3b**, traces product **K.7a** and 1-chloro-4-nitrobenzene were detected, and no **K.3b** reported by Dughera's group³¹⁷.

In further attempts to increase the homocoupling product yield, reactions were also performed in several conventional organic solvents. Unfortunately, none of them allowed the formation of the expected homodimer **K.3b** (entries 11-17). The more polar solvent in this series induced the formation of the de-diazotation product **K.7a** in good yields and the azo-product **K.4b** in moderate yields with or without air (entries 11-12), while the less polar solvents provided almost no transformation, only leading to traces amount of the side-products (entries 13-17). Protic solvents also led to low conversion and the main product was again the de-diazotation product **K.7a**, although in very low yields (entries 18-19).

In another report, by Cohen and co-workers³¹², a large excess of copper(I) perchlorate (CuClO₄ 5 eq.) has also been used to produce the homocoupling product (**K.3b**) in good yields of 82%, with only traces of side-products. This was achieved within a short reaction time in acetone containing traces of water under air (**Table 8**, entry 1). Using Cu^I-USY as a stoichiometric reagent under the same conditions did not lead to any transformation, except tiny amounts of *para*-nitrophenol **K.5a** (**Table 8**, entry 2).

One of the best conditions described in literature is the one reported by Capanec and co-workers.³¹³ Performed in dried acetonitrile under argon, this reaction required an excess of copper(I) triflate and produced the desired product **K.3b** in good yields together with low yields of the reduced product nitrobenzene **K.7a** (**Table 8**, entry 3). When the same amount of Cu^I-USY was used under the same conditions, only small amounts of the homocoupling product **K.3b** and the unexpected *para*-nitrophenol **K.5a** (~10% each), as well as traces amount of nitrobenzene **K.7a** were detected (**Table 8**, entry 4). Interestingly, a high yield of the corresponding azo-compound **K.4b** (71%) was obtained (**Table 8**, entry 4). This compound had never been found in Capanec's work, which motivated us to further explore the optimal reaction conditions for the Cu^I-USY-promoted reaction of aryldiazonium salts to generate the azo-product **K.4b**. Indeed, different amounts of Cu^I-USY (from 0.1 equiv. to 5 equiv.) were employed in the reaction to evaluate the optimal conditions (**Table 8**, entries 5-10).

Table 8. Trial reactions for the Cu^I-USY-promoted homocoupling of *para*-nitrobenzenediazonium tetrafluoroborate.^[a]



Entry	Catalyst	Solvent	Atm.	T (°C)	Time (h)	Yields of K.3b ^[b] (%)	Yields of K.4b ^[b] (%)	Yields of K.5a ^[b] (%)	Yields of K.7a ^[b] (%)
1 ^[c]	CuClO ₄ (5 eq.)	Acetone	air	rt	10 min	82	18	0	traces
2	Cu ^I -USY (5 eq.)	Acetone	air	rt	24	0	0	8	0
3 ^[d]	CuOTf (3 eq.)	MeCN	Ar	0-rt	2	66	0	0	28
4	Cu ^I -USY (3 eq.)	MeCN	Ar	rt	24	15	71	10	2
5	Cu ^I -USY (0.1 eq.)	MeCN	Ar	rt	24	1	3	1	2
6	Cu ^I -USY (1 eq.)	MeCN	Ar	rt	24	7	13	6	9
7	Cu ^I -USY (2 eq.)	MeCN	Ar	rt	24	18	30	17	16
8	Cu ^I -USY (2.5 eq.)	MeCN	Ar	rt	24	27	47	17	4
9	Cu ^I -USY (4 eq.)	MeCN	Ar	rt	24	17	66	12	3
10	Cu ^I -USY (5 eq.)	MeCN	Ar	rt	24	24	54	19	4
11	Cu ^I -USY (0.1 eq.)	DMSO	air	rt	24	22	35	15	30
12	Cu ^I -USY (3 eq.)	DMSO	air	rt	24	12	21	0.63	17
13	Cu ^I -USY (3 eq.)	DMSO	Ar	rt	24	12	21	0	18

^[a] Reactions run with *para*-nitrobenzenediazonium tetrafluoroborate (0.5 mmol, 1.0 equiv. with a 0.25 M concentration) and Cu^I-USY (X equiv.) in the mentioned solvent for 24 h under air, unless otherwise stated.

^[b] Yields estimated from the crude mixture ¹H NMR using 1,3,5-trimethoxybenzene as internal standard, unless otherwise stated.

^[c] Estimated yields reported by Cohen and co-workers³¹².

^[d] Isolated yields of **K.3b** and **K.7a** reported by Cepanec and co-workers³¹³.

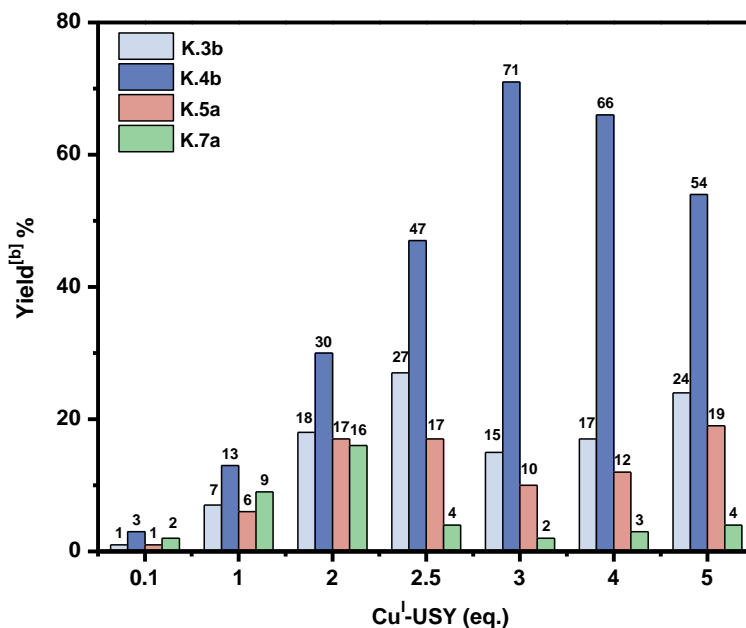


Figure 15. Screening of Cu^I-USY loading in coupling reaction of aryldiazonium salts.^[a]

^[a] Reactions run with *para*-nitrobenzenediazonium tetrafluoroborate (0.5 mmol, 1.0 equiv. with a 0.25 M concentration) and Cu^I-USY (X equiv.) in MeCN for 24 h under air, unless otherwise stated.

^[b] Yields estimated from the crude mixture ¹H NMR using 1,3,5-trimethoxybenzene as internal standard, unless otherwise stated.

The effect of Cu^I-USY loading on the product yield was shown in **Figure 15**. When the catalyst loading increased from 1 equiv. to 3 equiv., the yield of the azo-compound product (**K.4b**) was greatly improved compared to the yields of other products, but the former progressively decreased as the amount of Cu^I-USY continued to increase. The yield of **K.4b** peaked at 71% when the quantity of Cu^I-USY reached 3 equiv., before progressively falling to 54% for 5 equiv. of Cu^I-USY. Meanwhile, the yields of homocoupling product **K.3b** and nitrophenol **K.5a** also exhibited a similar trend and the yield of the former was slightly higher than that of the latter under the same Cu^I-USY loading. However, both yields of **K.3b** and **K.5a** reached the plateau when using 2.5 equiv. Cu^I-USY (27% and 17%), and started to decrease as Cu^I-USY loading further increased. Surprisingly, the yields of **K.3b** and **K.5a** increased again when using 5 equiv. Cu^I-USY, with yields similar to those obtained with 3 equiv. Cu^I-USY. It was noteworthy that the yield of the reduction product **K.7a** reached the maximum (16%) when Cu^I-USY increased to 2 equiv. and it was lower than 10% under all other conditions, which indicated that these reaction conditions were favorable for avoiding the hydrodediazotation reaction. The above results indicated that the yields of these four products were affected by the Cu^I-USY loading,

and high yields of the azo-product **K.4b** could be obtained by controlling the copper species loading.

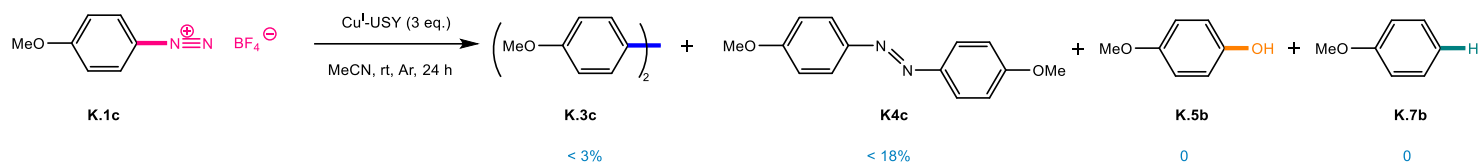
Furthermore, in our previous results, DMSO was a possible solvent to provide the azo-compound **K.4b** in a modest yield when using 0.1 equiv. Cu^I-USY as catalyst under air conditions (35%, **Table 8**, entry 11). The reaction was thus carried out under the similar conditions using higher amounts of Cu^I-USY (3 equiv.) to improve the yield of the product **K.4b** (**Table 8**, entry 12). However, all product yields significantly decreased (entry 12 vs 11). It should be noted that the inert atmosphere had no effect on the selectivity of these reactions under the same conditions (entry 13 vs 12).

In summary, these results showed that Cu^I-USY is not an efficient catalyst for the homocoupling of arenediazonium salts. At best, the reaction could afford the biaryl product in a modest 22% yield using DMSO as solvent (**Table 7**, entry 8). Alternatively, Cu^I-USY could efficiently and cleanly promote the de-diazotation of arenediazonium salts, since it provided 68% of this product with DMF as solvent (**Table 7**, entry 12).

In addition, a stoichiometric amount of Cu^I-USY can effectively promote the coupling of arene diazonium salts in MeCN under an argon atmosphere to synthesize the corresponding azo-compound **K.4b**. The latter could be obtained in yields as high as 71% when 3 equiv. Cu^I-USY was employed in the reaction (**Table 8**, entry 4). Unfortunately, the selectivity of the homocoupling towards **K.3b** cannot be significantly improved with increasing Cu^I-USY loading; a moderate yield of the product **K.3b** could be provided when the Cu^I-USY loading increased to 2.5 equiv. (27%, **Table 8**, entry 8).

5.2. Scope and limitations

Based on the results we obtained, the optimal conditions for the synthesis of azo-compound were 3 equiv. Cu^I-USY in MeCN at room temperature under argon atmosphere. Therefore, *para*-methoxybenzenediazonium tetrafluoroborate was chosen to evaluate the effect of the electron-donating group (methoxy group) (**Scheme 88**).



Scheme 88. Cu^I-USY-promoted homocoupling of *para*-methoxybenzenediazonium tetrafluoroborate.^[a]

^[a] Reaction run with *para*-methoxybenzenediazonium tetrafluoroborate **K.1c** (0.5 mmol, 1.0 equiv.) and Cu^I-USY (3 equiv.) in MeCN (2 mL) at room temperature under air for 24 h, unless otherwise stated.

As expected, the main product was still the corresponding azo-compound **K.4c**, but the yield was less than 18% after purification. Furthermore, only trace amounts of homocoupling product **K.3c** was detected. It seemed that **K.5b** and **K.7b** were not obtained in the reaction as there were several other compounds that could not be confirmed.

Obviously, further efforts are required to explore the reaction.

6. Conclusion

In this study, Cu^I-USY proved to be an efficient and easy-to handle heterogenous copper(I) catalyst in homocoupling of arylboronic acids. The reaction is performed under green and mild aerobic conditions without additional bases and ligands and showed a good tolerance of functional groups (e.g., methoxy, hydroxy, halide, nitro, etc.).

More precisely, the Cu^I-USY-catalyzed homocoupling of arylboronic acids, performed in MeOH at 60 °C under air, allows synthesizing a series of important biaryl scaffolds. The high copper-loaded catalyst (up to 80% Cu content) could be easily recovered by filtration, and directly re-engaged for the next reaction without calcination at least three times. However, a progressive erosion of the catalytic activity was observed, and the Sheldon test revealed that some leaching of copper species occurred in MeOH. Furthermore, various arylboronic acids carrying electron-donating groups (EDG) or electron-withdrawing groups (EWG) were screened, and they provided the desired dimers with yields up to 98%. *para*- or *ortho*-substituted arylboronic acids with EWG led to the expected homocoupling product in yields higher than those provided with other substituted analogs. Finally, a catalytic mechanism was proposed based on the formation of dimeric copper species with the help of MeOH.

On the other hand, Cu^I-USY was also applied to a cascade process combining the present homocoupling reaction and a Diels-Alder reaction. Moderate yields were observed in MeOH or in toluene, the classical solvent for the cycloaddition reaction with two different dienophiles. Further efforts are clearly required to improve this cascade, extend the product scope and to apply this simple and environmentally benign protocol to the synthesis of relevant compounds, natural or not. Nevertheless, further efforts are required to expand the application of this one-pot two-step protocol.

In addition, we demonstrated that the use of diazonium salts instead of classical aryl halides is feasible for the synthesis of biaryl compounds using Cu^I-based catalyst. So far, Cu^I-USY allowed to successfully produce the expected 4,4'-dinitrobiphenyl from 4-nitrobenzenediazonium tetrafluoroborate in MeCN at room temperature under an argon atmosphere, albeit in low yields (15%). However, a stoichiometric amount of Cu^I-USY (3 equiv.) was required. Interestingly, a high yield of the main product 4,4'-dinitroazobenzene (71%) was obtained during the reaction. Further efforts are nevertheless needed to explore the reaction.

**Chapter III. C_{aryl}-heteroatom bond formation towards phenols *via*
copper(I)-zeolite-catalyzed Chan-Lam-Evans coupling reactions**

1. Introduction

1.1. C_{aryl}-heteroatom bond formation

The significance of forming C_{aryl}-C_{aryl} bonds in the synthesis of important compounds or moieties (especially biaryls) in organic synthesis was already discussed in the previous chapter. Meanwhile, the formation of C_{aryl}-X (with X a heteroatom) bonds, which could create molecular diversities, also plays a pivotal role in the field of synthetic chemistry. The function of many organic compounds with backbone made of C-C bonds is often derived from the presence of heteroatoms, such as nitrogen, oxygen and sulphur.⁵ For instance, C-N bonds are common in pharmaceuticals, e.g. alstoscholarisine A. The latter, which is isolated from the leaves of *Alstonia scholaris*, can be used as neural stem cells activator (NSC) to promote adult NSC proliferation and differentiation³³¹. Furthermore, phenol, ether, ketone or ester C-O bonds are almost encountered in all natural products and can be found as pharmacophores in medically important compounds⁵ (**Figure 16**).

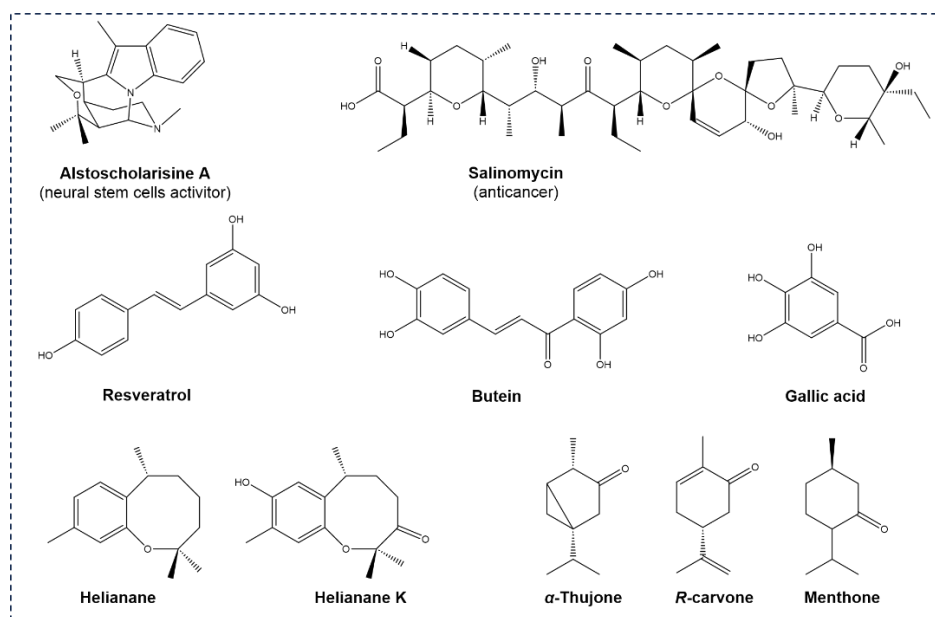
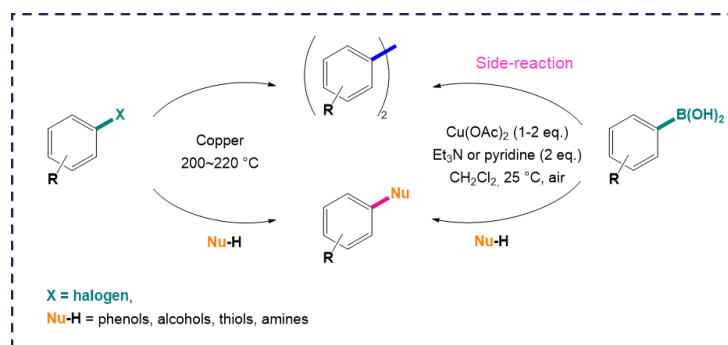


Figure 16. Representative examples of natural products containing C-N and C-O bonds.

The C_{aryl}-X bonds were first formed by Ullmann at the beginning of the last century. After his work on what it is nowadays called the homocoupling reaction of aryl halides (see Chapter II-2.1.),¹ Ullmann developed in 1903-1905 the formation of C_{aryl}-X bonds via copper-mediated cross-coupling reactions of aryl halides with different N- and O-nucleophiles. These reactions however originally required harsh conditions and often stoichiometric amount of copper (**Scheme 89, left**).

Inspired by these seminal works, chemists have been seeking new synthetic methods to improve the reaction conditions for the formation of $C_{\text{aryl}}\text{-X}$ bonds. Among the various developed methods (see below), the simultaneous disclosure by the groups of Chan-Lam^{10,11} and Evans⁹ of copper-mediated cross-coupling reactions at room temperature with arylboronic acid as one of the coupling partners, provided the opportunity to construct C-X bonds under much milder reaction conditions, making it clearly attractive compared to the Ullmann-type reaction conditions (**Scheme 89, right**).



Scheme 89. Cu-mediated Ullmann-type coupling (left) and Chan-Lam-type coupling (right), which provide access to biaryls, aryl ethers and amines.

Since then, the search for new catalytic systems and green technologies that allow these reactions to proceed under more sustainable conditions has become highly desirable in the last decade. However, these reactions were mostly carried out under palladium- and copper-catalyzed homogeneous conditions in the presence of bases and ligands, resulting in environmental problems and waste of resources. Although numerous heterogeneous catalysts, with the inherent advantage of easy separation, better handling characteristics and recyclability, are continuously developed in various organic transformations, this is not the case for Ullmann-type^{1,7,8,232,332,333} and Chan-Evans-Lam-type coupling reactions⁹⁻¹¹.

In particular, an extremely limited number of copper-based heterogeneous catalysts has been developed for Chan-Evans-Lam-type reactions³³⁴. Moreover, none of them relied on the use of zeolites as catalysts, although the potential of zeolite as an inexpensive and stable support material should not be underestimated.

As a tremendously useful heterogeneous catalyst, Cu^I-USY was mostly applied in cycloaddition and coupling reactions in organic synthesis with excellent catalytic performance (for more details, see Chapter I-2.3.2.2.6.). This motivated us to attempt forming $C_{\text{aryl}}\text{-X}$ bonds, and especially phenols (see below), *via* Cu-zeolite-catalyzed-Ullmann and Chan-Evans-Lam-type reactions. However, to the best of our knowledge, these C-O cross-coupling reactions mainly

focused on the synthesis of aryl ethers, and only a few examples related to the preparation of phenols.

1.2. Phenol synthesis

Phenols are common motifs that appear in a wide range of natural substances, from amino acids and hormones to flavonoids, alkaloids and antibiotics, usually contributing to their biological activities.^{335,336} For these reasons, phenols also are frequent scaffolds of pharmaceuticals, agrochemicals, but also of flavors and fragrances (**Figure 17**).³³⁷ For instance, phenols are an important class of antioxidants that can inhibit the oxidative degradation of a large number of biological aerobic organisms. A typical example is α -tocopherol, a well-known vitamin E component, which has been proved to be the most efficient phenol derivative to trap the damaging peroxy radicals in human blood plasma. Besides, salicylic acid bearing a phenol moiety can be used to relieve pain and fever.²⁵ Phenols are thus at the core of many important industrial products. In addition, phenols are serving as versatile synthetic intermediates.²⁵ Therefore, the synthesis of phenols, especially under mild and green conditions, continues to attract the attention of organic chemists.

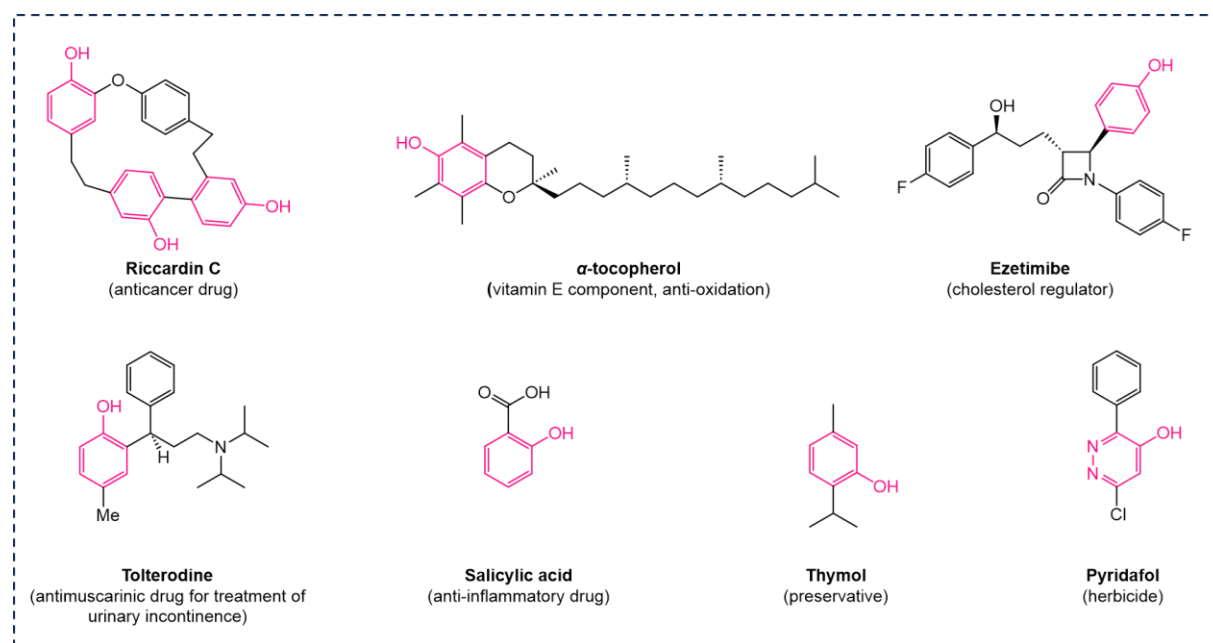


Figure 17. Representative examples of bioactive compounds containing a phenol motif.³³⁷

Obtaining phenol derivatives usually require nucleophilic aromatic substitution or oxidative processes under harsh conditions, especially at industrial scale, with obvious environmental and sustainability consequences.²⁵ Non-oxidative methods include nucleophilic aromatic

substitution of activated aryl halides and conversion of aryldiazonium salts. Within the development of the Buchwald-Hartwig palladium-catalyzed formation of C-O bonds from aryl halides in 2006,³³⁸ phenols have also been obtained from aryl halides under similar conditions but with hydroxide salts as nucleophiles³³⁹ instead of aliphatic alcohols or phenols³⁴⁰⁻³⁴⁴. With such easy-to-handle and cheap nucleophile, phenols could be directly synthesized from aryl halides in a more convenient and economical route. *Nevertheless, to the best of our knowledge, only a few homogeneous and two heterogeneous examples of Ullmann coupling reactions for the synthesis of phenols with hydroxide salts as nucleophiles have been reported* (see below).

In parallel, and although first observed as a side-reaction in the Chan-Evans-Lam-copper-promoted coupling of arylboronic acids,^{9,11} the hydroxylation of arylboronic acids have gained interest, mostly due to the availability of numerous boronic acids and to the mild conditions employed.³⁴⁵ However, most of these Chan-Evans-Lam variants still involve oxidative conditions with either hydrogen peroxide, *tert*-butyl hydroperoxide, oxone, peracids or quinones. Such conditions cannot always be compatible with functionalized arenes. *Furthermore, only five Chan-Lam-Evans C-O coupling reactions with hydroxide salts as nucleophiles have been developed towards phenols.*

To highlight the importance of designing and developing novel efficient heterogeneous catalysts for the Chan-Evans-Lam-type cross-coupling reactions, the introductory section will illustrate the development process of the formation of C_{aryl}-X bonds from original Ullmann reactions to the Chan-Evans-Lam coupling reactions with selected but non-exhaustive examples.

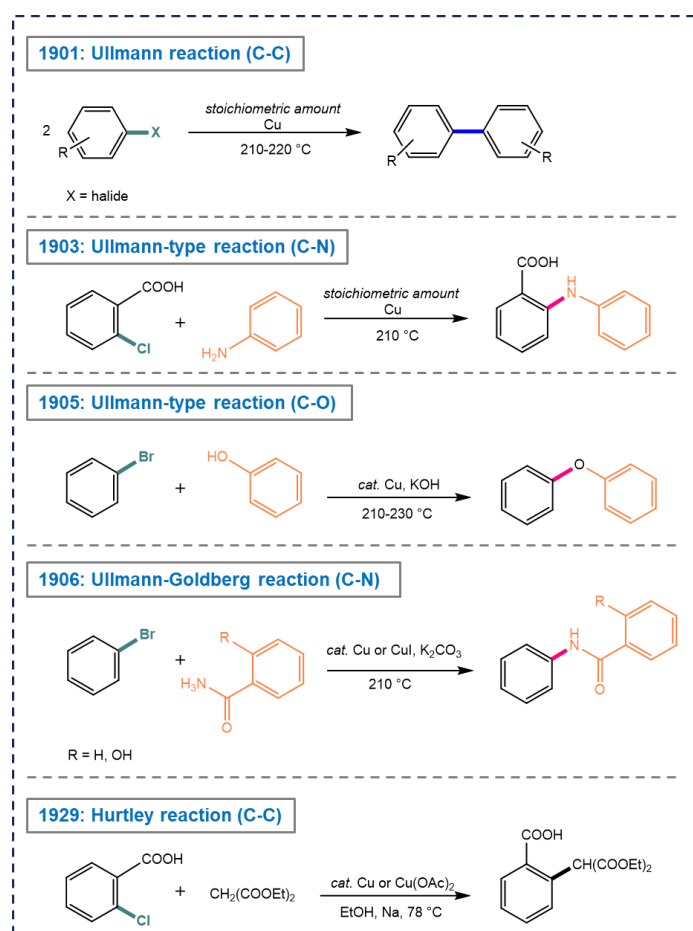
On the other hand, the synthesis of phenols using hydroxide salts (e.g., NaOH, KOH...) as nucleophiles will be discussed separately in each part to illustrate the scarcity of phenol syntheses by these methods in comparison to other advances in C_{aryl}-X bond formations.

2. The history of Ullmann-type reactions to Chan-Lam-type reactions

2.1. From Ullmann reactions...

In 1901, Ullmann¹ first formed aryl-aryl bonds through stoichiometric amount of copper-mediated homocoupling reactions of aryl halides to synthesize biaryls, leading to the so-called Ullmann reactions (**Scheme 90**). Shortly after, he again disclosed copper-mediated cross-couplings of aryl halides with aryl amines and copper-catalyzed cross-coupling between aryl halides and phenols, successfully forming C_{aryl}-N bonds⁷ (in 1903) and C_{aryl}-O bonds⁸ (in 1905),

respectively (**Scheme 90**). These two reactions were later known as the Ullmann condensations or Ullmann-type reactions. During 1906-1907, Goldberg successfully developed the catalytic version of the cross-coupling of aryl halides with aryl amines (or aryl amides) to construct C_{aryl}-N bonds with the help of catalytic amount copper powder²³² or copper salt (CuI)³³². She thus achieved the first shift from stoichiometric to catalytic conditions, and from copper metal to copper salt (**Scheme 90**). These reactions are also called Ullmann-Goldberg condensations. Inspired by these seminal works, Hurtley³³³ described the formation of C_{aryl}-C bond *via* a copper salt-catalyzed cross-coupling between aryl bromide and activated methylene compound malonic acid in 1929 (**Scheme 90**). This reaction was later also called Ullmann-type reaction.



Scheme 90. Early Ullmann coupling reactions.^{1,7,8,232,332,333}

However, these reactions were mostly promoted by a stoichiometric amount of copper under rather harsh conditions, such as high reaction temperatures (200-220 °C) and long reaction times (1 or 2 days). These features resulted in the production of huge amounts of resource and energy wastes, as well as high cost, making these methods unacceptable from economic and ecological perspectives. Besides, the resulting poor functional group tolerance and the moderate

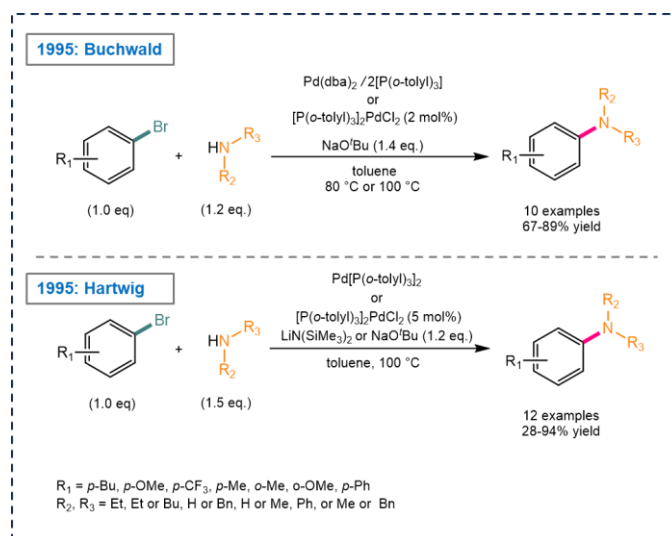
yields in most cases also greatly limited the synthetic scope of these transformations at that time. Nevertheless, Ullmann-type reactions extended the methodology of C_{aryl}-C_{aryl} bonds formation in the original Ullmann homocoupling reactions to the construction of C_{aryl}-O, C_{aryl}-N and C_{aryl}-C bonds in cross-coupling reactions, and produced diverse aromatic compounds with valuable pharmaceutical and biological potential, thus arousing a surge of scientific interest in this area to improve reaction conditions and expand their applications. Since the 1960s, some studies discovered that the Ullman-type reaction rate could be enhanced when the arylation reaction was performed in the presence of ligand or other additives or even other metals.²⁴⁷⁻²⁵⁴ Although the exact roles of these reagents were not established unequivocally at that time, they provided a faster route to perform these coupling reactions from a practical perspective.

2.1.1. Palladium-catalyzed Ullmann coupling reactions

The emergence of the Pd-catalyzed cross-coupling reaction in the 70's³⁴⁶ and their large development in the 80's-90's led some groups to apply such Pd-catalysis to Ullmann-type reactions.

In 1995, Buchwald's^{347,348} and Hartwig's groups³⁴⁹ first formed C_{aryl}-N bonds under palladium catalysis in toluene at 80-100 °C with varying yields of the products. These reactions are now called the Buchwald-Hartwig coupling reaction (**Scheme 91**). However, a special ligand (P(*o*Tol)₃) and base (NaO^tBu) were required in the reaction. Besides, only a few specific groups could be tolerant since substrates which are sensitive to basic conditions could not be employed. Furthermore, primary or secondary acyclic amines only led to low yields.

After these pioneering works, numerous catalytic systems based on palladium complexes have been developed to further improve the reaction conditions and expand the reaction scope³⁵⁰. Similarly, the palladium-catalyzed Ullmann coupling reactions, which facilitated the formation of C_{aryl}-O and C_{aryl}-C bonds to synthesize phenols, aryl ethers,^{351,352} (substituted) phenyl compounds and symmetrical biaryls from activated aryl halides, have been also flourishing with more attractive reaction conditions.³⁵⁰ It should be mentioned that the corresponding C_{aryl}-heteroatom (N, O, S) bond cross-coupling was less well established prior to the discovery of the Buchwald-Hartwig coupling reaction. Herein, we will give some examples of palladium-catalyzed Ullmann-type cross-coupling reactions between aryl halides and amines in promoting C_{aryl}-N bond formations.



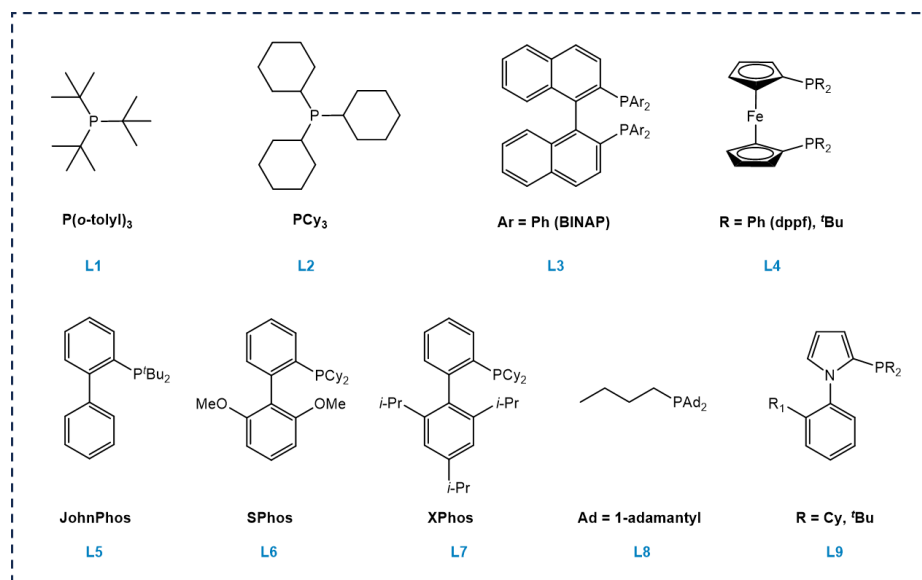
Scheme 91. Palladium-catalyzed Buchwald–Hartwig reactions under homogeneous conditions.³⁴⁷⁻³⁴⁹

2.1.1.1. Palladium-catalyzed homogeneous Buchwald–Hartwig reactions

The classical copper-mediated Ullmann–Goldberg reaction involved harsh conditions with very high temperatures and/or strong bases through generate aryl amines and aryl ethers from aryl halides (**Scheme 90**). The recent modification by Buchwald and Hartwig through palladium-catalyzed coupling reaction greatly improved the reaction conditions (**Scheme 91**). In order to solve the problems in the original reactions (such as limited scope and low yields in some cases), different catalytic systems were developed based on shifting ligand and base.

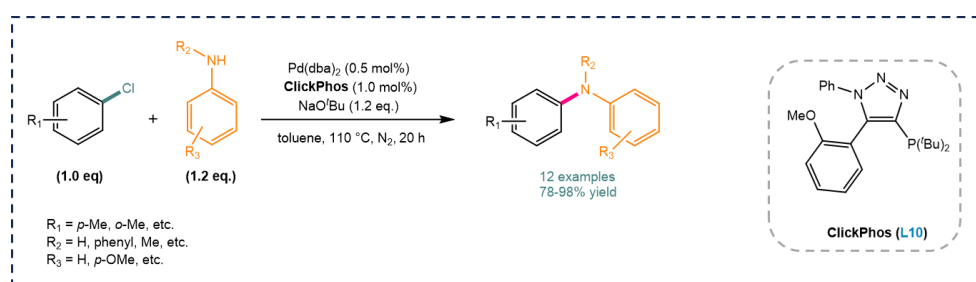
Taking the ligand as an example, $\text{P}(o\text{-tolyl})_3$ (**Scheme 92, L1**) was originally used as a ligand for the Buchwald–Hartwig reactions, resulting in poor yields in the reaction of primary amines with aryl halides.^{347,353,354} During this period, PCy_3 (Cy = cyclohexyl) (**Scheme 92, L2**) was also developed for the reaction of secondary amines with aryl halides, but a high temperature (120 °C) and a special base (NaO^tBu) were still required in the reaction.³⁵⁵ Shortly after, Buchwald³⁴⁸ and Hartwig³⁴⁹ developed a second generation of ligands based on chelating diphosphine (BINAP and dppf) ligands (**Scheme 92, L3 and L4**) to improve the reaction. With such ligands, a broader scope of *N*-nucleophiles including primary alkyl amines, anilines and hetero aromatic halides were achieved for the Pd-catalyzed C-N cross-coupling of aryl halides.³⁵⁰ However, these ligands were ineffective for reactions with unactivated aryl chlorides.^{348,349,356} In the late 1990s, Buchwald and co-workers reported a series of monophosphine ligands derived from biphenyl, such as JohnPhos (**Scheme 92, L5**), SPhos (**Scheme 92, L6**) and Xphos (**Scheme 92, L7**)³⁵⁷, which proved effective for conducting the amination reactions at room-temperature.³⁵⁸⁻³⁶¹ In the early 21st century, Beller *et al.*

synthesized two novel monophosphine ligands (**Scheme 92**, **L8** and **L9**); the former (**L8**) could promote the Pd-catalyzed coupling of sterically hindered amines³⁶², while the latter (**L9**) showed excellent reactivity towards a wide range of substrates.^{363,364} Since then, different monophosphine ligands have been continuously developed for the Pd-catalyzed amination reaction of aryl halides.



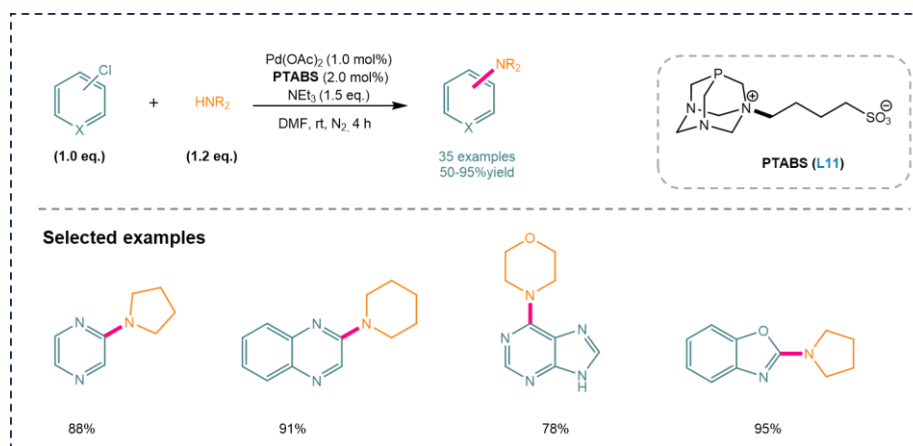
Scheme 92. Examples of ligands for Pd-catalyzed Buchwald–Hartwig reactions.

In 2006, Zhang *et al.*³⁶⁵ developed various triazole-based monophosphine ligands (**ClickPhos**, **L10**) for palladium-catalyzed cross-coupling reactions of aryl chlorides. Palladium complexes with this type of ligand exhibited excellent catalytic activity in the reaction, providing products yields up to 98% (**Scheme 93**).



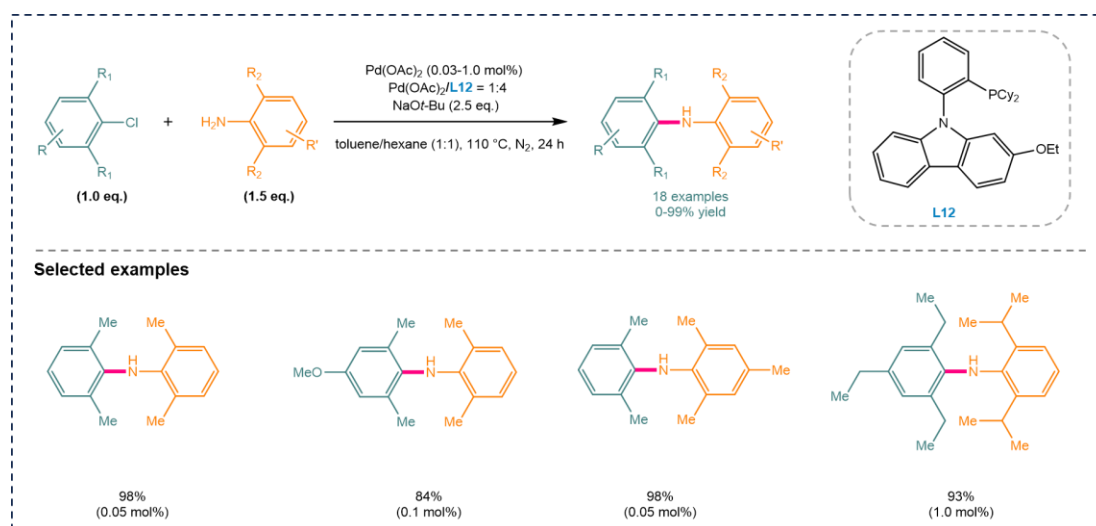
Scheme 93. Pd(dba)₂-catalyzed homogeneous Buchwald–Hartwig reaction with ClickPhos ligand.³⁶⁵

Kapdi and co-workers³⁶⁶ in 2018 reported a water-soluble phosphotriazene ligand (PTABS, **L11**) for the Buchwald–Hartwig reaction of chloroheteroarenes. The introduction of this ligand and NEt₃ as the base allowed the palladium-catalyzed reaction to proceed efficiently at room temperature with up to 95% yields of the expected products (**Scheme 94**).



Scheme 94. Pd(OAc)₂-catalyzed homogeneous Buchwald–Hartwig reaction in the presence of PTABS.³⁶⁶

In 2019, Kwong's group³⁶⁷ used 2-(9*H*-carbazol-9-yl)phenyl-based phosphine ligand **L12** to promote the Pd(OAc)₂-catalyzed C-N cross-coupling of aryl chlorides, affording substituted diarylamines smoothly in high products yields (up to 99%) (**Scheme 95**).



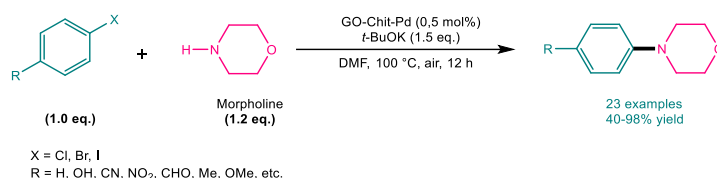
Scheme 95. Pd(OAc)₂-catalyzed homogeneous Buchwald–Hartwig reaction with phosphine ligand.³⁶⁷

2.1.1.2. Palladium-catalyzed heterogeneous Buchwald–Hartwig reactions

To extend the lifetime of the catalyst and minimize its negative impact on the environment, as well as to solve the difficulty of recovering the catalyst from the product, several solid materials have been explored to support the palladium species for the Buchwald–Hartwig reactions.

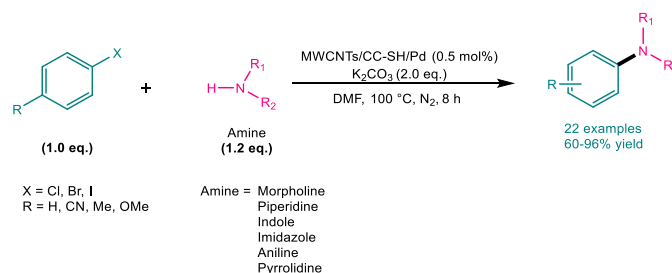
In 2018, Azadi and co-workers³⁶⁸ prepared Pd nanoparticles deposited on chitosan functionalized graphene oxide (GO-Chit) to promote the C-N cross-coupling of aryl halides for the synthesis of *N*-arylamines (**Scheme 96**). A variety of aryl halides and amines have been

employed under the optimal conditions, providing the products in yields up to 98%. Reusability study of the catalyst indicated that the catalyst, recovered by centrifugation, could be recycled at least five times without obvious loss in catalytic activity (from 90% to 87%). The hot filtration test indicated that only slight quantities of palladium were lost in the solvent during the reaction.



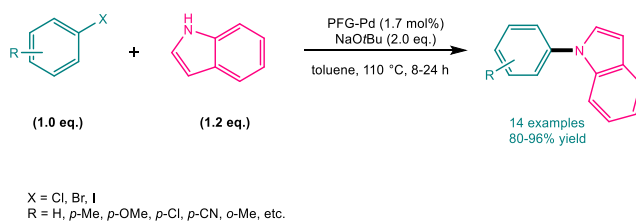
Scheme 96. GO-Chit-Pd-catalyzed heterogeneous Buchwald-Hartwig reaction.³⁶⁸

In 2019, Veisi and co-workers³⁶⁹ immobilized palladium nanoparticles on thio-modified-multi-walled carbon nanotubes (MWCNTs) for the C-N bonds cross-coupling reaction, affording high yields of the expected products (60-96%) (**Scheme 97**). The catalyst could be recycled for 6 times in the reaction, and a Sheldon test and ICP analysis indicated that no significant palladium species were leached into the solvent.



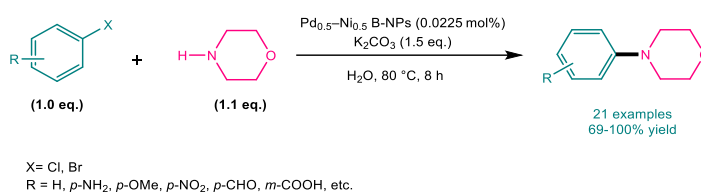
Scheme 97. MWCNTs/CC-SH/Pd-catalyzed heterogeneous Buchwald-Hartwig reaction.³⁶⁹

Fareghi-Alamdari' group³⁷⁰ developed a immobilized Pd(0) nanoparticles on phosphine functionalized graphene (PFG) for the Buchwald-Hartwig reactions in 2016 (**Scheme 98**). This catalyst efficiently promoted the formation of the C-N bonds, affording high yields of the desired products (80-96%). The PFG-Pd catalyst could be used at least 5 times during the recyclability study. Furthermore, ICP analysis showed that a small amount of Pd (about 1.5%) was lost after five reusability runs in comparison with the fresh catalyst.



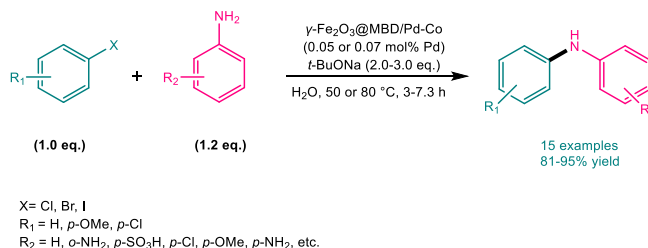
Scheme 98. PFG-Pd-catalyzed heterogeneous Buchwald–Hartwig reaction.³⁷⁰

In 2014, Heshmatpour and co-worker³⁷¹ reported an efficient palladium–nickel bimetallic nanoparticles (Pd–Ni B-NPs) for the *N*-arylation (**Scheme 99**). The addition of the second metal, nickel, to the catalytic system improved the activity, selectivity, and stability of the catalyst in the transformation and produced quantitative yields of the product in some cases. The optimal molar ratios of these two metals are 1:1 (Pd_{0.5}–Ni_{0.5} B-NPs). This catalytic system could be recycled six times without loss of catalytic activity. The leaching of Pd species into the solution was very low as shown by ICP analysis. This was the first time that the catalyst was used in the C–N coupling reaction of aryl chlorides with amines.



Scheme 99. Pd_{0.5}–Ni_{0.5} B-NPs-catalyzed heterogeneous Buchwald–Hartwig reaction.³⁷¹

More recently, Sobhani' group³⁷² developed a novel Pd–Co bimetallic alloy encapsulated in melamine-based dendrimer supported on magnetic nanoparticles (γ -Fe₂O₃@MBD/Pd–Co), allowing the Buchwald–Hartwig reaction to be performed in water with low amount of palladium loading (**Scheme 100**). The encapsulation of γ -Fe₂O₃ by melamine-based dendrimer dispersed the catalyst in water, leading to higher catalytic activity compared with the monometallic counterparts. The magnetic catalyst could be easily recovered and reused ten times without losing activity, while keeping its structure unaltered.



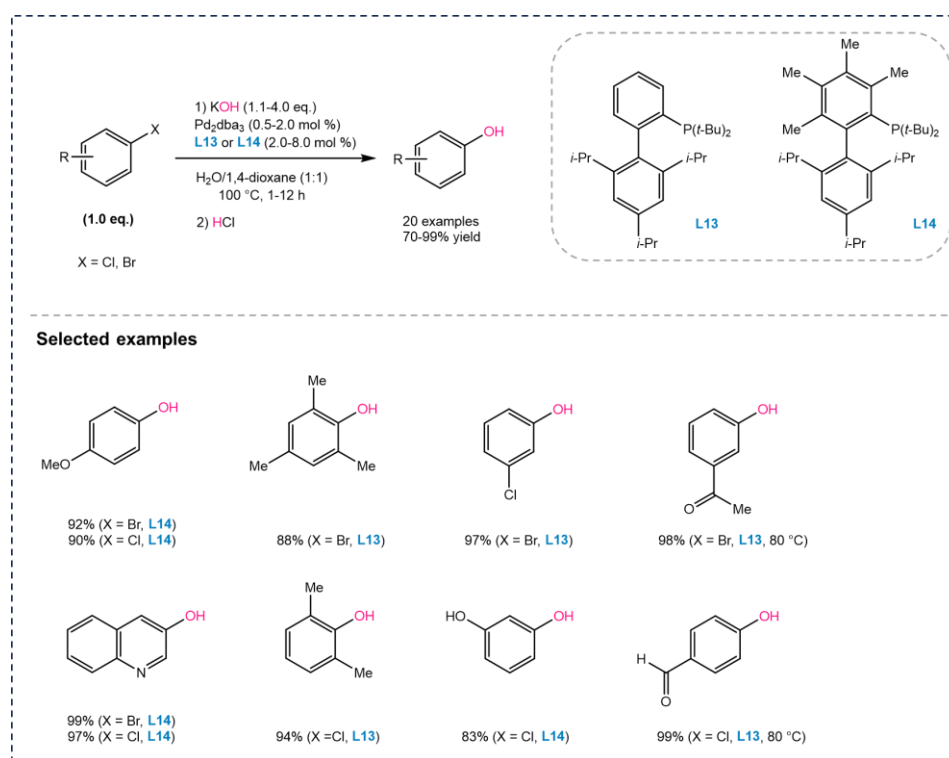
Scheme 100. γ -Fe₂O₃@MBD/Pd–Co-catalyzed heterogeneous Buchwald–Hartwig reaction.³⁷²

2.1.2. Palladium-catalyzed hydroxylation of aryl halides towards phenols

As mentioned previously, this section will demonstrate the synthesis of phenols by palladium-catalyzed hydroxylation of aryl halides with hydroxide salts as nucleophiles. To our knowledge, only five examples have been reported under homogeneous conditions. Most of them catalyzed by a palladium complex with a special phosphine ligand. *Furthermore, no Pd-catalyzed heterogeneous hydroxylation of aryl halides has been reported to date.*

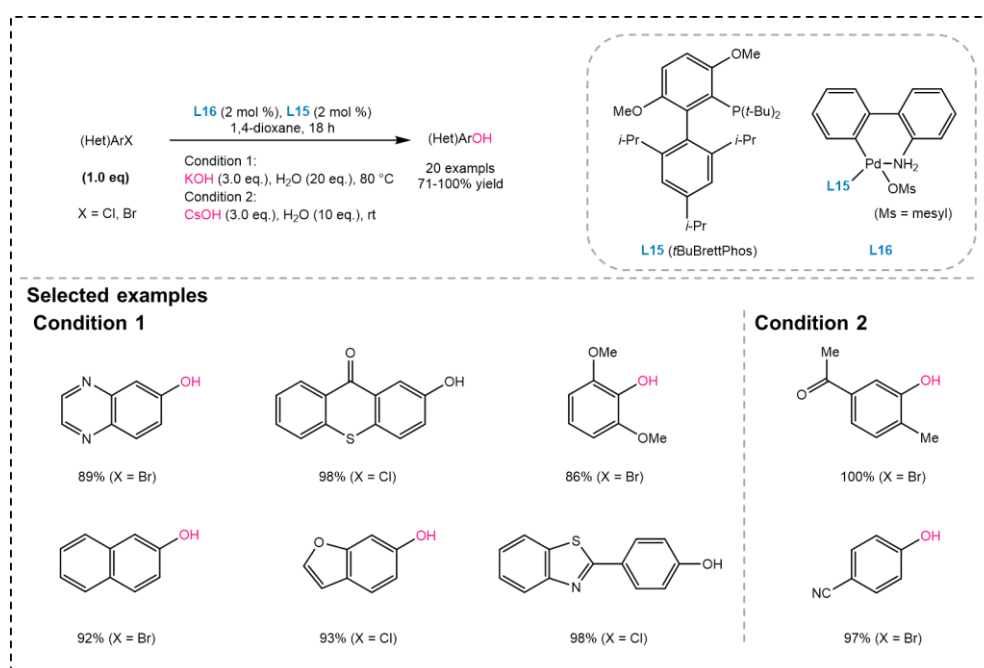
2.1.2.1. Palladium-catalyzed homogeneous hydroxylation of aryl halides

In 2006, Buchwald and co-workers³³⁸ reported the direct and selective synthesis of phenols *via* a palladium complex-catalyzed reaction of aryl halides and potassium hydroxide (KOH) (**Scheme 101**). This was the first time that hydroxide salts (e.g., KOH, NaOH) had been used as nucleophiles to directly synthesize phenols in Ullmann-type C-O coupling reactions. With the catalyst tris(dibenzylideneacetone)dipalladium(0) (Pd₂dba₃) and external highly active monophosphine-based ligand **L13** or **L14**, the model reaction of 3-bromoanisole and KOH could proceed in a mixture of 1,4-dioxane/ H₂O at 100 °C, providing 94% yield of the only product 3-methoxyphenol. The combination of Pd₂dba₃ and **L13** or **L14** provided an efficient route for the synthesis of phenols from a variety of aryl bromides and chlorides bearing electron-donating groups and functionalized heteroaryl halides.



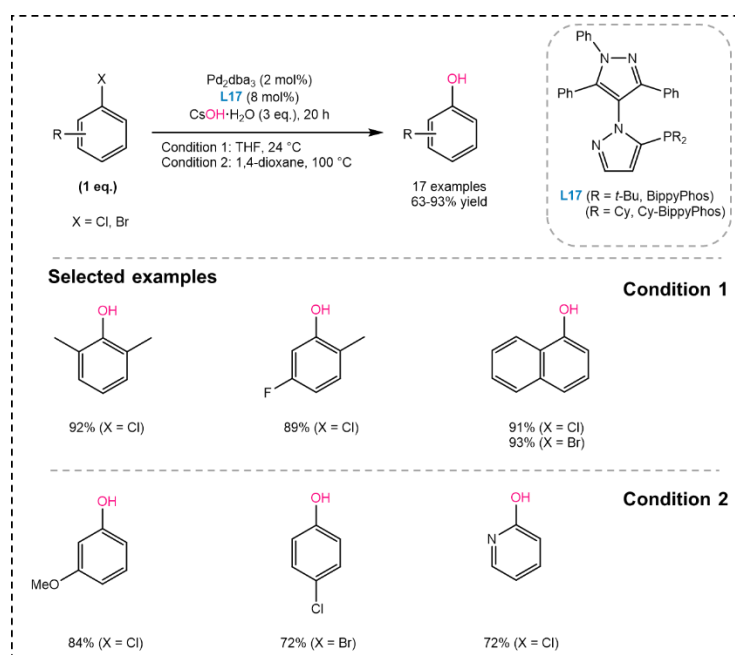
Scheme 101. Pd-catalyzed hydroxylation of aryl halides towards phenols.³³⁸

In 2014, Buchwald and co-workers³⁷³ again developed a hydroxylation of (hetero)aryl halides catalyzed by a palladacycle precatalyst (**L16**) in the presence of a biarylphosphine ligand (*t*BuBrettPhos) (**L15**). The reactions allowed the cross-coupling of (hetero)aryl halides with both potassium and cesium hydroxides to afford a diversity of phenols and hydroxylated heteroarenes in good to excellent yields (**Scheme 102**). Notably, when KOH was used as nucleophile, the reaction proceeded at 80 °C in the presence of 20 equiv. of water, whereas with CsOH as nucleophile, the reaction could occur smoothly at room temperature with only 10 equiv. of water.



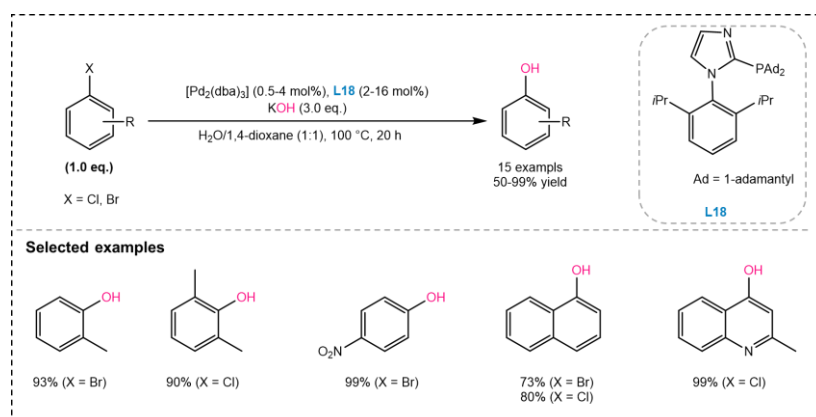
Scheme 102. Pd complex-catalyzed hydroxylation of aryl halides.³⁷³

Stradiotto *et al.*³⁷⁴ in 2013 used a mixture of Pd₂dba₃ and 5-(di-*tert*-butylphosphino)-1',3',5'-triphenyl-1'*H*-[1,4']bipyrazole (BippyPhos) (**L17**) for the hydroxylation of (hetero)aryl halides and CsOH. A variety of (hetero)aryl halides could be efficiently converted to the corresponding phenols in THF at room temperature in the presence of this catalyst (**Scheme 103**). Moreover, the employment of this catalytic system first allowed the palladium complex-catalyzed hydroxylation of aryl halide to be conducted under air with unpurified and as-received reaction solvents.



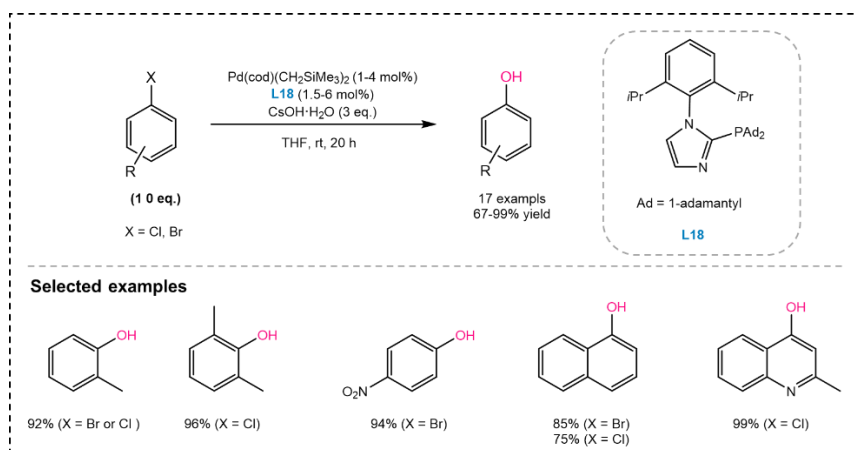
Scheme 103. Pd complex-catalyzed hydroxylation of aryl halides.³⁷⁴

In 2009, Beller's group³⁷⁵ reported a Pd complex-catalyzed hydroxylation of aryl halides with KOH in the presence of imidazolylphosphine ligand **L18**. A variety of phenols were obtained from the corresponding aryl halides substituted in moderate to high yields (50-99%) with the catalytic system $[\text{Pd}_2(\text{dba})_3]/\text{L18}$ at 100 °C in a mixed media of $\text{H}_2\text{O}/1,4\text{-dioxane}$ (1:1) (**Scheme 104**).



Scheme 104. Palladium-catalyzed synthesis of phenols from aryl halides and KOH.³⁷⁵

In the next year, this group used the same ligand **L18** and $\text{Pd}(\text{cod})(\text{CH}_2\text{SiMe}_3)_2$ (cod = 1,5-cyclooctadienyl) to efficiently promote the hydroxylation of aryl halides with CsOH at room temperature in THF (**Scheme 105**).³⁷⁶ This was the first time that the hydroxylation of aryl chlorides and aryl bromides could be catalyzed at room temperature by the combination of a novel palladium precursor $[\text{Pd}(\text{cod})(\text{CH}_2\text{SiMe}_3)_2]$ with the imidazole-based ligand **L18**.

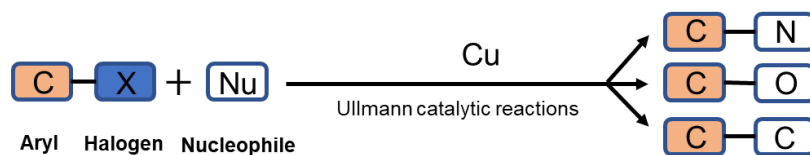


Scheme 105. Palladium-catalyzed hydroxylation of aryl halides and CsOH at room temperature.³⁷⁶

While palladium catalysts are booming in Ullmann coupling reactions, chemists are still working on seeking for ligands adaptable to the copper-based catalyzed Ullmann coupling reactions and improving reaction conditions since the expensive and toxic palladium cannot fulfill the long-term demands of industrial production and pharmaceutical synthesis from an economic and ecological perspective [Pd: ~\$350 per gram; Cu: ~\$0.01 per gram].

2.1.3. Copper-catalyzed Ullmann coupling reactions

In 2001, Buchwald's³⁷⁷ and Taillefer's group³⁷⁸ made major breakthroughs with the discoveries of versatile and efficient new copper/ligand systems for C-N, C-O or C-C cross-coupling (**Scheme 106**), allowing the use of catalytic amount of metal under mild conditions (90-110 °C). Since then, a variety of copper salts-based catalytic systems have been disclosed for the Ullmann-type reactions, which have been reviewed by Florian Monnier and Marc Taillefer.²⁴⁵ It is worth noting that most studies on Ullmann-type C-O cross-coupling reactions have been devoted to the synthesis of aryl ethers without much attention to the production of phenols.

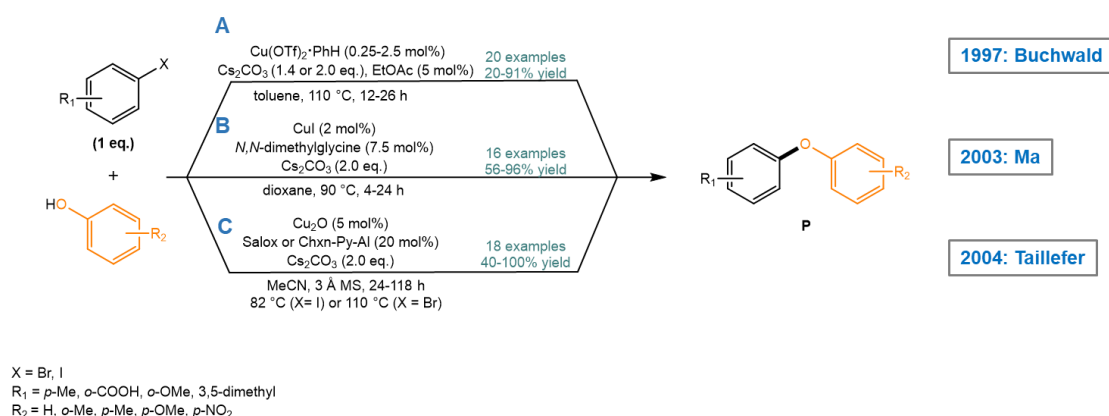


Scheme 106. Scope of copper-based Ullmann catalytic reactions.^{245,377,378}

Here, we briefly introduce some pioneering works based on copper-catalyzed C-O bond formation towards to aryl ethers, which underwent similar development as for the construction of C-N bonds during this period.

2.1.3.1. Copper-catalyzed homogeneous reactions

In 1997, Buchwald's group²⁵⁰ first used a catalytic amount of copper(I) triflate complex ((CuOTf)₂·PhH) to form C-O bond under Ullmann-type conditions with a novel base, i.e. cesium carbonate (Cs₂CO₃). (**Scheme 107, A**), affording excellent yields of the product (**P**). Inspired by this seminal work, Ma *et al.*³⁷⁹ developed an efficient C-O coupling reaction with catalytic amount of CuI with *N,N*-dimethylglycine as ligand and Cs₂CO₃ as a base to synthesize various desired products (**P**) in 96% yields (**Scheme 107, B**). Taillefer and co-workers³⁸⁰ also applied catalytic amounts of CuI and Cu₂O with Cs₂CO₃ to construct C-O bonds in 2004, providing the expected aryl ether (**P**) in yields ranging from 20% to 91% (**Scheme 107, C**). Since then, a variety of catalytic systems based on CuI (or CuBr) and Cs₂CO₃ have been disclosed, but the absence of catalyst recovery/recycling and the need for additives make this reaction conditions still costly, toxic and environmentally unfriendly. Therefore, the search for new reusable heterogeneous copper-based catalysts was still highly desirable.



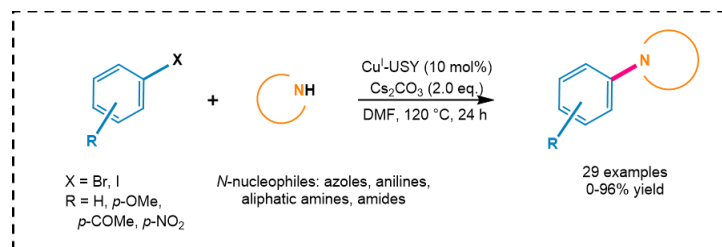
Scheme 107. Copper-catalyzed Ullmann-type *O*-arylation reactions.^{250,379,380}

2.1.3.2. Copper-catalyzed heterogeneous reactions

With the rapid development of reusable heterogeneous catalysts, some copper-loaded heterogeneous catalysts have emerged for catalyzing Ullmann-type reactions. Of the handful of catalysts that have been developed, most of them were suitable only for C-N coupling reactions, and very few have been developed for the formation of C-O and C-C bonds in cross-coupling reactions.^{264,381,382}

In 2018, our research group successfully used Cu^I-USY for the formation of C-O bonds, C-N bonds and C-C bonds in Ullmann-type reactions.^{39,40} More than 50 products were synthesized under milder conditions without additional ligand.⁴⁰ For instance, Cu^I-USY could promote the

formation of C-N bonds to synthesize various aromatic amines with yields up to 96% (**Scheme 108**).⁴⁰ The catalyst could be recycled up to five times without losing its activity in this reaction. However, the use of the toxic solvents, toluene or DMF, and base were inevitable in these reactions.



Scheme 108. Cu^I-USY-catalyzed Ullmann coupling reactions for C-N bond formation.⁴⁰

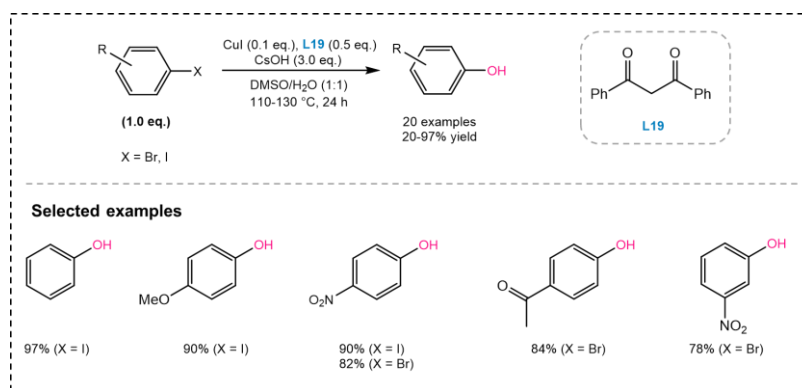
2.1.4. Copper-catalyzed hydroxylation of aryl halides towards phenols

This section will present the synthesis of phenols by copper-catalyzed hydroxylation of aryl halides using hydroxide salts as nucleophiles. Several copper salts-based catalysts have been developed to promote the hydroxylation of aryl halides under homogeneous conditions. Most catalytic systems in these limited examples are relying on the combinations of CuI with various ligands.

However, only two copper-catalyzed heterogeneous versions have been reported to date.

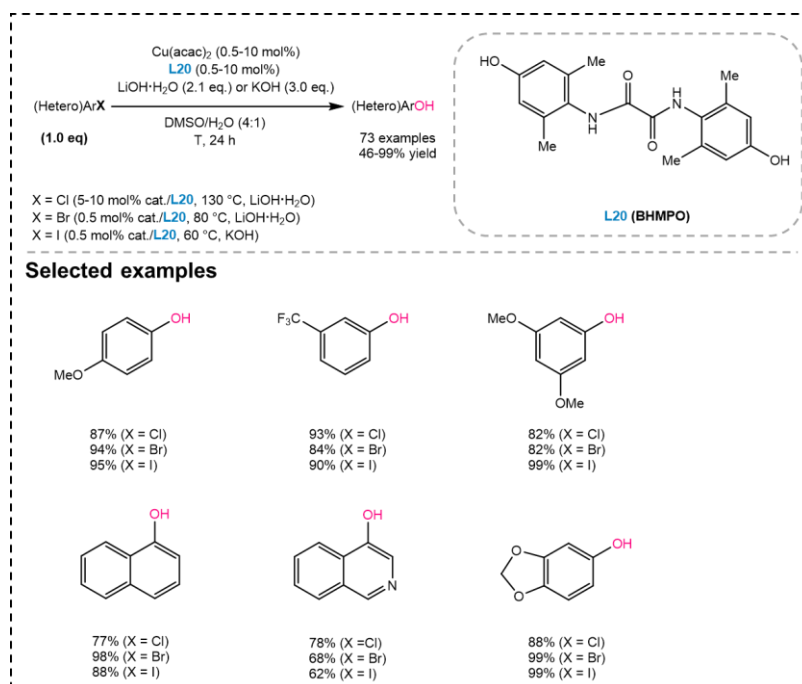
2.1.4.1. Copper-catalyzed homogeneous hydroxylation of aryl halides

In 2009, Taillefer and co-workers³³⁹ reported a copper-catalyzed homogeneous hydroxylation of aryl halides with cesium hydroxide. The copper catalyst derived from CuI and simple diketone ligand (**L19**) could efficiently and selectively promote the reaction of activated/unactivated aryl iodides or bromides in a mixed solvent of water and DMSO at 110-130 °C, with the yields of the corresponding phenols up to 97% (**Scheme 109**). This highly selective reaction avoided the formation of the biaryl ether by-product. The convenience of using a hydroxide ion as nucleophile and the inexpensive copper catalytic system made this protocol very competitive. However, high temperature and toxic solvent were required.



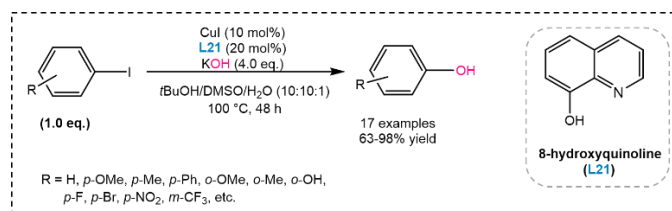
Scheme 109. Copper-catalyzed hydroxylation of aryl iodides and aryl bromides.³³⁹

In 2016, Ma's group³⁸³ reported a copper complex-catalyzed direct hydroxylation of (hetero)aryl halides with lithium hydroxide. The combination of $\text{Cu}(\text{acac})_2$ and *N,N'*-bis(4-hydroxy-2,6-dimethylphenyl)oxalamide (**L20**) (BHMPO) in a mixed media of DMSO/ H_2O (4:1) provided an efficient catalytic system for the hydroxylation of (hetero)aryl halides (**Scheme 110**). A variety of (hetero)aryl chlorides containing either electron-donating or -withdrawing groups were smoothly converted at 130 °C with 5 mol% catalyst/ligand, affording the corresponding phenols and hydroxylated heteroarenes in high and excellent yields. Interestingly, the hydroxylation reactions of more reactive aryl bromides and iodides could be conducted at relatively lower temperatures (80 °C and 60 °C, respectively) with lower catalyst loadings (0.5 mol% Cu).



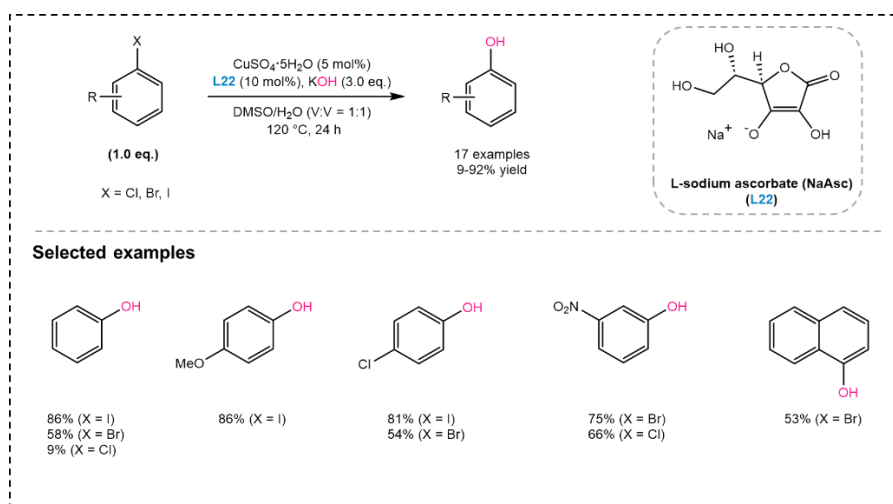
Scheme 110. Cu-catalyzed hydroxylation of (hetero)aryl halides.³⁸³

In 2010, Ma *et al.*³⁸⁴ developed a CuI-catalyzed direct hydroxylation of aryl iodides with KOH as nucleophile. The reaction proceeded efficiently in a mixed solvent system (*t*-BuOH/DMSO/H₂O) at 100 °C in the presence of 8-hydroxyquinoline (**L21**) as ligand, affording the expected phenols in good to excellent yields (**Scheme 111**). However, the reactivity of aryl bromides was found to be rather low under these reaction conditions.



Scheme 111. Cu-catalyzed hydroxylation of aryl iodides.³⁸⁴

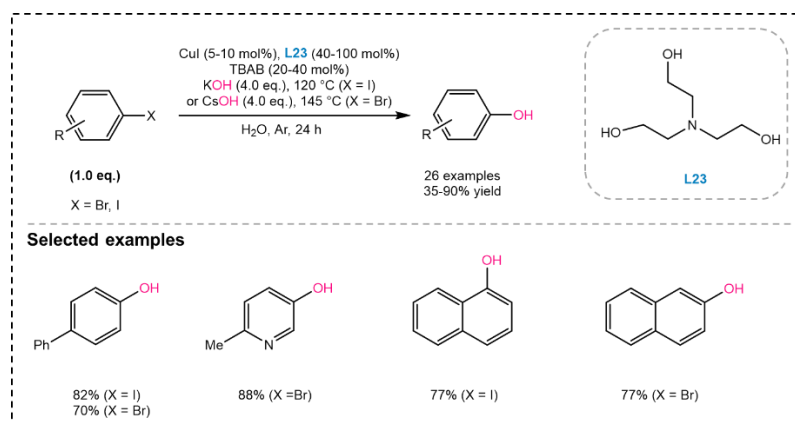
In 2015, Wang and co-workers³⁸⁵ reported a direct hydroxylation of aryl halides and KOH catalyzed by CuSO₄·5H₂O with L-sodium ascorbate (NaAsc) (**L22**) as ligand. The reaction was conducted in a mixed reaction solvent of DMSO/H₂O (1:1) at 120 °C for 24 h with the help of 5 mol% CuSO₄·5H₂O and 10 mol% NaAsc (**Scheme 112**). A wide range of functionalized aryl halides were employed under the current conditions, providing the desired phenols in yields up to 92%.



Scheme 112. Cu₂SO₄-catalyzed hydroxylation of aryl halides.³⁸⁵

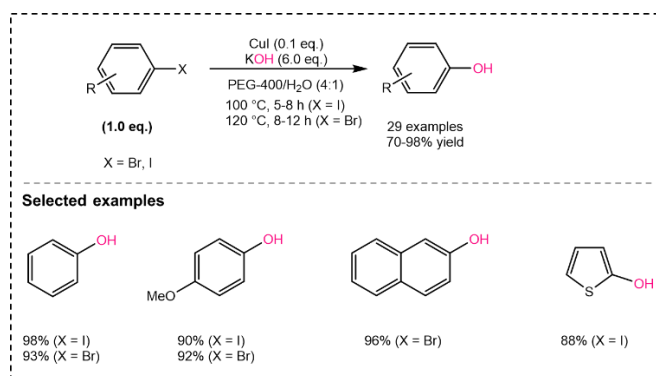
In 2014, Wang *et al.*³⁸⁶ developed a CuI/triethanolamine catalytic system for the direct hydroxylation of aryl halides using KOH or CsOH as nucleophile. The reaction could be performed in water with a phase-transfer catalyst *n*Bu₄NBr (TBAB) at 120-145 °C under argon atmosphere (**Scheme 113**). A wide range of aryl halides with different functional groups such as nitro groups, aldehydes, carbonyls, carboxylic acids, hydroxy groups, fluoride groups and

bromide groups, could be tolerated for the reaction under current conditions, providing 35-90% yields of the expected phenols.



Scheme 113. Copper-catalyzed hydroxylation of aryl halides.³⁸⁶

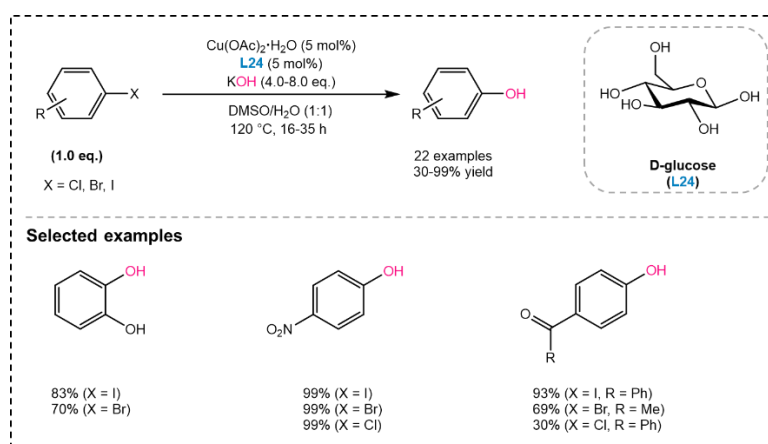
Chen *et al.*³⁸⁷ in 2011 developed a simple and efficient CuI-based catalytic system for the direct hydroxylation of aryl halides with potassium hydroxide as nucleophile in the absence of ligand (**Scheme 114**). Polyethylene glycol (PEG), an inexpensive, non-toxic and thermally stable reaction media, was first used as a cosolvent of water in the reaction. Various substituted phenols were synthesized with yields up to 98% through the hydroxylation of functionalized aryl iodides and less reactive aryl bromides at 100-120 °C in a mixed solvent of PEG-400/H₂O (4:1).



Scheme 114. Copper-catalyzed hydroxylation of aryl halides.³⁸⁷

Sekar and co-workers³⁸⁸ developed an effective and environmentally benign catalyst system (D-glucose/Cu(OAc)₂) for the hydroxylation of various aryl halides with KOH. This was the first time that readily available glucose (**L24**) had been used directly as a ligand in a transition-metal-catalyzed organic transformation. The optimal reaction conditions for this reaction were 5 mol% of Cu(OAc)₂ and 5 mol% of D-glucose in mixed solvent of DMSO/H₂O (1:1) solvent

at 120 °C (**Scheme 115**). A library of substituted aryl halides was effectively converted to the corresponding phenols under the present reaction conditions. Aryl iodides bearing both electron-donating and electron-withdrawing groups, as well as *ortho*-substituted aryl bromides containing electron-donating groups, provided moderate to excellent yields (52-99%). As for aryl chlorides, *para*-nitrochlorobenzene also provided high yield of the expected phenol, but aryl chloride substituted with a weak electron-withdrawing benzoyl group led to less yield (99% vs 30%). It was noteworthy that even aryl halides containing base-sensitive groups ketones and acid-sensitive cyano groups, survived well during the reaction. The catalyst and D-glucose could be easily removed from organic phase to aqueous phase by extracting the reaction mixture with water. This process provided a greener and sustainable way to synthesize phenols.

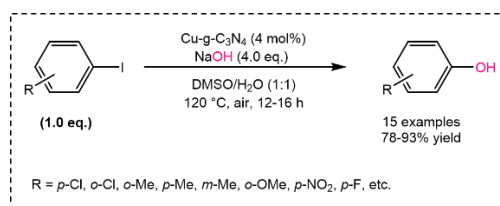


Scheme 115. Copper-catalyzed hydroxylation of aryl halides.³⁸⁸

2.1.4.2. Copper-catalyzed heterogeneous hydroxylation of aryl halides

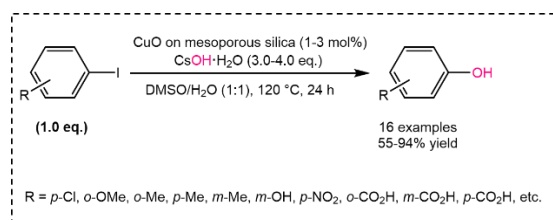
To our knowledge, only two publications of copper-catalyzed hydroxylation of aryl halides under heterogeneous conditions have been reported.

Han *et al.*³⁸⁹ in 2014 synthesized a copper-doped graphitic carbon nitride catalyst (Cu-g-C₃N₄) for the hydroxylation of aryl iodides and NaOH in the absence of ligand. With this efficient and recyclable catalyst, the reaction could proceed in a mixture of DMSO/H₂O at 120 °C under air, affording the corresponding phenols in good to excellent yields (**Scheme 116**). Various phenols were synthesized in yields ranging from 78% to 93% under the current conditions. The recyclability of Cu-g-C₃N₄ was explored with the coupling reaction of iodobenzene with NaOH. The results showed that the catalyst could be recovered and recycled at least 5 times without significant loss of activity. Phenol could be successfully produced with 99% yield under the optimal conditions in a large-scale experiment (10 g).



Scheme 116. Cu-g-C₃N₄-catalyzed hydroxylation of aryl iodides.³⁸⁹

Another example was proposed by Lee and co-workers³⁹⁰ in 2011. They developed a heterogeneous CuO supported on mesoporous silica for the synthesis of phenols from aryl iodides and CsOH. The reaction could proceed at 120 °C in a mixture of DMSO /water (1:1) with the help of 1 mol% catalyst and without the need of external ligand (**Scheme 117**). Various functionalized aryl halides were employed in the current conditions, providing the corresponding phenols in good to excellent yields. The recyclability of the catalyst was investigated for the reaction of *para*-iodoanisole and CsOH, and the results showed that the catalyst could be reused at least four times without significant loss of activity.



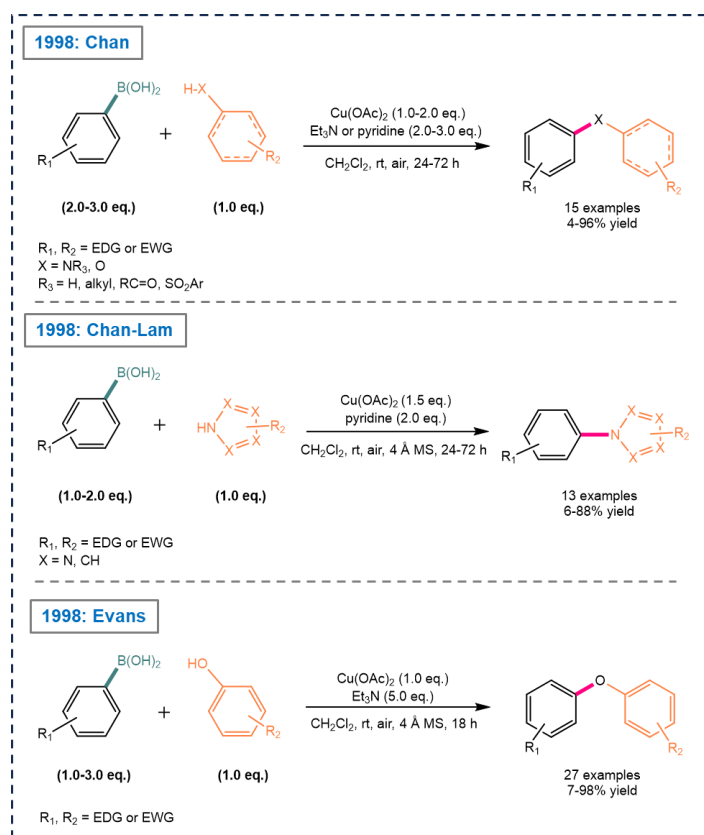
Scheme 117. CuO supported on mesoporous silica-catalyzed hydroxylation of aryl iodides.³⁹⁰

2.2. ... to Chan-Lam-type reactions

In 1979, N. Miyaura and A. Suzuki discovered that alkenyl, alkynyl and arylboronic acids could be engaged in palladium-catalyzed cross-coupling reactions.^{238,239} This finding started a burst in cross-coupling reactions of arylboronic acids and their applications in aryl-aryl bond formations, but also induced the seminal work on copper-promoted Chan-Lam-Evans coupling reactions to form C_{aryl}-O and C_{aryl}-N bonds.

In 1998, Chan¹⁰, Lam¹¹ and Evans⁹ proposed concomitantly milder reaction conditions by replacing the aryl halide partner, peculiar to the Ullmann coupling reaction, with an arylboronic acid (ABA) (**Scheme 118**). Such a shifting enabled the synthesis of aryl ethers and aryl amines at room temperature with various *O*- and *N*-nucleophiles, respectively. Accordingly, such coupling reactions were named Chan-Lam-Evans reactions. The new method has gained widespread interest due to the availability of numerous boronic acids, the mild conditions

employed,³¹⁹ and broader functional group tolerance compared to aryl halides. However, a stoichiometric amount of copper(II) with excess base was still necessary to promote these reactions.



Scheme 118. First reports of the Chan-Lam-Evans reactions.⁹⁻¹¹

In the last decades, various synthetic approaches have been developed to form $\text{C}_{\text{aryl}}\text{-N}$ and $\text{C}_{\text{aryl}}\text{-O}$ bonds in Chan-Lam-type reactions. Furthermore, these reactions were most carried out with bases and ligands under palladium or copper-catalyzed homogeneous conditions, only a small amount of heterogeneous versions of these reactions have been disclosed to date. The next section will present various examples of Chan-Lam-type reactions performed under homogeneous and heterogeneous conditions, respectively.

2.2.1. Homogeneous and heterogeneous Chan-Lam-type reactions

Various homogeneous Chan-Lam-type reactions have been reported in the last decades with stoichiometric or catalytic copper salts or complex, which have been detailed in Dong *et al.*'s review³³⁴. However, an extremely limited number of heterogeneous versions were reported in the literature. Among them, most approaches focused on the construction of C-N bonds. Herein, we take the C-N bond formation as an example to introduce the Chan-Lam-type reactions.

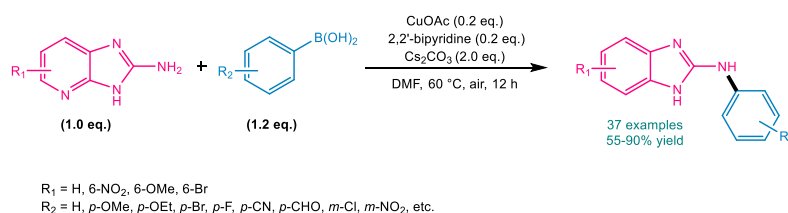
2.2.1.1. Homogeneous Chan-Lam-type reactions

Wu and co-workers³⁹¹ developed an efficient protocol to produce *N*-arylpyridin-2-amine derivatives (**Scheme 119**). The copper-mediated reaction of 2-aminopyridine with ABAs had widely functional group tolerance and provided the expected products with moderate to good yields.



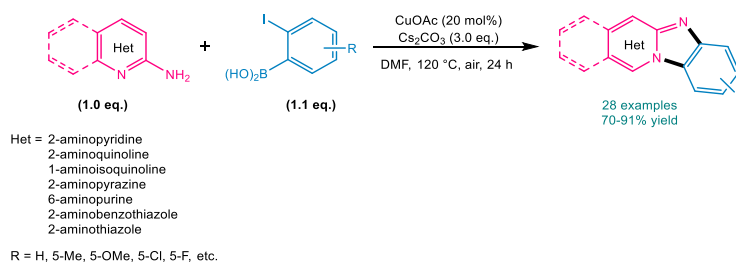
Scheme 119. Cu(OAc)₂·H₂O-mediated Chan-Lam-type reaction.³⁹¹

Das's group³⁹² reported selective *N*-arylation of aminobenzimidazoles *via* a copper(II)-catalyzed Chan-Lam-type reaction. It was noting that the reaction represented the first example of Cu-catalyzed selective C-NH₂ arylation (**Scheme 120**).



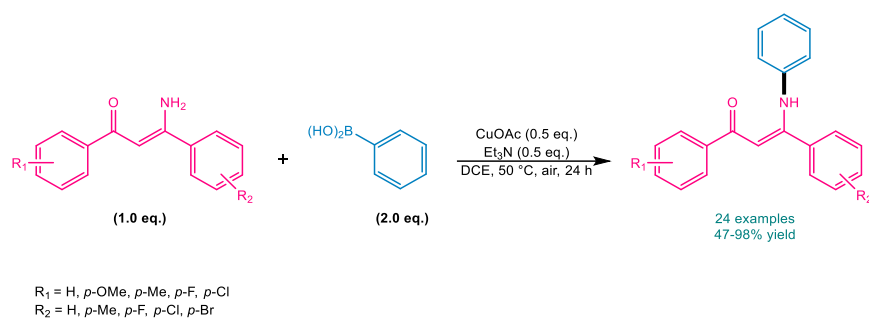
Scheme 120. CuOAc-promoted Chan-Lam-type reaction.³⁹²

Das *et al.*³⁹³ achieved Cu(II)-catalyzed inter/intramolecular C-N bond formation to synthesize various benzimidazole-fused heterocycles without ligand under air (**Scheme 121**).



Scheme 121. CuOAc-catalyzed Chan-Lam-type reaction.³⁹³

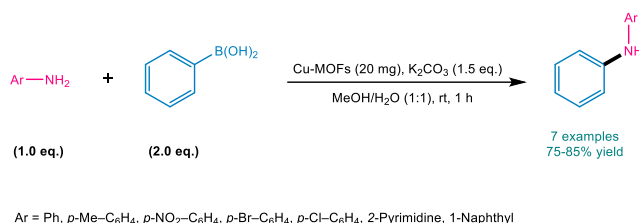
Ma and co-workers³⁹⁴ reported the Chan-Lam coupling reactions of enaminones with aromatic boronic acids, providing an efficient route to yield *N*-aryl enaminones. This protocol exhibited an excellent functional group compatibility (**Scheme 122**).



Scheme 122. CuOAc-promoted Chan-Lam-type reaction.³⁹⁴

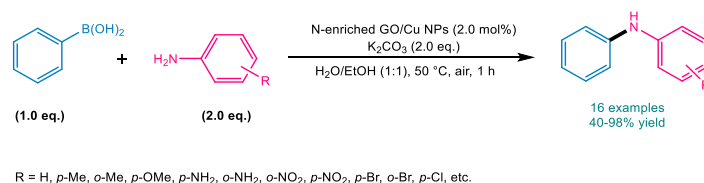
2.2.1.2. Heterogeneous Chan-Lam-type reactions

Naimi-Jamal and co-workers³⁹⁵ prepared a copper-based nanoporous MOF material, $\text{Cu}_2(\text{BDC})_2(\text{BPY})$ (BDC = benzene-1,4-dicarboxylate; BPY = 4,4'-bipyridine), as an efficient and recyclable heterogeneous catalyst for the Chan-Lam-type reactions. This catalyst could be reused for several times without obvious activity loss (**Scheme 123**).



Scheme 123. Cu-MOFs-catalyzed Chan-Lam-type reaction.³⁹⁵

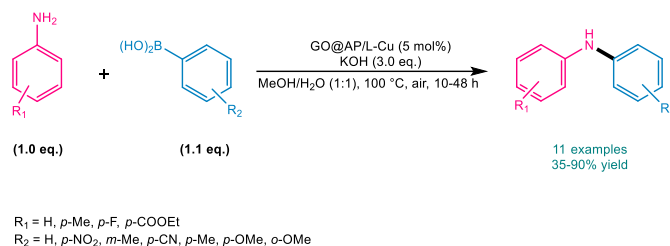
Seyedi *et al.*³⁹⁶ also synthesized copper nanoparticles immobilized on nitrogen-enriched graphene oxide (N-enriched GO) as an efficient catalyst for the Chan-Lam reactions (**Scheme 124**). This catalyst could promote the Chan-Lam coupling reaction of aniline derivatives and *N*-heterocycles under green and mild conditions. This catalyst could be easily recovered and reused six times without losing activity.



Scheme 124. N-enriched GO/Cu NPs-catalyzed Chan-Lam-type reaction.³⁹⁶

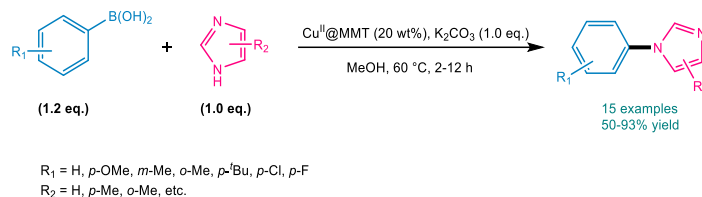
Sharma and co-workers³⁹⁷ reported an efficient and reusable heterogeneous catalyst for Chan-Lam reactions (**Scheme 125**). The catalyst was prepared by supporting the Cu(II) ligand complex on graphene oxide (GO) (GO@AP/L-Cu). The reaction conditions proved to be simple

and clean with this catalyst, providing products yields up to 90%. Additionally, the catalyst showed negligible activity loss after being reused for four times.



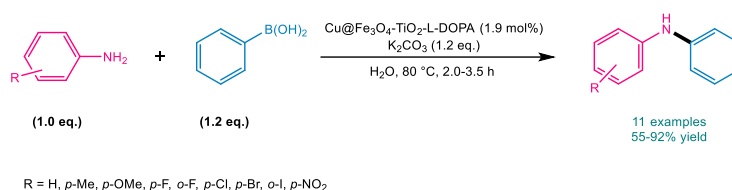
Scheme 125. GO@AP/L-Cu-catalyzed Chan-Lam-type reaction.³⁹⁷

Bora *et al.*³⁹⁸ disclosed an efficient and simple catalytic protocol for the Chan-Lam reactions of ABAs and *N*-nucleophiles including imidazoles (**Scheme 126**). The copper salt was intercalated within montmorillonite (MMT) K-10 to form the Cu(II)@MMT catalytic system. The latter exhibited interesting performance for the formation of C-N bonds in Chan-Lam-type reactions, affording the expected products in yields ranging from 50% to 93%.



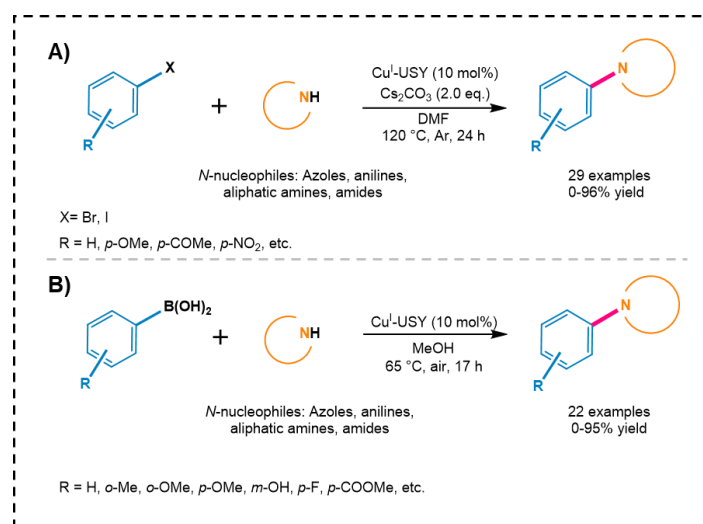
Scheme 126. Cu(II)@MMT-catalyzed Chan-Lam-type reaction.³⁹⁸

Paul and co-workers³⁹⁹ developed an efficient copper-doped magnetic catalyst (Cu@Fe₃O₄-TiO₂-L-DOPA) for the C-N bond Chan-lam-type reaction (**Scheme 127**). Cu nanoparticles were immobilized on the Fe₃O₄-TiO₂-L-DOPA support material with an aqueous solution of NaBH₄. This catalyst could promote phenylboronic acid to couple with various substituted anilines smoothly in the absence of ligand. The catalyst could be recycled at least 6 times without significant activity loss.



Scheme 127. Cu@Fe₃O₄-TiO₂-L-DOPA-catalyzed Chan-Lam-type reaction.³⁹⁹

It is worth mentioning that our group has made great progress in the formation of C-N bonds catalyzed by Cu^I-USY in previous work.⁴² Compared to our Ullmann conditions which utilize aryl halides as coupling partners and require high temperature (120 °C), toluene or DMF as solvent and the presence of an additional base⁴⁰ (**Scheme 128, top**), our Chan-Lam-Evans Cu^I-USY-catalyzed conditions are milder and greener, as they only required refluxing in methanol under air without any base and ligand (**Scheme 128, bottom**). These results again proved that Cu^I-USY is a highly efficient catalyst for the Chan-Lam-type C-N bond cross-coupling.



Scheme 128. Representative examples of Ullmann coupling (top)⁴⁰ and Chan-Lam-Evans coupling reactions (bottom) for C-N bond formation.⁴²

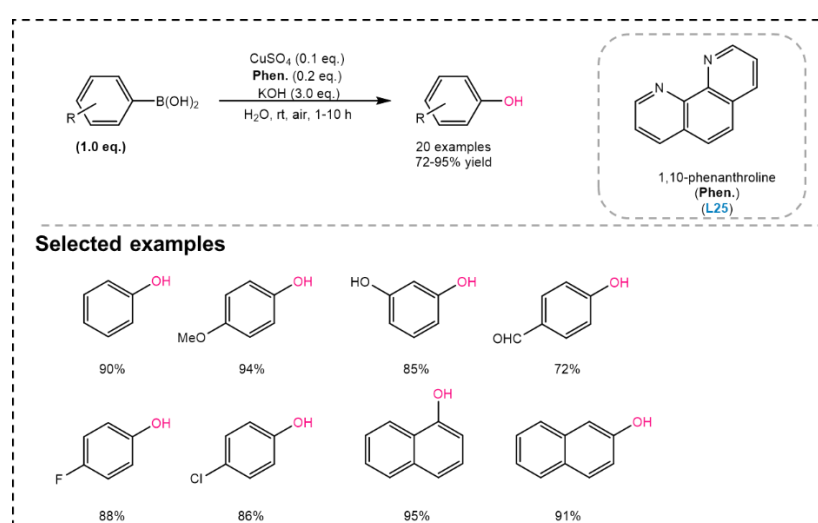
However, the formation of the C-O bonds towards phenols or aryl ethers with compatible *O*-nucleophiles through Cu^I-USY-catalyzed Chan-Lam-type reactions has not yet been fully developed.

2.2.2. Hydroxylation of arylboronic acids towards phenols *via* Chan-Evans-type reactions

Recently, Zhang *et al.*³⁴⁵ published a review on the synthesis of functionalized phenols from aromatic boronic acids and their derivatives. A series of reaction systems have been comprehensively demonstrated, including traditional thermal homogeneous and heterogeneous catalysis, electrocatalytic systems and photocatalytic, as well as oxidant involved catalyst-free systems. However, only five examples related on oxidative hydroxylation of aromatic boronic compounds using hydroxide salts as nucleophiles.

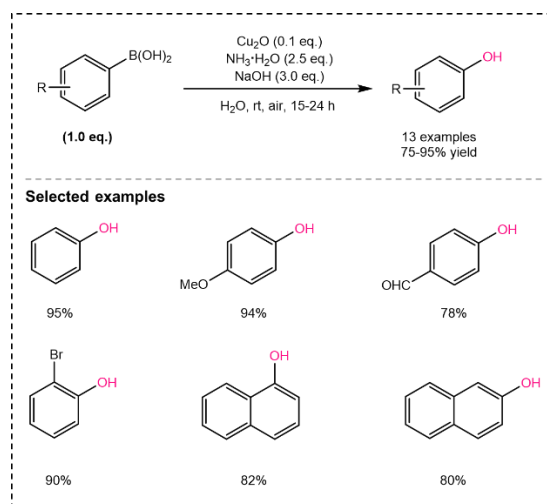
2.2.2.1. Hydroxylation of arylboronic acids towards phenols under homogeneous conditions

In 2010, Hu and co-workers⁴⁰⁰ reported an efficient copper(II) salt-catalyzed oxidative hydroxylation of arylboronic acids with KOH to synthesize phenols (**Scheme 129**). The reaction proceeded at room temperature in water using cheap CuSO₄ and 1,10-phenanthroline (Phen.) as catalyst and ligand (**L25**), respectively. With such catalyst, various substituted phenols bearing electron-donating groups could be efficiently prepared in higher yields than those bearing electron-withdrawing groups. This represented the first copper-catalyzed oxidative hydroxylation of arylboronic acids for the synthesis of functionalized phenols.



Scheme 129. CuSO₄-catalyzed hydroxylation of arylboronic acids.⁴⁰⁰

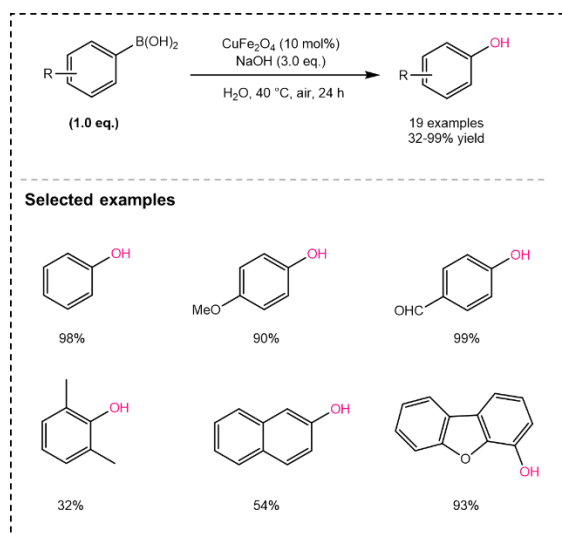
Shortly after, Fu *et al.*⁴⁰¹ reported Cu₂O/NH₃ complex-catalyzed hydroxylation of arylboronic acids towards phenols in the absence of ligand in water under ambient conditions (**Scheme 130**). It should be noted that ammonia acted as the ligand and additive in the reaction. The optimal reaction conditions were Cu₂O/NH₃ complex (0.1 equiv.) as the catalyst and NaOH as the nucleophile (3 equiv.). Various substituted arylboronic acids were employed under the present conditions, providing good to excellent yields of the corresponding phenols (75-95%). The results indicated that arylboronic acids bearing electron-donating groups showed higher reactivity than the ones containing electron-withdrawing groups. Moreover, the catalyst system in water could be reused up to five times, with the yield decreasing from 92% to 82%. Notably, the catalytic system was also applicable for the preparation of aryl iodides, aryl azides, aryl sulfones and arylamines from arylboronic acids.



Scheme 130. Copper-catalyzed oxidative hydroxylation of arylboronic acids.⁴⁰¹

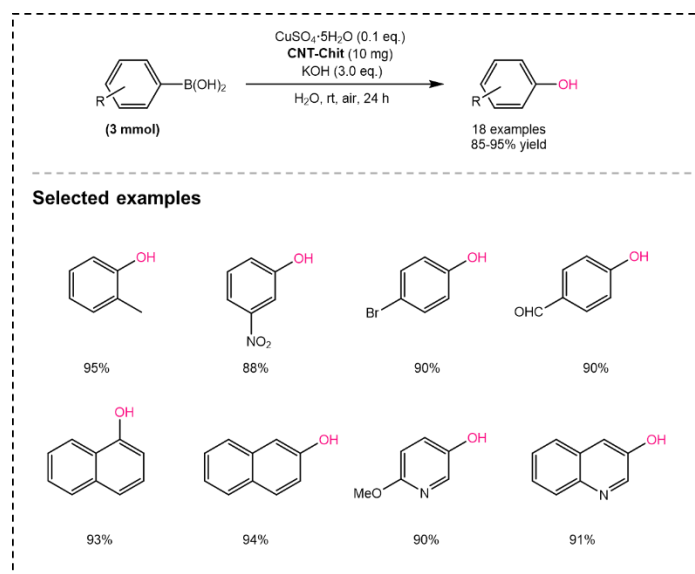
2.2.2.2. Hydroxylation of arylboronic acids towards phenols under heterogeneous conditions

Wang *et al.*⁴⁰² developed an oxidative hydroxylation of arylboronic acids catalyzed by magnetic CuFe_2O_4 nanoparticles in the absence of ligand and additive (**Scheme 131**). Using this inexpensive, readily available and air-stable catalyst in water under ambient conditions, the reaction effectively converted various substituted arylboronic acids to the corresponding phenols in moderate to good yields (32-99%). The electronic effect of the substituted functional groups (including electron-donating groups, neutral groups, and electron withdrawing groups) in arylboronic acids did not exhibit obvious reactivity differences. The catalyst could be completely recovered with an external magnet and could be reused and recycled at least six times without obvious loss of catalytic activity. When using H_2^{18}O as the solvent under the present conditions, 63% of the phenols contained ^{18}O atom and 31% of phenols contained ^{16}O atom products, indicating that the oxygen source for the phenol production was mostly water.



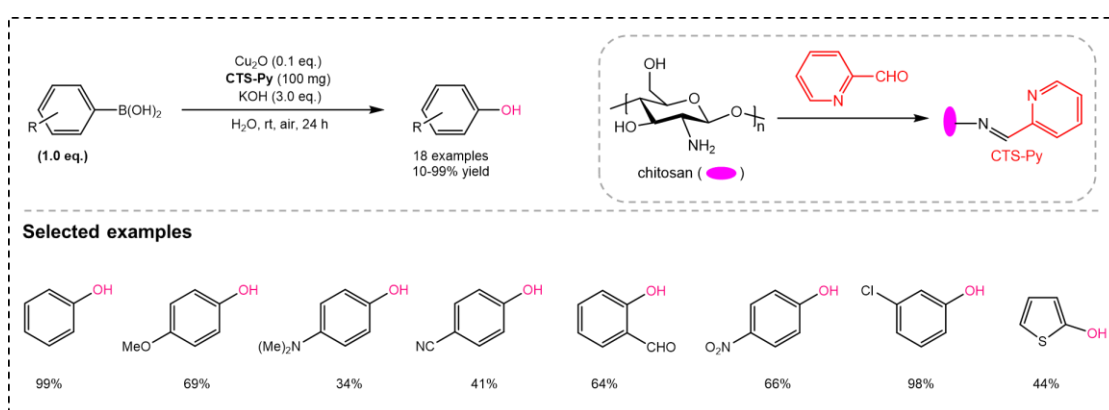
Scheme 131. Magnetic CuFe_2O_4 -catalyzed aerobic hydroxylation of arylboronic acids.⁴⁰²

In 2018, Kim and co-workers⁴⁰³ prepared a novel carbon nanotube (CNT)-chitosan (CNT-Chit) nanohybrid film material for the copper-catalyzed aerobic hydroxylation of aromatic boronic acids in aqueous media (**Scheme 132**). A variety of arylboronic acids containing electron-donating or electron-withdrawing groups were smoothly transformed into the corresponding phenols with high yields (85-95%) at room temperature in water using Cu_2SO_4 salt supported on recyclable and reusable CNT-Chit film as catalyst without any extra additives. The catalyst could be recovered by simply filtration with water and drying in air after each run, and directly reused for the next run. The catalyst recovered could be recycled up to five times without obvious loss of activity in terms of the purified product yields (from 98% to 95%).



Scheme 132. Copper-based heterogeneous hydroxylation of arylboronic acids.⁴⁰³

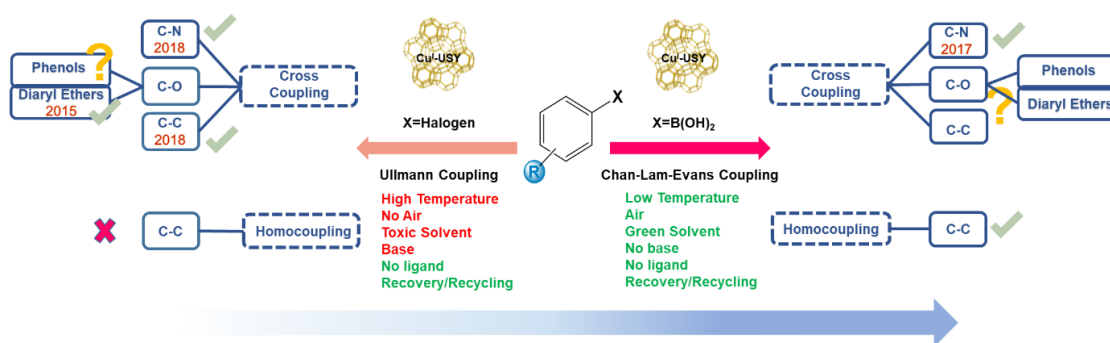
In a subsequent study, the same group⁴⁰⁴ further synthesized a pyridine-modified chitosan support (CTS-Py) for the copper-catalyzed oxidative hydroxylation of aromatic boronic acids with KOH in water (**Scheme 133**). The CTS-Py acted as a biopolymer ligand of the copper salt Cu_2O in the reaction. 99% yield of phenol could be obtained in the model hydroxylation reaction of phenylboronic acids using such an efficient catalyst. Regardless of the electronic effects of the substituted groups, various substituted arylboronic acids were successfully transformed to the corresponding phenolic compounds in moderate to high yields. The catalytic system exhibited compatible tolerance to various functional groups such as alkoxy, amino, carbonyl, nitro, and chloro functionalities. Unfortunately, this catalyst could only be reused once, and the product yield decreased significantly from 89% to 17%.



Scheme 133. Cu_2O -based heterogeneous hydroxylation of arylboronic acids.⁴⁰⁴

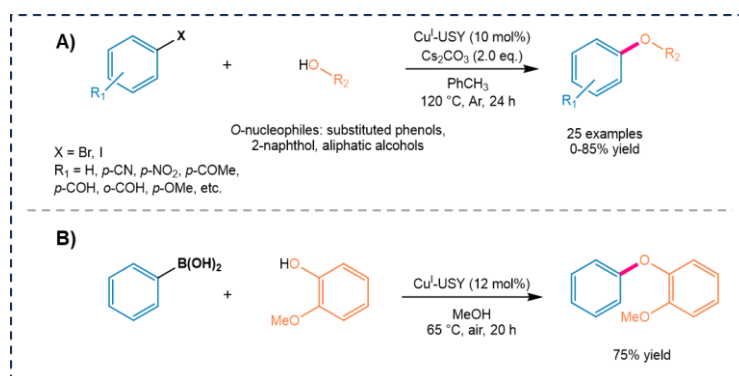
3. Our current research progresses and theme

The fact that zeolites can easily be loaded with various transition metal ions,^{160,318} as well as our recent success in forming C_{aryl}-X bonds to synthesize aryl azides⁴¹, aryl ethers^{39,40} or *N*-derivatives⁴² via copper(I)-zeolite-catalyzed Ullmann-type reactions^{39,40} and Chan-Lam-type reactions^{41,42}, motivated us to explore the formation of C_{aryl}-O bonds using copper(I)-zeolite as catalyst in Ullmann-type and Chan-Lam-type reactions (**Scheme 134**).



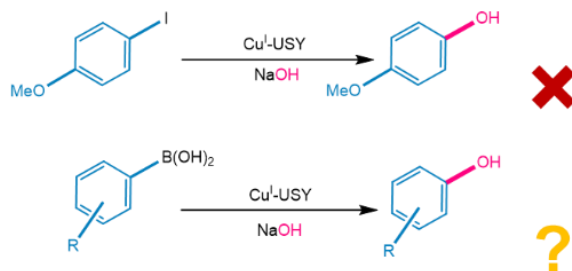
Scheme 134. Comparison of Ullmann and Chan-Lam-Evans coupling processes for C-heteroatom and C-C bonds formation.³⁹⁻⁴²

Our previous results showed that Cu^I-USY could indeed catalyze Ullmann-type C-O (**Scheme 135, top**), but also Chan-Lam-type C-N coupling reactions (**Scheme 134**). Preliminary results revealed that Chan-Evans-type C-O coupling reaction towards aryl ether could as well be catalyzed by Cu^I-USY (**Scheme 135, bottom**). However, the examination of the literature, as reported in the previous section, suggested us to investigate the formation of phenol, with the goal of achieving milder and greener conditions than the usual conditions, especially industrial ones.



Scheme 135. Cu^I-USY-catalyzed Ullmann-type coupling (top)⁴⁰ and Chan-Lam-Evans coupling reactions (bottom) for the synthesis of aryl ethers.

Therefore, my research has so far focused on the following aspects: exploring and expanding the Chan-Evans type C-O cross-coupling reactions between arylboronic acids and the easy-to-handle and cheap hydroxide salts (e.g., NaOH, KOH...) as nucleophilic species to synthesize phenol compounds. Indeed, preliminary experiments showed that the Ullmann version could not be applied to such reaction (**Scheme 136**).



Scheme 136. Comparison of Cu^I-USY-catalyzed Ullmann reaction and Chan-Lam-type reactions.

4. Chan-Lam-Evans coupling reactions for C-O bond formation towards phenols

4.1. The optimization of reaction conditions

The initial investigation was conducted with the reactive *para*-methoxyphenylboronic acid as the model substrate and easy-to-handle and cheap hydroxide anion as nucleophilic species. Cu^I-USY was first used as the catalyst in this reaction owing to its excellent performance in our earlier works.

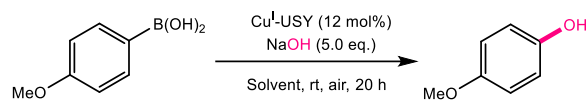
Our experiments were usually performed at room temperature because of the instability of phenol when heated under air⁴⁰⁵⁻⁴⁰⁷ in our preliminary results. In addition, considering the importance of protic solvents for copper(I)-zeolite-catalyzed related reactions in our earlier works,^{41,42} several protic solvents were investigated in the present reaction (**Table 9**).

It was surprising that ethanol could not allow the reaction to occur, while MeOH, the optimal solvent in our previous work, only provided a very low amount of phenol product (entries 1-2). Nevertheless, water was able to produce the expected phenol in high yield (entry 3), making this process even greener and more sustainable. Furthermore, control experiments confirmed that this hydroxylation is not a simple hydrolysis of the arylboronic acid, nor an aromatic nucleophilic substitution reaction. Indeed, only tiny amount of phenol could be detected in the absence of hydroxide anion (entry 4), and no reaction occurred without catalyst (entry 5). In addition, heating proved deleterious since the known phenol oxidation easily occurred when exposed to oxygen (entry 6 *vs* 3). Under such heating conditions, yields were moderate or even low despite faster reaction rates (entries 7-8 *vs* 3).

With the optimal solvent condition in hand, the amounts of hydroxide and of catalyst were then optimized. Dividing the amount of hydroxide by two would lower the phenol yield in the same proportion (entry 9 *vs* 3), and doubling its amount surprisingly provided a decreased yield (entry 10 *vs* 3). The latter result might be due to the known zeolite sensitivity to bases.^{297,300,323,324} The reaction efficiency clearly showed that around 5 equivalents of sodium hydroxide (NaOH) was the optimum (**Figure 18, left**). Furthermore, a similar result was obtained with another common hydroxide source, potassium hydroxide (KOH), under the same conditions (entry 13).

Also, reducing the amount of catalyst also lowered the phenol yield (entry 11 *vs* 3), while increasing it did not significantly change the product yield (entry 12 *vs* 3).

Table 9. Screening of solvents metal hydroxides and the catalyst loading for the Cu^I-USY-catalyzed Chan-Evans-type coupling of *para*-methoxyphenylboronic acid.^[a]



Entry	Solvent	Cu ^I -USY (mol%)	NaOH (eq.)	Time (h)	Yield (%) ^[b]
1	EtOH	12	5	20	Traces ^[c]
2	MeOH	12	5	20	<5 ^[c]
3	H ₂ O	12	5	20	80
4	H ₂ O	12	-	20	<5 ^[c]
5	H ₂ O	-	5	20	0
6 ^[d]	H ₂ O	12	5	20	0 ^[c]
7 ^[d]	H ₂ O	12	5	6	54 ^[c]
8 ^[e]	H ₂ O	12	5	1.5	16
9	H ₂ O	12	2.5	20	38
10	H ₂ O	12	10	20	68 ^[c]
11	H ₂ O	6	5	20	62
12	H ₂ O	24	5	20	84
13 ^[f]	H ₂ O	12	5	20	78

^[a] Reactions run with *para*-methoxyphenylboronic acid (0.5 mmol, 1 equiv.), NaOH and Cu^I-USY (12 mol%) were stirred in 2 mL solvent at room temperature under air, unless otherwise stated.

^[b] Yields of isolated pure product after flash chromatography, unless otherwise mentioned.

^[c] Yield estimated by ¹H NMR using 1,3,5-trimethoxybenzene as internal standard.

^[d] Reaction performed at 50 °C.

^[e] Reaction performed at 100 °C.

^[f] Reaction run with KOH as the nucleophile.

A plateau seemed to be reached at around 12 mol% of Cu^I-USY (**Figure 18, right**).

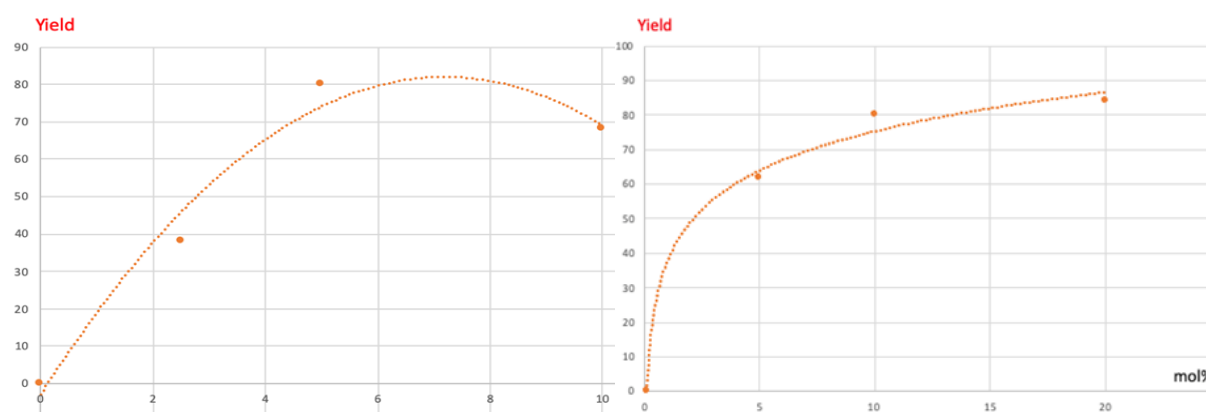
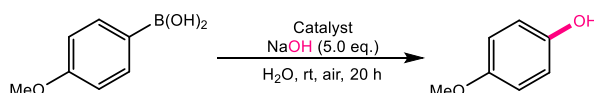


Figure 18. Cu^I-USY-catalyzed hydroxylation of *para*-methoxyphenylboronic acid: influence of the amount of NaOH (left) and of catalyst loading (right).

With the optimized conditions in hand, the potential of other catalysts in this reaction was investigated (**Table 10**). Interestingly, using Cu^{II}-USY also led to the hydroxylation product in yield similar to the one achieved with Cu^I-USY (entry 2 vs 1). This result suggested that the copper species within zeolite was probably oxidized when the reaction was performed under air. To check this hypothesis, the reaction was performed under argon with Cu^I-USY as catalyst. Such conditions induced low conversion (33%) and only returned a small amount of phenol, although the yield relative to conversion (61%) remained good and quite close to the one achieved with Cu^I-USY (85%) (entry 3 vs 1). This result not only confirmed that oxygen was required for this reaction, as for classical Chan-Lam-Evans C-O couplings, but led to clues regarding the mechanism of such reaction (see below). In addition, the use of copper(I) chloride (CuCl) also gave the phenol products with similar conversion but slightly lower yields compared to the Cu^I-USY-catalyzed reaction (entry 4 vs 1), while cupric chloride (CuCl₂) provided lower conversion and yield compared to the one under Cu^{II}-USY catalysis (entry 5 vs 2). Furthermore, no reaction occurred with the native commercial USY zeolite or without any catalyst (entries 6-8). The present results clearly showed that this reaction is catalytic due to copper(I) or (II) ions loaded in a zeolite. It should be pointed out that Chan-Lam-Evans C-O and C-N couplings usually required at least stoichiometric amount of copper salts and proceed best with copper(II) salts, notably copper(II) acetate.³¹⁹

Table 10. Screening of catalyst.^[a]

Entry	Catalyst	Copper Loading (mol%)	Conversion (%) ^[b]	Yield (%) ^[b]
1	Cu ^I -USY	12	94	80 ^[c]
2	Cu ^{II} -USY	12	91	79
3 ^[d]	Cu ^I -USY	12	33	20
4	CuCl	12	94	73
5	CuCl ₂	12	80	66
6	H-USY	-	2	0
7	NH ₄ -USY	-	0	0
8	None	-	0	0

^[a] Reactions run with *para*-methoxyphenylboronic acid (0.5 mmol, 1 equiv.), NaOH (2.5 mmol, 5 equiv.) and catalyst (X mol%) were stirred in 2 mL water for 20 h at room temperature under air, unless otherwise stated.

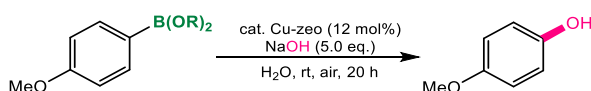
^[b] Conversion and yield estimated by ¹H NMR using 1,3,5-trimethoxybenzene as internal standard.

^[c] Yields of isolated pure product after flash chromatography.

^[d] Reaction under Ar.

The role of the boronic moiety in this hydroxylation reaction was then surveyed with the optimal conditions described above (**Table 11**). As suspected, the nature of the boronic moiety influenced the reaction outcome. Interestingly, starting from the pinacol boronic ester led to very high yield of phenol with Cu^I-USY as catalyst (entry 3 *vs* 1) but to lower conversion and yield with Cu^{II}-USY (entry 4 *vs* 2). In contrast, *N*-methyliminodiacetic acid (MIDA) derivative only led to modest yields (entries 5-6 *vs* 3-4 and 1-2), and a lower efficacy of Cu^{II}-USY *vs* Cu^I-USY was observed (entry 5 *vs* 6). A trifluoroborate analog was also engaged in this reaction, but it was not surprising that the hydroxide medium led to successive exchange of the fluoride linked to boron. Indeed, combined ¹H and ¹⁹F NMR analyses allowed to detect difluorohydroxyboronate in solution, especially 20% boronic acid derivative could be observed under Cu^{II}-catalysis conditions (entry 8). These results suggest that the observed reactivity difference is probably linked to the hydrolysis rate of the boronate moiety. The chelating MIDA ligand could only be slowly displaced by the hydroxide added and thus the corresponding boronate only slowly reacted.

Table 11. Influence of the boronic moiety.^[a]



Entry	-B(OR) ₂	The type of catalyst	Conversion (%) ^[b]	Yield (%) ^[b]
1		Cu ^I -USY	94	80
2		Cu ^{II} -USY	91	79
3		Cu ^I -USY	99	95
4		Cu ^{II} -USY	77	68
5		Cu ^I -USY	100	35+6 ^[c]
6		Cu ^{II} -USY	100	27+7 ^[c]
7		Cu ^I -USY	100	80
8		Cu ^{II} -USY	100	60+20 ^[d]

^[a] Reactions run with boron derivative (0.5 mmol, 1 equiv.), NaOH (2.5 mmol, 5 equiv.) and catalyst (12 mol%) were stirred in 2 mL water for 20 h at room temperature under air, unless otherwise stated.

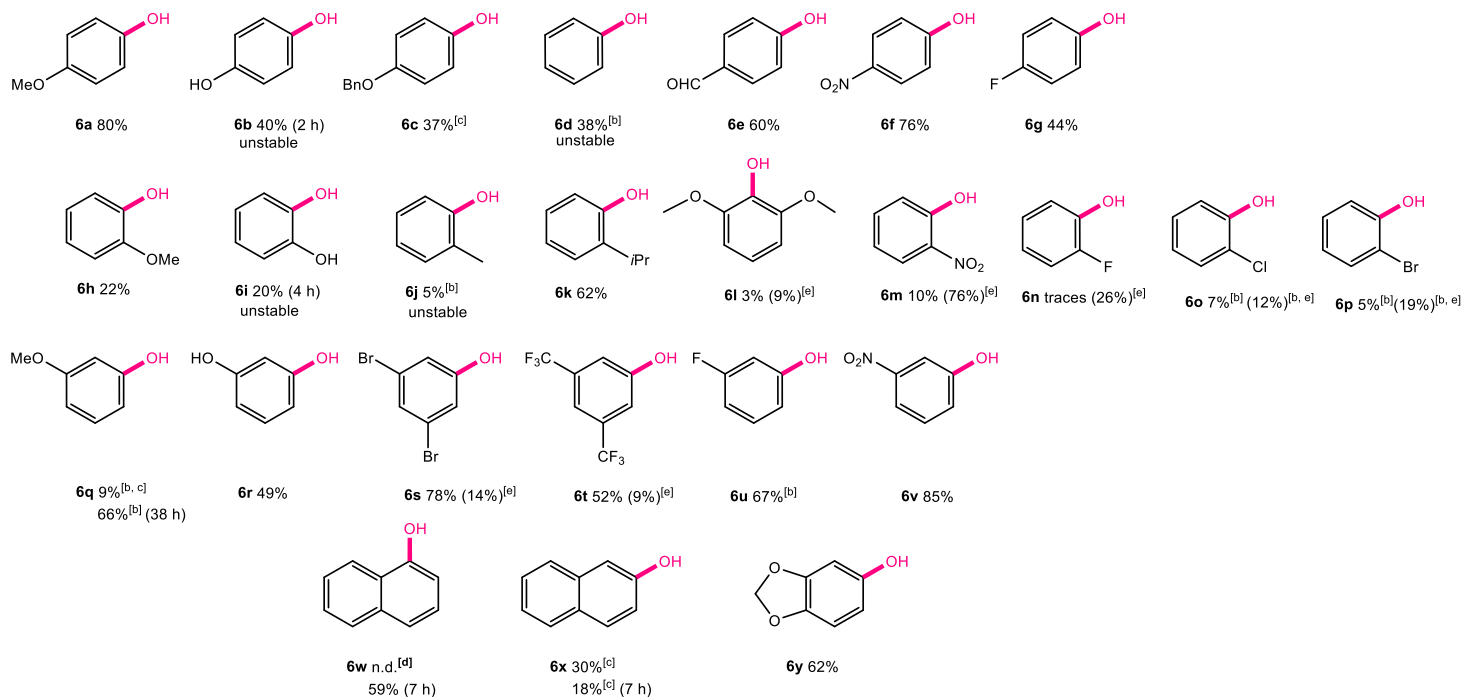
^[b] Conversion and yield estimated by ¹H NMR using 1,3,5-trimethoxybenzene as internal standard.

^[c] Yields of homocoupling product.

^[d] Yields of boronic acid derivative.

4.2. Reaction scope and limitation

Once optimized conditions and the right boronic precursor were set up, the possibility and limits of this new phenol heterogeneous synthesis was explored. A series of *ortho*-, *meta*- and *para*-substituted substrates with electron-withdrawing or electron-donating groups (EWG, EDG respectively) were selected to study the electronic effect in the reaction (**Scheme 137**).



Scheme 137. Cu^I-USY-catalyzed Chan-Evans-type C-O cross-coupling towards phenols.^[a]

^[a] Reactions run with boronic acid (0.5 mmol, 1 equiv.), NaOH (2.5 mmol, 5 equiv.) and Cu^I-USY (12 mol%) were stirred in 2 mL water for 20 h at room temperature under air, unless otherwise stated.

^[b] Yield estimated by ¹H NMR using dimethyl terephthalate as internal standard.

^[c] Incomplete conversion.

^[d] Not detected.

^[e] Yield of homocoupling product.

The *para* series usually gave the expected phenols in good to high yields (see **6a**, **6e**, and **6f**), without significant differences between EWG and EDG (see **6a** and **6f**). In some cases, such as **6b** or **6g**, the product proved very sensitive to the reaction conditions. The hydroquinone **6b** formed from the hydroxylation of *para*-hydroxyphenyl boronic acid quickly oxidized and decomposed, which not surprisingly gave a moderate yield after 2 h. Such behavior was checked with a benzylated analog and with phenol itself. The former led to the monoprotected hydroquinone **6c** with 37% yield based on the incomplete conversion (41%) after 20 h, suggesting that the protected boronic acid analog was less reactive than the *para*-hydroxyphenylboronic acid. Furthermore, the simple phenol **6d** was obtained with 38% yield together with side-products, suggesting that the so-produced phenol also suffered from the

oxidative decomposition. A control experiment was consequently performed with pure phenol placed under the reaction conditions. As suspected, the result revealed its decomposition (up to 60%) upon the reaction course (20 h) and an approximative 40% yield could be estimated by NMR.

The *ortho* series proved to be the most sensitive to such over-oxidation, and the corresponding phenols were obtained in low to modest yields.^{408,409} This degradation problem was alleviated with a substituent less prone to oxidation, and the reaction work as well as for other boronic acids, providing the corresponding phenols in good yields (see **6k**). In some cases, the corresponding homocoupling product was observed under the present basic reaction conditions.

With substituent(s) at the *meta* position, stability problems were less pregnant, and good to high yields of phenols were achieved (52-85%). Slightly better yields were obtained from boronic acids carrying EWG compared to those with EDG (67-85% vs 49-66%), see e.g. **6q** vs **6v**), suggesting some electronic effect of the substituent(s). α - and β -naphthyl boronic acids were more or less efficiently converted to the corresponding naphthols. No product was obtained from the α -substituted analog and a low yield was achieved with the β -substituted derivative (10 vs 30%).

Such results are reminiscent of the behavior of *ortho*- vs *meta*-substituted derivatives mentioned above. Indeed, when the reaction time was reduced to 7 h, a good yield (59%) of the α -substituted phenol **6w** was obtained. However, the product (**6x**) from the unstable β -analog was less formed after the reaction time was reduced to 7 h probably because the β -naphthyl boronic acid slowly reacted as it was not completely converted even within 20 h. Similarly, the 3,4-(methylenedioxy)phenylboronic acid reacted as a *para*- and *meta*-substituted phenylboronic acid and the corresponding phenol **6y** was obtained in good yield. The latter is a natural product, named sesamol, one of the nutritional components from sesame seeds and its oil, which exhibits antioxidant and antidepressant activities, as well as the capacity to lower lipids.⁴¹⁰

4.3. Recyclability study of catalyst and gram-scale experiment

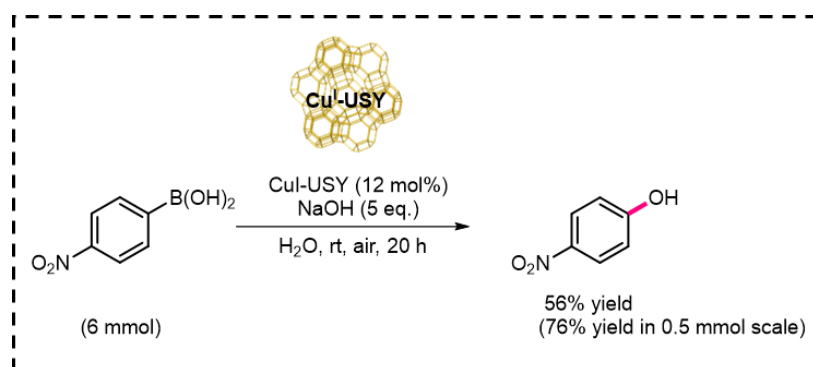
Using heterogeneous catalysts usually offers the advantage of facile catalyst recovery and possibility of reusing it for further reaction. This aspect was obviously checked for the present reaction. After each reaction, the insoluble zeolite material was easily recovered by filtration through a nylon 66 membrane (0.2 μm) and washed sequentially with 2M NaOH, H₂O, and MeOH to separate organic materials from catalytic material. This recovered solid was then re-

engaged in the hydroxylation reaction after drying under vacuum. However, variable results were obtained from several parallel experiments. Furthermore, only 75% of the solid zeolite introduced could be recovered.

Although it was not so strong, the basic reaction conditions probably led to some desilication of the silicoaluminate zeolitic material. Zeolite treatment with aqueous NaOH solution is well known to induce the formation of mesopores within zeolites, but also decrease the surface area and microporosity of zeolites, as well as partly damage the zeolite structure depending on zeolite composition and on the concentration of sodium hydroxide.⁴¹¹⁻⁴¹³ Thus, it seemed that Cu^I-USY was not recyclable in the present reaction conditions but still reusable.

Nevertheless, the Cu^I-USY-catalyzed-Chan-Evans-type hydroxylation reaction which was performed in water without additional ligand under air at room temperature, provided a greener and milder new protocol for the synthesis of phenols.

Moreover, the possibility of scale-up of our protocol was investigated with 1 gram (6 mmol) of *para*-nitrophenylboronic acid (**Scheme 138**) under standard conditions using 12 mol% Cu^I-USY. Although a slightly lower yield of the expected phenol product was obtained compared to the one at 0.5 mmol small scale, this result clearly showed that it is possible to scale up this reaction.

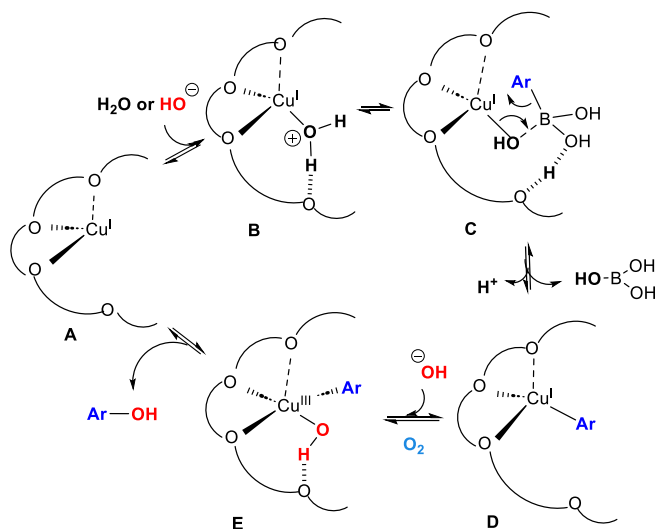


Scheme 138. Gram-scale study of Cu^I-USY-catalyzed Chan-Evans-type C-O cross-coupling.

4.4. Mechanism

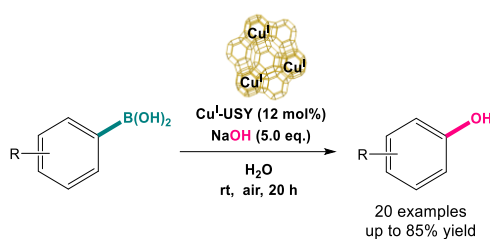
In the present reaction as in related ones,^{41,42} the zeolite framework exhibits the role of a huge stabilizing ligand for copper ions, especially copper(I). Their locations within this USY zeolite are known³²⁸ (For details, see Chapter II-4.5., **Figure 14**). It has been shown that those copper species located at site III' along the main pore are coordinatively unsaturated, which made them the most reactive (**A** in **Scheme 139**). The latter could thus coordinate to water or to a hydroxide

anion, and the resulting hydroxy complex (**B**) could then interact with the boronic acid. Transmetalation (**C**) will then occur to provide an arylcopper(I) species (**D**). In the presence of hydroxide and oxygen, an arylcopper(III) hydroxide⁴¹⁴ could be produced (**E**) and the latter should then evolve through reductive elimination, providing the corresponding phenol and regenerating the copper(I) species.



Scheme 139. Mechanistic proposal for the Cu^I-USY-catalyzed Chan-Lam-type C-O cross-coupling reaction.

5. Conclusion



In this study, we demonstrated that Cu^I-USY was proved to be an efficient and easy-to-handle supported copper(I) catalyst in Chan-Evans-type C-O cross coupling reactions. The easy-to-handle and cheap hydroxide anion was selected as nucleophilic species to synthesize various phenols moieties under Cu^I-USY catalysis. Very simple practical and green conditions, namely in water at room temperature under air, were found for efficiently promoting the desired C-O coupling process. This was the first heterogeneous copper(I)-zeolite catalyst to directly prepare phenols *via* Chan-Evans-type reactions. Unfortunately, the catalyst could not be recycled. Nevertheless, the reaction showed a large tolerance of functional groups (e.g., methoxy, hydroxy, halide, nitro, etc.). At this point, some twenty arylboronic acids were examined with coupling efficiency up to 85%, among which *meta*-substituted arylboronic acids proved to be the more suitable for producing phenols in high yields. Furthermore, a mechanism was proposed.

Nevertheless, further efforts were required to expand the application of this protocol.

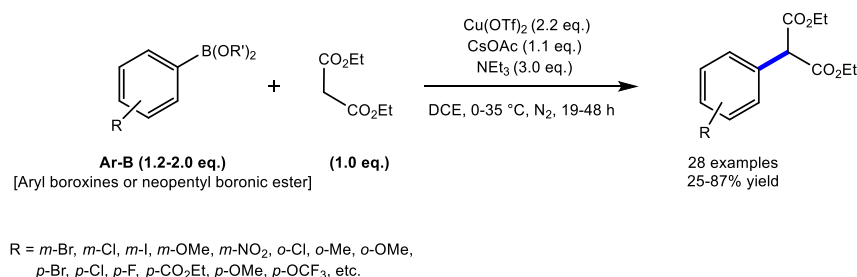
Chapter IV. Copper(I)-zeolite-catalyzed cross-dehydrogenative coupling (CDC) reaction to form C-C bonds and their applications on the synthesis of THIQ derivatives

1. Introduction

In the previous chapters, we have explored new catalytic systems based on copper(I)-zeolites, especially Cu^I-USY, to improve the formation of C-C bonds in Ullmann-type reactions. While achieving some interesting and inspiring results, we also observed some limitations of Cu^I-USY in these reactions:

- Cu^I-USY could not really promote the intermolecular cross-coupling of aryl halides to form C-C bonds. C-C bonds could be formed under these catalytic conditions, but only with activated methylene compounds acting as nucleophiles.
- A base (Cs₂CO₃), non-green solvent (toluene or DMF), and unsatisfactory temperature (120-140 °C) were still required in Cu^I-USY-catalyzed Ullmann-type reactions.

Alternatively, the formations of C-C bonds through Chan-Lam-type cross-coupling reactions were still very challenging in organic synthesis. Only one example has been reported to date under homogeneous conditions.⁴¹⁵ This reaction was mediated by stoichiometric copper salts in the presence of base and ligand using aryl boroxines or boronic esters as starting materials (**Scheme 140**).

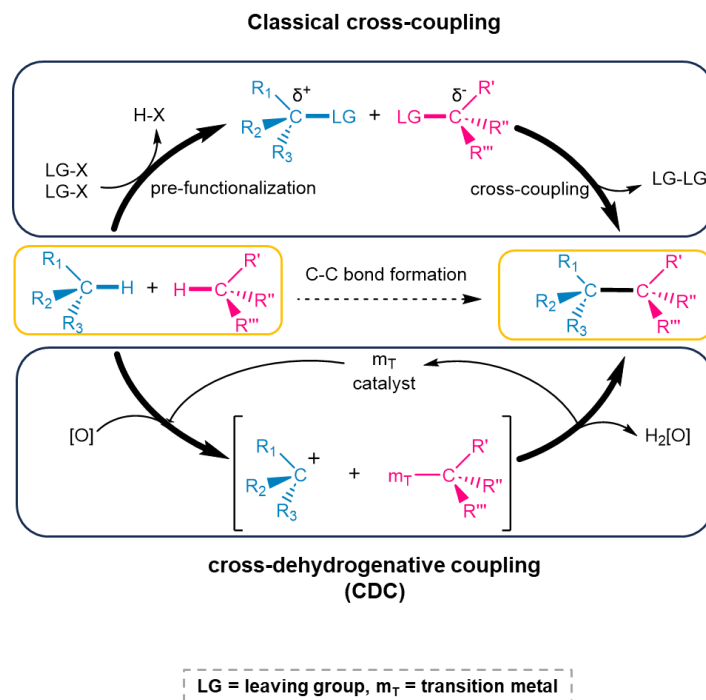


Scheme 140. Cu(OTf)₂-mediated Chan-Lam-Evans-type cross-coupling reactions for the formation of C-C bonds.⁴¹⁵

More importantly, these transition metal-catalyzed coupling reactions (**Scheme 141, top**) commonly required a functionalized partner to form the C-C bonds required to synthesize the desired products. Such processes inevitably produce unwanted by-product(s), leading to chemical wastes. Additionally, a pre-functionalization synthetic step is required to install the desired leaving group in each substrate. None of these could meet the requirements of green chemistry and sustainable development.

To solve these problems, chemists have been looking for more efficient and greener catalytic methodologies to construct C-C bonds in recent years.⁴¹⁶⁻⁴¹⁸ Among them, the cross-

dehydrogenative coupling (CDC) reaction emerged, which was one of the most sustainable and efficient synthetic strategies for constructing C–C bonds.⁴¹⁹



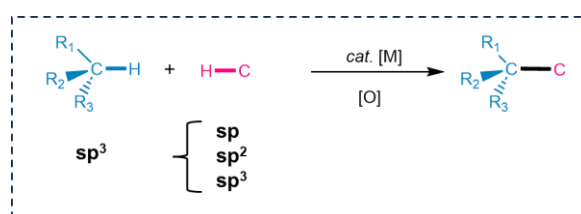
Scheme 141. Strategies for selective C-C bond formation.⁴

Inspired by the breakthrough achievements in catalytic C-H functionalizations,⁴²⁰ Li's group⁴ first coined in 2009 the concept of CDC reaction (**Scheme 141, bottom**). CDC reactions allowed the formation of C-C bonds directly from two coupling substrates with different C-H bonds in the presence of oxidant. This strategy assumed that the catalyst/mediator activated one of the C-H bonds to form a carbon nucleophile *in situ*. Meanwhile, the oxidation of the second C-H bond *in situ* generated an electrophilic carbon. Subsequently, a coupling reaction occurred between these two intermediates to provide a new C-C bond (**Scheme 141, bottom**). Under ideal conditions, the only waste product would be water if oxygen is used as the terminal oxidant in the method. Such a coupling allows to omit the preparation of functionalized starting materials, leading to shorter and more efficient synthetic schemes. As an attractive and challenging goal in organic synthesis⁴²¹, this reaction has attracted widespread interest since its appearance and studies in this field have increased dramatically in recent years. Various transition metals such as Ru⁴²², Rh⁴²³, Pd^{424,425}, Fe⁴²⁶⁻⁴²⁸, Co⁴²⁸, Ni, Cu⁴²⁹ and Mn²⁴⁵ have been applied to promote this reaction. Compared to other scarce and costly transition metals, Fe and Cu have been increasingly used due to their lower toxicity, lower cost, and high abundance. Furthermore, novel catalytic systems that differ from the thermally induced reaction, have been

exploited in the last decade,^{419,430} relying on photoredox, microwave, or electrochemical activations, etc., for the connection of different C-H bonds in C_{sp}-H, C_{sp2}-H, and C_{sp3}-H.^{9,10,431,432}

The formation of direct C_{sp3}-C bonds in CDC reactions (**Scheme 142**) induced a variety of chemo-, regio- and stereoselectivity problems, so it is regarded as one of the most challenging tasks in current organic synthesis.

Pioneer in this field, Li's group has been devoted to the functionalization of C_{sp3}-H bonds with other C-H bonds in CDC reactions and this group has achieved fruitful results.⁴³³ Among these results, the alkylation of *N,N*-dialkylanilines and tetrahydroisoquinolines (THIQs),^{434,435} have been developed to such an extent that it is now a reference system for evaluating the performance of new catalytic systems.



Scheme 142. Cross-dehydrogenative coupling for C_{sp3}-C bond formations.⁴³³

Tetrahydroisoquinoline motif is widely present in natural products, and most of them exhibit a broad range of biological and pharmacological activities⁴³⁶. Among them, 1-substituted tetrahydroisoquinolines, *i.e.* the nitrogen-containing heterocyclic moiety with a stereocenter at C-1 carbons (**Figure 19**), are privileged scaffolds in drugs and pharmaceuticals^{27,437-439}. For instance, 1-benzyl-1,2,3,4-tetrahydroisoquinolines are dopamine receptor antagonists (**Figure 20, left**)^{440,441}. (±)-*O*-methyarmepavine isolated from the leaves of *Annona squamosa* could effectively inhibit the growth and development of larvae of *Callosobruchus chinensis* on red gram pest^{442,443} (**Figure 20, right**).

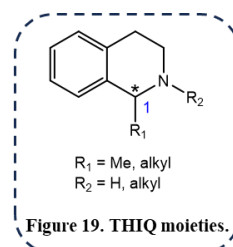


Figure 19. THIQ moieties.

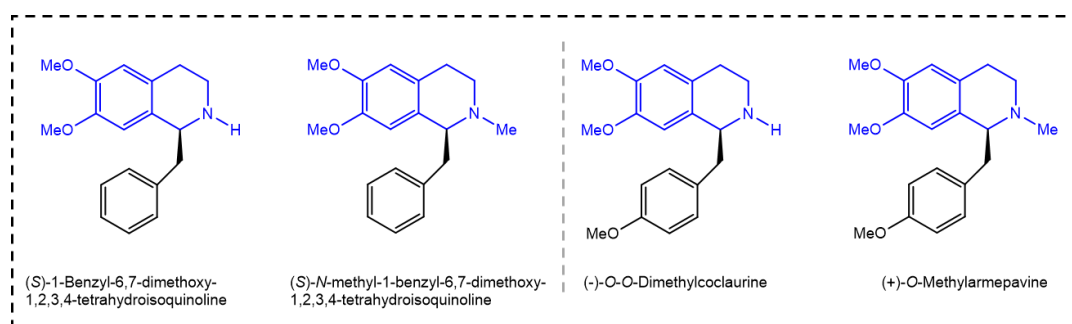
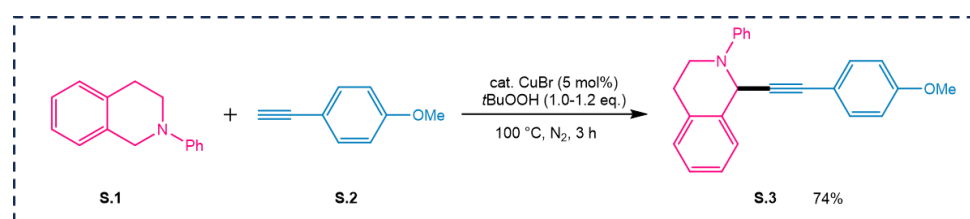


Figure 20. Examples of tetrahydroisoquinoline alkaloids.⁴⁴⁰⁻⁴⁴³

Various methodologies have been developed to construct such compounds⁴⁴⁴. The mostly used approaches are the Pictet-Spengler cyclization, Bischler-Napieralski cyclization/reduction.⁴⁴⁵ Subsequently, the asymmetric Pictet-Spengler reaction⁴⁴⁶⁻⁴⁵¹ and asymmetric hydrogenation of iminium intermediates⁴⁵² were developed to improve reaction selectivity⁴⁵³. However, these methods are usually accompanied by moderate to poor yield, unsatisfactory regio- and stereoselectivity, harsh reaction conditions, complicated operation and multistep procedures, as well as the high costs of starting material and reagents. Therefore, seeking for more efficient and/or simpler synthetic strategies to synthesize THIQs are still highly attractive.

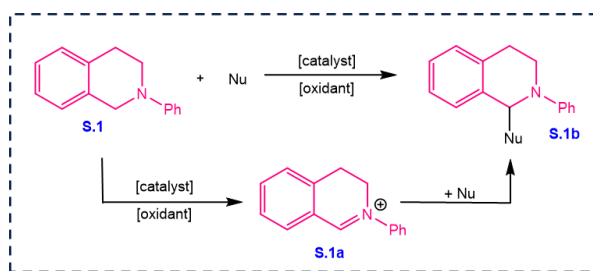
In 2004, Li's group⁴⁵⁴ first disclosed a new copper-based catalytic 1-alkynylation of THIQ (**S.1**) (**Scheme 143**), providing a more straightforward and efficient strategy for synthesizing C-1-substituted THIQ derivatives (**S.3**). This reaction was promoted by a catalytic system made of copper bromide (CuBr) and *tert*-butyl hydroperoxide (TBHP, *t*BuOOH). Such combination activated C_{sp3}-H bond and C_{sp}-H bond, and the resulting intermediates reacted to form C-C bond, providing 74% yields of the expected coupling product (**S.3**). This seminal work provided a new route to catalyze C-C bond formation based on the C_{sp3}-H bond activation of prochiral CH₂ groups, compared with the previous methods relying on forming a stereogenic carbon center by nucleophilic addition to the prochiral carbon atom bearing a double bond.

Since, CDC reactions with THIQ and terminal alkynes have been constantly developed based on the well-known system combining CuBr as a catalyst and TBHP as the oxidant.⁴⁵⁵⁻⁴⁵⁹



Scheme 143. CuBr-catalyzed 1-alkynylation of THIQ derivative.⁴⁵⁴

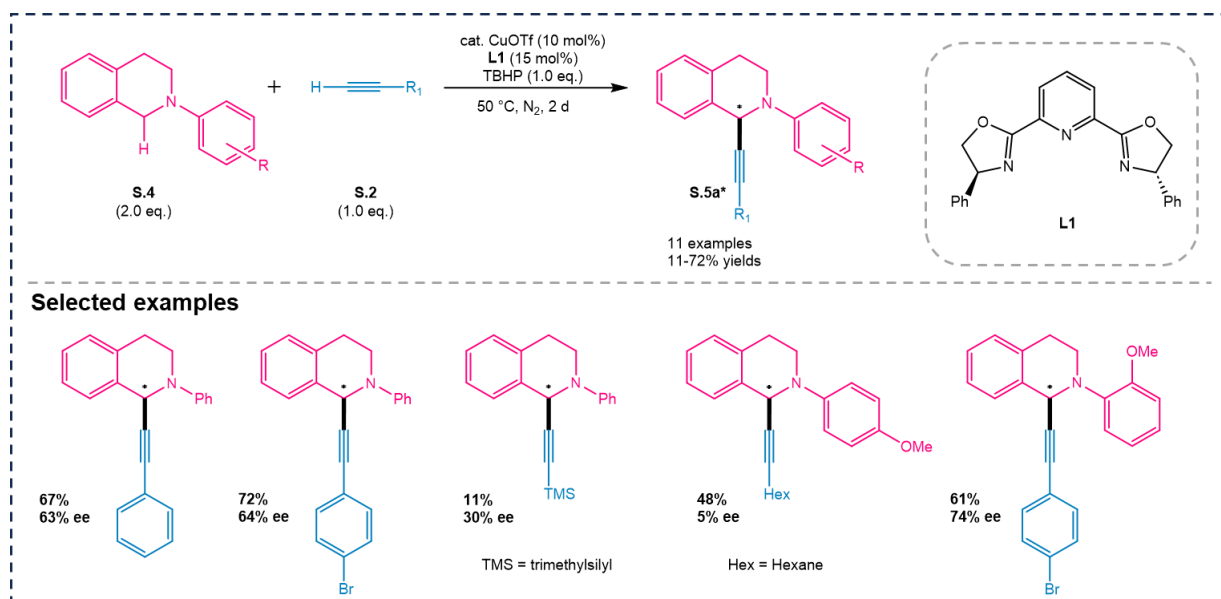
Meanwhile, the generally proposed hypothesis about the CDC reaction of *N*-phenyl tetrahydroisoquinoline (**S.1**) was that an intermediate iminium species **S.1a** was generated under the catalytic conditions, and reacted with nucleophiles to produce **S.1b** (**Scheme 144**). Furthermore, in order to control the stereoselectivity, diverse chiral catalysts and ligands have been developed to induce the stereochemistry of the so-formed C-1 stereocenter.



Scheme 144. Mechanistic proposal for the CDC reaction of S.1.

2. THIQ derivatives through CDC reactions-State of the art

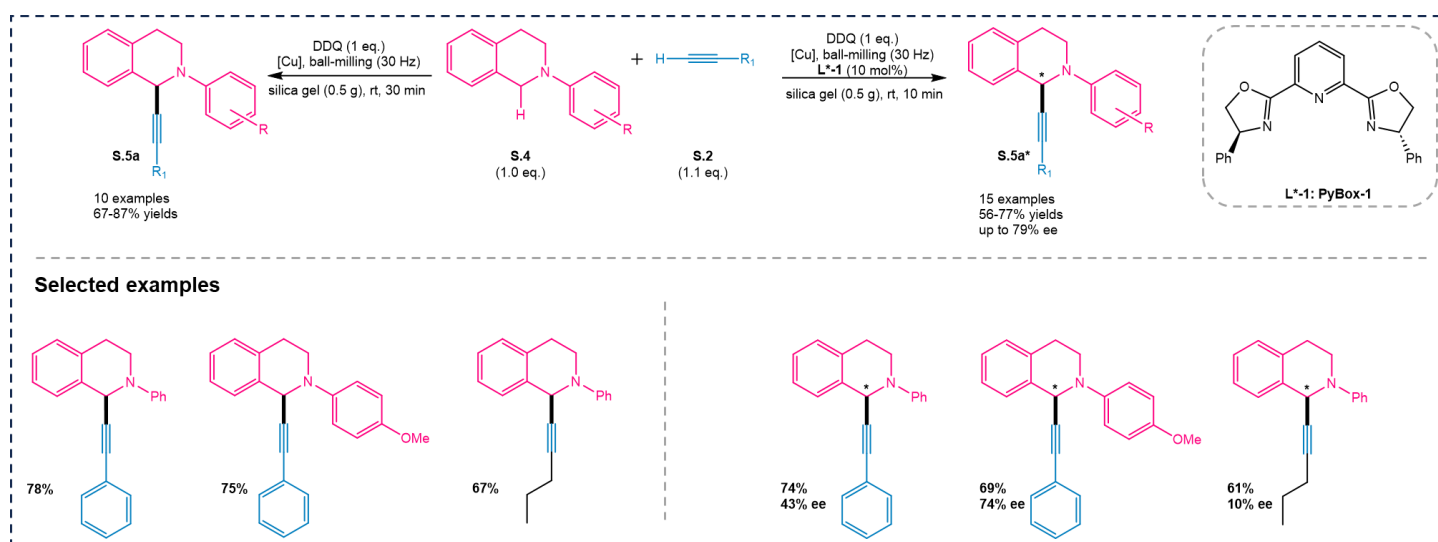
Following their first report of synthesizing C-1-substituted THIQ derivatives *via* CDC reaction of S.1 and substituted phenylacetylene, Li and co-workers^{460,461} successfully performed enantioselective CDC versions, with alkynes and various THIQs (S.4) using a series of chiral ligands (Scheme 145). CuOTf combined with PyBox-based chiral ligand L1 proved to be the optimal catalyst. With such catalyst, the *N*-phenyl THIQ (S.4) smoothly reacted with phenylacetylene at 50 °C in the presence of THBP and molecular sieves under an inert atmosphere, and provided the desired product with 63% enantiomeric excesses (ee). Among the explored terminal alkyne substrates (S.2), aromatic alkynes exhibited the best reaction outcomes with good yields of the desired products. The substituents on the aryl ring had no apparent influence on the reaction enantioselectivity and on the product yield. However, aliphatic alkynes gave the desired product with lower yields and enantiomeric excesses.



Scheme 145. Enantioselective alkylation of tetrahydroisoquinolines.^{460,461}

In 2011, Su's⁴⁶² group disclosed a novel solvent-free method, based on high-speed ball-milling, for the alkynylation of *N*-substituted THIQ (**S.4**) using DDQ (2,3-dichloro-5,6-dicyano-1,4-benzoquinone) as the oxidant (**Scheme 146, left**). They replaced the stainless-steel balls with copper balls, affording 67-87% yields of the expected products (**S.5a**) in a short reaction time (30 minutes) at 30 Hz. The reaction proceeded smoothly with aliphatic and aromatic alkynes, and provided slightly better outcomes with aromatic substrates than that with aliphatic alkynes. Furthermore, the copper balls easily recovered from the reactor could efficiently promote the reaction again in the absence of any additional catalyst. This mechanically induced ball-milling technique was thus applied for the first time to CDC reactions, providing a simple, green and cost-effective alternative approach for the synthesis of THIQ derivatives (**S.5a**).

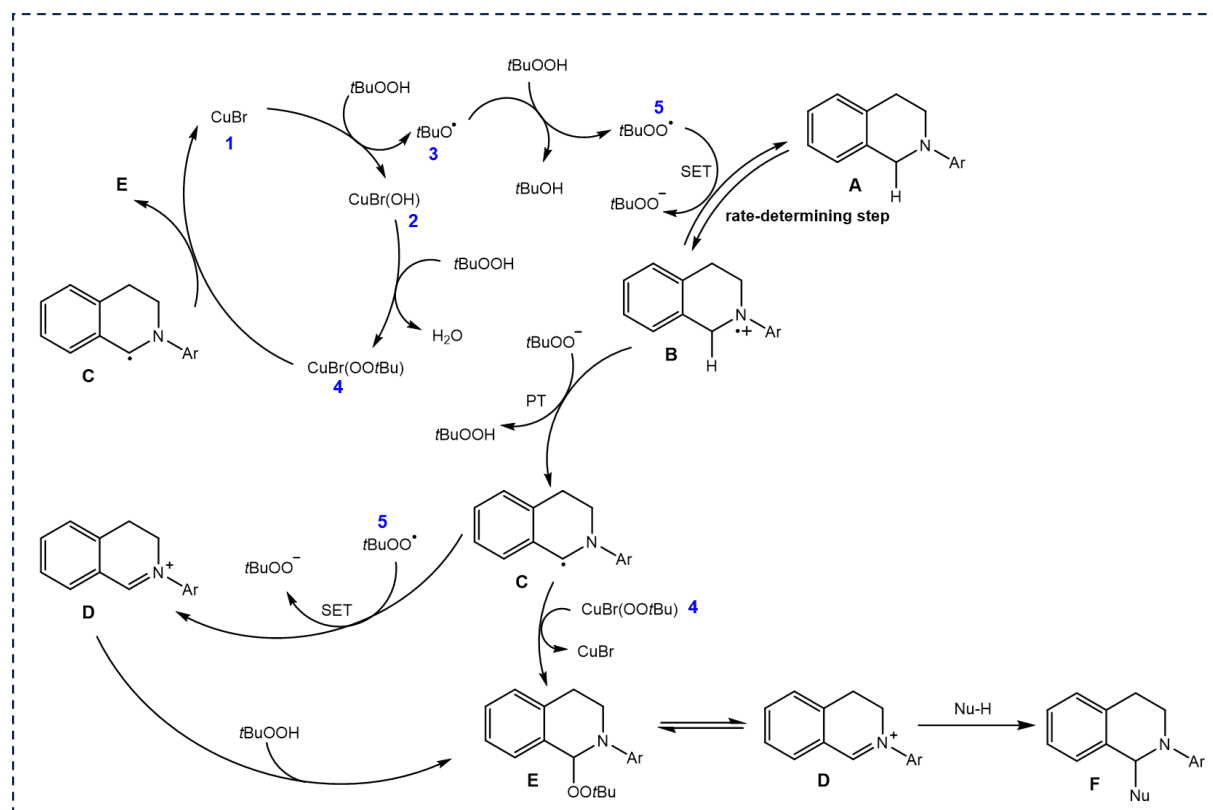
Shortly after, Su's group⁴⁶³ developed an enantioselective version of this protocol with a PyBox ligand (**L*-1**), affording the desired products (**S.5a***) in enantiomeric excesses up to 79% (**Scheme 146, right**).



Scheme 146. Mechanically induced diastereo- and enantio-selective CDC reactions of THIQs with alkynes.^{462,463}

During the same period, two groups, lead by Klussmann^{464,465} and Doyle⁴⁶⁶, investigated the copper-catalyzed CDC reaction through detailed isotope-labeling experiments and kinetic studies. From that, they proposed a mechanism for the CDC reaction of *N*-phenyl THIQ (**Scheme 147**). They both proposed that the reaction of CuBr and TBHP generates a copper(II) species **2** and a *tert*-butyloxy radical **3**. Then **2** and **3** reacted with another TBHP molecule, respectively to form a *tert*-butylperoxy copper complex **4** and a *tert*-butylperoxy radical **5**. The latter was demonstrated to be the thermodynamically favoured oxidant. This radical **5** was

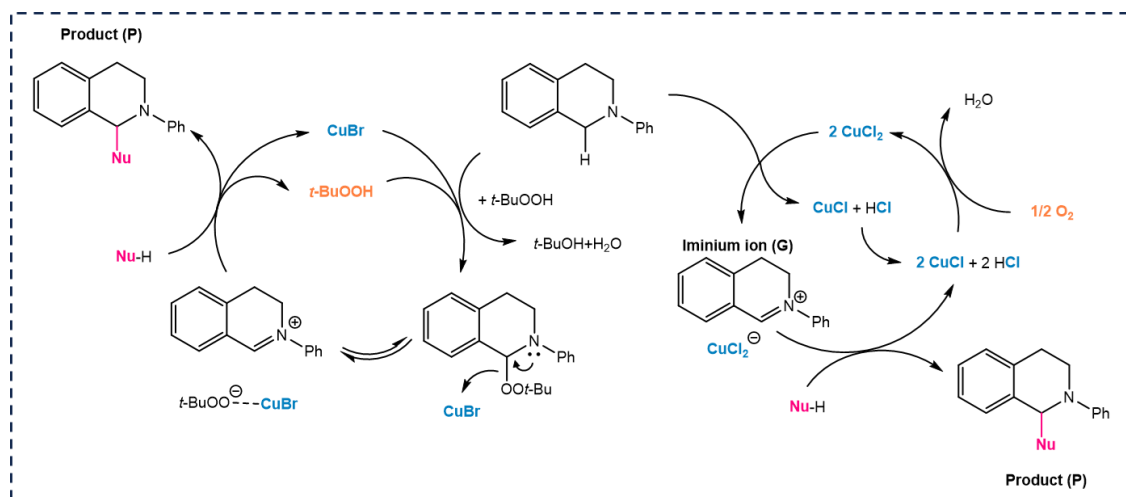
engaged in a single-electron transfer (SET) process with THIQ **A**. This SET step was regarded as the rate-determining step of the reaction. Once formed, the resulting radical cation **B** underwent a proton-transfer (PT) process to obtain the α -amino radical **C**. Then, the radical **C** underwent a second SET with another molecule of **5** to generate the corresponding iminium species **D**. The peroxide **E**, which could be produced either by **D** and TBHP or **C** and copper complex **4**, was proved to be the precursor of the expected product **F**. Finally, the nucleophile attacked the iminium intermediate **D**, affording the product **F**.



Scheme 147. Proposed mechanism for the oxidation of THIQ by TBHP with CuBr.⁴⁶⁴⁻⁴⁶⁶

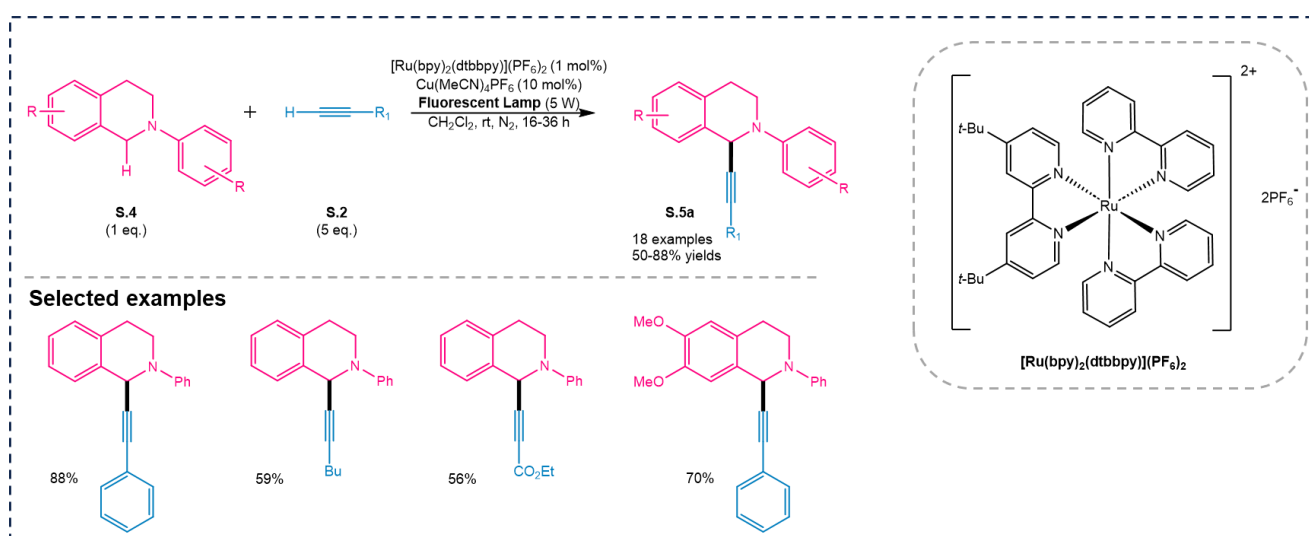
Furthermore, Klusmann's group⁴⁶⁵ also studied the CuCl₂-catalyzed CDC reaction with oxygen as the terminal oxidant. Their investigations allowed revealing the difference between the two copper-catalyzed systems (**Scheme 148**). In the CuCl₂·2H₂O/O₂ system, the iminium ion (**G**), which was generated *via* Cu^{II}-catalyzed oxidation, proved to be the key intermediate in the presence of oxygen. The iminium **G** reacted with the activated nucleophile to yield the product (**P**). The oxygen played a crucial role in the reoxidation of the reduced copper(I) species. It was shown that the reactivity of the nucleophile has a significant effect on the reaction. Therefore, only reagents with high nucleophilicity could be employed in the reaction. However, in the CuBr/TBHP system, the α -amino peroxide **E** (see **Scheme 147**) served as the true intermediate during the catalytic cycle and was demonstrated as the precursor to the iminium

ion intermediate **D** (see **Scheme 147**). As this procedure mostly underwent radical processes, it was independent of the reactivity of the nucleophiles, making it possible to construct new coupling reactions with substrates of low nucleophilicity but reactive to carbon radicals. These results may explain why most CDC reactions of THIQ with relatively weak nucleophiles as alkynes^{460,461,463,467,468} need to be performed with the CuBr/TBHP system.



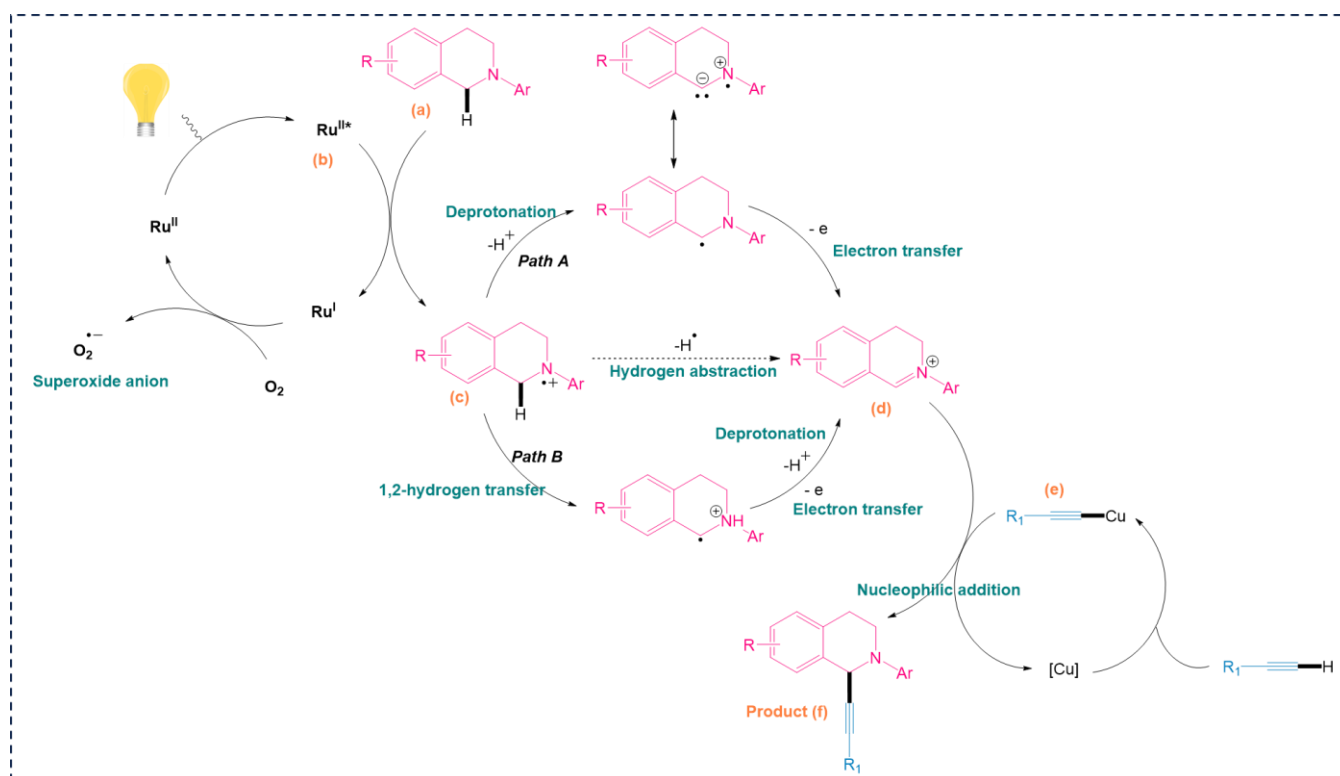
Scheme 148. Comparison of catalytic system CuBr/TBHP and CuCl₂/O₂.⁴⁶⁵

In 2012, Rueping *et al.*⁴⁶⁹ first published a dual catalytic system that consisted in a photoredox catalyst [Ru(bpy)₂(dtbbpy)](PF₆)₂ and a metal catalyst Cu(MeCN)₄PF₆ for the CDC reaction (**Scheme 149**). With visible light as the renewable energy source, various THIQs (**S.4**) could smoothly react with terminal alkynes under mild conditions, producing up to 88% of valuable products (**S.5a**). From the perspective of green chemistry, this dual catalytic CDC reaction represents a cost-effective and environmentally benign approach, opening a new route for the synthesis of valuable fine chemicals. Nevertheless, the solvent remains far from green.



Scheme 149. Photoredox-induced CDC reactions of THIQs with terminal alkynes.⁴⁶⁹

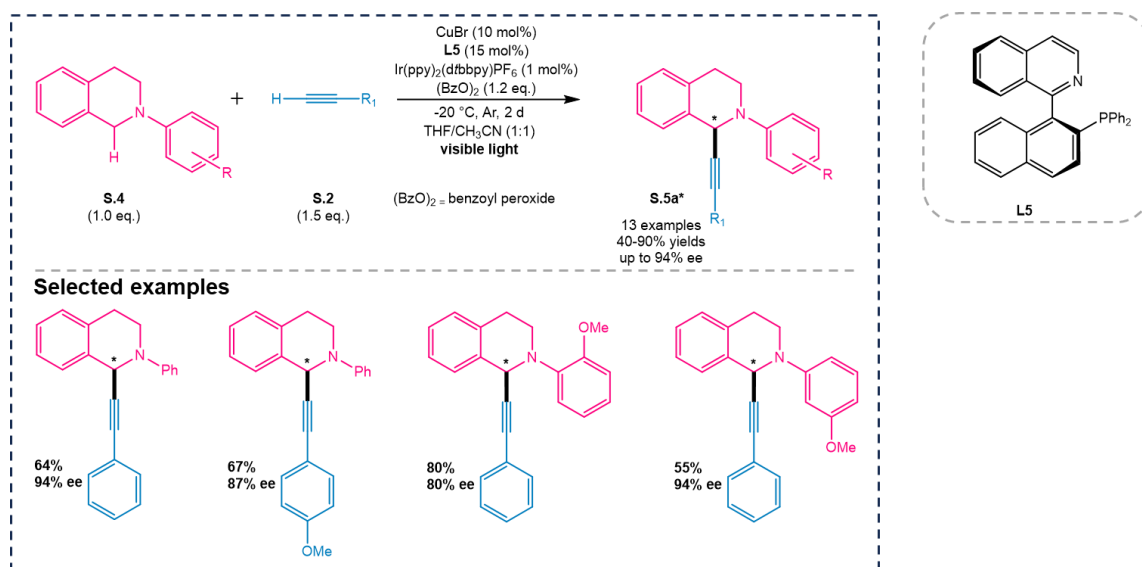
The authors⁴⁶⁹ also proposed a possible mechanism for the reaction based on experimental results and relevant literature (**Scheme 150**): THIQ (**a**) was oxidized to the corresponding amine radical cation (**c**) *via* an excited ruthenium catalyst (**b**); then radical cation (**c**) could generate iminium ions (**d**) through a hydrogen (H^\cdot) abstraction process. Two other possible pathways (path **A** and path **B**), in which the two steps of deprotonation and electron transfer occurred in a different order, could also produce iminium ions (**d**). Finally, the latter underwent a nucleophilic addition to the alkyne–copper (**e**) intermediate generated from the alkyne to provide the final product (**f**).



Scheme 150. A proposed mechanism of photoredox-induced CDC of THIQs with terminal alkynes.⁴⁶⁹

In 2015, Li's group⁴⁶⁸ disclosed another efficient dual copper and photoredox catalytic system to improve the CDC of THIQs and terminal alkynes (**Scheme 151**). This method provided the expected product yields up to 90% with 96% ee compared to the previous works^{460,463}, in which yield and enantiomeric excess of the optically active product were obtained in a moderate range. The reaction was promoted by a combination of photoredox catalyst ($[\text{Ru}(\text{bpy})_3](\text{PF}_6)_2$ or $[\text{Ir}(\text{ppy})_2(\text{dtbbpy})]\text{PF}_6$) with a chiral copper catalyst ($\text{CuBr}/\text{chiral ligand}$) under visible light conditions at room temperature with benzoyl peroxide ($(\text{BzO})_2$) as the sole oxidant, providing products **S.5a*** in excellent yields and enantiomeric excesses compared to previous works.^{460,461,463} Beneficially, this new approach could produce valuable chemicals that could

not be obtained using these catalysts alone. Such a synergic catalytic system consisting of a photocatalyst and a transition metal catalyst, with low photocatalyst loading (1 mol%) and simply available light energy, is an attractive green synthesis tool in organic chemistry.

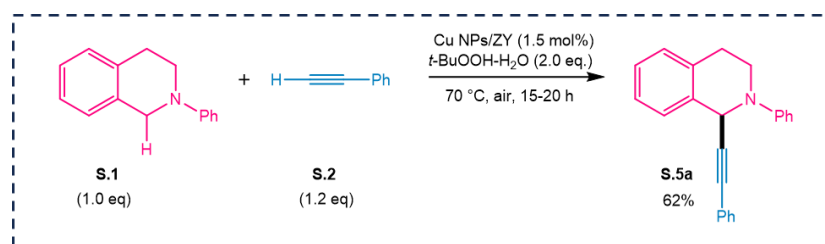


Scheme 151. Enantioselectivity of the CDC reaction between THIQs and terminal alkynes in the presence of a photocatalyst and visible light.⁴⁶⁸

In summary, the combination of copper(I) species, (chiral) ligands and TBHP is still regarded as the most critical catalytic system for the (asymmetric) CDC reactions of THIQs and terminal alkynes. These homogeneous metal species-catalyzed organic transformations are not green enough. Unfortunately, to the best of our knowledge, only one copper-based heterogeneous version has so far been reported⁴⁷⁰ (see below).

In 2015, Moglie and co-workers⁴⁷⁰ published the first copper-based heterogeneous CDC reaction of THIQ (**S.1**) and a terminal alkyne (**S.2**) catalyzed by Cu nanoparticles (Cu NPs) on various support materials. Cu NPs supported on zeolite Y proved to be the most effective catalyst with *tert*-butyl hydroperoxide as the oxidant. In contrast to the previously reported methodologies involving copper catalysts, this reaction could be catalyzed by 1.5 mol% catalyst without solvent and inert atmosphere (**Scheme 152**). The catalyst was prepared by a reduction reaction, in which Cu NPs were readily generated from copper(II) chloride, lithium metal and a catalytic amount of 4,4'-di-*tert*-butylbiphenyl (DTBB) (10 mol%) in anhydrous THF at room temperature.^{471,472} Beneficially, the catalyst could be reused over seven cycles without significant loss of activity and could be easily recovered by centrifugation after each run and directly reused in the recycling procedure. The Sheldon test result indicated that no copper species leached into the solvent. The use of this copper-doped heterogeneous and recyclable

catalyst provided an economical and sustainable approach for the synthesis of alkynyl THIQs via CDC reactions, indicating that zeolite Y was a promising support material for the active metal species that catalyzed CDC reactions.



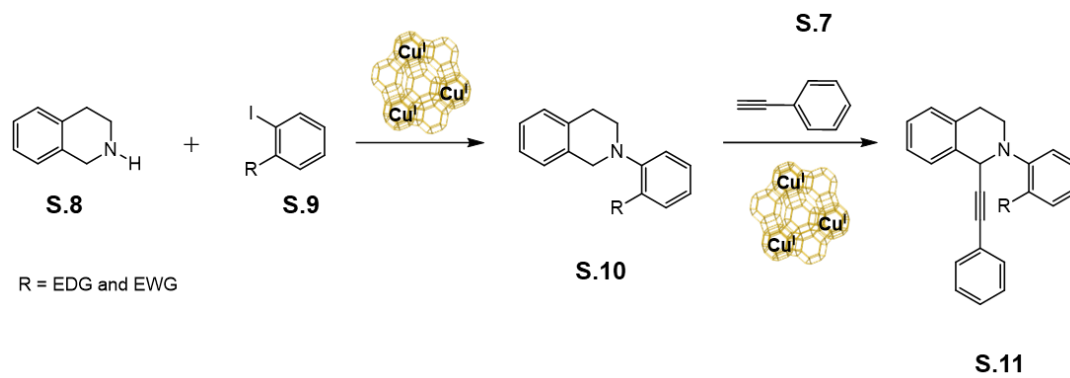
Scheme 152. Cu NPs/ZY-catalyzed 1-alkynylation of THIQ derivative.⁴⁷⁰

3. Promising research themes

Based on this context, the catalytic performance of our copper(I)-zeolite as heterogeneous catalysts was evaluated in CDC reactions, especially for the direct formation of C_{sp3}-C_{sp} bond. As mentioned before, the alkynylation of *N,N*-dimethylaniline has been regarded as a reference system for evaluating the performance of new catalytic systems. *Therefore, to begin our study, Cu^I-USY was employed as catalyst for the alkynylation of N,N-dimethylaniline (S.6) with phenylacetylene (S.7).*

Furthermore, the excellent biological activities of THIQ moieties motivated us to prepare 2-aryl-1,2,3,4-tetrahydroisoquinolines (THIQs), which are essential starting materials for the syntheses of various THIQ derivatives. *Hence, a multi-step procedure was designed for the synthesis of a new C-1-substituted tetrahydroisoquinoline derivative (S.11) based on the Cu^I-USY-catalyzed alkynylation of 2-aryl-1,2,3,4-tetrahydroisoquinoline (S.10) (Scheme 153).*

The cheap and commercially available chemical 1,2,3,4-tetrahydroisoquinoline was selected as the starting material (S.8). The first step would be preliminary performed using the Ullmann condensation conditions that we developed for the C-N bond formations⁴⁰. Then, the so-obtained compound (S.10) would react with phenylacetylene (S.7) in a CDC reaction in order to prepare the desired product (S.11). It should be mentioned that zeolite-based catalysts will be preferentially used throughout the overall process to better follow the Green Chemistry principles.



Scheme 153. Proposed synthesis of THIQ derivative.

4. Our research progresses

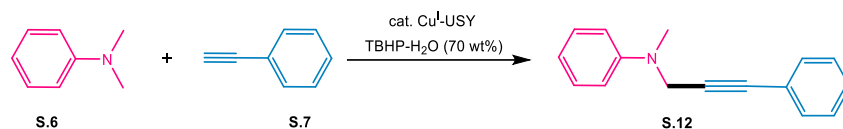
4.1. Preliminary results

The feasibility of direct catalytic alkynylation of C_{sp3}-H bonds in a cross-dehydrogenative coupling (CDC) reaction was assessed. Initial investigations were conducted under conditions similar to those reported in the literature⁴⁷⁰, which used copper nanoparticles on zeolite Y (Cu NPs/ZY) to catalyze the alkynylation of *N,N*-dimethylaniline (**S.6**) with phenylacetylene (**S.7**) (**Table 12**, entry 1). The same reaction was first performed with Cu^I-USY as catalyst at room temperature under air with a 1.5 mol% catalyst loading and *tert*-butyl hydroperoxide aqueous solution (TBHP·H₂O) as the oxidant. However, the product (**S.12**) was not observed after 6 h and even after increasing reaction time and temperature compared to the reported one⁴⁷⁰ (entries 2-3 vs 1).

Subsequently, the reaction was performed in MeCN, known to be a good solvent for CuBr₂-catalyzed CDC reaction (entry 4).⁴⁷³ Interestingly, the expected product (**S.12**) was progressively obtained at elevated temperatures, with a product yield of 79% at 85 °C (entry 6 vs 5), comparable to the reported condition (entry 6 vs 4).

This was the first Cu^I-USY-catalyzed alkynylation reaction of *N,N*-dimethylaniline (**S.6**), although the result of the reaction obtained with this catalyst did not significantly differ from the one reported in the literature⁴⁷³ (entry 6 vs 4). Cu^I-USY could promote such reaction under air at mild temperature, which was more sustainable conditions than those reported by Li's group⁴⁵⁴. The latter employed concentrated TBHP (in decane) at 100 °C under an inert atmosphere. With this promising result in hand, we embarked on the preparation of important THIQ derivatives (**S.11**, see above).

Table 12. Preliminary optimization studies for Cu^I-USY-catalyzed cross-dehydrogenative coupling of tertiary amines and terminal alkynes.



Entry	Cat. (mol%)	S.6 (eq.)	S.7 (eq.)	TBHP-H ₂ O (70 wt%) (eq.)	Solvent (2 mL)	Time (h)	T/°C	Condition	Yields of S.12 (%) ^[b]
1 ^[c]	CuNPs/ZY (1.5)	1	1.2	2	-	15-20	70	air	98
2	Cu ^I -USY (1.5)	1	1.2	2	-	6	rt	air	- ^[e]
3	Cu ^I -USY (1.5)	1	1.2	2	-	13	50	air	- ^[e]
4 ^[d]	CuBr ₂ (10)	3	1	2	MeCN	6	80	air	84
5	Cu ^I -USY (10)	3	1	2	MeCN	6	50	air	traces
6	Cu ^I -USY (10)	3	1	2	MeCN	6	85	air	79

^[a] Reaction run with *N,N*-dimethylaniline and phenylacetylene, and Cu^I-USY in the presence of *t*-BuOOH-H₂O, unless otherwise stated.

^[b] Isolated yield.

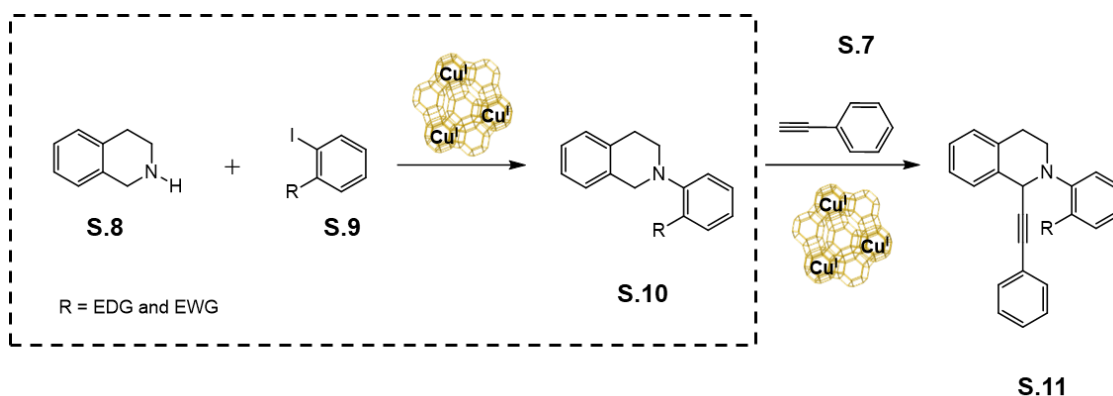
^[c] 98% isolated yield reported by Alonso's group⁴⁷⁰.

^[d] 84% isolated yield reported by Xu and co-workers⁴⁷³.

^[e] Not detected.

4.2. The synthesis of THIQ derivative

With the above-mentioned positive result with Cu^I-USY as catalyst in a CDC reaction, we started exploring such reaction with THIQ. In this context, we first attempted preparing *N*-aryl THIQ derivatives, and then looked at CDC reactions with such starting materials (**Scheme 154**).



Scheme 154. Proposed synthesis process of THIQ derivative **S.11**.

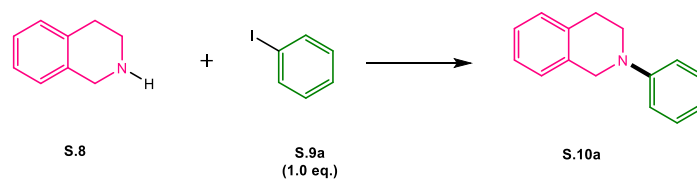
4.2.1. C-N bond cross-coupling

In this approach, the first step was to prepare 2-aryl-1,2,3,4-tetrahydroisoquinolines (**S.8**+**S.9**→**S.10**) (**Scheme 154**).

In order to verify the possibility of C-N bond formation, **S.8** was first reacted with the simple phenyl iodide (**S.9a**; R = H) under the conditions of our developed Cu^I-USY-catalyzed Ullmann-type C-N cross-coupling reaction⁴⁰ (**Table 13**, entries 1-2). The reaction was first performed with **S.9a** (1.0 equiv.), **S.8** (1.5 equiv.) and Cu^I-USY (10 mol%) in DMF in the presence of Cs₂CO₃ (2.0 equiv.) at 120 °C under argon during 24 h. However, the yield of the expected product **S.10a** was very low (entries 1-2), indicating that Cu^I-USY could not really catalyze the arylation of **S.9a** to form the expected amine (**S.10a**) under such conditions.

In 2009, Taillefer *et al.*²⁴⁵ reported a detailed review of copper-catalyzed Ullmann-type C-N cross coupling. Among them, CuI-based catalytic system was one of the most frequently used strategies for the C-N Ullmann-type coupling reactions. For instance, Buchwald and co-workers⁴⁷⁴ used CuI to catalyze the coupling of alkylamines and aryl iodides in the presence of base (K₃PO₄) and ligand (ethylene glycol) under air, providing the expected products in yields up to 95%. Therefore, CuI (5 mol%) was employed in the arylation of **S.9a** (1.0 equiv.) with **S.8** (1.2 equiv.) in the presence of K₃PO₄ (2.0 equiv.) and ethylene glycol (2 equiv.). Under such conditions, the desired product **S.10a** was obtained with yields higher than the one, achieved with Cu^I-USY, but nevertheless moderate (~ 40-50%) (entries 3-4).

Table 13. the arylation of S.9a.



Entry	Cat. (mol%)	S.8 (eq.)	Ligand (eq.)	Base (eq.)	Solvent	T (°C)	Time (h)	Yield of S.10a (%) ^[b]
1	Cu ^I -USY (10)	1.5	-	Cs ₂ CO ₃ (2)	DMF	120 (Ar)	24	15
2								10
3	CuI (5)	1.2	ethylene glycol (2)	K ₃ PO ₄ (2)	2- propanol	80 (air)	16	47
4								44

^[a] Reaction run with 1,2,3,4-tetrahydroisoquinoline (**S.8**) and iodobenzene (**S.9a**) (1 equiv.), unless otherwise stated.

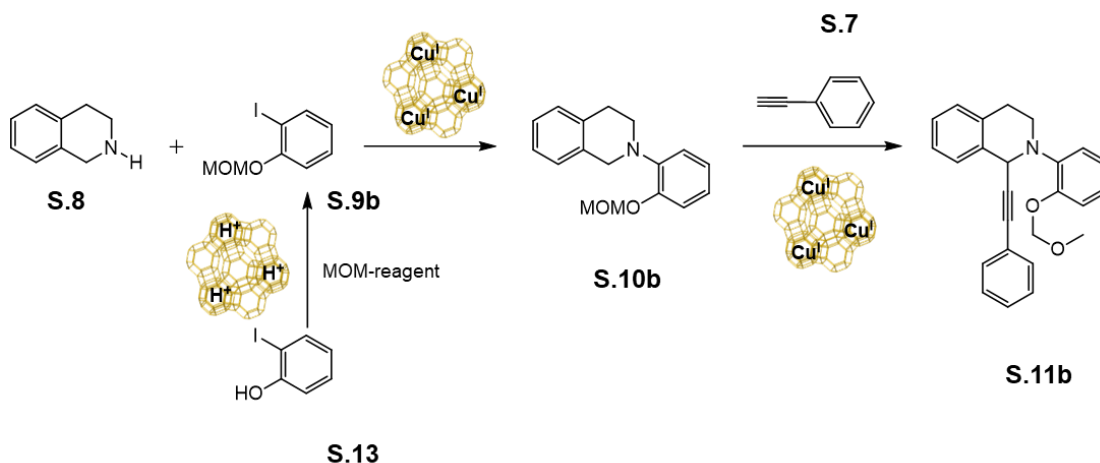
^[b] Isolated yield.

Based on these promising results, we envisaged to including functional group(s) to the 2-substituted THIQ **S.10**. An interesting group is methoxymethyl ether (MOM), which is often employed to protect hydroxyl group and can be easily installed and removed in a defined synthesis procedure. Therefore, a two-step process was designed to prepare the molecular **S.10b** with a MOM group. The latter **S.10b** will then be alkynylated in the Cu^I-USY-catalyzed CDC reaction developed above to further synthesize compound **S.11b** (**Scheme 155**). The general procedures were as follows;

(I) H-USY was used to catalyze the installation of a MOM group onto *ortho*-iodophenol (**S.13**) to generate the intermediate **S.9b**;

(II) **S.9b** was then employed for the Cu^I-USY-catalyzed Ullmann-type C-N cross-coupling, to produce the 2-aryl-THIQ (**S.10b**);

(III) The so-obtained **S.10b** was utilized to Cu^I-USY-catalyzed alkynylation with phenylacetylene (**S.7**) to synthesize the product **S.11b**.



Scheme 155. Proposed synthesis process of THIQ derivative S.11b.

4.2.1.1. The protection of *ortho*-iodophenol (S.13)

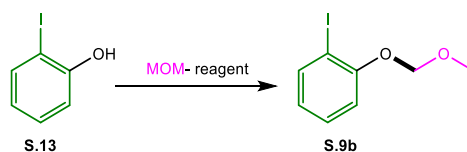
A frequently used and classical methodology^{167,475,476} for the installation of MOM protecting group is using chloromethyl methyl ether (MOMCl) as reagent. As expected, the use of MOMCl reagent in dichloromethane (CH₂Cl₂) with *N,N*-diisopropylethylamine (DIPEA) as base, the desired product **S.9b** could be obtained with a yield of over 90% (**Table 14**, entries 1-2) at room temperature under argon after 16-22 h. However, from the green chemistry perspective, the protocol was not satisfying considering the highly toxic of MOMCl.

In 2018, our group⁴⁰ successfully used dimethoxymethane (DMM) as a MOM-reagent to install a MOM group on a multi-substituted phenol. This procedure was promoted by phosphorus pentoxide (P₂O₅) in CH₂Cl₂ at 0 °C, smoothly affording 84% yields of the corresponding protected product. Such method was thus applied to the present work.

As H-USY behaves as a superacid,⁷² we attempted using such acidic zeolite to catalyze the protection reaction of *ortho*-iodophenol (**S.13**). DMM was employed as the MOM-reagent in these experiments. The reaction was performed under the conditions we have developed⁴⁰, without additional solvent at 40 °C for 24 h (entry 3). Unfortunately, only the starting material was recovered in the crude. This result indicated that H-USY could not promote the protection reaction of *ortho*-iodophenol when DMM was used as the protecting reagent.

Therefore, we switched to P₂O₅ as acidic catalyst for the protection of **S.13** (entries 4-6). Under the conditions we have developed⁴⁰, the expected product **S.9b** was obtained in yields up to 90%.

Table 14. the protection of *ortho*-iodophenol S.13.



Entry	MOM-reagent (eq.)	Acid (eq.)	Base (eq.)	Solvent	T (°C)	Time (h)	Yield of S.9b (%) ^[b]
1	MOMCl (2.7)	-	DIPEA (1.26)	CH ₂ Cl ₂	rt (Ar)	16	90
2	MOMCl (2.0)	-	DIPEA (1.26)	CH ₂ Cl ₂	rt (Ar)	22	97
3	DMM (15)	Fresh H-USY (5)	-	-	42 (air)	24	0
4	DMM (15)	P ₂ O ₅ (5)	-	CH ₂ Cl ₂	0 (air)	4	68
5	DMM (15)	P ₂ O ₅ (5)	-	CH ₂ Cl ₂	0 (air)	5	89
6	DMM (15)	P ₂ O ₅ (5)	-	CH ₂ Cl ₂	0 (air)	7	90

^[a] Reaction run with *ortho*-iodophenol (1 equiv.), unless otherwise stated.

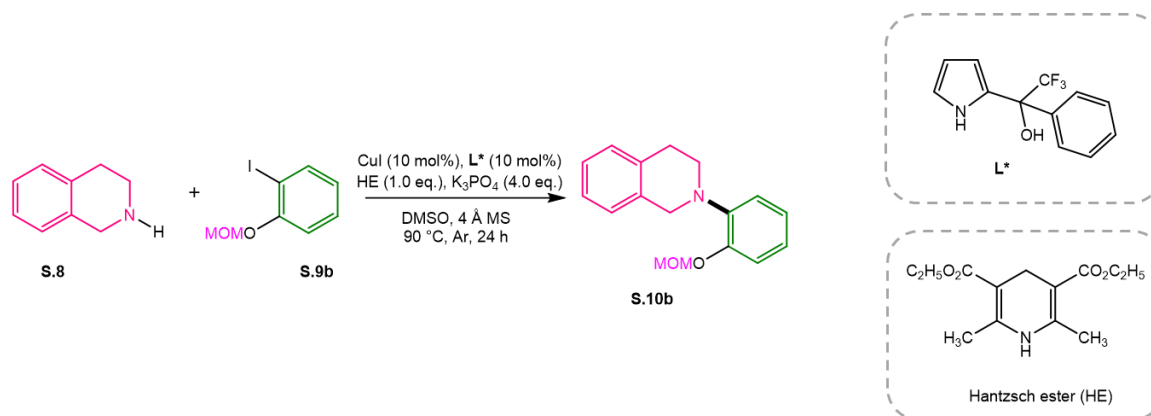
^[b] Isolated yield.

4.2.1.2. The arylation of S.8

As mentioned before, Cu^I-USY was prioritized for this reaction under the conditions we developed⁴⁰. However, the expected product **S.10b** could not be obtained under the Cu^I-USY-catalyzed Ullmann-type C-N coupling reaction condition (**Table 15**, entry 1). Furthermore, the screening results of several solvents showed that the CuI-based catalytic system as mentioned above also could not efficiently promote the reaction (entry 2-6). This could be due to the fact that the aryl iodide bearing an *ortho*-OMOM group sterically hindered the copper-catalyzed arylation reaction. Copper-catalyzed Ullmann-type amination with hindered partners remains an unsolved problem to date.⁴⁷⁷ Only a few examples showed that aryl iodides substituted with an *ortho* methyl group could be tolerated in the reaction.⁴⁷⁸⁻⁴⁸⁴ Recently, Cook's group⁴⁸⁵ reported a novel pyrrolyl benzyl alcohol **L*** as ligand for the coupling of *ortho*-substituted aryl iodides with sterically hindered amines. With such ligand and a reductant Hantzsch ester (HE), they successfully synthesized a variety of arylated amines in yields up to 95%. These results

motivated us to use this ligand for the present experiment. As expected, under similar conditions, an excellent yield of the expected product **S.10b** was obtained in CuI-catalyzed arylation of **S.8** in the presence of base and additive (entries 7-8, 80% and 89%).

Table 15. The arylation of S.8.



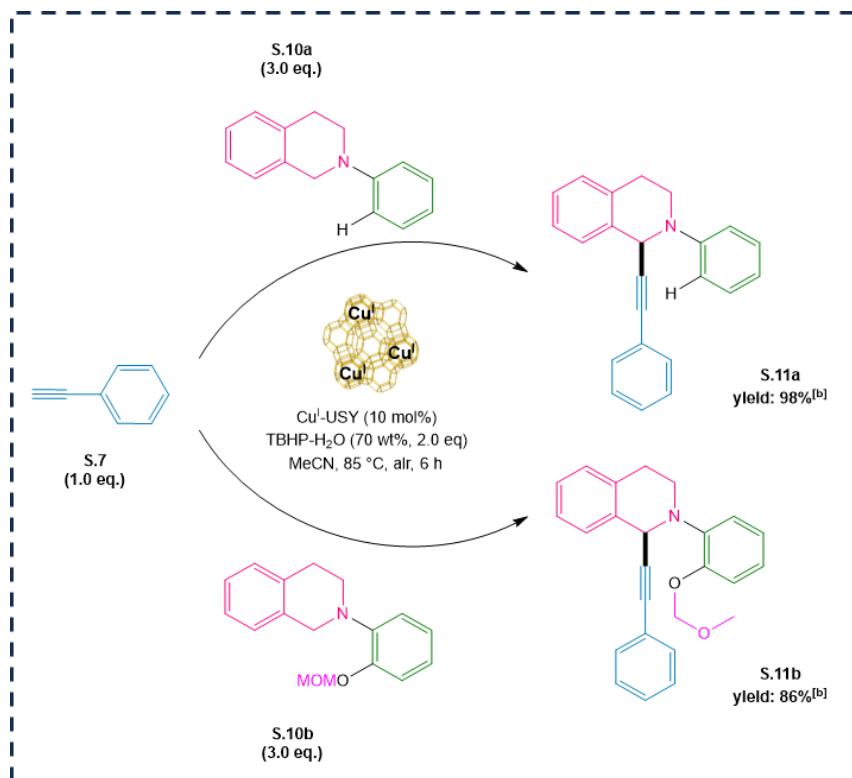
Entry	Cat. (mol%)	S.8 (eq.)	Ligand (eq.)	Base (eq.)	Solvent (mL)	T (°C)	Time (h)	Yield of S.10b (%) ^[b]
1	Cu ^I -USY (10)	1.5	-	Cs ₂ CO ₃ (2)	DMF	120 (Ar)	24	7
2	CuI (10)	1.5	ethylene glycol (2)	K ₃ PO ₄ (2)	2-propanol	90 (Ar)	24	12
3	CuI (10)	1.5	ethylene glycol (2)	K ₃ PO ₄ (2)	2-propanol	90 (air)	24	10
4	CuI (10)	1.5	ethylene glycol (2)	K ₃ PO ₄ (2)	1-butanol	120 (Ar)	24	28
5	CuI (10)	1.5	ethylene glycol (2)	K ₃ PO ₄ (2)	1-butanol	120 (Ar)	24	19
6	CuI (10)	1.5	ethylene glycol (2)	K ₃ PO ₄ (2)	2-methyl-2-butanol	110 (Ar)	24	2
7	CuI (10)	2	prepared ligand L* (0.1)	K ₃ PO ₄ (4)	DMSO (4 Å MS)	90 (N ₂)	24	80
8	CuI (10)	2	prepared ligand L* (0.1)	K ₃ PO ₄ (4)	DMSO (4 Å MS)	90 (N ₂)	24	89

^[a] Reaction run with 1,2,3,4-tetrahydroisoquinoline and **S.9b** (1 equiv.), unless otherwise stated.

^[b] Isolated yield.

4.2.2. CDC reaction of 2-aryl-substituted THIQs (S.10a and S.10b) with terminal alkyne (S.7)

With these precursors in hands, the CDC reactions of **S.10** with alkyne **S.7** were achieved with the Cu^I-USY-catalyzed protocol developed above. Rewardingly, high yields of products **S.11** were achieved (Scheme 156).



Scheme 156. Cu^I-USY-catalyzed CDC reactions of **S.10** with **S.7**.^[a]

^[a] Reaction run with **S.7** (1.0 equiv.) and **S.10** (3.0 equiv.), with 10 mol% Cu^I-USY in 2 mL MeCN at 85 °C for 6 h, unless otherwise stated.

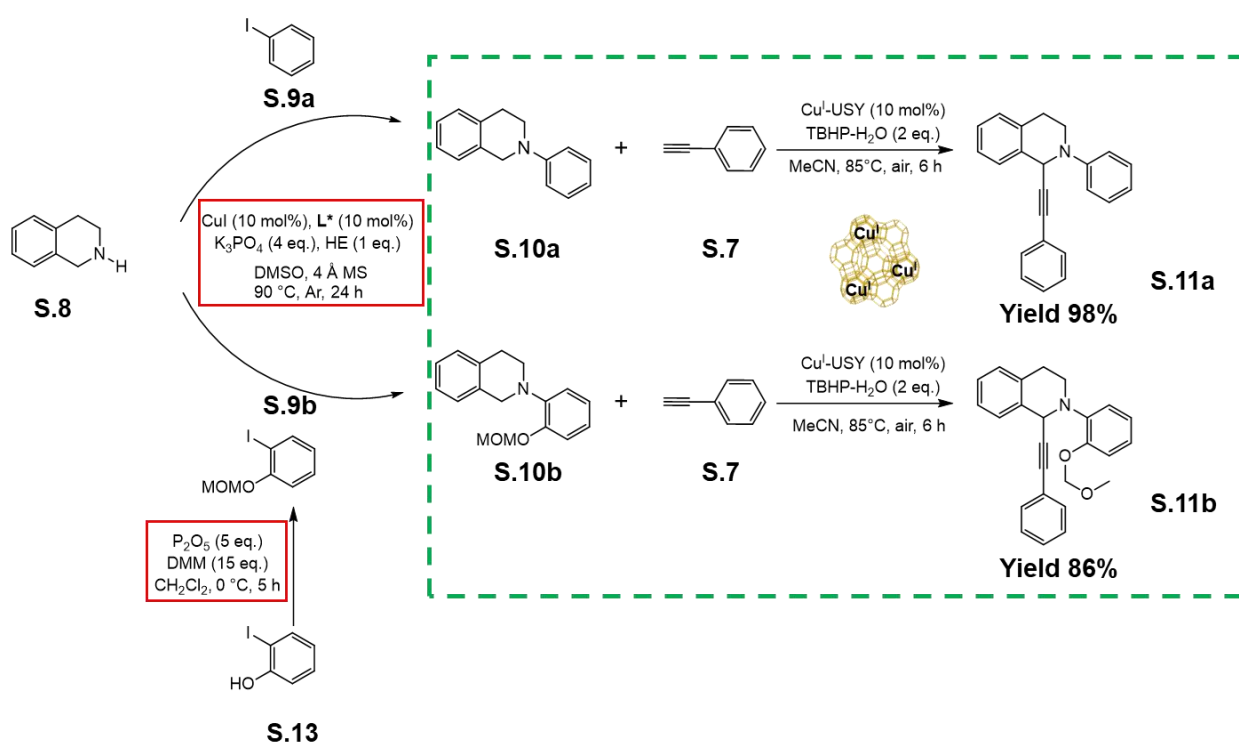
^[b] Isolated yield.

With these promising results in hands, the substrates scope with regard to various *ortho*-substituted aryl iodides and terminal alkynes is currently being explored. On the other hand, the application of the prepared **S.11b** in the synthesis of THIQ derivatives will also be investigated.

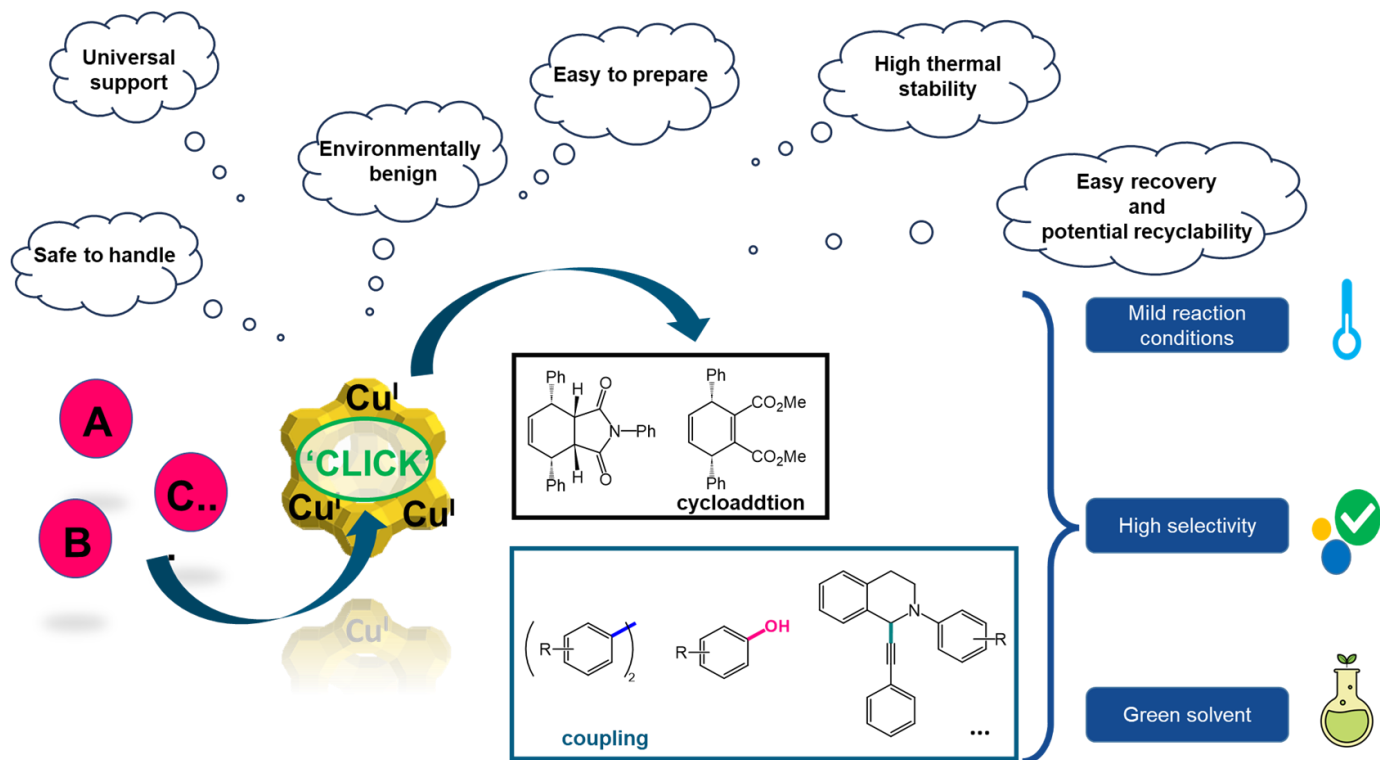
5. Conclusion

In conclusion, Cu^I-USY proved to be an efficient heterogeneous catalyst for the CDC reactions of tertiary amines and terminal alkynes in the presence of aqueous TBHP in MeCN. Contrary to previously reported methodologies, Cu^I-USY-catalyzed CDC could be conducted at milder temperatures under air conditions, which were more sustainable and economical. Preliminary results indicated that the catalyst did not significantly improve the product yield compared to other homogeneous copper catalysts. Nevertheless, Cu^I-USY deserved to be prioritized due to its ease of handling and recovery. Furthermore, this protocol has been applied to the synthesis of THIQ derivative **S.11**.

Nevertheless, further efforts are still required to optimize the reaction conditions.



General conclusions and perspectives



1. General conclusions

This thesis aimed to evaluate the potential of Cu^I-zeolite as heterogeneous catalyst for the synthesis of aromatic compounds. Cu^I-USY, as a hierarchical zeolite with large internal cages, could be easily prepared *via* a simple two-step ‘solid-solid calcination-ion exchange’ method and performed excellent in various organic transformations. Therefore, we envisaged developing more sustainable synthetic methodologies to form the C_{aryl}-C_{aryl} bonds accessing to valuable aromatic molecules or motifs with the help of the heterogeneous Cu^I-USY catalyst. The construction of some C_{aryl}-heteroatom (C_{aryl}-X) bonds has also been studied to expand the application scope of the catalyst.

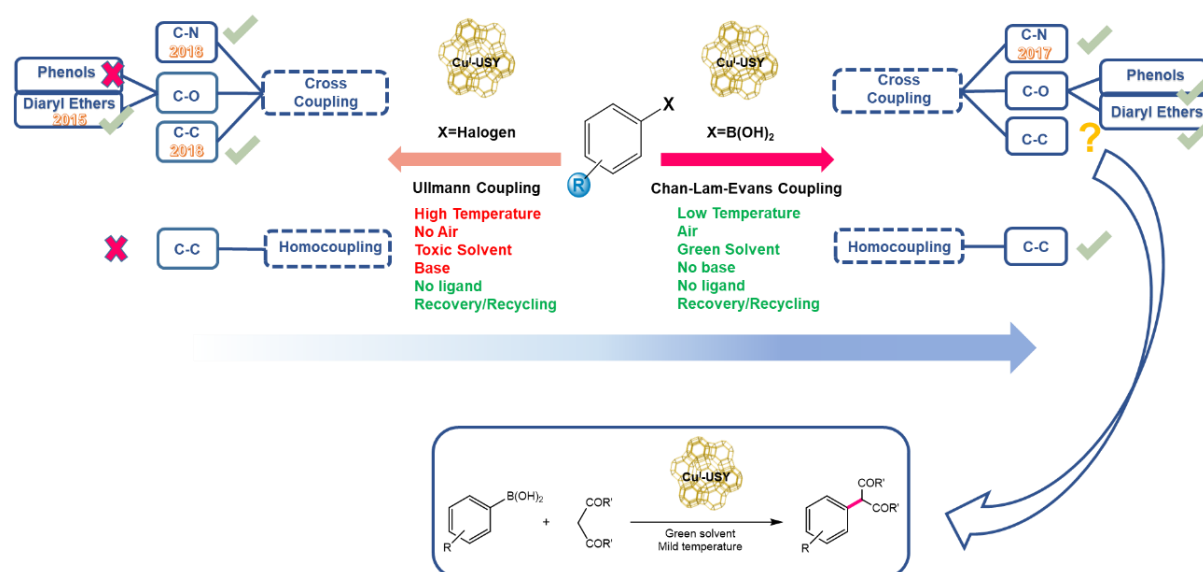
Overall, Cu^I-USY proved to be an efficient catalyst to form C_{aryl}-C_{aryl} bonds and C_{aryl}-X bonds for the synthesis of various aromatic compounds, such as biaryls, phenols, and THIQ alkaloids. These reactions are usually performed in greener solvent in the absence of additional base and ligand, which is highly desirable from an economic and ecological point of view.

2. Perspectives

Aromatic molecules or scaffolds (e.g., biaryls, phenols and alkaloids, etc.), are often encountered in numerous natural products and biologically active compounds. These valuable natural products are often found in plants, animals, and microorganisms. However, some of them can only be extracted in tiny amounts, which has greatly limited their potential applications. Therefore, chemists are dedicated to developing approaches to form C_{aryl}-C_{aryl} bands and C_{aryl}-X bonds to afford these compounds. Cu^I-USY-catalyzed homocoupling and Chan-Lam-type reactions provides simple and rapid reaction routes to construct C_{aryl}-C_{aryl} bonds and C_{aryl}-X bonds accessing to biaryls, phenols, aryl ethers and amines, which are usually prepared in complex procedures with unsatisfying conditions. With the simple small molecule arylboronic acid as the coupling partner, these products could be obtained in green solvents under mild conditions in a Cu^I-USY-catalyzed one-step process. These conditions greatly reduce the reaction cost and minimize the waste of resources. The cheap and easily available copper(I)-zeolite-based heterogeneous catalyst can be reused and recycled, which alleviates the serious environmental problems caused by metal homogeneous catalysis.

Therefore, further optimization and expansion of the potential of Cu^{I} -USY in the formation of $\text{C}_{\text{aryl}}\text{-C}$ bonds remains an attractive and promising aspect to synthesize valuable aromatic compounds or scaffolds of natural products.

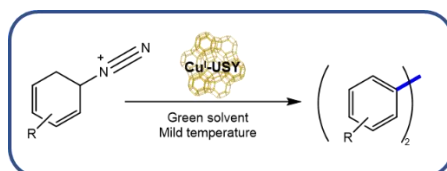
In our previous works, the formation of $\text{C}_{\text{aryl}}\text{-C}_{\text{aryl}}$ bonds towards symmetrical biphenyl compounds in Cu^{I} -USY-catalyzed homocoupling of arylboronic acids have been achieved, but the synthesis of biaryl derivatives in Chan-lam-type $\text{C}_{\text{aryl}}\text{-C}$ bond cross coupling reactions have not been realized. However, asymmetric aromatic structures appear to be more common and useful in drug development. Thus, it would be interesting to perform Cu^{I} -USY-catalyzed Chan-Lam-type cross coupling reactions to form $\text{C}_{\text{aryl}}\text{-C}$ bonds. The initial reaction is expected to be carried out between arylboronic acids and activated methylene compounds as coupling partners (**Scheme 157**), since the latter are one of the possible C -nucleophile species to form $\text{C}_{\text{aryl}}\text{-C}$ bonds under harsh conditions in Ullmann-type reactions in our previous works⁴⁰. Surprisingly, examples under Chan-Lam conditions are still scarce in the literature with only one recent example⁴¹⁵ so far reported under homogeneous and again quite harsh conditions. There is thus ample room to improve this highly relevant tool and we are confident to do this by developing a Cu^{I} -USY-catalyzed version in a more sustainable synthetic procedure.



Scheme 157. Comparison of Cu^{I} -USY-catalyzed Ullmann and Chan-Lam-Evans coupling processes for C-heteroatom and C-C bonds formation.³⁹⁻⁴²

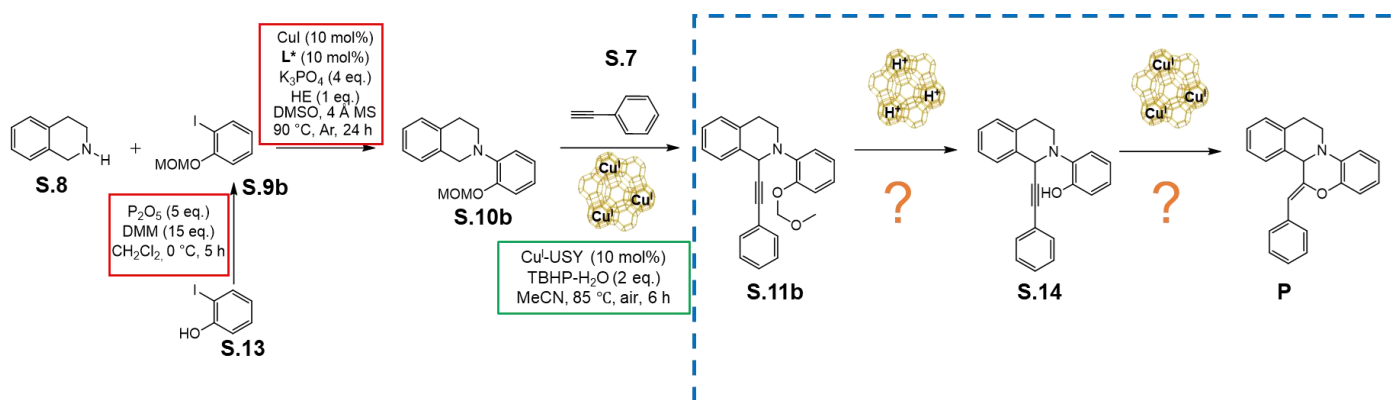
Furthermore, aryldiazonium salts, as a kind of promising alternative to aryl halides, exhibit greater advantages in the construction of $\text{C}_{\text{aryl}}\text{-C}_{\text{aryl}}$ bonds since the former can be conveniently prepared from the corresponding anilines and are commonly applied in organic transformations at room temperature. Furthermore, ionic liquids and deep eutectic solvents as green solvents

have been utilized in the homocoupling of aryldiazonium salts, providing the possibility to develop another greener and milder conditions to form C-C bonds. Therefore, further efforts were required to explore the Cu^I-USY-catalyzed homocoupling reaction conditions of aryldiazonium salts (**Scheme 158**). The search for suitable and greener reaction conditions in which Cu^I-USY remains efficient as catalytic system still needed to be investigated.



Scheme 158. Cu^I-USY-catalyzed homocoupling of arenediazonium salts.

Finally, considering the potential pharmaceutical value of THIQ moieties, we envisage synthesizing possible THIQ derivatives, such as **P**, an unknown compound, in a one-pot process (**Scheme 159**). Simple and efficient synthetic methodologies from **S.11b** to the desired product **P** are currently investigated. Of course, Cu^I-USY will be prioritized in these transformations from green chemistry perspective. Once the unprecedented product **P** will be synthesized, its biological and pharmacological activities will be identified, especially within the context of the constant demand for innovative and highly bioactive structures or ingredients, and applied to all conceivable aspects of human life.



Scheme 159. the synthesis of THIQ derivatives.

Résumé en français

Table des matières

1. Contexte général et objectifs du travail de thèse	i
1.1. <i>Introduction</i>	i
1.2. <i>Zéolithes</i>	ii
1.3. <i>Objectifs du travail de thèse</i>	iii
2. Résultats et discussions	v
2.1. <i>Formation de liaisons C_{aryl}-C_{aryl} via des réactions de type homocouplage catalysées par des zéolithes dopées au cuivre(I)</i>	v
2.2. <i>Formation de liaisons C_{aryl}-hétéroatome vers les phénols via des réactions de couplage de Chan-Lam-Evans catalysées par des zéolithes dopées au cuivre(I)</i>	xii
2.3. <i>Réactions de couplage déshydrogénatif croisé catalysées par des zéolithes dopées au cuivre(I) pour former des liaisons C-C et leurs applications à la synthèse de dérivés de tétrahydroisoquinoléine</i>	xv
3. Conclusions générales	xviii
4. Références	xix

1. Contexte général et objectifs du travail de thèse

1.1. Introduction

Les structures du type benzénique sont une caractéristique prédominante dans de nombreux composés biologiquement actifs. La plupart d'entre eux se présentent sous forme de motifs biaryle, phénol et isoquinoléine (**Fig. 1**), que l'on trouve dans de nombreux produits naturels et dans certains intermédiaires synthétiques importants. Par exemple, le motif biaryle composée de liaison $C_{aryl}-C_{aryl}$ est un élément de base utile pour certains produits pharmaceutiques, tels que ceux de la famille des régulateurs de pression artérielle, les sartans (**Fig. 1, A**). Les phénols, naturels ou non, constituent une classe importante d'antioxydants, capables d'inhiber la dégradation oxydative qui intervient dans la plupart des organismes aérobies (**Fig. 1, B**). Par exemple, l' α -tocophérol, un composant bien connu de la vitamine E, s'est avéré être le dérivé phénolique le plus efficace pour piéger les radicaux peroxy nocifs dans le plasma sanguin, entre autres humain. D'autre part, l'acide salicylique contenant une fraction phénol peut être utilisé pour soulager douleurs et fièvres¹. Les dérivés de l'isoquinoléine sont aussi largement présents dans la nature² et dans de nombreux médicaments. Par exemple, la célèbre papavérine est un médicament antispasmodique important et les 1-benzyl-1,2,3,4-tétrahydroisoquinolines (THIQ) sont des antagonistes des récepteurs de la dopamine (**Fig. 1, C**).³

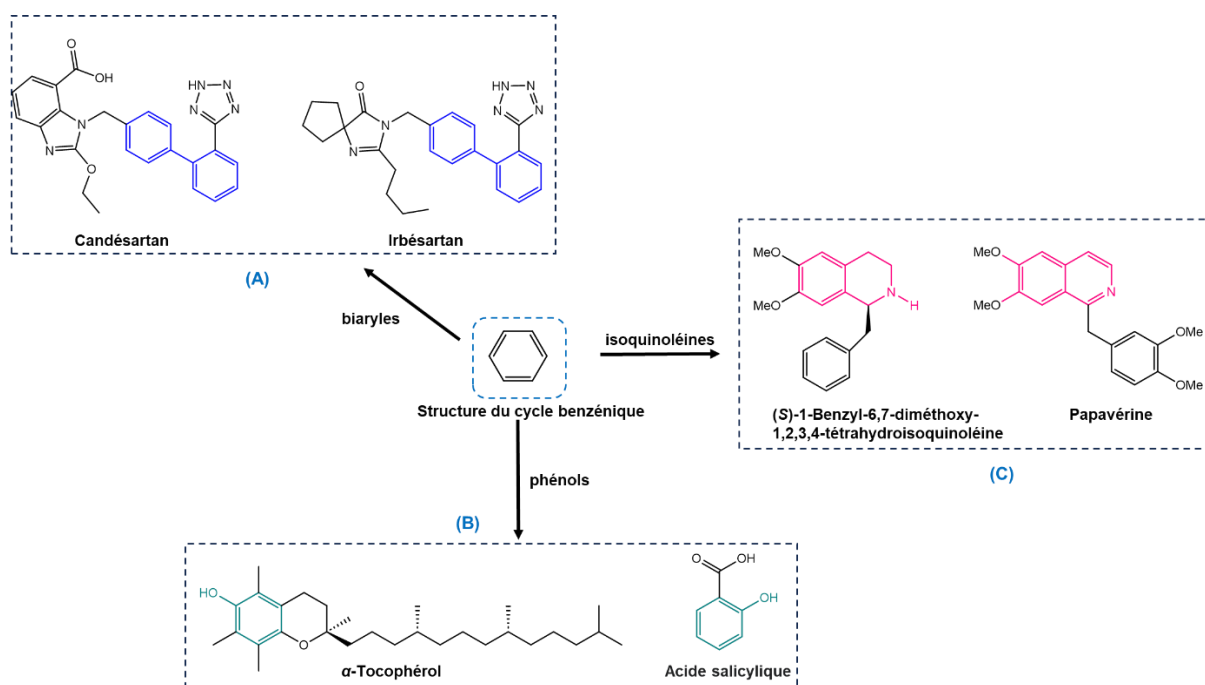


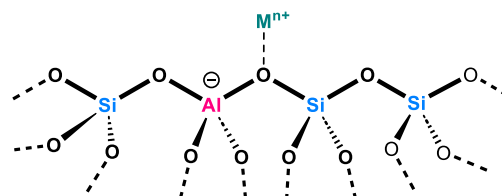
Figure 1. Exemples représentatifs de composés bioactifs présentant les motifs biaryle (A), phénol (B) et isoquinoléine (C).¹⁻³

En conséquence, la formation de liaisons $C_{\text{aryl}}-C_{\text{aryl}}$ et $C_{\text{aryl}}-X$ (avec X étant un atome hétéroatomique) est devenue importante pour la synthèse de tels composés utiles. Plus d'un siècle après l'émergence de la réaction d'Ullmann⁴ et de ses réactions dérivées (appelées de type Ullmann ; pour plus de détails, voir ci-dessous),^{5,6} les premières réactions de liaison $C_{\text{aryl}}-C_{\text{aryl}}$ et de formation de $C_{\text{aryl}}-X$ médiées par le cuivre, une variété de méthodes ont été décrites pour former ces liaisons, mais les réactions de couplage médiées par les métaux de transition restent toujours les méthodes les plus utilisées.⁷⁻⁹ Cependant, les réactions initiales nécessitaient généralement des quantités stœchiométriques, voire sur-stœchiométriques, de métal de transition dans des conditions difficiles, telles qu'une température élevée et un long temps de réaction. Ces procédures n'étaient ni durables ni économiques. Sur la base du concept éco-environnemental de « chimie verte », les chimistes organiciens ont cherché à développer de nouvelles méthodes catalytiques et plus bénignes pour construire des liaisons $C_{\text{aryl}}-C_{\text{aryl}}$ et $C_{\text{aryl}}-X$.

Compte tenu des impacts négatifs de la pollution de l'environnement, de la consommation d'énergie et des coûts élevés causés par l'utilisation d'espèces métalliques, le remplacement des catalyseurs métalliques homogènes standards par des catalyseurs hétérogènes faciles d'accès et recyclables est devenu un domaine d'intérêt croissant au cours des dernières décennies, mais il s'agit toujours d'une tâche difficile en synthèse organique. L'une des méthodes de préparation des catalyseurs hétérogènes consiste à immobiliser des ions métalliques sur des matériaux solides inorganiques. Parmi eux, les zéolithes naturelles ou synthétiques ont été privilégiées en raison de leur faible coût, de leur stabilité et de leur grande sélectivité^{10,11}.

1.2. Zéolithes

Les zéolithes, sortes d'aluminosilicates cristallins naturels ou synthétiques (**Fig. 2**), sont des matériaux de support très recherchés en raison de leur simplicité de préparation, disponibles dans le commerce à bas prix (< 1€/g) et d'une excellente stabilité hydrothermale. À ce jour, 240 types de zéolithes avec des topologies différentes (cage ou canal) ont été décrites.¹² Ces matériaux hautement microporeux ont de grandes surfaces spécifiques ($SSA > 400 \text{ m}^2/\text{g}$), des sites acides abondants et des tailles et nombres de pores différents, ce qui les rend



M^{n+} : counter cation, p.ex., Na^+ , Mg^{2+} dans les zéolithes naturelles; H^+ ou NH_4^+ et cations de métaux (de transition) dans les zéolithes synthétiques

Figure 2. Composition chimique et structure des zéolithes.

fréquemment utilisés comme catalyseurs efficaces pour divers processus, dont ceux à grande échelle de la pétrochimie. En conséquence, les zéolites font partie des catalyseurs industriels hétérogènes les plus courants et les plus appliqués.¹³ Cependant, l'application des zéolites, en particulier des zéolites dopées aux métaux de transition, reste étonnamment sous-estimée en synthèse organique.

1.3. Objectifs du travail de thèse

Sur cette base, l'objectif principal de cette thèse est de développer des méthodologies de synthèse plus durables pour synthétiser des motifs ou molécules aromatiques (cf **Fig. 1**) à l'aide de catalyseurs hétérogènes issus de zéolites dopées au Cu^I. Ce travail rentre dans le contexte général du laboratoire visant à élargir le champ d'application des zéolites en synthèse organique.

Les présents travaux se concentrent sur une zéolithe métallée particulière, Cu^I-USY (zéolithe Y Ultra-Stable), présentant une faible toxicité, un faible coût et un catalyseur à forte charge en cuivre par rapport à d'autres catalyseurs à base de métaux. Ce catalyseur peut être facilement préparé à l'aide d'une méthode simple en deux étapes par échange d'ions lors de calcination solide-solide¹⁴ (**Sch. 1**). Tout d'abord, la zéolithe NH₄-USY commercial est calciné à 550 °C pendant 12 h pour fournir son analogue H-USY. Celle-ci est ensuite mélangée avec du CuCl et ce mélange est chauffé à 350 °C pendant 3 jours sous flux d'azote pour former le catalyseur attendu. La charge finale de cuivre dans le catalyseur ainsi obtenu, déterminée par ICP-AES, est d'environ 3,0 mmol/g, ce qui correspond à un taux d'échange allant jusqu'à 80%.

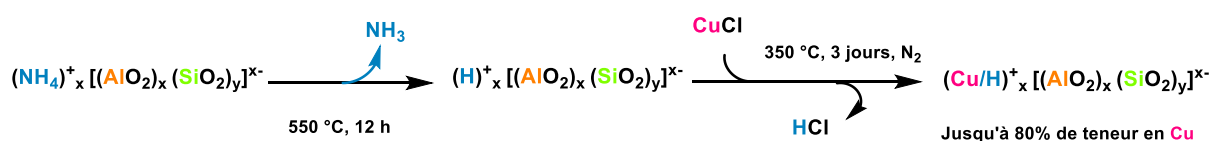


Schéma 1. Préparation du Cu^I-USY.¹⁴

Cette zéolithe Cu^I-USY s'est avérée être un catalyseur hétérogène polyvalent, capable de promouvoir une grande quantité de transformations organiques, y compris la cycloaddition d'azide-alcyne catalysée par le cuivre (CuAAC)^{15,16}, l'homocouplage de Glaser¹⁷, ainsi que les réactions de couplage d'Ullmann^{18,19} et de Chan-Lam-Evans^{20,21} (**Sch. 2**). Qui plus est, s'est avérée recyclable et utilisable recyclable et utilisable dans des conditions vertes.

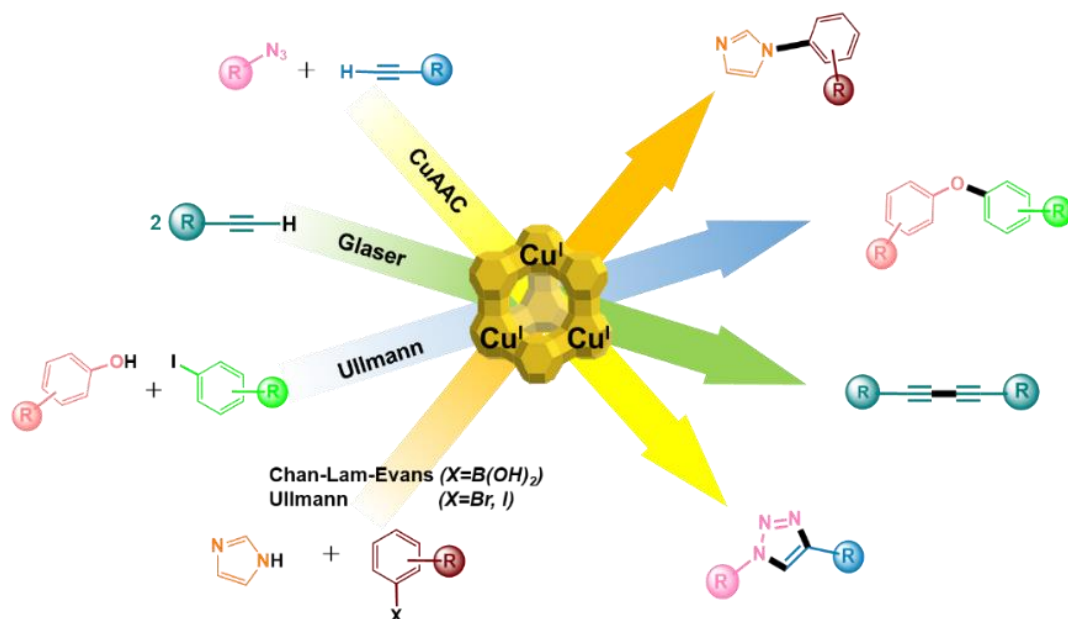


Schéma 2. Le catalyseur hétérogène Cu^I-USY en synthèse organique.¹⁵⁻²¹

Pour surmonter les problèmes associés aux réactions de Ullmann et de type Ullmann mentionné précédemment (**Sch. 3, à gauche**), les chimistes ont cherché de nouvelles méthodes de synthèse pour améliorer les conditions de réaction pour la formation des liaisons C_{aryl}-C et C_{aryl}-X. La réaction de type Chan-Lam-Evans (**Sch. 3, à droite**), qui est basée sur le remplacement du partenaire halogénure d'aryle propre à la réaction d'Ullmann par un acide arylboronique (ABA), a permis la formation de liaisons C_{aryl}-X dans des conditions simples et plus douces, ce qui la rend attrayante par rapport aux conditions de couplage originales de type Ullmann. Cependant, il y a encore quelques limites à ces réactions, notamment l'utilisation de quantité stoechiométrique de sel de cuivre Cu(OAc)₂ et de solvant non vert CH₂Cl₂.

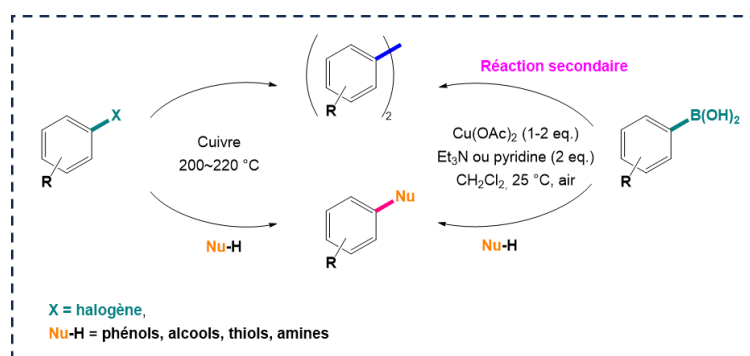


Schéma 3. Couplage de type Ullmann/Ullmann médié par le cuivre (à gauche) et couplage homologue/de type Chan-Lam (à droite), qui permettent d'accéder aux biaryles, aux éthers aryliques et aux amines.

Comme le montre le **Sch. 2**, la zéolithe Cu^I-USY a permis la formation efficace de liaisons C_{aryl}-N et C_{aryl}-O vers les arylamines et les éthers aryliques *via* des réactions de couplage croisé de

type Ullmann et de type Chan-Lam-Evans. Compte tenu des excellentes performances de Cu^I-USY dans la catalyse de telles réactions de couplage, nous avons poursuivi dans ce travail l'exploration du potentiel catalytique de Cu^I-USY:

- pour former des liaisons C_{aryl}-C_{aryl} *via* des couplages de type Ullmann et des réactions d'homocouplage associées (voir section 2.1),
- pour former des liaisons C_{aryl}-O *via* des réactions de type Chan-Lam-Evans (voir section 2.2).

Parallèlement, le couplage déshydrogénatif croisé (CDC) catalysé par Cu^I-USY a été également étudié pour la synthèse de dérivés THIQ *via* la formation de liaisons C_{sp3}-C_{sp} (voir section 2.3).

2. Résultats et discussions

Cette partie résume les résultats obtenus à partir de plusieurs réactions de couplage catalysées par Cu^I-USY pour la synthèse de biaryles, de phénols et de dérivés THIQ *via* la formation de liaisons C-C et C-X. De plus, l'application des motifs importants ainsi obtenus a également été explorée dans les réactions de Diels-Alder pour la construction d'hétérocycles d'intérêt avec des économies d'atomes élevées. Il convient de noter que Cu^I-USY est toujours priorisé tout au long du processus afin de mieux mettre en œuvre les principes de la chimie verte.

2.1. Formation de liaisons C_{aryl}-C_{aryl} via des réactions de type homocouplage catalysées par des zéolithes dopées au cuivre(I)

Les synthèses connues de biaryles par la formation de liaisons C_{aryl}-C_{aryl} en synthèse organique reposent principalement sur des réactions de couplage croisé²² ou d'homocouplage catalysées par les métaux.²³ Par rapport aux réactions de couplage croisé, seules quelques publications ont décrit la formation de biaryles symétriques par des réactions d'homocouplage.

Comme mentionné précédemment, l'homocouplage des halogénures d'aryle (réaction d'Ullmann)⁴ est grandement limité par les conditions difficiles et la rareté des systèmes catalytiques hétérogènes développés. Ainsi, la synthèse de biaryles symétriques dans des protocoles plus économiques et respectueux de l'environnement est devenue un sujet d'intérêt général.

L'homocouplage a souvent été considéré comme une réaction secondaire dans diverses transformations organiques. Cependant, un tel homocouplage pourrait fournir un accès rapide et pratique aux biaryles symétriques *via* la formation de liaisons C_{aryl}-C_{aryl}.

Ainsi, l'homocouplage des acides arylboroniques (ABA) a été considéré comme une réaction secondaire dans les réactions de couplage de Chan-Lam-Evans (voir ci-dessus). Cependant, une telle homocombinaison d'acides arylboroniques a permis la synthèse de biaryles symétriques en formant des liaisons $C_{\text{aryl}}-C_{\text{aryl}}$ à une température douce sous air, ce qui la rend très attrayante par rapport aux conditions de réaction d'Ullmann d'origine.

L'homocouplage médié par le cuivre(I) des sels d'aryldiazonium a également été initialement découvert comme une réaction secondaire lors d'études sur la réaction de Sandmeyer des sels d'aryldiazonium et de l'halogénure de cuivre (**Sch. 4**), mais ce travail fondateur ouvre la possibilité de synthétiser rapidement des biaryles symétriques en utilisant les sels d'aryldiazonium comme seul partenaire de couplage. Comme ces sels d'aryldiazonium peuvent être facilement préparés à partir des anilines correspondantes avec du nitrite de sodium (NaNO_2) dans une solution acide froide ou avec de l'acide nitreux (HNO_2), ils sont devenus des alternatives intéressantes aux électrophiles courants, tels que les halogénures d'aryle ou les triflates²⁴, pour les formations de liaisons $C_{\text{aryl}}-C_{\text{aryl}}$ par des réactions d'homocouplage.

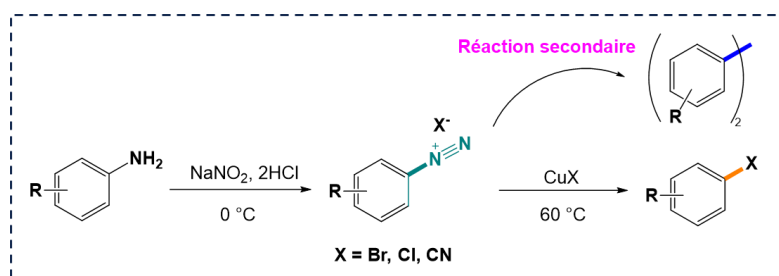


Schéma 4. Réaction de Sandmeyer.

Sur cette base, nous avons envisagé d'explorer le potentiel de $\text{Cu}^{\text{I}}\text{-USY}$ pour former des liaisons $C_{\text{aryl}}-C_{\text{aryl}}$ dans l'homocouplage des halogénures d'aryle et des ABAs et des sels d'aryldiazonium, respectivement, dans le but de synthétiser des biaryles symétriques dans des conditions plus vertes et plus douces.

Dans des études antérieures de notre groupe, nous avons montré que $\text{Cu}^{\text{I}}\text{-USY}$ n'était pas capable de catalyser la réaction d'homocouplage d'Ullmann (**Sch. 5**). Cependant, les résultats expérimentaux préliminaires ont indiqué que $\text{Cu}^{\text{I}}\text{-USY}$ pouvait catalyser avec succès l'homocouplage de l'acide *para*-méthoxybenzèneboronique et l'homocouplage du tétrafluoroborate de *para*-nitrobenzènediazonium vers des biaryles symétriques. Par conséquent, nous nous sommes concentrés sur l'optimisation, la portée de la réaction et les applications des réactions d'homocouplage catalysées par $\text{Cu}^{\text{I}}\text{-USY}$ des ABAs et des sels d'aryldiazonium.

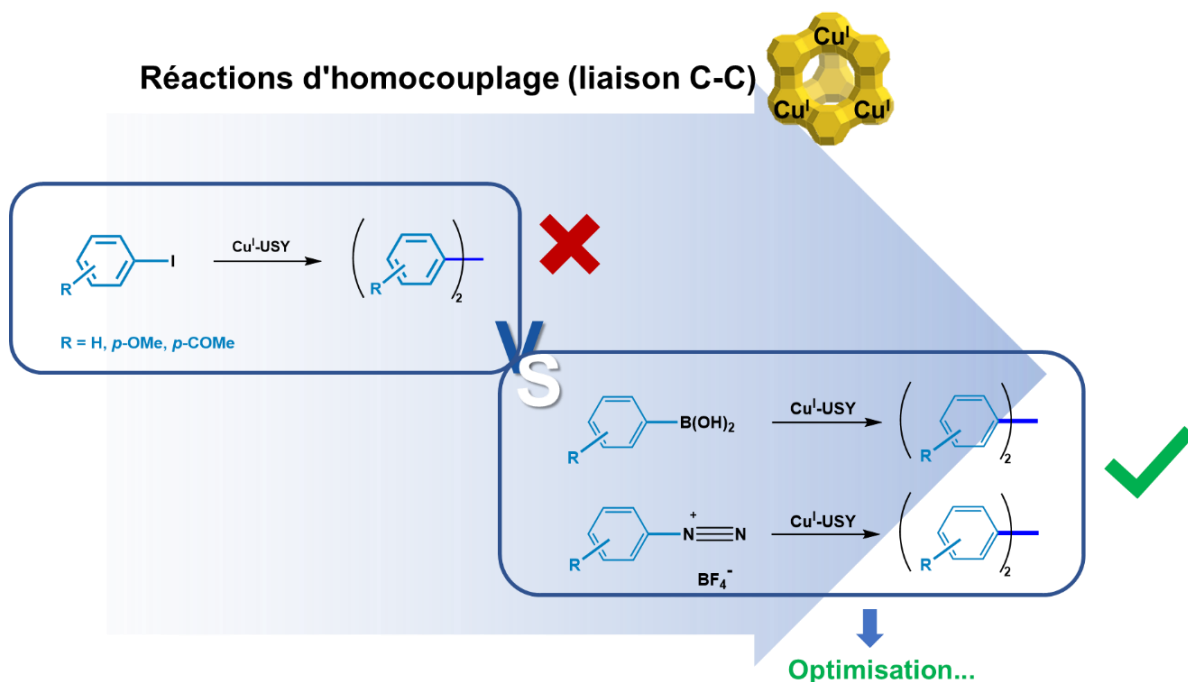


Schéma 5. Comparaison de différentes réactions d'homocouplage catalysées par Cu^{I} -USY vers les biaryles.

2.1.1. Homocouplage des acides arylboroniques catalysé par Cu^{I} -USY

L'acide *para*-méthoxyphénylboronique a été choisi comme substrat modèle pour optimiser les conditions réactionnelles sous catalyse Cu^{I} -USY. Une série de paramètres ont été étudiés, tels que les solvants, les charges des catalyseurs, les températures et l'atmosphère de réaction. Le reflux dans le méthanol sous l'air sans base ni ligand supplémentaire s'est avéré être les conditions optimales pour favoriser la réaction d'homocouplage catalysée par Cu^{I} -USY des acides arylboroniques (Sch. 6). Ces conditions sont plus vertes et plus douces que les conditions de réaction d'Ullmann.

Dans les conditions ainsi optimisées, des expériences de contrôle (c'est-à-dire en utilisant la zéolithe NH_4 -USY commerciale native, sa forme H-USY calcinée et le CuCl , ainsi qu'en l'absence de catalyseur) ont été réalisées. Les résultats ont montré que le rôle catalytique critique joué par la combinaison des ions $\text{Cu}(\text{I})$ et de la zéolithe USY puisque le produit n'a été observé que lors de l'utilisation de CuCl ou Cu^{I} -USY comme catalyseur.

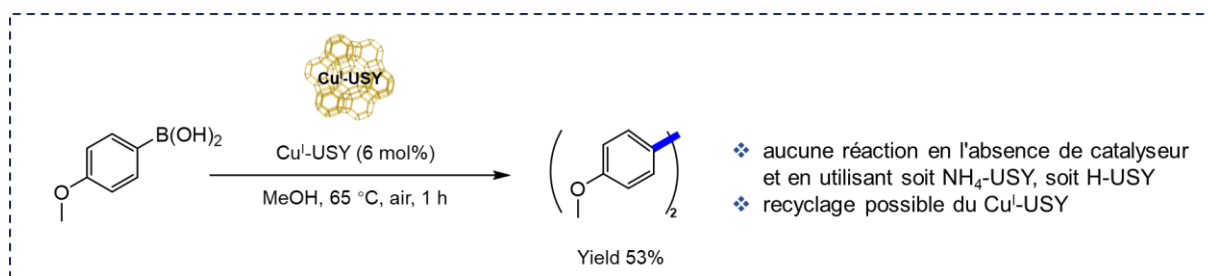


Schéma 6. Conditions de réaction optimales avec l'acide *para*-méthoxyphénylboronique comme substrat modèle pour former des liaisons C-C.^[a]

^[a] Réactions avec de l'acide *para*-méthoxyphénylboronique (0.5 mmol, 1.0 équiv.) et du Cu^I-USY (6 mol%) dans du MeOH (2 mL) à 65 °C pendant 1 h à l'air, sauf indication contraire.

Avec ces résultats prometteurs, nous avons ensuite exploré la portée et les limites du substrat des réactions de type homocouplage catalysées par Cu^I-USY développées avec divers acides arylboroniques portant des groupes déficients ou riches en électrons. 25 exemples ont été obtenus avec des rendements allant jusqu'à 99% (pour quelques exemples illustratifs, voir **Sch. 7**). Après avoir exploré les conditions de réaction optimisées et la portée du substrat, nous avons cherché à comprendre les mécanismes sous-jacents de ces réactions. En outre, leurs applications dans les réactions de Diels-Alder ont également été étudiées (voir ci-dessous).

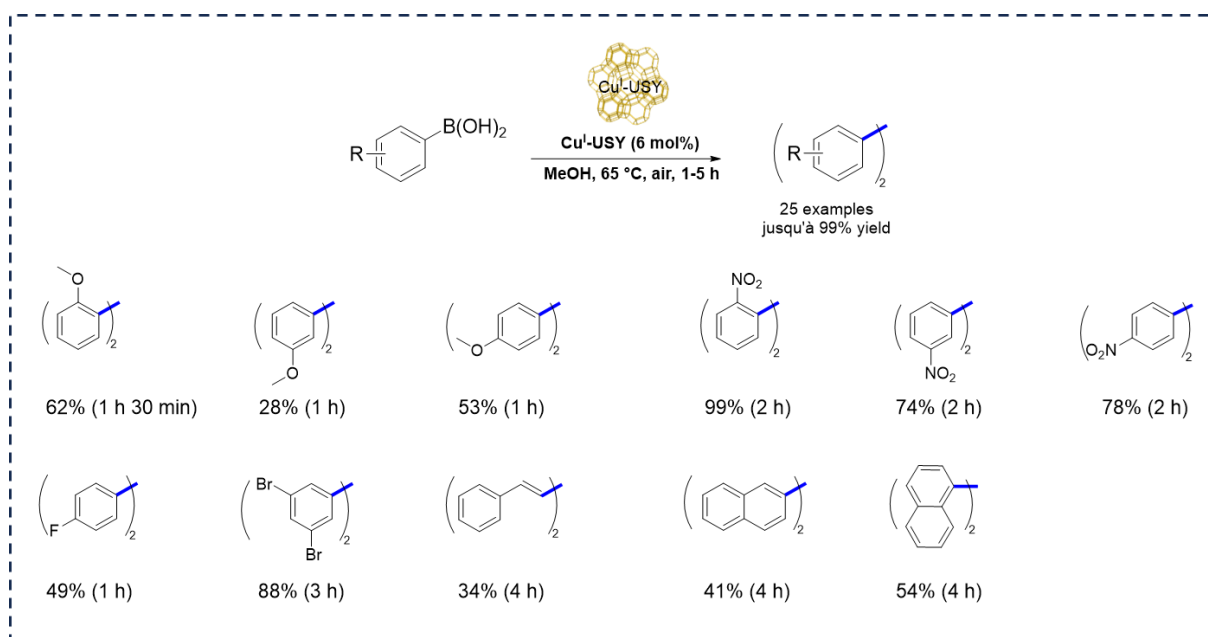


Schéma 7. Homocouplage catalysé par Cu^I-USY de divers acides arylboroniques substitués.^[a]

^[a] Toutes les réactions se déroulent avec de l'acide boronique 1a (0.5 mmol, 1.0 équiv.) et du Cu^I-USY (6 mol%) dans du MeOH (2 mL) à 65 °C pendant 1 à 5 h à l'air jusqu'à ce que le matériau de départ soit complètement converti, sauf indication contraire.

La récupérabilité et la recyclabilité du Cu^I-USY ont également été passées au crible afin d'évaluer leur hétérogénéité pour chaque nouveau procédé. Par conséquent, deux réactions d'homocouplage catalysé par Cu^I-USY (à l'échelle de 2.5 mmol) ont été examinées avec le substrat de réaction modèle acide para-méthoxyphénylboronique (**Fig. 3, A**) et l'un des acides boroniques ortho-nitrophénylboroniques les plus réactifs (**Fig. 3, B**).

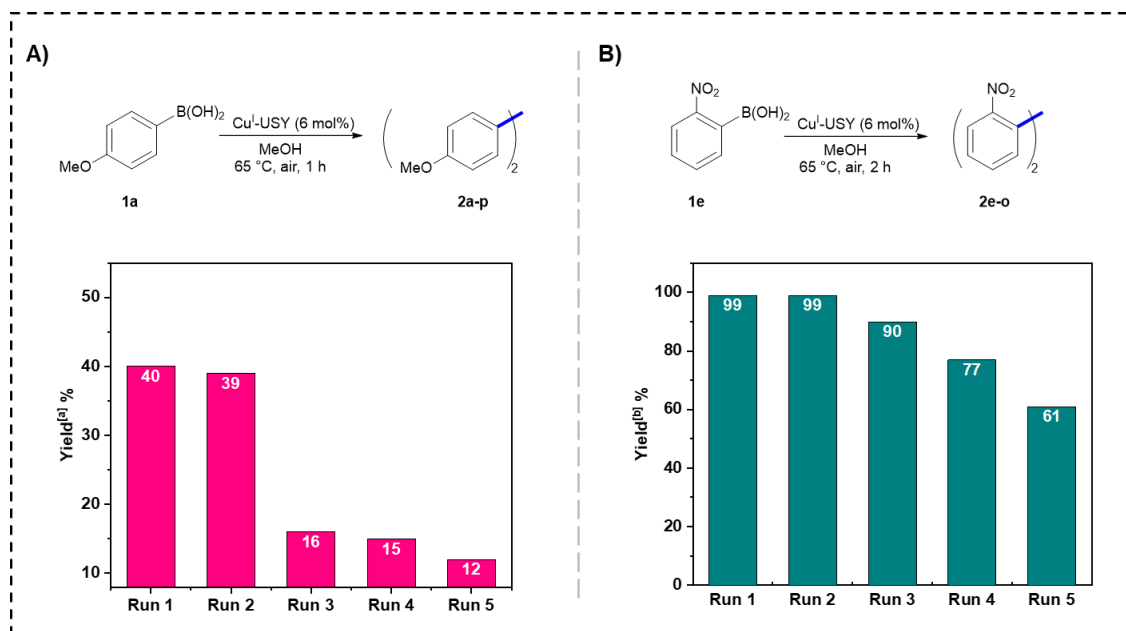


Figure 3. Etudes de recyclage de Cu^I-USY dans la réaction d'homocouplage successif.

^[a] Rendements estimés par RMN ¹H en utilisant le téréphtalate de diméthyle comme étalon interne.

^[b] Rendement isolé.

Le catalyseur à haute teneur en cuivre (jusqu'à 80% de teneur en Cu) peut être facilement récupéré par filtration et directement réengagé pour la réaction suivante sans calcination. Comme le montre la **Fig. 3**, le Cu^I-USY peut être recyclé dans les deux réactions au moins deux fois. Cependant, une érosion progressive de l'activité catalytique a été observée de la troisième à la cinquième tentative, ce qui suggère que de multiples lavages de solvants pourraient éroder l'activité du catalyseur.

Afin d'identifier plus précisément la raison de cette érosion de l'activité catalytique, un test de Sheldon a été effectué à l'aide d'acide *ortho*-nitrophénylboronique dans les mêmes conditions de réaction (**Fig. 4**). Les résultats préliminaires ont révélé que de petites quantités d'espèces de cuivre actives sont lessivées de Cu^I-USY à la solution de MeOH, puisque la réaction continue de fonctionner dans les mêmes conditions de réaction après avoir retiré le catalyseur Cu^I-USY. Bien que le rendement du produit soit passé de 29% à 55% après filtration (barre verte), il est très différent du rendement quantitatif obtenu en présence de Cu^I-USY pendant la même période

(barre bleue). La lixiviation des espèces de cuivre est probablement une autre raison de la diminution progressive du rendement dans l'étude de recyclabilité, bien que cela doive encore être confirmé par le titrage de la teneur en Cu dans le mélange brut par analyse ICP.

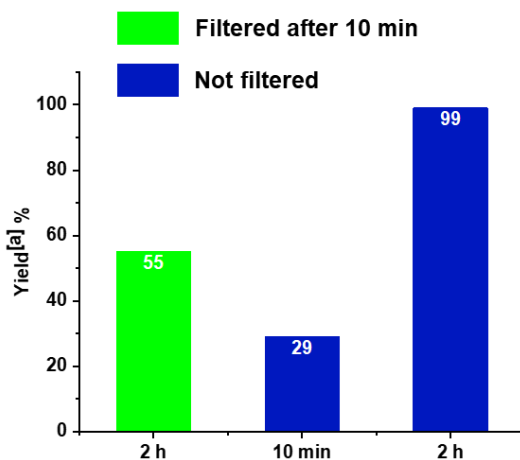


Figure 4. Test de Sheldon pour l'homocouplage catalysé par Cu^I-USY de l'acide *ortho*-nitrophénylboronique.

^[a] Rendements estimés par RMN ¹H en utilisant le téréphtalate de diméthyle comme étalon interne.

D'autre part, le diène obtenu à partir de l'homocouplage de l'acide arylboronique a été appliqué dans différentes réactions de Diels-Alder (en utilisant le *N*-phényl maléimide et le dicarboxylate d'acétylène comme diénophiles, respectivement) pour synthétiser des composés cyclohexènes plus complexes dans des procédés en deux étapes catalysées par Cu^I-USY (**Sch. 8**).

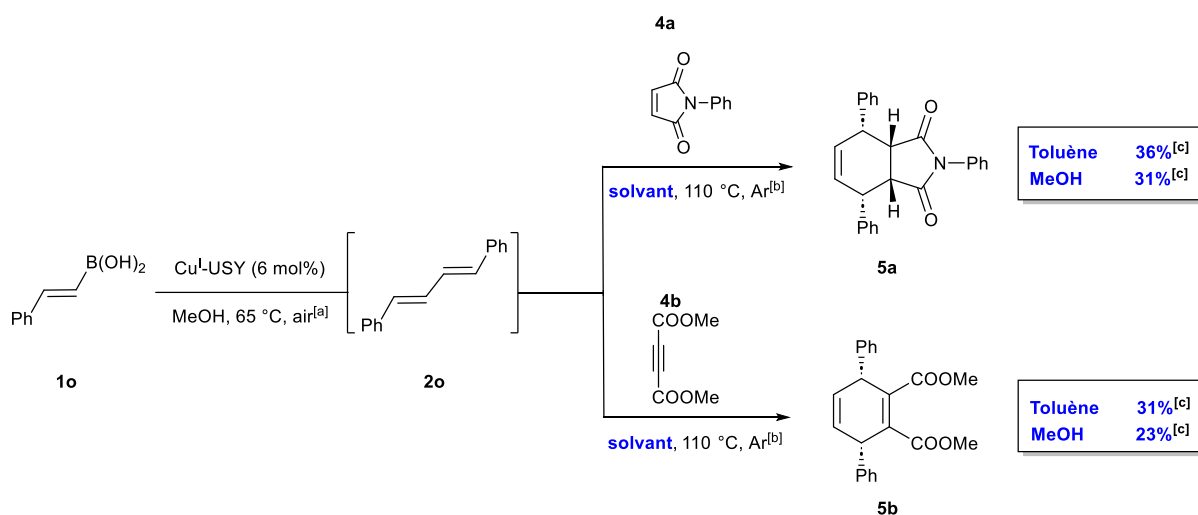


Schéma 8. Procédé en cascade catalysé par Cu^I-USY.

^[a] Fonctionnement de la réaction avec l'acide *E*-2-phénylvinyloboronique **1o** (0.5 mmol, 1.0 équiv.) et du Cu^I-USY (6 mol%) dans MeOH (2 mL) à 65 °C sous air pendant 3 h jusqu'à ce que le matériau de départ soit complètement converti.

^[b] Essai de réaction avec l'acide *E*-2-phénylvinylboronique **1o** (0.5 mmol, 1.0 équiv.) et du Cu^I-USY (6 mol%) dans MeOH (2 mL) à 65 °C à l'air pendant 3 h, puis addition du diénophile correspondant (0.5 mmol, 1.0 équiv.), suivie d'une agitation dans le solvant mentionné à 110 °C pendant 24 h sous argon, sauf indication contraire.

^[c] Rendements estimés par RMN ¹H en utilisant le téréphthalate de diméthyle comme étalon interne.

En effet, les adduits de Diels-Alder **5a** et **5b** ont été obtenus dans ces conditions, mais les rendements globaux sont restés modestes. Nos études ont montré qu'il était nécessaire de changer de solvant entre les deux étapes. En effet, lorsque le *N*-phényl maléimide **4a** a été utilisé comme diénophile, un rendement légèrement supérieur de l'adduit **5a** attendu a été obtenu dans le toluène par rapport à celui dans le MeOH (36% vs 31%). De même avec le dicarboxylate d'acétylène **4b**, le rendement du produit souhaité **5b** observé était aussi meilleur dans le toluène par rapport au MeOH (23% vs 31%) comme diénophile.

Néanmoins, ce procédé séquentiel en un pot catalysé par Cu^I-USY a fourni une méthode simple et efficace pour obtenir les produits de **5a** et **5b** dans une procédure de synthèse plus simple et économe en atomes.

2.1.2. Homocouplage catalysé par Cu^I-USY de sels d'aréné diazonium

Dans cette étude, le tétrafluoroborate de *para*-nitrobenzènediazonium a été choisi comme substrat modèle pour la réaction d'homocouplage catalysée par Cu^I-USY (**Sch. 9**). Plusieurs solvants courants et conditions de température ont été explorés. Les résultats expérimentaux préliminaires ont montré que Cu^I-USY a permis de produire avec succès le 4,4'-dinitrobiphényle attendu à partir du tétrafluoroborate de *para*-nitrobenzènediazonium dans le MeCN à température ambiante sous une atmosphère d'argon, bien qu'avec de faibles rendements (15%). Cependant, nos études ont montré que le rendement était fonction de la quantité de cuivre. Ainsi, une quantité sur-stœchiométrique de Cu^I-USY (3 équiv.) s'est avérée nécessaire. Il est intéressant de noter que le produit principal s'est révélé être le 4,4'-dinitroazobenzène, obtenu avec un bon rendement (71%). Le *para*-nitrophénol inattendu (~10%), ainsi que des traces de nitrobenzène ont été détectés. Des efforts supplémentaires sont clairement nécessaires pour explorer cette nouvelle réaction et contrôler sa sélectivité.

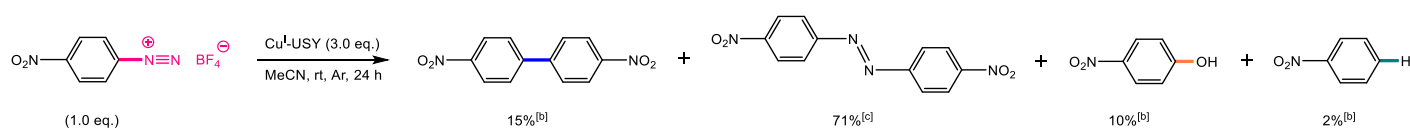


Schéma 9. Homocouplage catalysé par Cu^I-USY du tétrafluoroborate de *para*-nitrobenzènediazonium.^[a]

^[a] Réactions avec du tétrafluoroborate de *para*-nitrobenzènediazonium (0,5 mmol, 1.0 équiv. avec une concentration de 0,25 M) et du Cu^I-USY (3.0 équiv.) dans du MeCN à température ambiante sous air pendant 24 h, sauf indication contraire.

^[b] Rendements estimés à partir du mélange brut RMN ¹H en utilisant le 1,3,5-triméthoxybenzène comme étalon interne, sauf indication contraire.

^[c] Rendement isolé.

2.2. Formation de liaisons C_{aryl}-X vers les phénols via des réactions de couplage de type Chan-Lam-Evans catalysées par des zéolithes dopées au cuivre(I)

Comme mentionné précédemment, les liaisons C_{aryl}-X ont été formées pour la première fois par Ullmann au début du siècle dernier. Par rapport aux conditions difficiles de ces réactions originales, les réactions de couplage croisé de type Chan-Lam-Evans avec les acides arylboroniques comme l'un des partenaires de couplage, ont fourni la possibilité de construire des liaisons C_{aryl}-N et C_{aryl}-O dans des conditions de réaction beaucoup plus douces, ce qui les rend clairement attrayantes par rapport aux conditions de réaction originales de type Ullmann.

Cependant, à notre connaissance, ces réactions de couplage croisé C_{aryl}-O de type Chan-Lam-Evans se sont principalement concentrées sur la synthèse d'éthers aryliques et seulement quelques rapports liés à la préparation de phénols.

Comme mentionné précédemment, les phénols sont des motifs courants qui apparaissent dans une large gamme de substances naturelles et de nombreux produits industriels importants. Ils servent ainsi souvent d'intermédiaires synthétiques polyvalents.²⁵

Par conséquent, la synthèse des phénols, en particulier dans des conditions douces et vertes, continue d'attirer l'attention des chimistes organiciens. L'obtention de dérivés phénoliques nécessite généralement une substitution aromatique nucléophile ou des processus oxydatifs dans des conditions difficiles, en particulier à l'échelle industrielle, avec des conséquences évidentes sur l'environnement et la durabilité.²⁶ Les méthodes non oxydantes comprennent la substitution aromatique nucléophile des halogénures d'aryle activés et la conversion des sels d'aryldiazonium. Dans le cadre du développement de la formation de liaisons C-O catalysée par le palladium de Buchwald-Hartwig à partir d'halogénures d'aryle en 2006,²⁶ des phénols ont également été obtenus à partir d'halogénures d'aryle dans des conditions similaires, mais avec des sels d'hydroxyde comme nucléophiles²⁷ au lieu d'alcools aliphatiques^{28,29}, ou phénols³⁰⁻³². Avec de tels nucléophiles faciles à manipuler et bon marché, les phénols pourraient être directement synthétisés à partir d'halogénures d'aryle par une voie plus pratique et économique. Néanmoins, à notre connaissance, seuls quelques exemples de couplage de type

Ullmann en conditions homogènes et deux en conditions hétérogènes ont été rapportés pour la synthèse de phénols avec des sels d'hydroxyde en tant que nucléophiles.

En parallèle, et bien qu'elle ait été observée pour la première fois comme une réaction secondaire dans le couplage des acides arylboroniques favorisé par Chan-Evans-Lam-cuivre,^{33,34} l'hydroxylation des acides arylboroniques a gagné en intérêt, principalement en raison de la disponibilité de nombreux acides boroniques et des conditions douces employées.³⁵ Néanmoins, seules cinq réactions de couplage C_{aryl}-O de Chan-Lam-Evans avec des sels d'hydroxyde en tant que nucléophiles ont été développées pour accéder à des phénols.

Cette situation actuelle nous a motivés à étudier la synthèse du phénol dans ces deux réactions, dans le but d'obtenir des conditions plus douces et plus vertes que les conditions habituelles, en particulier industrielles.

Par conséquent, mes recherches se sont jusqu'à présent concentrées sur les aspects suivants : l'exploration et l'expansion des réactions de couplage croisé C-O de type Chan-Evans entre les acides arylboroniques et les sels d'hydroxyde faciles à manipuler et bon marché (par exemple, NaOH, KOH...) en tant qu'espèces nucléophiles pour synthétiser des composés phénoliques. En effet, des expériences préliminaires ont montré que la version d'Ullmann ne pouvait pas être appliquée à une telle réaction (**Sch. 10**).

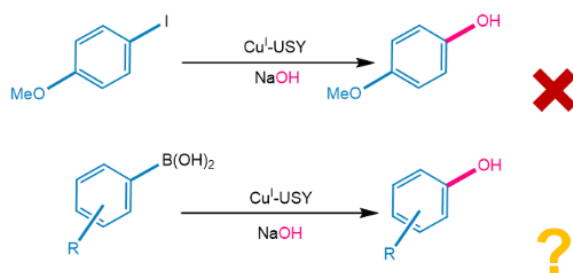


Schéma 10. Comparaison de la réaction d'Ullmann catalysée par Cu^I-USY et des réactions de type Chan-Lam.

2.2.1. Réactions de couplage C-O de type Chan-Lam catalysées par Cu^I-USY vers les phénols

L'acide *para*-méthoxyphénylboronique a été choisi comme substrat modèle pour optimiser les conditions réactionnelles sous catalyse Cu^I-USY. Divers paramètres ont été étudiés, tels que les solvants, les charges des catalyseurs, les températures et l'atmosphère de réaction.

L'utilisation de 12 mol% de Cu^I-USY dans l'eau à température ambiante sous air s'est avérée être la condition la plus efficace pour la formation de phénols, offrant un rendement de 80% du

produit (**Sch. 11**). Il s'agit du premier catalyseur hétérogène capable de préparer directement des phénols par des réactions de type Chan-Evans.

Il est intéressant de noter que cette formation de phénols peut ainsi être réalisée dans des conditions très « vertes ».

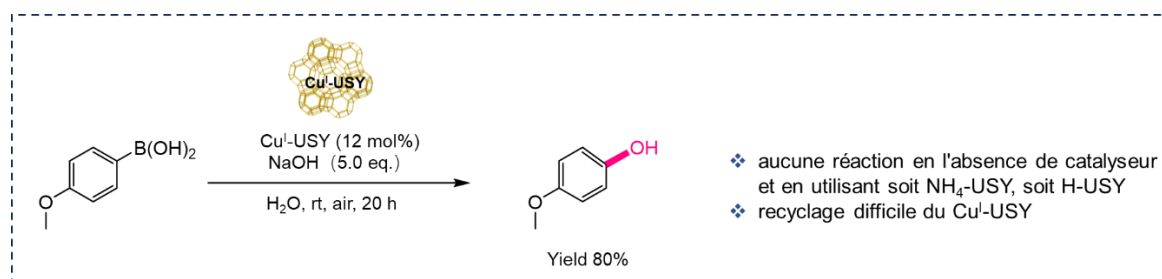


Schéma 11. Conditions de réaction optimales avec l'acide *para*-méthoxyphénylboronique comme substrat modèle pour former des liaisons C-O.^[a]

^[a] Réactions avec de l'acide *para*-méthoxyphénylboronique (0.5 mmol, 1.0 équiv.) et du Cu^I-USY (12 mol%) dans H₂O (2 mL) à température ambiante pendant 20 h à l'air, sauf indication contraire.

Dans les conditions ainsi optimisées, des expériences de contrôle (c'est-à-dire en utilisant la zéolithe commerciale native NH₄-USY, sa forme H-USY calcinée et le CuCl, ainsi qu'en l'absence de catalyseur) ont été réalisées. Les résultats ont également montré que le rôle critique joué par la combinaison des ions Cu(I) et de la zéolithe USY en tant qu'aucun produit ne pouvait être obtenu en l'absence d'espèces de cuivre. Malheureusement, le catalyseur n'a pas pu être recyclé.

Avec ces résultats prometteurs, nous avons ensuite exploré la portée et les limites du substrat des réactions de couplage croisé C-O de type Chan-Lam catalysées par Cu^I-USY avec divers acides arylboroniques portant des groupes déficients ou riches en électrons. 20 exemples ont été obtenus avec des rendements allant jusqu'à 85% (pour quelques exemples illustratifs, voir **Sch. 12**). Après avoir exploré les conditions de réaction optimisées et la portée du substrat, nous avons cherché à comprendre les mécanismes sous-jacents de ces réactions.

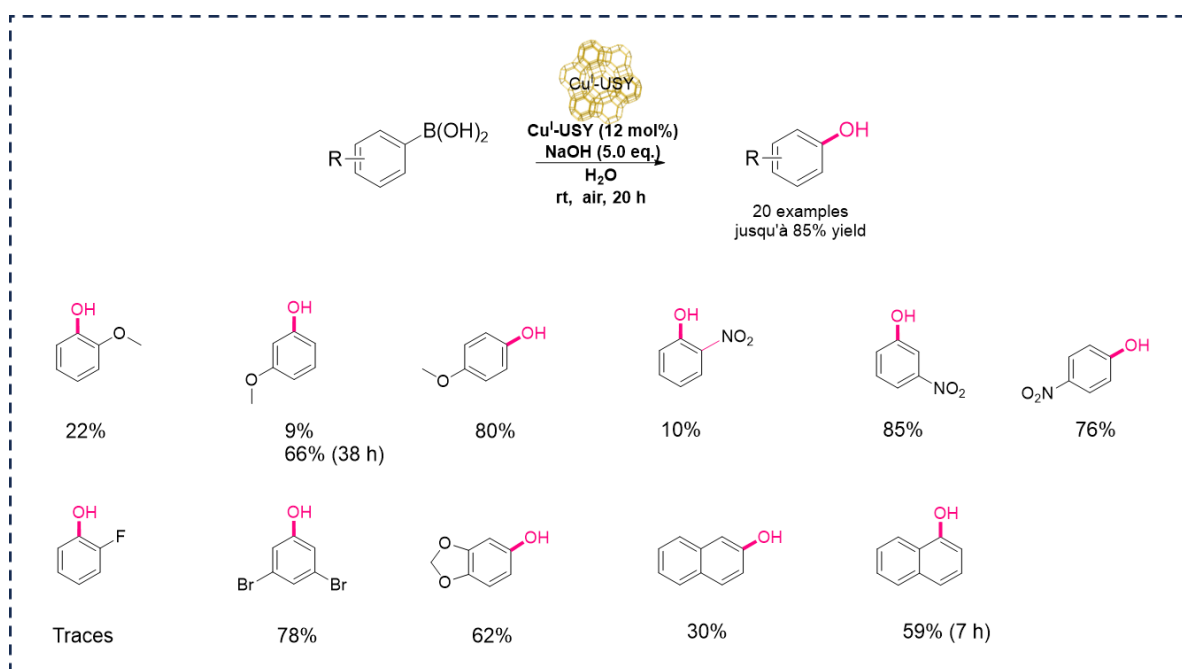


Schéma 12. Couplage croisé C-O de type Chan-Evens catalysé par Cu^{I} -USY vers les phénols.^[a]

^[a] Les réactions fonctionnent avec de l'acide boronique (0.5 mmol, 1.0 équiv.), du NaOH (2.5 mmol, 5.0 équiv.) et du Cu^{I} -USY (12 mol%) ont été mélangés dans 2 mL d'eau pendant 20 h à température ambiante sous l'air, sauf indication contraire.

2.3. Réactions de couplage déshydrogénatif croisé catalysées par des zéolithes dopées au cuivre(I) pour former des liaisons C-C et leurs applications sur la synthèse de dérivés de tétrahydroisoquinoléine

La réaction de couplage déshydrogénatif croisé (CDC), proposée il y a une quinzaine d'années,³⁶ est l'une des stratégies de synthèse les plus durables et les plus efficaces pour construire des liaisons C-C directement à partir de liaisons C-H (**Sch. 13**). Cette réaction continue d'être développée et d'être explorée, notamment en conditions hétérogènes pour lesquelles seules quelques versions sont connues.

Du point de vue de la chimie verte, la réaction CDC est un protocole véritablement économe en atomes, simple et respectueux de l'environnement, qui a fasciné de nombreux chimistes et nous a motivés à exploiter le potentiel de notre matériau cuivre(I)-zéolithe dans cette réaction. Les méthodes ainsi développées fourniraient la base pour synthétiser de précieux motifs THIQ catalysés par notre zéolithe de cuivre(I).

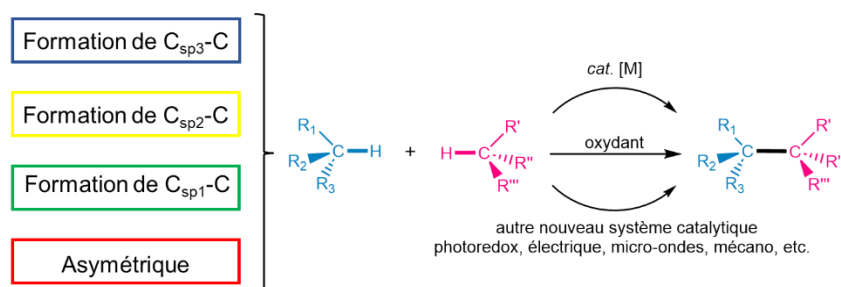


Schéma 13. Couplage déshydrogénatif croisé pour les formations de liaisons C-C.³⁶

Comme mentionné précédemment, le motif THIQ est souvent rencontrée dans les produits naturels biologiquement actifs,³⁷ ce qui a suscité un grand intérêt et a motivé la synthèse de divers analogues synthétiques.³⁸ De ce fait, diverses méthodologies ont été développées pour construire de tels motifs³⁹, mais peu d'études ont rapporté des versions hétérogènes basées sur la réaction de CDC. Par conséquent, nous envisageons de préparer divers substrats de type THIQ (**S.10**) pour la synthèse ultérieure de dérivés plus complexes et/ou fonctionnalisés (par exemple **S.11**) en utilisant la réaction CDC catalysée par Cu^I-USY (**Sch. 14**). De plus, les réactions catalysées par des zéolithes seront priorisées tout au long du processus afin de se conformer autant que possible aux principes de la chimie verte.

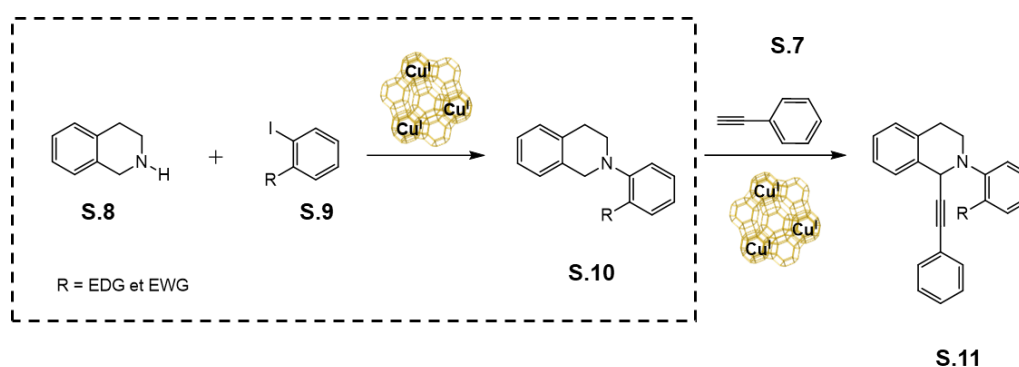


Schéma 14. Proposition de synthèse de dérivés THIQ.

Afin de vérifier les capacités de Cu^I-USY à réaliser des réactions de type CDC, la réaction modèle CDC entre la *N,N*-diméthylaniline et du phénylacétylène a été explorée dans diverses conditions. Les résultats préliminaires obtenus ont indiqué que la Cu^I-USY est bien capable de catalyser de telles réactions, et ce avec de bons voire très bons rendements (~80%; **Sch. 15**).

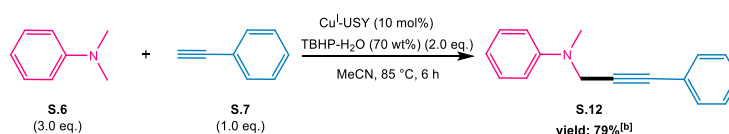


Schéma 15. Etudes préliminaires pour le couplage déshydrogénatif croisé catalysé par Cu^I-USY d'amines tertiaires et d'alcynes terminales.^[a]

^[a] Réaction avec **S.6** (3.0 équiv.) et **S.7** (1.0 équiv.), avec 10 mol% Cu^I-USY dans 2 mL de MeCN à 85 °C pendant 6 h, sauf indication contraire.

^[b] Rendement isolé.

De plus, en série THIQ, Cu^I-USY s'est révélée encore plus active et a fourni les alcynyl THIQ attendues avec d'excellents rendements, quasi quantitatifs (**Sch. 16**).

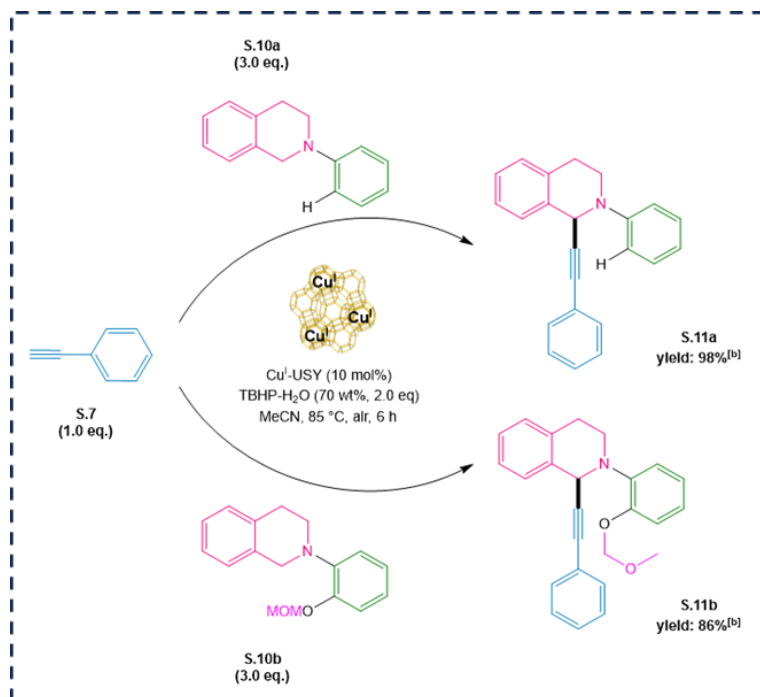


Schéma 16. Réactions CDC catalysées par Cu^I-USY de **S.10** avec **S.7**.^[a]

^[a] Réaction effectuée avec **S.7** (1.0 équiv.) et **S.10** (3.0 équiv.), avec 10 mol% de Cu^I-USY dans 2 mL de MeCN à 85 °C pendant 6 h, sauf indication contraire.

^[b] Rendement isolé.

Avec ces résultats prometteurs en main, la possibilité d'exploiter d'autres substrats avec divers alcynes terminaux est actuellement explorée.

3. Conclusions générales

Au travers cette étude, nous avons montré que la zéolithe Cu^I-USY est capable de catalyser la formation de liaisons C_{aryl}-C_{aryl} et C_{aryl}-O pour préparer des composés biaryles et des phénols *via* des réactions d'homocouplage et de couplage croisé C-O de type Chan-Lam-Evans, et ce dans des conditions plus douces et plus vertes.

En plus d'être un catalyseur hétérogène efficace, cette zéolithe s'est avérée recyclable, et active selon les réactions dans des solvants verts tels que l'eau.

De plus, nous avons démontré que l'utilisation de sels de diazonium à la place des halogénures d'aryle classiques est réalisable pour la synthèse de composés biaryles à l'aide de zéolithe de cuivre(I). Qui plus est, une sorte d'homocouplage de diazoniums en azobenzènes a été mise en évidence par action de Cu^I-USY. Cette nouvelle réaction mériterait d'être étudiée plus avant.

D'autre part, nous avons pu montrer que Cu^I-USY est capable de catalyser efficacement des réactions de type CDC entre des anilines ou des THIQ et des alcynes terminaux. Ces formations de liaisons C_{sp3}-C_{sp} pourrait ainsi être appliquées à la synthèse de dérivés THIQ plus complexes d'intérêt biologique.

Les méthodologies développées dans ce travail fournissent ainsi des alternatives catalytiques plus vertes de formation de liaisons C-C et C-O pour la synthèse de produits naturels. D'un point de vue bénéfique, ce travail a aussi apporté de nouvelles contributions au remarquable champ d'application des zéolithes, en particulier Cu^I-USY, en synthèse organique.

4. Références

1. Nguyen, M. T.; Kryachko, E. S.; Vanquickenborne, L. G. *General and theoretical aspects of phenols, The Chemistry of Phenols*, 1st ed.; John Wiley & Sons, **2004**.
2. Hesse, M. *Alkaloide*, 1st ed.; Weinheim: Wiley-VHC, **2000**.
3. (a) Manske, R. H.; Holmes, H. L. *The Alkaloids: Chemistry and Physiology*, 1st ed.; New York: Academic Press, **2005**;
(b) Charifson, P. S.; Wyrick, S. D.; Hoffman, A. J.; Simmons, R. M. A.; Bowen, J. P.; McDougald, D. L.; Mailman, R. B. *J. Med. Chem.* **1988**, *31*(10), 1941-1946.
4. Ullmann, F.; Bielecki, J. *Ber. Dtsch. Chem. Ges.* **1901**, *34*(2), 2174-2185.
5. Ullmann, F. *Ber. Dtsch. Chem. Ges.* **1903**, *36*(2), 2382-2384.
6. Ullmann, F.; Sponagel, P. *Ber. Dtsch. Chem. Ges.* **1905**, *38*(2), 2211-2212.
7. Stanforth, S. P. *Tetrahedron* **1998**, *54*(3-4), 263-303.
8. Hassan, J.; Sévignon, M.; Gozzi, C.; Schulz, E.; Lemaire, M. *Chem. Rev.* **2002**, *102*(5), 1359-1470.
9. Negishi, E. I.; De Meijere, A. *Handbook of Organopalladium Chemistry for Organic Synthesis*, 1st ed.; John Wiley & Sons, **2003**.
10. Anastas, P. T.; Warner, J. C. *Green Chemistry: Theory and Practice*, 1st ed.; Oxford University Press, **2000**.
11. Millini, R.; Bellussi, G. *Zeolite Science and Perspectives*, 1st ed.; Royal Society of Chemistry: London, **2017**.
12. Santi, K. *Zeolites in Industrial Separation and Catalysis*, 1st ed.; Wiley-VCH, **2010**.
13. Van Bekkum, H.; Flanigen, E. M.; Jacobs, P. A.; Jansen, J. C. *Introduction to Zeolite Science and Practice*, 3rd ed.; Elsevier: Amsterdam, **2007**.
14. Kuhn, P.; Pale, P.; Sommer, J.; Louis, B. *J. Phys. Chem. C.* **2009**, *113*, 2903-2910.
15. Chassaing, S.; Kumarraja, M.; Sido, A. S. S.; Pale, P.; Sommer, J. *Org. Lett.* **2007**, *9*(5), 883-886.
16. Chassaing, S.; Sido, A. S. S.; Alix, A.; Kumarraja, M.; Pale, P.; Sommer, J. *Chem. Eur. J.* **2008**, *14*(22), 6713-6721.
17. Kuhn, P.; Alix, A.; Kumarraja, M.; Louis, B.; Pale, P.; Sommer, J. *Eur. J. Org. Chem.* **2009**, (3), 423-429.
18. Garnier, T.; Danel, M.; Magné, V.; Pujol, A.; Beneteau, V.; Pale, P.; Chassaing, S. *J. Org. Chem.* **2018**, *83*(12), 6408-6422.
19. Magné, V.; Garnier, T.; Danel, M.; Pale, P.; Chassaing, S. *Org. Lett.* **2015**, *17*(18), 4494-4497.
20. Clerc, A.; Béneteau, V.; Pale, P.; Chassaing, S. *ChemCatChem* **2020**, *12*(7), 2060-2065.
21. Garnier, T.; Sakly, R.; Danel, M.; Chassaing, S.; Pale, P. *Synthesis* **2017**, *49*(6), 1223-1230.
22. Alberico, D.; Scott, M. E.; Lautens, M. *Chem. Rev.* **2007**, *107*, 174-238.
23. Mondal, S. *ChemTexts*, **2016**, *2*(4), 17.
24. Mo, F.; Qiu, D.; Zhang, L.; Wang, J. *Chem. Rev.* **2021**, *121*(10), 5741-5829.

25. Rappoport, Z. *The Chemistry of Phenols*, 1st ed.; John Wiley & Sons, **2004**.
26. Anderson, K. W.; Ikawa, T.; Tundel, R. E.; Buchwald, S. L. *J. Am. Chem. Soc.* **2006**, *128*(33), 10694-10695.
27. Tlili, A.; Xia, N.; Monnier, F.; Taillefer, M. *Angew. Chem. Int. Ed.* **2009**, *121*(46), 8881-8884.
28. Vorogushin, A. V.; Huang, X.; Buchwald, S. L. *J. Am. Chem. Soc.* **2005**, *127*(22), 8146-8149.
29. Torraca, K. E.; Huang, X.; Parrish, C. A.; Buchwald, S. L. *J. Am. Chem. Soc.* **2001**, *123*(43), 10770-10771.
30. Burgos, C. H.; Barder, T. E.; Huang, X.; Buchwald, S. L. *Angew. Chem. Int. Ed.* **2006**, *118*(26), 4427-4432
31. Kataoka, N.; Shelby, Q.; Stambuli, J. P.; Hartwig, J. F. *J. Org. Chem.* **2002**, *67*(16), 5553-5566.
32. Shelby, Q.; Kataoka, N.; Mann, G.; Hartwig, J. *J. Am. Chem. Soc.* **2000**, *122*(43), 10718-10719.
33. Evans, D. A.; Katz, J. L.; West, T. R. *Tetrahedron Lett.* **1998**, *39*(19), 2937-2940.
34. Lam, P. Y.; Clark, C. G.; Saubern, S.; Adams, J.; Winters, M. P.; Chan, D. M.; Combs, A. *Tetrahedron Lett.* **1998**, *39*(19), 2941-2944.
35. Hao, L.; Ding, G.; Deming, D. A.; Zhang, Q. *Eur. J. Org. Chem.* **2019**, *2019*(44), 7307-7321.
36. Li, C. *J. Acc. Chem. Res.* **2009**, *42*(2), 335-344.
37. Pyne, M. E.; Kevvai, K.; Grewal, P. S.; Narcross, L.; Choi, B.; Bourgeois, L.; Dueber, J. E.; Martin, V. J. *J. Nat. Commun.* **2020**, *11*, 3337.
38. Pyne, M. E.; Martin, V. J. *J. Curr. Opin. Green Sustain. Chem.* **2022**, *33*, 100561.
39. Kim, A. N.; Ngamnithiporn, A.; Du, E.; Stoltz, B. M. *Chem. Rev.* **2023**, *123*(15), 9447-9496.

Part three. Experimental part.

General information and general procedures

All commercially available starting reagents and analytical grade solvents were purchased ready to use without further purification, unless otherwise stated. Deuterated solvent CDCl_3 was purchased from Euriso-Top and dried over molecular sieves (4 Å) prior to use. Anhydrous DMSO was purchased from Aldrich as Sure/Seal™ bottles keeping the solvent over activated 4 Å molecular sieves. Anhydrous THF was obtained from distillation over sodium. Anhydrous reactions were carried out in flame-dried glassware and under an inert argon atmosphere using standard Schlenk techniques. Evaporation of solvents was conducted under reduced pressure at 40 °C using a rotary evaporator.

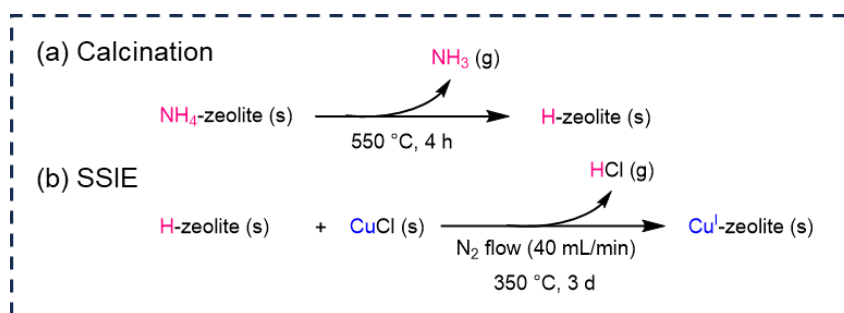
Reactions were monitored by thin-layer chromatography (TLC) which was carried out on silica plates (Merck 60 F254 silica gel) using UV-light, KMnO_4 and ninhydrine (for amines and imines) stains for visualization. Column chromatography was performed on silica gel 60 (40-63 µm, Meck) using cyclohexane/EtOAc mixtures as eluents, unless otherwise stated.

Infrared (IR) spectra were obtained on a Bruker Alpha II Fourier transform spectrometer, analyzed and recorded in wavenumbers (cm^{-1}).

^1H and ^{13}C NMR spectra were recorded on Bruker Avance spectrometers at 300, 400 or 500 MHz for ^1H NMR experiments and 126 MHz for ^{13}C NMR experiments at room temperature. ^{19}F NMR spectra were recorded at 282 MHz or 471 MHz on a 500 MHz spectrometer (equipped with a CP BBO 500S1BBF-H-D-05 Z probe) at 298 K and are referenced externally to CFCl_3 in CDCl_3 at 0.00 ppm. Chemical shifts (δ) and coupling constants (J) are given in parts per million (ppm) and Hertz (Hz), respectively. Chemical shifts (δ) are reported relative to the residual solvent as an internal standard (CDCl_3 : $\delta = 7.26$ ppm for ^1H NMR and $\delta = 77.16$ ppm for ^{13}C NMR). Data are presented as follows: chemical shift (δ), multiplicity (standard abbreviations), coupling constants (J), integration, assignment (where possible). The signal multiplicity is given according to the following abbreviations: s (singlet), d (doublet), t (triplet), q (quartet) and m (multiplet).

Low-(MS) and high-resolution mass spectrometry (HR MS) analysis were obtained using a micrOTOF spectrometer (Bruker Corporation, Billerica, MA, USA) equipped with an orthogonal electrospray interface (ESI) or atmospheric pressure chemical ionization (APCI), and a TSQ Quantum mass spectrometer (THERMO) equipped with an electron ionization (EI). Mass spectra were obtained from the “service de Spectroscopie de Masse” of the Fédération de Chimie “Le Bel” (FR2010).

(I) General procedure for the preparation of copper(I)-doped zeolites *via* SSIE.

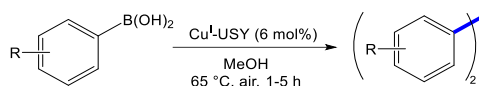


Cu^I-doped zeolites were prepared according to the solid-state ion-exchange (SSIE) reaction procedure reported by Louis and co-workers in 2009.³¹⁸ Briefly, commercial NH₄-zeolite purchased from Zeolyst International[®] was loaded into an oven and then heated at 550 °C for 4 h to provide the corresponding H-zeolite. So-formed H-zeolite (1.0 g with zeolite = USY, ZSM-5, MOR, β) and cuprous chloride (CuCl, 1.0 eq. related to the number of H-zeolite protons) were ground by a mortar and pestle for 5 min under air to afford a homogeneous mixture of H-zeolite/CuCl. Subsequently, the mixture was poured into a tubular glass reactor which was sealed and connected to a flow manifold. The H-zeolite/CuCl mixture was then heated in a furnace to 350 °C under flowing nitrogen (40 mL/min). After 3 days heating, the furnace was cooled down to room temperature and nitrogen feed was stopped, resulting in the expected Cu-exchanged zeolites, i.e., Cu^I-USY, Cu^I-ZSM-5, Cu^I-MOR and Cu^I- β , with exchange rates up to 80%. The formed catalyst was stored under argon before using. Cu^I-USY is the most attractive catalyst in our reactions, and ICP analysis showed that the copper content of the material is 3.0 mmol/g.

(II) General procedure for the preparation of copper(II)-doped zeolites *via* aqueous ion exchange (AIE) method.

The commercial NH₄-USY (1 g) was suspended in 80 mL of an aqueous solution of Cu(OAc)₂·H₂O (0.1 M). The suspension was vigorously stirred at 80 °C for 3 hours. After cooling to room temperature, the mixture was filtrated through a Millipore funnel. The solid was rinsed with distilled water and dried in an oven at 80°C. The exchange procedure was repeated twice. Finally, the preformed catalyst was calcinated in a furnace under air at 550 °C for 5 h to give Cu^{II}-USY as a dark grey solid.

(III) General procedure for the Cu^I-USY-catalyzed homocoupling of arylboronic acids towards biaryl compounds.

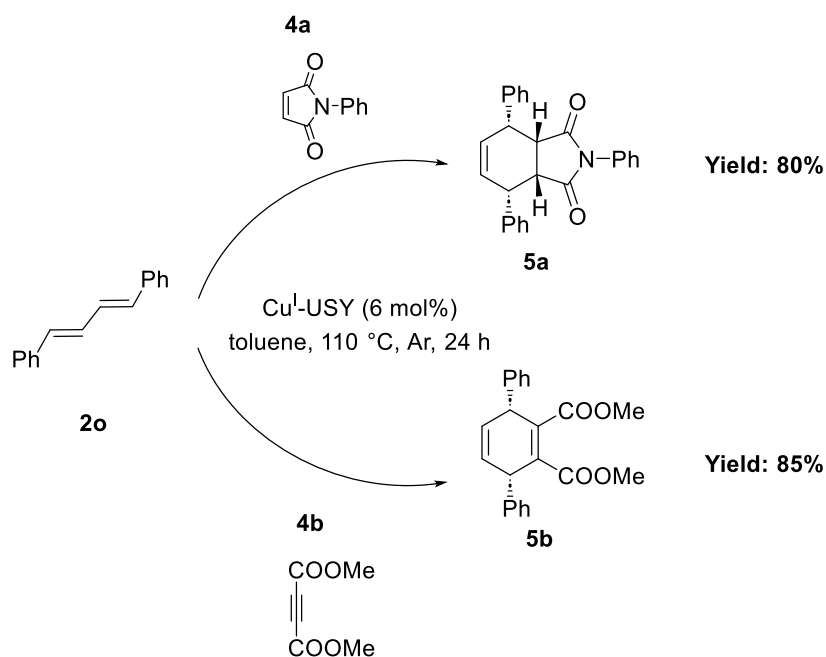


Arylboronic acid (0.5 mmol, 1.0 equiv.), Cu^I-USY (10 mg, 6 mol% of copper species) and MeOH (2 mL, *c* = 0.25 mol/L) were successively added to a 50 mL Schlenk flask (with a magnetic stirring bar). The reaction mixture was stirred at 65 °C under air and monitored by TLC until full consumption of the starting material. Then the reaction was cooled down to room temperature. After addition of 15 mL of EtOAc, the mixture was stirred for additional 2 h and then filtered over a filter funnel (50 ml, 4 (10-16 μm)) with celite and washed with ethyl acetate (4 × 5 mL). The filtrate was concentrated under reduced pressure and the crude was purified by flash chromatography over silica gel using cyclohexane/EtOAc mixture.

(IV) Procedure for recycling study of Cu^I-USY in homocoupling reaction.

The recyclability and stability of Cu^I-USY were studied in the homocoupling of 4-methoxyphenylboronic acid and 2-nitrophenylboronic acid, respectively. At the end of a run, the zeolite was recovered by filtration over a Nylon 66 Millipore membrane (0.45 μm) and further washed with EtOAc. After drying under reduced pressure for a while night, the so-obtained solid was used as a catalyst in the next run.

(V) Procedure for the Cu^I-USY-catalyzed Diels-Alder reaction.



In a screwcap reaction tube, 1,4-diphenyl-1,3-butadiene **2o** (0.5 mmol, 1 equiv.), dienophile *N*-phenyl maleimide **4a** and Cu^I-USY (6 mol%) were successively added in toluene (2 mL), and

the tube was then sealed under argon. After 24 h heating at 110 °C, the Cu^I-USY was removed by hot filtration with celite and washed with EtOAc. After cooling the filtered solution to room temperature, toluene was decanted and the solid was washed 4 times with cold diethyl ether (4 × 10 mL). The solid was dried to give the desired product 2,4,7-triphenyl-3a,4,7,7a-tetrahydro-1*H*-isoindole-1,3(2*H*)-dione (**5a**) as a white solid. Yield: 80%.

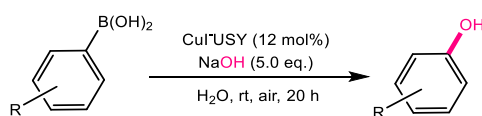
The procedure is similar in the case of acetylene dicarboxylate **4b** as the dienophile, excepted that after cooling down to room temperature, the solution was evaporated to obtain a yellow crude. The solid was then washed with 2-propanol and hexane to provide the title compound, namely dimethyl 3,6-diphenylcyclohexa-1,4-diene-1,2-dicarboxylate (**5b**), as a colorless solid. Yield: 85%.

(VI) General procedure for the Cu^I-USY-catalyzed homocoupling of *para*-nitrobenzenediazonium salt.

The arenediazonium salt (0.5 mmol, 1.0 equiv.), Cu^I-USY (20 mg, 12 mol% of copper species) and solvent (2 mL, *c* = 0.25 mol/L) were successively added to a 50 mL Schlenk flask (with a stirring bar). The reaction mixture was stirred at room temperature under air for 24 h. The catalyst was then removed by filtration with celite and washed with EtOAc (4 × 5 mL). The filtrate was concentrated under reduced pressure and the yield of the product was evaluated by ¹H NMR spectra using 1,3,5-trimethoxybenzene as the internal standard.

When the mixture urea: choline chloride (2:1) was used as the solvent, the reaction was heated and stirred at 50 °C under air for 24 h. Once cooled to room temperature, the reaction mixture was diluted with a 10 mL mixture Et₂O:H₂O (1:1) and further extracted with Et₂O (2 × 5 mL). The combined organic layers were washed with water and brine, dried over Na₂SO₄ and filtered. The solvent was removed under reduced pressure and the yield of the product was estimated by ¹H NMR spectra of the crude using 1,3,5-trimethoxybenzene as the internal standard.

(VII) General procedure for the Cu^I-USY-catalyzed Chan–Lam-type C–O cross-coupling reactions towards phenols.



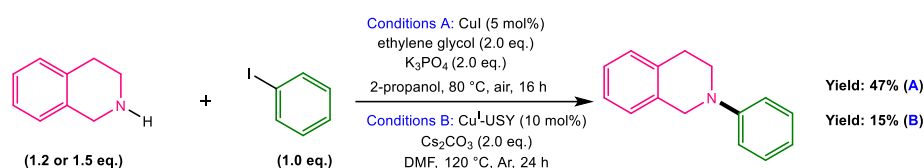
In a 50 mL Schlenk tube were successively added the arylboronic acid (0.5 mmol, 1 equiv.), an aqueous solution of sodium hydroxide (100 mg of crushed pellets/2 mL of water, 2.5 mmol, 5

equiv.) and Cu^I-USY (20 mg, 12 mol% of copper species). After 20 h stirring under air at room temperature, the pH was adjusted to around 6 by addition of aqueous 0.25 M HCl, and the resulting aqueous layer was then extracted with EtOAc (3 × 15 mL). The organic layers were then combined, dried over Na₂SO₄, filtered and evaporated. The resulting crude was purified by column chromatography eluting with appropriate cyclohexane/EtOAc mixture to afford the expected phenolic compounds.

(VIII) General procedure for the recycling study of Cu^I-USY in Chan–Lam-type C–O cross-coupling reaction.

The recyclability and stability of Cu^I-USY in basic water was studied through hydroxylation of *para*-methoxyphenylboronic acid. After each run, Cu^I-USY was recovered by filtration on a Nylon 66 membrane and successively washed with 2M NaOH, H₂O and MeOH to separate the inorganic and organic materials from the catalytic material. After drying under reduced pressure for a whole night, the zeolite was then directly used for the next run.

(IX) Procedures for the synthesis of 2-phenyl-1,2,3,4-tetrahydroisoquinoline.

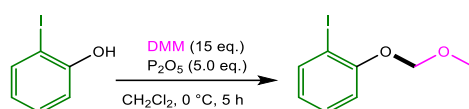


Conditions A: Copper(I) iodide (10 mg, 5 mol%) and potassium phosphate (425 mg, 2.0 mmol) were added into a septum screw-capped tube equipped with a stirring bar, followed by the addition of 2-propanol (1 ml), ethylene glycol (111 μl, 2.0 mmol), 1,2,3,4-tetrahydroisoquinoline (150 μl, 1.2 mmol) and iodobenzene (112 μl, 1.0 mmol, 1 equiv.) by microsyringe at room temperature. The tube was capped and the reaction mixture was heated to 80°C and stirred for 16 h. Once cooled to room temperature, the reaction mixture was diluted with Et₂O (5 ml) and water (5 ml) and further extracted with Et₂O (4 × 10 mL). The organic layer was collected and washed with water, brine and dried over Na₂SO₄. All volatiles were removed under reduced pressure and the crude was purified by column chromatography over silica gel eluting with cyclohexane/EtOAc (9.5:0.5). Yield: 47%.

Conditions B: In a screwcap reaction tube equipped with a stirring bar, were successively added Cu^I-USY (30 mg, 10 mol% of copper species), *N,N*-dimethylformamide (DMF) as solvent (1 mL), iodobenzene (1 mmol, 1.0 equiv.), 1,2,3,4-tetrahydroisoquinoline (1.5 mmol, 1.5 equiv.),

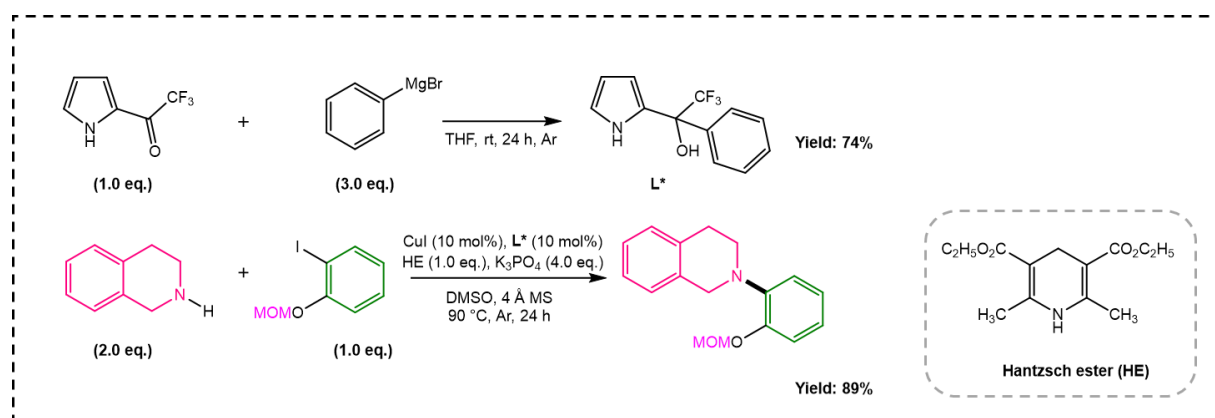
and cesium carbonate (2 mmol, 2.0 equiv.). The tube was flushed with inert gas (argon) for 15 s before sealing. Next, the reaction mixture was heated at 120 °C for 24 h. After cooling to room temperature, the solid materials were removed by filtration over a Millipore membrane and further washed with Et₂O (1 × 20 mL). The resulting organic phase was washed with aqueous 1 M NaOH (3 × 10 mL), water (3 × 10 mL) and brine (1 × 10 mL), dried over Na₂SO₄, filtered, and evaporated under reduced pressure. The crude was purified by column chromatography eluting with a cyclohexane/EtOAc (9.5:0.5) mixture to furnish the title compound product. Yield: 15%.

(X) Procedure for the phenol protection of *ortho*-iodophenol.



To a stirred ice-cold solution of CH₂Cl₂ (10 mL) containing *ortho*-iodophenol (1 mmol, 1.0 equiv.) was added dimethoxymethane (CH₂(OCH₃)₂) (1.33 mL, 15 mmol, 15 equiv.) and P₂O₅ (710 mg, 5 mmol, 5 equiv.). The resulting mixture was stirred at 0 °C for 5 h. The liquid phase was then transferred into a separatory funnel, and the solid residue was washed with CH₂Cl₂ (3 × 20 mL). The combined CH₂Cl₂ layers were washed with saturated aqueous NaHCO₃ (1 × 60 mL), aqueous 1 M NaOH (2 × 50 mL), water (1 × 60 mL), and brine (1 × 60 mL), dried over Na₂SO₄, filtered, and evaporated. The crude was purified by column chromatography on silica gel eluting with cyclohexane/EtOAc (9.5:0.5). Yield: 90%.

(XI) Procedure for the arylation of 1,2,3,4-tetrahydroisoquinoline.

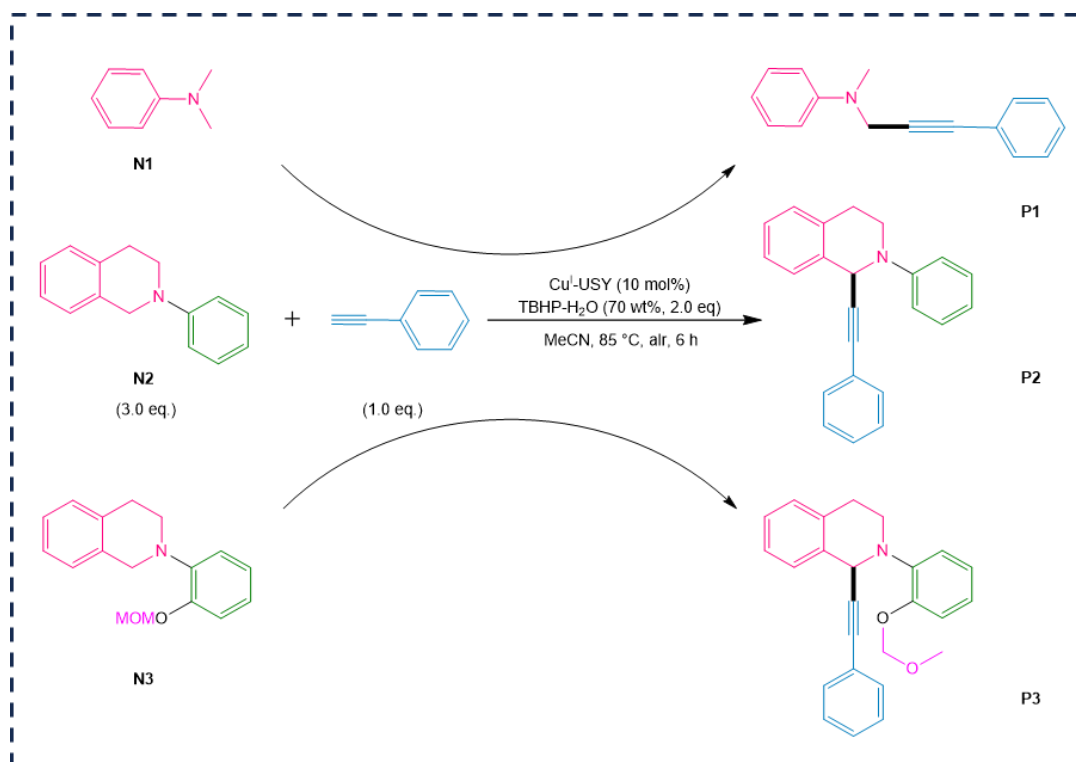


(a) The ligand L* was prepared according to a reported procedure⁴⁸⁵. To a solution of 2-(trifluoroacetyl)pyrrole (2 mmol, 1.0 equiv.) in anhydrous THF (2 mL) was added dropwise at

room temperature phenylmagnesium bromide (1M in THF, 6 mL, 6 mmol, 3.0 equiv.). After stirring overnight at room temperature, the reaction was quenched by adding 10 mL of aqueous 1M HCl and the mixture was extracted with EtOAc (2 × 10 mL). The organic layers were then combined and washed with 10 mL of saturated aqueous NaHCO₃ and brine, respectively, dried over Na₂SO₄, filtered, and evaporated. The crude was purified by column chromatography on silica gel eluting with cyclohexane/EtOAc (9:1). Yield: 74%.

(b) An oven-dried screwcap reaction tube (with a magnetic stir bar) was charged with 4 Å powdered molecular sieves (approx. 100 mg) and sealed. The molecular sieves were then activated by flame-drying the tube under high vacuum for 5 min. Next, the reaction tube was cooled to room temperature and then were successively added CuI (10 mol%), the ligand **L*** (10 mol%) and 1,2,3,4-tetrahydroisoquinoline (0.8 mmol, 2 equiv.), K₃PO₄ (1.6 mmol, 4 equiv.), Hantzsch ester (0.4 mmol, 1 equiv.), aryl iodide (0.4 mmol, 1 equiv.) and anhydrous DMSO (2 mL). The reaction tube was flushed with inert gas (argon) for 15 s before sealing. Then, the reaction was heated and stirred at 90 °C in a preheated oil bath for 24 h. When the reaction was complete, the mixture was cooled to room temperature and diluted with EtOAc (20 mL). The organic layer was washed with saturated aqueous NaCl solution (3 × 20 mL) and water (1 × 20 mL). The combined organic layers were dried over Na₂SO₄, filtered, and concentrated in a rotary evaporator. The crude was purified by flash column chromatography on silica gel using cyclohexane/EtOAc (9.5:0.5) mixture as eluent. Yield: 89%.

(XII) General procedure for Cu^I-USY-catalyzed cross-dehydrogenative coupling of tertiary amines and phenylacetylene.

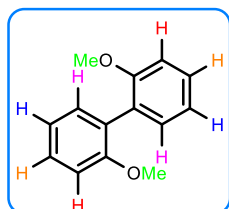


Cu^I-USY (10 mol%), phenylacetylene (0.25 mmol, 1.0 equiv.), amine (N1 or N2 or N3) (0.75 mmol, 3.0 equiv.), TBHP (70 wt.% aqueous solution, 0.50 mmol, 2.0 equiv.), and MeCN (2.5 mL) were successively added to a screwcap reaction tube equipped with a stirring bar. Then the tube was sealed, and the reaction mixture was heated to 85 °C and stirred at 450 rpm for 6 h. After cooling down to room temperature, 20 mL of 5 wt.% aqueous Na₂S₂O₃ were added to the mixture to quench the excess TBHP. Then, the resulting mixture was extracted with EtOAc (3 × 15 mL) and the combined organic phases were washed with brine, dried over Na₂SO₄ and filtered. The solvent was removed by rotary evaporation. The crude was purified by column chromatography over silica gel using cyclohexane/EtOAc (9.5:0.5) as eluent.

Analytical data of compounds from Chapter II

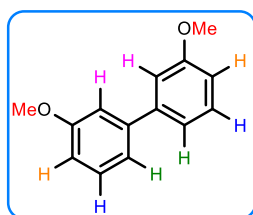
(a) Biaryl compounds

2,2'-Dimethoxy-1,1'-biphenyl (2a-o) (CAS: 4877-93-4)²⁹⁷



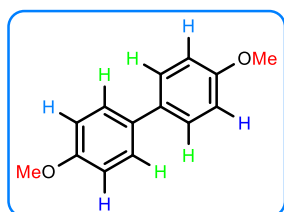
Using the general procedure III, the title compound **2a-o** was isolated as a white solid. Time reaction: 90 min. Yield: 62%. $R_f = 0.67$ (cyclohexane/EtOAc 7:3). IR (neat, cm^{-1}): 3057, 3024, 2962, 2929, 2835, 1590, 1500, 1481, 1455, 1427, 1298, 1283, 1253, 1226, 1164, 1126, 1111, 1054, 1020, 1000. $^1\text{H NMR}$ (300 MHz, CDCl_3): $\delta = 7.37\text{-}7.31$ (m, **2H**), $7.28\text{-}7.25$ (m, **2H**), $7.05\text{-}6.97$ (m, **2H2H**), 3.79 (s, **6H**) ppm. $^{13}\text{C NMR}$ (126 MHz, CDCl_3): $\delta = 157.0$ (Cq), 131.5, 128.6, 127.8, 120.3, 111.1 (Cq), 55.7 (CH_3) ppm. MS (EI) m/z (rel intensity): 214 $[\text{M}]^+$ (100), 199 (18), 184 (38).

3,3'-Dimethoxy-1,1'-biphenyl (2a-m) (CAS: 6161-50-8)⁴⁸⁶



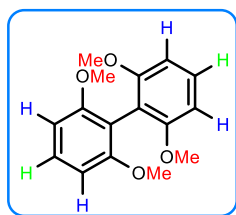
Using the general procedure III, the yield of title compound **2a-m** was estimated by $^1\text{H NMR}$ using dimethyl terephthalate as internal standard. Time reaction: 1h. Yield: 28%. $R_f = 0.72$ (cyclohexane/EtOAc 7:3). $^1\text{H NMR}$ (500 MHz, CDCl_3): $\delta = 7.35$ (t, $J = 7.9$ Hz, **2H**), $7.20\text{-}7.17$ (m, **2H**), $7.13\text{-}7.12$ (m, **2H**), $6.91\text{-}6.89$ (m, **2H**), 3.87 (s, **6H**) ppm.

4,4'-Dimethoxy-1,1'-biphenyl (2a-p) (CAS: 2132-80-1)²⁹⁷



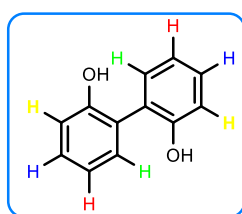
Using the general procedure III, the title compound **2a-p** was isolated as a white solid. Time reaction: 1h. Yield: 53%. $R_f = 0.65$ (cyclohexane/EtOAc 7:3). IR (neat, cm^{-1}): 2957, 2914, 2839, 1603, 1568, 1497, 1464, 1435, 1328, 1273, 1240, 1182, 1137, 1039, 1011, 996. $^1\text{H NMR}$ (300 MHz, CDCl_3): $\delta = 7.53\text{-}7.45$ (m, **4H**), $7.00\text{-}6.92$ (m, **4H**), 3.85 (s, **6H**) ppm. $^{13}\text{C NMR}$ (126 MHz, CDCl_3): $\delta = 158.9$ (Cq), 133.7, 127.9, 114.3 (Cq), 55.6 (CH_3) ppm. MS (EI) m/z (rel intensity): 214 $[\text{M}]^+$ (100), 190 (100), 171 (43), 156 (11), 128 (18).

2,2',6,6'-Tetramethoxy-1,1'-biphenyl (2a-o,o) (CAS: 19491-10-2)²⁹⁷



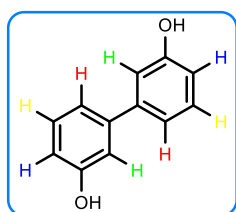
Using the general procedure III, the yield of the title compound **2a-o,o** was estimated by ¹H NMR using dimethyl terephthalate as internal standard. Time reaction: 5 h. Yield: 4%. **R_f** = 0.76 (cyclohexane/EtOAc 7:3). ¹H NMR (300 MHz, CDCl₃): δ = 7.29 (t, *J* = 8.1 Hz, **2 H**), 6.66 (d, *J* = 8.1 Hz, **4 H**), 3.72 (s, **12 H**) ppm.

2,2'-Dihydroxy-1,1'-biphenyl (2b-o) (CAS: 1806-29-7)³⁰⁶



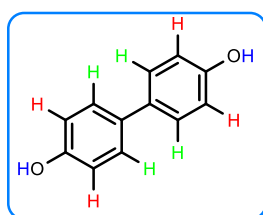
Using the general procedure III, the title compound **2b-o** was isolated as a yellow solid. Time reaction: 2 h. Yield: 46%. **R_f** = 0.34 (cyclohexane/EtOAc 7:3). **IR** (neat, cm⁻¹): 3268, 3171, 2919, 2850, 1705, 1605, 1588, 1572, 1480, 1437, 1370, 1340, 1267, 1211, 1111, 1093, 1045, 1005, 937. ¹H NMR (500 MHz, CDCl₃): δ = 7.56-7.53 (m, **2H**), 7.50-7.47 (m, **2H**), 7.29-7.24 (m, **2H2H**), 5.77 (s, **2H**) ppm. ¹³C NMR (126 MHz, CDCl₃): δ = 153.0 (Cq), 131.4, 130.2, 123.6, 121.8, 116.8 ppm. **MS** (ESI) *m/z* (rel intensity): 186 [M]⁺ (100).

3,3'-Dihydroxy-1,1'-biphenyl (2b-m) (CAS: 612-76-0)⁴⁸⁷



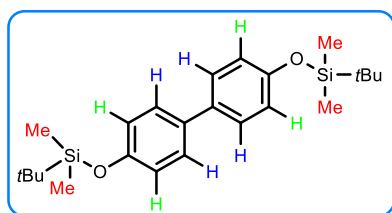
Using the general procedure III, the yield of the title compound **2b-m** was estimated by ¹H NMR using dimethyl terephthalate as internal standard. Time reaction: 3 h. Yield: 19%. ¹H NMR (300 MHz, CDCl₃): δ = 7.30-7.27 (m, **2H**), 7.14-7.12 (m, **2H**), 7.04-7.03 (m, **2H**), 6.84-6.82 (m, **2H**) ppm.

4,4'-Dihydroxy-1,1'-biphenyl (2b-p) (CAS: 92-88-6)⁴⁸⁷



Using the general procedure III, the title compound **2b-p** was isolated as an orange solid. Time reaction: 2 h. Yield: 25%. **R_f** = 0.5 (cyclohexane/EtOAc 7:3). **IR** (neat, cm⁻¹): 3344, 3020, 2954, 2921, 2852, 1887, 1705, 1608, 1589, 1494, 1420, 1377, 1294, 1234, 1173, 1134, 1116, 1020, 1001. ¹H NMR (500 MHz, DMSO-d₆): δ = 9.40 (s, **2H**), 7.37-7.35 (m, **4H**), 6.80-6.77 (m, **4H**) ppm. ¹³C NMR (126 MHz, DMSO-d₆): δ = 156.2 (Cq), 131.2, 127.0, 115.6 ppm. **MS** (ESI) *m/z* (rel intensity): 186 [M]⁺ (100).

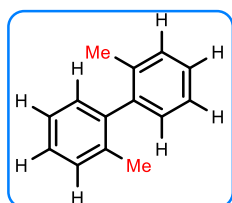
4,4'-bis((*tert*-Butyldimethylsilyloxy)-1,1'-biphenyl (2c-p) (CAS: 1492015-05-0)³⁰⁰



The title compound **2c-p** was obtained using the general procedure III. Time reaction: 2 h. Yield: 79%. $R_f = 0.75$ (cyclohexane/EtOAc 9.5:0.5). $^1\text{H NMR}$ (500 MHz, CDCl_3): $\delta = 7.42\text{--}7.39$ (m, **4H**), $6.89\text{--}6.86$ (m, **4H**), 1.00 (s, **18H**), 0.22 (s, **12H**) ppm. $^{13}\text{C NMR}$ (126 MHz, CDCl_3): $\delta = 154.9$ (Cq),

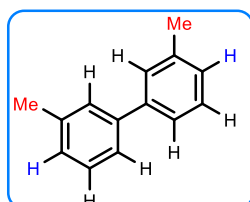
134.2, 127.8, 120.4, 25.9, 18.4, -4.2 ppm.

2,2'-Dimethyl-1,1'-biphenyl (2d-o) (CAS: 605-39-0)²⁹⁷



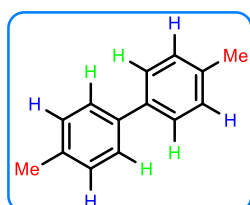
Using the general procedure III, the yield of title compound **2d-o** was estimated by $^1\text{H NMR}$ using dimethyl terephthalate as internal standard. Time reaction: 3 h. Yield: 7%. $^1\text{H NMR}$ (300 MHz, CDCl_3): $\delta = 7.43\text{--}7.38$ (m, 4H), $7.36\text{--}7.31$ (m, 2H), $7.19\text{--}7.14$ (m, 2H), 2.43 (s, **6H**) ppm.

3,3'-Dimethyl-1, 1'-biphenyl (2d-m) (CAS: 612-75-9)²⁹⁷



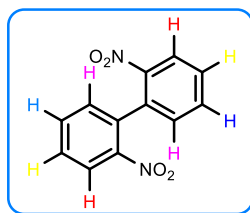
Using the general procedure III, the yield of title compound **2d-m** was estimated by $^1\text{H NMR}$ using dimethyl terephthalate as internal standard. Time reaction: 3 h. Yield: 27%. $R_f = 0.56$ (cyclohexane). $^1\text{H NMR}$ (500 MHz, CDCl_3): $\delta = 7.41\text{--}7.37$ (m, 4H), $7.35\text{--}7.29$ (m, 2H), $7.18\text{--}7.14$ (m, **2H**), 2.42 (s, **6H**) ppm. $^{13}\text{C NMR}$ (126 MHz, CDCl_3): $\delta = 141.5$ (Cq), 138.4, 128.7, 128.1, 128.0, 124.3, 21.7 (CH_3) ppm.

4,4'-Dimethyl-1, 1'-biphenyl (2d-p) (CAS: 613-33-2)²⁹⁷



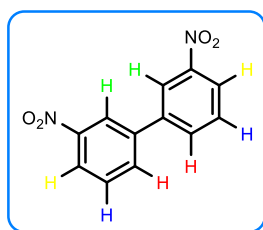
Using the general procedure III, the yield of title compound **2d-p** was estimated by $^1\text{H NMR}$ using dimethyl terephthalate as internal standard. Time reaction: 1 h. Yield: 25%. IR (neat, cm^{-1}): 3021, 2913, 2852, 1902, 1500, 1487, 1445, 1311, 1178, 1112, 1037, 1005, 837, 816, 724, 547, 501, 427. $^1\text{H NMR}$ (300 MHz, CDCl_3): $\delta = 7.50\text{--}7.46$ (m, **4H**), $7.26\text{--}7.21$ (m, **4H**), 2.39 (s, **6H**) ppm. $^{13}\text{C NMR}$ (126 MHz, CDCl_3): $\delta = 138.4$ (Cq), 136.8, 129.6, 126.9, 21.2 (CH_3) ppm. MS (EI) m/z (rel intensity): 182 [M]⁺ (100).

2,2'-Dinitro-1,1'-biphenyl (2e-o) (CAS: 2436-96-6)³⁰⁵



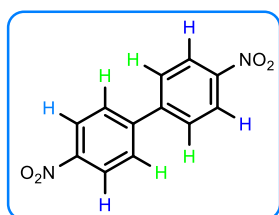
Using the general procedure III, the title compound **2e-o** was isolated as an orange solid. Time reaction: 2 h. Yield: 99%. $R_f = 0.41$ (cyclohexane/EtOAc 7:3). IR (neat, cm^{-1}): 1605, 1571, 1514, 1467, 1349, 1297, 1163, 1145, 1103, 1006, 955. $^1\text{H NMR}$ (300 MHz, CDCl_3): $\delta = 8.23\text{-}8.21$ (m, **2H**), 7.69 (td, $^3J = 7.5$ Hz, $^4J = 1.4$ Hz, **2H**), 7.62-7.58 (m, **2H**), 7.31-7.29 (m, **2H**) ppm. $^{13}\text{C NMR}$ (126 MHz, CDCl_3): $\delta = 147.2$ (Cq), 134.2 (Cq), 133.5, 130.9, 129.2, 124.9 ppm. MS (EI) m/z (rel intensity): 198 $[\text{M}-\text{NO}_2]^+$ (100), 168 (44), 139 (42), 115 (30).

3,3'-Dinitro-1,1'-biphenyl (2e-m) (CAS: 958-96-3)²⁹⁷



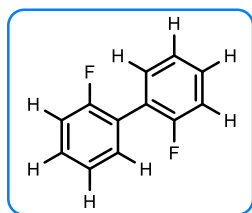
Using the general procedure III, the title compound **2e-m** was isolated as a yellow solid. Time reaction: 2 h. Yield: 74%. $R_f = 0.64$ (cyclohexane/EtOAc 7:3). IR (neat, cm^{-1}): 3384, 3092, 3080, 2922, 2852, 1706, 1622, 1593, 1519, 1464, 1417, 1344, 1300, 1266, 1214, 1103, 1082, 998. $^1\text{H NMR}$ (300 MHz, CDCl_3): $\delta = 8.52\text{-}8.49$ (m, **2H**), 8.33-8.29 (m, **2H**), 7.99-7.96 (m, **2H**), 7.73-7.68 (m, **2H**) ppm. $^{13}\text{C NMR}$ (126 MHz, CDCl_3): $\delta = 148.7$ (Cq), 140.2, 133.1, 130.2, 123.1, 122.0 ppm. MS (ESI, m/z): 244 $[\text{M}]^+$ (100).

4,4'-Dinitro-1,1'-biphenyl (2e-p) (CAS: 1528-74-1)⁴⁸⁶



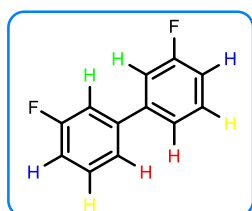
Using the general procedure III, the title compound **2e-p** was isolated as a yellow solid. Time reaction: 2 h. Yield: 78%. $R_f = 0.66$ (cyclohexane/EtOAc 7:3). IR (neat, cm^{-1}): 3096, 2921, 2857, 2444, 1928, 1794, 1597, 1508, 1476, 1393, 1375, 1338, 1260, 1180, 1106, 1006. $^1\text{H NMR}$ (500 MHz, CDCl_3): $\delta = 8.38\text{-}8.33$ (m, **4H**), 7.81-7.77 (m, **4H**) ppm. $^{13}\text{C NMR}$ (126 MHz, CDCl_3): $\delta = 148.1$, 145.0, 128.4, 124.4 ppm. MS (EI) m/z (rel intensity): 244 $[\text{M}]^+$ (100), 214 (34), 151 (44).

2,2'-Difluoro-1,1'-biphenyl (2f-o) (CAS: 388-82-9)⁴⁸⁸



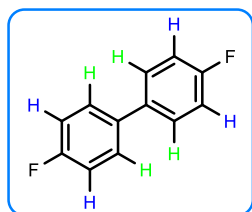
Using the general procedure III, the title compound **2f-o** was isolated as a white solid. Time reaction: 2 h. Yield: 34%. $R_f = 0.77$ (cyclohexane/EtOAc 7:3). **IR** (neat, cm^{-1}): 3201, 2922, 2852, 2261, 1432, 1411, 1192. **^1H NMR** (300 MHz, CDCl_3): $\delta = 7.41\text{-}7.35$ (m, 4H), 7.24-7.21 (m, 2H), 7.19-7.15 (m, 2H) ppm. **^{13}C NMR** (126 MHz, CDCl_3): $\delta = 159.9$ (d, $J = 248.6$ Hz, Cq), 131.7 (d, $J = 7.6$ Hz), 129.9 (d, $J = 8.3$ Hz), 124.2, 116.0 (d, $J = 21.1$ Hz), 115.8 (d, $J = 22.5$ Hz) ppm. **^{19}F NMR** (500 MHz, CDCl_3): $\delta = -114.8$ ppm. **MS** (EI) m/z (rel intensity): 190 $[\text{M}]^+$ (100).

3,3'-Difluoro-1,1'-biphenyl (2f-m) (CAS: 396-64-5)⁴⁸⁸



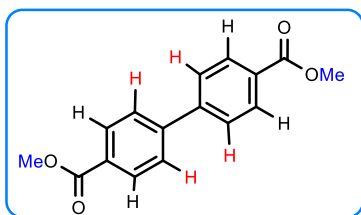
Using the general procedure III, the title compound **2f-m** was isolated as a colorless solid. Time reaction: after 24 h at room temperature. Yield: 87%. $R_f = 0.77$ (cyclohexane/EtOAc 7:3). **IR** (neat, cm^{-1}): 3208, 2955, 2920, 2851, 2261, 2081, 1611, 1580, 1453, 1420, 1410, 1377, 1258, 1193, 1157, 1028, 935. **^1H NMR** (500 MHz, CDCl_3): $\delta = 7.44\text{-}7.39$ (m, 2H), 7.37-7.34 (m, 2H), 7.29-7.26 (m, **2H**), 7.09-7.05 (m, **2H**) ppm. **^{13}C NMR** (126 MHz, CDCl_3): $\delta = 163.3$ (d, $J = 246.1$ Hz, Cq), 142.3 (dd, $J = 7.7$ Hz, $J = 2.3$ Hz, Cq), 130.5 (d, $J = 8.4$ Hz), 122.9 (d, $J = 2.9$ Hz), 114.8 (d, $J = 21.2$ Hz), 114.2 (d, $J = 22.3$ Hz) ppm. **^{19}F NMR** (500 MHz, CDCl_3): $\delta = -112.8$ ppm. **MS** (EI) m/z (rel intensity): 190 $[\text{M}]^+$ (100).

4,4'-Difluoro-1,1'-biphenyl (2f-p) (CAS: 398-23-2)⁴⁸⁶



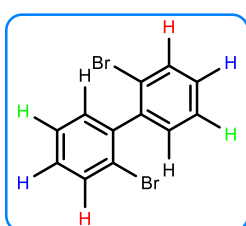
Using the general procedure III, the title compound **2f-p** was isolated as a pale yellow solid. Time reaction: 24 h at room temperature. Yield: 81%. $R_f = 0.81$ (cyclohexane/EtOAc 7:3). **IR** (neat, cm^{-1}): 3068, 3048, 2921, 2853, 1891, 1594, 1487, 1394, 1320, 1226, 1156, 1108, 1004, 803. **^1H NMR** (500 MHz, CDCl_3): $\delta = 7.52\text{-}7.45$ (m, **4H**), 7.15-7.08 (m, **4H**) ppm. **^{13}C NMR** (126 MHz, CDCl_3): $\delta = 162.4$ (d, $J = 245.0$ Hz, Cq), 136.4 (d, $J = 3.0$ Hz), 128.6 (d, $J = 8.0$ Hz), 115.7 (d, $J = 21.0$ Hz) ppm. **^{19}F NMR** (500 MHz, CDCl_3): $\delta = -115.7$ ppm. **MS** (EI) m/z (rel intensity): 190 $[\text{M}]^+$ (100).

Dimethyl biphenyl-4,4'-dicarboxylate (2g-p) (CAS: 792-74-5)⁴⁸⁶



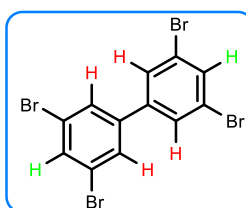
Using the general procedure III, the yield of the title compound **2g-p** was estimated by ¹H NMR using dimethyl terephthalate as internal standard. Time reaction: 2 h. Yield: 48%. ¹H NMR (300 MHz, CDCl₃): δ = 8.13 (d, J = 8.3 Hz, **4H**), 7.69 (d, J = 8.3 Hz, **4H**), 3.95 (s, **6H**) ppm.

2,2'-Dibromobiphenyl (2h-o) (CAS: 13029-09-9)⁴⁸⁷



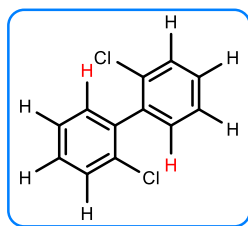
Using the general procedure III, the title compound **2h-o** was isolated as a white solid. Time reaction: 2 h. Yield: 14%. R_f = 0.77 (cyclohexane/EtOAc 7:3). IR (neat, cm⁻¹): 3055, 2955, 2922, 2852, 1919, 1799, 1733, 1698, 1631, 1616, 1583, 1560, 1453, 1421, 1264, 1255, 1159, 1120, 1074, 1044, 1024, 1001. ¹H NMR (500 MHz, CDCl₃): δ = 7.69-7.67 (m, **2H**), 7.40-7.37 (m, **2H**), 7.28-7.24 (m, **2H2H**) ppm. ¹³C NMR (126 MHz, CDCl₃): δ = 142.2 (Cq), 132.7, 131.1, 129.5, 127.3, 123.6 (Cq) ppm. MS (ESI, m/z): 312 [M]⁺ (100), 310 (46), 311 (7), 313 (14), 314 (50), 315 (7).

3,3',5,5'-Tetrabromo-1,1'-biphenyl (2h-m,m) (CAS: 16400-50-3)²⁹⁷



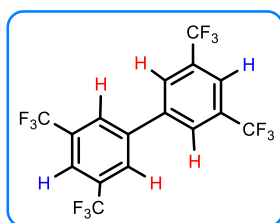
Using the general procedure III, the title compound **2h-m,m** was isolated as a white solid. Time reaction: 3 h. Yield: 88%. R_f = 0.8 (cyclohexane/EtOAc 7:3). IR (neat, cm⁻¹): 3100, 3064, 2921, 2851, 1775, 1727, 1576, 1539, 1404, 1385, 1362, 1096, 1066, 986. ¹H NMR (500 MHz, CDCl₃): δ = 7.701-7.693 (m, **2H**), 7.593-7.589 (m, **4H**) ppm. ¹³C NMR (126 MHz, CDCl₃): δ = 141.9 (Cq), 134.0, 129.1, 123.7 (Cq) ppm. MS (ESI, m/z): 470 [M]⁺ (100), 466 (20), 468 (72), 469 (12), 471 (20), 472 (72), 473 (12), 474 (20).

2,2'-Dichlorobiphenyl (2i-o) (CAS: 13029-08-8)²⁹⁷



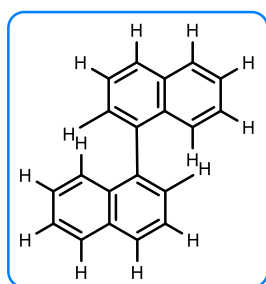
Using the general procedure III, the title compound **2i-o** was isolated as a white solid. Time reaction: 2 h. Yield: 64%. $R_f = 0.82$ (cyclohexane/EtOAc 7:3). IR (neat, cm^{-1}): 3057, 2957, 2923, 2854, 1963, 1927, 1808, 1728, 1626, 1566, 1487, 1461, 1422, 1261, 1241, 1159, 1127, 1084, 1055, 1026, 1004, 946. $^1\text{H NMR}$ (500 MHz, CDCl_3): $\delta = 7.51\text{--}7.47$ (m, **2H**), 7.37-7.32 (m, 4H), 7.30-7.27 (m, 2H) ppm. $^{13}\text{C NMR}$ (126 MHz, CDCl_3): $\delta = 138.5$ (Cq), 133.6, 131.3, 129.6, 129.4, 126.6 ppm. MS (ESI, m/z): 223 $[\text{M}]^+$ (100).

3,3',5,5'-Tetrakis(trifluoromethyl)-1,1'-biphenyl (2j) (CAS: 396-44-1)³⁰⁰



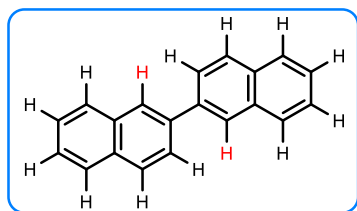
Using the general procedure III, the title compound **2j** was isolated as a white solid. Time reaction: 3 h. Yield: 70%. $R_f = 0.48$ (cyclohexane). IR (neat, cm^{-1}): 3097, 2927, 1616, 1457, 1348, 1275, 1175, 1119, 1104, 1072, 929. $^1\text{H NMR}$ (300 MHz, CDCl_3): $\delta = 7.69$ (bs, **4H**), 7.59 (bs, **2H**) ppm. $^{13}\text{C NMR}$ (126 MHz, CDCl_3): $\delta = 140.6$ (Cq), 133.0 (q, $J = 33.8$ Hz, Cq), 127.7 (q, $J = 2.9$ Hz), 125.3 (q, $J = 273.0$ Hz, Cq), 122.8 (sept, $J = 3.8$ Hz) ppm. $^{19}\text{F NMR}$ (500 MHz, CDCl_3): $\delta = -62.9$ ppm. MS (EI) m/z (rel intensity): 426 $[\text{M}]^+$ (100).

1,1'-Binaphthalene (2k) (CAS: 604-53-5)⁴⁸⁷



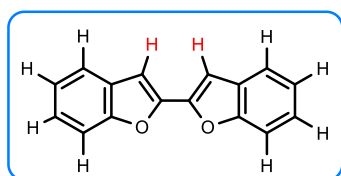
Using the general procedure III, the title compound **2k** was isolated as a white solid. Time reaction: 4 h. Yield: 54%. $R_f = 0.48$ (cyclohexane). IR (neat, cm^{-1}): 3040, 1586, 1504, 1378, 1327, 1256, 1211, 1199, 1178, 1162, 1130, 1013, 968. $^1\text{H NMR}$ (300 MHz, CDCl_3): $\delta = 7.97\text{--}7.95$ (m, 4H), 7.62-7.59 (m, 2H), 7.51-7.47 (m, 4H), 7.41-7.40 (m, 2H), 7.31-7.28 (m, 2H) ppm. $^{13}\text{C NMR}$ (126 MHz, CDCl_3): $\delta = 138.6$, 133.6, 133.0, 128.3, 128.0, 127.9, 126.7, 126.1, 125.9, 125.5 ppm. MS (ESI) m/z (rel intensity): 254 $[\text{M}]^+$ (100).

2,2'-Binaphthalene (2l) (CAS: 612-78-2)²⁹⁷



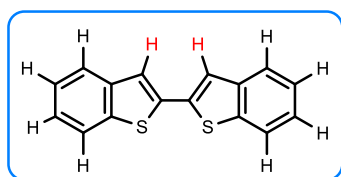
Using the general procedure III, the title compound **2l** was isolated as a white solid. Time reaction: 4 h. Yield: 41%. $R_f = 0.74$ (cyclohexane/EtOAc 7:3). **IR** (neat, cm^{-1}): 3053, 2921, 2852, 1593, 1461, 1376, 1259, 1129, 1093, 1021. **¹H NMR** (500 MHz, CDCl_3): $\delta = 8.18$ (s, **2H**), 7.98-7.88 (m, 8H), 7.49-7.55 (m, 4H) ppm. **¹³C NMR** (126 MHz, CDCl_3): $\delta = 138.5, 133.9, 132.8, 128.7, 128.4, 127.8, 126.5, 126.3, 126.2, 125.9$ ppm. **MS** (ESI) m/z (rel intensity): 254 $[M]^+$ (100).

2,2'-Bibenzofuran (2m) (CAS: 41014-29-3)²⁹⁷



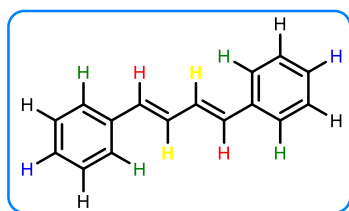
Using the general procedure III, the title compound **2m** was isolated as a white solid. Time reaction: 2 h. Yield: 31%. $R_f = 0.81$ (cyclohexane/EtOAc 7:3). **IR** (neat, cm^{-1}): 3158, 3122, 3065, 3056, 3034, 3016, 1940, 1899, 1863, 1820, 1780, 1625, 1611, 1515, 1467, 1438, 1342, 1299, 1253, 1216, 1170, 1152, 1140, 1102, 1046, 1008. **¹H NMR** (500 MHz, CDCl_3): $\delta = 7.65$ -7.63 (m, 2H), 7.56-7.54 (m, 2H), 7.35-7.32 (m, 2H), 7.29-7.26 (m, 2H), 7.17-7.16 (m, **2H**) ppm. **¹³C NMR** (126 MHz, CDCl_3): $\delta = 155.2, 147.8, 128.7, 125.2, 123.5, 121.5, 111.4, 103.8$ ppm. **MS** (ESI, m/z): 234 $[M]^+$ (100).

2,2'-Dibenzothiophene (2n) (CAS: 65689-53-4)⁴⁸⁹



Using the general procedure III, the title compound **2n** was isolated as a white solid. Time reaction: 2 h. Yield: 13%. $R_f = 0.76$ (cyclohexane/EtOAc 7:3). **IR** (neat, cm^{-1}): 3051, 3027, 2958, 2918, 2850, 1418, 1249. **¹H NMR** (300 MHz, CDCl_3): $\delta = 7.82$ -7.77 (m, 4H), 7.52 (s, **2H**), 7.38-7.32 (m, 4H) ppm. **¹³C NMR** (126 MHz, CDCl_3): $\delta = 140.3, 139.6, 137.3, 125.1, 124.9, 123.9, 122.3, 121.5$ ppm. **MS** (ESI) m/z (rel intensity): 266 $[M]^+$ (100).

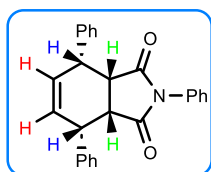
(1E, 3E)-1,4-Diphenylbuta-1,3-diene (2o) (CAS: 538-81-8)⁴⁸⁸



Using the general procedure III, the title compound **2o** was isolated as a white solid. Time reaction: 4 h. Yield: 34%. $R_f = 0.31$ (cyclohexane). **IR** (neat, cm^{-1}): 3078, 3054, 3015, 2924, 2854, 1952, 1870, 1731, 1592, 1571, 1488, 1443, 1292, 1176, 1073, 983, 912. **$^1\text{H NMR}$** (500 MHz, CDCl_3): $\delta = 7.47\text{--}7.44$ (m, **4H**), 7.36–7.31 (m, **4H**), 7.26–7.22 (m, **2H**), 7.00–6.94 (m, **2H**), 6.71–6.65 (m, **2H**) ppm. **$^{13}\text{C NMR}$** (126 MHz, CDCl_3): $\delta = 137.5$ (Cq), 133.0, 129.4, 128.8, 127.7, 126.5 ppm. **MS** (ESI) m/z (rel intensity): 206 $[\text{M}]^+$ (100).

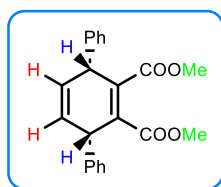
2,4,7-Triphenyl-3a,4,7,7a-tetrahydro-1H-isoindole-1,3(2H)-dione (5a)

(CAS: 20929-47-9)⁴⁹⁰



Using the general procedure V, the title compound **5a** was isolated as a white solid. Time reaction: 24 h of reaction. Yield: 36%. $R_f = 0.37$ (cyclohexane/EtOAc 7:3). **IR** (neat, cm^{-1}): 3062, 3029, 2946, 2835, 1780, 1705, 1596, 1495, 1453, 1374, 1165, 750, 702, 673, 618, 576, 495. **$^1\text{H NMR}$** (500 MHz, CDCl_3): $\delta = 7.45\text{--}7.24$ (m, 13H), 7.06–6.94 (m, 2H), 6.60–6.48 (m, **2H**), 3.93 (d, $J = 4.9$ Hz, **2H**), 3.66 (dd, $J = 4.9$ Hz, $J = 2.2$ Hz, **2H**) ppm. **$^{13}\text{C NMR}$** (126 MHz, CDCl_3): $\delta = 175.1, 139.3, 131.8, 131.6, 129.1, 129.0, 128.6, 128.5, 127.4, 126.5, 46.7, 41.9$ ppm. **MS** (ESI) m/z (rel intensity): 380 $[\text{M}+\text{H}]^+$ (100).

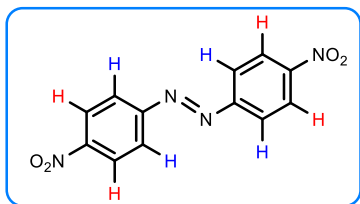
Dimethyl 3,6-diphenylcyclohexa-1,4-diene-1,2-dicarboxylate (5b) (CAS: 49538-77-4)⁴⁹¹



Using the general procedure V, the title compound **5b** was isolated as a colorless solid. Time reaction: 20 h. Yield: 31%. $R_f = 0.52$ (cyclohexane/EtOAc 7:3). **IR** (neat, cm^{-1}): 1740, 1650, 1610, 1500, 1450–1400, 1265, 1150, 1000, 855, 795, 760, 750, 740, 700. **$^1\text{H NMR}$** (300 MHz, CDCl_3): $\delta = 7.40\text{--}7.26$ (m, 10H), 5.80–5.77 (m, **2H**), 4.48–4.52 (m, **2H**), 3.56 (s, **6H**) ppm. **$^{13}\text{C NMR}$** (126 MHz, CDCl_3): $\delta = 167.9$ (Cq), 141.2, 135.6, 128.7, 128.3, 127.1, 126.0, 52.0, 44.0 ppm. **MS** (ESI) m/z (rel intensity): 348 $[\text{M}]^+$ (100).

(b) azo-compound

4,4'-Dinitroazobenzene (K.4b) (CAS: 3646-57-9)⁴⁹²

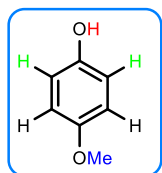


Using the general procedure VI, the expected compound **K.4b** was isolated as a light orange solid. Time reaction: 24 h. Yield: 71%. $R_f = 0.49$ (cyclohexane/EtOAc 9:1). $^1\text{H NMR}$ (500 MHz, acetone- d_6): $\delta = 8.29\text{-}8.26$ (m, **4H**), $7.74\text{-}7.71$ (m, **4H**) ppm. $^{13}\text{C NMR}$ (126 MHz, acetone- d_6): $\delta = 147.8$ (Cq), 141.6 (Cq), 130.7 , 126.1 ppm. **MS** (ESI) m/z (rel intensity): 272 [M] $^+$ (100).

Analytical data of compounds from Chapter III

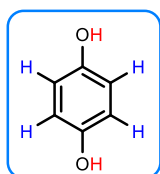
Phenol compounds

4-Methoxyphenol (6a) (CAS: 150-76-5)⁴⁰⁰



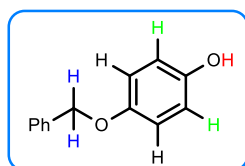
Using the general procedure VII, the expected **6a** was isolated as a white solid. Time reaction: 20 h. Yield: 80%. $R_f = 0.70$ (cyclohexane/EtOAc 8:2). **IR** (neat, cm^{-1}): 3345, 1510, 1350, 1025. **^1H NMR** (500 MHz, CDCl_3): $\delta = 6.80\text{-}6.76$ (m, **2H**), 4.39 (bs, **1H**), 3.76 (s, **3H**) ppm; **^{13}C NMR** (126 MHz, CDCl_3): $\delta = 153.9$ (Cq), 149.6, 116.4, 115.3, 55.9 (CH_3) ppm. **MS** (ESI) m/z (rel intensity): 125 [M-H]⁻ (100).

Hydroquinone (6b) (CAS: 123-31-9)⁴⁹³



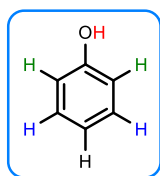
Using the general procedure VII, the expected **6b** was isolated as a white solid. Time reaction: 2 h. Yield: 40%. $R_f = 0.2$ (cyclohexane/EtOAc 7:3). **IR** (neat, cm^{-1}): 3130, 1510, 1365, 1095. **^1H NMR** (500 MHz, acetone- d_6): $\delta = 7.67$ (bs, **2H**), 6.65 (s, **4H**) ppm. **^{13}C NMR** (126 MHz, acetone- d_6): $\delta = 150.3$ (Cq), 115.7 ppm. **MS** (EI) m/z (rel intensity): 110 [M]⁺ (100).

4-(Benzyloxy)phenol (6c) (CAS: 103-16-2)⁴⁹⁴



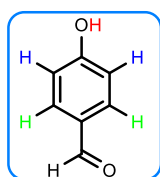
Using the general procedure VII, the expected **6c** was isolated as a white solid. Time reaction: 20 h. Yield: 37%. $R_f = 0.42$ (cyclohexane/EtOAc 7:3). **IR** (neat, cm^{-1}): 3422, 1500, 1219, 1015, 819. **^1H NMR** (500 MHz, CDCl_3): $\delta = 7.43\text{-}7.30$ (m, 5H), 6.88-6.85 (m, 2H), 6.78-6.74 (m, 2H), 5.00 (s, **2H**), 4.41 (s, **1H**) ppm. **^{13}C NMR** (126 MHz, CDCl_3): $\delta = 153.2$ (Cq), 149.8 (Cq), 137.4, 128.7, 128.0, 127.6, 116.2, 116.1, 70.9 ppm. **MS** (EI) m/z (rel intensity): 200 [M]⁺ (100).

Phenol (6d) (CAS: 108-95-2)⁴⁰⁰



Using the general procedure VII, the expected **6d** was determined by ¹H NMR using 1,3,5-trimethoxybenzene as internal standard. Time reaction: 20 h. Yield: 38%. **R_f** = 0.56 (cyclohexane: EtOAc 7:3). ¹H NMR (300 MHz, CDCl₃): δ = 7.28-7.21 (m, **2H**), 6.96-6.91 (m, **1H**), 6.85-6.80 (m, **2H**), 5.08 (bs, **1H**) ppm.

4-Hydroxybenzaldehyde (6e) (CAS: 123-08-0)⁴⁹⁵



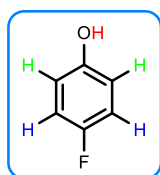
Using the general procedure VII, the expected **6e** was isolated as a white solid. Time reaction: 20 h. Yield: 60%. **R_f** = 0.30 (cyclohexane/EtOAc 7:3). **IR** (neat, cm⁻¹): 3250, 1570, 1165, 815. ¹H NMR (500 MHz, CDCl₃): δ = 9.88 (s, **1H**), 7.83-7.81 (m, **2H**), 6.98-6.95 (m, **2H**), 5.67 (bs, **1H**) ppm. ¹³C NMR (126 MHz, CDCl₃): δ = 191.1 (Cq), 161.3 (Cq), 132.6, 130.1, 116.1 ppm. **MS** (ESI) m/z (rel intensity): 121 [M-H]⁻ (100).

4-Nitrophenol (6f) (CAS: 100-02-7)⁴⁰⁰



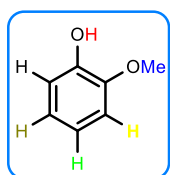
Using the general procedure VII, the expected **6f** was isolated as a yellow solid. Time reaction: 20 h. Yield: 76%. **R_f** = 0.33 (cyclohexane/EtOAc 7:3). **IR** (neat, cm⁻¹): 3350, 1590, 1485, 1330, 1290. ¹H NMR (500 MHz, CDCl₃): δ = 8.19-8.16 (m, **2H**), 6.93-6.91 (m, **2H**) ppm. ¹³C NMR (126 MHz, CDCl₃): δ = 161.2 (Cq), 136.8 (Cq), 126.3, 115.9 ppm. **MS** (EI) m/z (rel intensity): 139 [M]⁺ (100), 109 (35), 65 (30).

4-Fluorophenol (6g) (CAS: 371-41-5)⁴⁰⁰



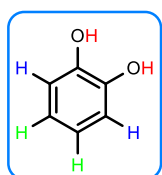
Using the general procedure VII, the expected **6g** was isolated as a lightly tan solid. Time reaction: 20 h. Yield: 44%. **R_f** = 0.48 (cyclohexane/EtOAc 7:3). **IR** (neat, cm⁻¹): 3328, 2921, 2852, 1712, 1491, 1201, 1094, 1009, 826. ¹H NMR (500 MHz, CDCl₃): δ = 6.93 (dd, ³J(H-H) = ³J(H-F) = 8.6 Hz, **2H**), 6.77 (dd, ³J(H-H) = 8.5 Hz, ⁴J(H-F) = 4.3 Hz, **2H**), 5.04 (bs, **1H**) ppm. ¹³C NMR (126 MHz, CDCl₃): δ = 156.2 (Cq), 150.5 (Cq), 115.2, 115.0 ppm. **MS** (EI) m/z (rel intensity): 111 [M-H]⁻ (100).

2-Methoxyphenol (6h) (CAS: 90-05-1)⁴⁰⁰



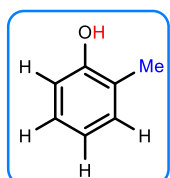
Using the general procedure VII, the expected **6h** was estimated by ¹H NMR using dimethyl terephthalate as internal standard. Time reaction: 20 h. Yield: 22%. **R_f** = 0.66 (cyclohexane/EtOAc 7:3). ¹H NMR (300 MHz, CDCl₃): δ = 6.95-6.84 (m, 4H), 5.60 (bs, **1H**), 3.89 (s, **3H**).

2-Hydroxyphenol (6i) (CAS: 120-80-9)⁴⁹⁶



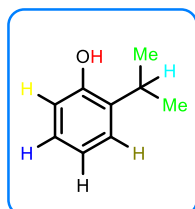
Using the general procedure VII, the expected **6i** was isolated as a yellow solid. Time reaction: 4 h. Yield: 20%. **R_f** = 0.26 (cyclohexane/EtOAc 7:3). **IR** (neat, cm⁻¹): 3443, 3320, 3052, 1923, 1882, 1762, 1692, 1618, 1596, 1512, 1467, 1360, 1278, 1254, 1237, 1184, 1163, 1093, 1039, 936, 916, 848, 768, 739, 624, 553. ¹H NMR (500 MHz, acetone-d₆): δ = 7.76 (s, **2H**), 6.83-6.79 (m, **2H**), 6.69-6.66 (m, **2H**) ppm. ¹³C NMR (126 MHz, acetone-d₆): δ = 146.0 (Cq), 120.7, 116.2 ppm. **MS** (ESI) m/z (rel intensity): 109 [M-H]⁻ (100).

2-Cresol (6j) (CAS: 95-48-7)⁴⁰⁰



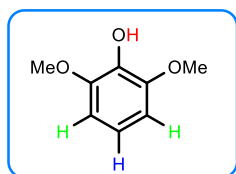
Using the general procedure VII, the expected **6j** was determined by ¹H NMR using dimethyl terephthalate as internal standard. Time reaction: 20 h. Yield: 5%. ¹H NMR (300 MHz, CDCl₃): δ = 7.18-7.10 (m, 2H), 6.91-6.87 (m, 1H), 6.82-6.80 (m, 1H), 5.17 (s, **1H**), 2.30 (s, **3H**) ppm.

2-Isopropylphenol (6k) (CAS: 88-69-7)⁴⁹⁷



Using the general procedure VII, the expected **6k** was isolated as a light-yellow solid. Time reaction: 20 h. Yield: 62%. **R_f** = 0.56 (cyclohexane/EtOAc 8:2). **IR** (neat, cm⁻¹): 3520, 3380, 2960, 1450, 825. ¹H NMR (500 MHz, CDCl₃): δ = 7.21 (dd, ³J = 7.5 Hz, ⁴J = 1.7 Hz, **1H**), 7.10-7.04 (m, **1H**), 6.94-6.89 (m, **1H**), 6.75 (dd, ³J = 7.9 Hz, ⁴J = 1.3 Hz, **1H**), 4.81 (s, **1H**), 3.32 (sept, ³J = 6.9 Hz, **1H**), 1.27 (d, ³J = 6.9 Hz, **6H**) ppm. ¹³C NMR (126 MHz, CDCl₃): δ = 152.8 (Cq), 134.5, 126.8, 126.5, 121.1, 115.4, 27.1, 22.7 ppm. **MS** (ESI) m/z (rel intensity): 135 [M-H]⁻ (100).

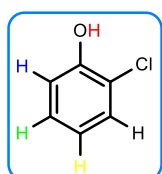
2,6-Dimethoxyphenol (6l) (CAS: 91-10-1)⁴⁹⁵



The expected **6l** was obtained using the general procedure VII. Yield: 3%.

$R_f = 0.46$ (cyclohexane/EtOAc 7:3). $^1\text{H NMR}$ (500 MHz, CDCl_3): $\delta = 6.81$ (t, $J = 8.4$ Hz, **1H**), 6.59 (d, $J = 8.3$ Hz, **2H**), 5.52 (s, **1H**), 3.89 (s, **6H**).

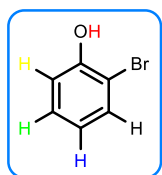
2-Chlorophenol (6o) (CAS: 95-57-8)⁴⁹⁵



Using the general procedure VII, the expected **6o** was estimated by $^1\text{H NMR}$ using dimethyl terephthalate as internal standard. Time reaction: 20 h. Yield: 7%.

$^1\text{H NMR}$ (300 MHz, CDCl_3): $\delta = 7.34$ (dd, $^3J = 8.0$ Hz, $^4J = 1.6$ Hz, 1H), 7.17 (ddd, $^3J = 8.2$ Hz, $^3J = 7.4$ Hz, $^4J = 1.6$ Hz, 1H), 7.01 (dd, $^3J = 8.2$ Hz, $^4J = 1.6$ Hz, 1H), 6.86 (ddd, $^3J = 8.0$ Hz, $^3J = 7.4$ Hz, $^4J = 1.6$ Hz, 1H), 5.64 (s, **1H**).

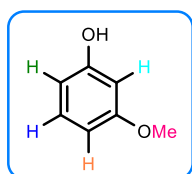
2-Bromophenol (6p) (CAS: 95-56-7)⁴⁹⁵



Using the general procedure VII, the expected **6p** was estimated by $^1\text{H NMR}$ using dimethyl terephthalate as internal standard. Time reaction: 20 h. Yield: 5%.

$^1\text{H NMR}$ (300 MHz, CDCl_3): $\delta = 7.46$ (dd, $^3J = 8.0$ Hz, $^4J = 1.6$ Hz, 1H), 7.22 (ddd, $^3J = 8.7$ Hz, $^3J = 7.3$ Hz, $^4J = 1.6$ Hz, 1H), 7.02 (dd, $^3J = 8.2$ Hz, $^4J = 1.6$ Hz, 1H), 6.80 (ddd, $^3J = 8.0$ Hz, $^3J = 7.3$ Hz, $^4J = 1.6$ Hz, 1H), 5.57 (s, **1H**).

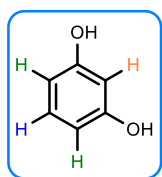
3-Methoxyphenol (6q) (CAS: 150-19-6)⁴⁰⁰



Using the general procedure VII, the expected **6q** was isolated as a yellow solid. Time reaction: 38 h. Yield: 66%. $R_f = 0.46$ (cyclohexane/EtOAc 7:3).

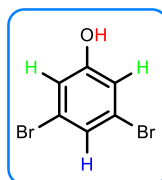
IR (neat, cm^{-1}): 3380, 1590, 1140. $^1\text{H NMR}$ (500 MHz, CDCl_3): $\delta = 7.15$ -7.12 (m, **1H**), 6.52-6.50 (m, **1H**), 6.45-6.42 (m, **1H1H**), 3.78 (s, **3H**) ppm. $^{13}\text{C NMR}$ (126 MHz, CDCl_3): $\delta = 161.1$ (Cq), 156.8 (Cq), 130.3, 107.9, 106.6, 101.6, 55.4 (CH_3) ppm. MS (ESI) m/z (rel intensity): 125 [$\text{M}+\text{H}$] $^+$ (100), 193 (55), 309 (37).

3-Hydroxyphenol (6r) (CAS: 108-46-3)⁴⁰⁰



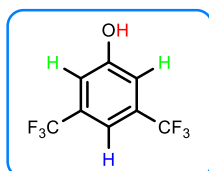
Using the general procedure VII, the expected **6r** was isolated as a white solid. Time reaction: 20 h. Yield: 49%. $R_f = 0.30$ (cyclohexane/EtOAc 7:3). **IR** (neat, cm^{-1}): 3182, 1609, 1475, 1272, 1217, 1143, 1074, 956, 763, 679, 538. **^1H NMR** (500 MHz, CDCl_3): $\delta = 7.08$ (t, $^3J = 8.1$ Hz, **1H**), 6.41 (dd, $^3J = 8.1$ Hz, $^4J = 2.4$ Hz, **2H**), 6.35 (t, $^4J = 2.4$ Hz, **1H**) ppm. **^{13}C NMR** (126 MHz, CDCl_3): $\delta = 158.9$ (Cq), 130.2, 106.7, 102.9 ppm. **MS** (EI) m/z (rel intensity): 110 $[\text{M}]^+$ (100), 86 (25), 84 (35), 82 (25).

3,5-Dibromophenol (6s) (CAS: 626-41-5)⁴⁹⁸



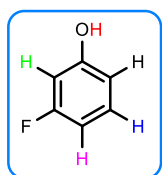
Using the general procedure VII, the expected **6s** was isolated as an orange solid. Time reaction: 20 h. Yield: 78%. $R_f = 0.56$ (cyclohexane/EtOAc 7:3). **IR** (neat, cm^{-1}): 3128, 2955, 2921, 2852, 1695, 1569, 1466, 1418, 1364, 1350, 1284, 1230, 1211, 1101, 1082, 890, 838, 748, 664. **^1H NMR** (500 MHz, CDCl_3): $\delta = 7.25$ -7.24 (m, **1H**), 6.96-6.95 (d, $^4J = 1.7$ Hz, **2H**), 5.19 (bs, **1H**) ppm. **^{13}C NMR** (126 MHz, CDCl_3): $\delta = 156.8$ (Cq), 126.9, 123.3, 118.0 ppm. **MS** (ESI) m/z (rel intensity): 251 $[\text{M}-\text{H}]^-$ (100), 249 (52), 250 (4), 252 (7), 253 (48), 254 (4).

3,5-bis(Trifluoromethyl)phenol (6t) (CAS: 349-58-6)⁴⁹⁹



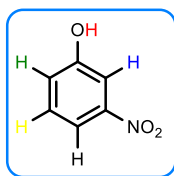
Using the general procedure VII, the expected **6t** was isolated as a liquid. Time reaction: 20 h. Yield: 52%. $R_f = 0.51$ (cyclohexane/EtOAc 7:3). **^1H NMR** (500 MHz, CDCl_3): $\delta = 7.43$ (s, **1H**), 7.28 (s, **2H**), 6.70 (bs, **1H**) ppm. **^{13}C NMR** (126 MHz, CDCl_3): $\delta = 156.9$ (Cq), 133.1 (q, $J = 33.4$ Hz, Cq), 123.2 (q, $J = 272.5$ Hz, Cq), 116.0 (m), 114.3 ppm. **MS** (EI) m/z (rel intensity): 230 $[\text{M}]^+$ (100).

3-Fluorophenol (6u) (CAS: 372-20-3)⁴⁰⁰



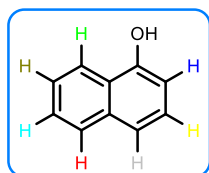
Using the general procedure VII, the expected **6u** was estimated by **^1H NMR** using dimethyl terephthalate as internal standard. Time reaction: 20 h. Yield: 67%. $R_f = 0.55$ (cyclohexane/EtOAc 7:3). **^1H NMR** (300 MHz, CDCl_3): $\delta = 7.22$ -7.14 (m, 1H), 6.67-6.56 (m, 3H), 4.90 (s, **1H**).

3-Nitrophenol (6v) (CAS: 554-84-7)⁴⁰⁰



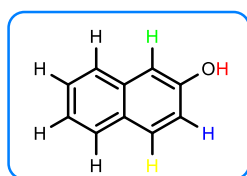
Using the general procedure VII, the expected **6v** was isolated as a yellow solid. Time reaction: 20 h. Yield: 85%. $R_f = 0.43$ (cyclohexane/EtOAc 7:3). **IR** (neat, cm^{-1}): 3384, 3110, 3090, 2921, 2852, 1966, 1749, 1623, 1516, 1467, 1348, 1298, 1212, 1077, 999, 934, 873, 816, 793, 736, 670, 589. **¹H NMR** (500 MHz, CDCl_3): $\delta = 7.83\text{-}7.81$ (m, **1H**), $7.72\text{-}7.70$ (m, **1H**), $7.43\text{-}7.40$ (m, **1H**), $7.18\text{-}7.16$ (m, **1H**), 5.23 (s, **1H**) ppm. **¹³C NMR** (126 MHz, CDCl_3): $\delta = 156.3$ (Cq), 149.3 (Cq), 130.5, 122.0, 116.1, 110.7 ppm. **MS** (ESI) m/z (rel intensity): 138 $[\text{M-H}]^-$ (100).

Naphthalen-1-ol (6w) (CAS: 90-15-3)⁴⁰⁰



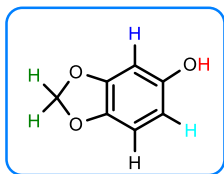
Using the general procedure VII, the expected **6w** was isolated as a lightly brown solid. Time reaction: 7 h. Yield: 59%. $R_f = 0.48$ (cyclohexane/EtOAc 7:3). **IR** (neat, cm^{-1}): 3249, 2924, 1708, 1577, 1455, 1384, 1264, 1080, 1013, 788, 763, 708, 565, 416. **¹H NMR** (500 MHz, CDCl_3): $\delta = 8.19\text{-}8.17$ (m, **1H**), $7.83\text{-}7.81$ (m, **1H**), $7.51\text{-}7.48$ (m, 2H), 7.45 (d, $^3J = 8.3$ Hz, 1H), 7.31 (t, $^3J = 7.8$ Hz, 1H), 6.82 (d, $^3J = 7.4$ Hz, **1H**), 5.22 (bs, **1H**) ppm. **¹³C NMR** (126 MHz, CDCl_3): $\delta = 151.3$, 134.8, 127.7, 126.5, 125.8, 125.3, 124.3, 121.5, 120.7, 108.6 ppm. **MS** (EI) m/z (rel intensity): 144 $[\text{M}]^+$ (100), 116 (75), 115 (50).

Naphthalen-2-ol (6x) (CAS: 135-19-3)⁴⁰⁰



Using the general procedure VII, the expected **6x** was isolated as a white solid. Time reaction: 20 h. Yield: 30%. $R_f = 0.53$ (cyclohexane/EtOAc 7:3). **IR** (neat, cm^{-1}): 3281, 1629, 1600, 1509, 1464, 1214, 1171, 958, 904, 842, 812, 740, 479. **¹H NMR** (300 MHz, CDCl_3): $\delta = 7.78\text{-}7.76$ (m, 2H), 7.69 (d, $^3J = 8.2$ Hz, **1H**), $7.45\text{-}7.42$ (m, 1H), $7.35\text{-}7.32$ (m, 1H), 7.15 (d, $^4J = 2.5$ Hz, **1H**), 7.11 (dd, $^3J = 8.8$ Hz, $^4J = 2.6$ Hz, **1H**), 4.96 (bs, **1H**) ppm. **¹³C NMR** (126 MHz, CDCl_3): $\delta = 153.3$ (Cq), 134.6, 129.9, 128.9, 127.8, 126.6, 126.4, 123.6, 117.7, 109.5 ppm. **MS** (EI) m/z (rel intensity): 144 $[\text{M}]^+$ (100), 115 (50).

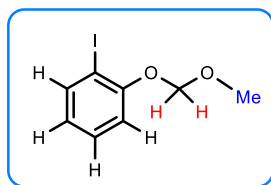
Sesamol (6v) (CAS: 533-31-3)⁴⁹³



Using the general procedure VII, the expected **6y** was isolated as a white solid. Time reaction: 20 h. Yield: 62%. $R_f = 0.33$ (cyclohexane/EtOAc 8:2). **IR** (neat, cm^{-1}): 3340, 1570, 1250, 900, 745. **^1H NMR** (500 MHz, CDCl_3): $\delta = 6.65$ (d, $^3J = 8.3$ Hz, **1H**), 6.43 (d, $^4J = 2.5$ Hz, **1H**), 6.25 (dd, $^3J = 8.3$ Hz, $^4J = 2.5$ Hz, **1H**), 5.90 (s, **2H**), 4.71 (bs, **1H**) ppm. **^{13}C NMR** (126 MHz, CDCl_3): $\delta = 150.7$ (Cq), 148.4 (Cq), 141.7 (Cq), 108.3, 106.8, 101.3, 98.4 ppm. **MS** (ESI) m/z (rel intensity): 137 $[\text{M}-\text{H}]^-$ (15), 227 (100), 283 (55).

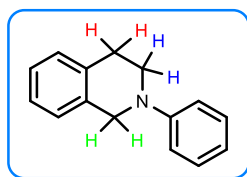
Analytical data of compounds from Chapter IV

1-Iodo-2-(methoxymethoxy)benzene (S.9b) (CAS: 80778-47-8)⁵⁰⁰



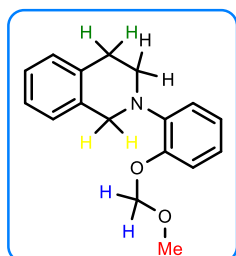
Using the general procedure X, the expected **S.9b** was isolated as a colorless liquid. Yield: 90%. $R_f = 0.52$ (cyclohexane/EtOAc 9.5:0.5). **IR** (neat, cm^{-1}): 3061, 2993, 2955, 2929, 2901, 2845, 2825, 2786, 1583, 1469, 1437, 1402, 1307, 1271, 1233, 1199, 1151, 1118, 1081, 1044, 1017, 978, 919, 788, 747, 709, 643, 528, 433. **$^1\text{H NMR}$** (500 MHz, CDCl_3): $\delta = 7.79\text{--}7.77$ (m, 1H), 7.30–7.27 (m, 1H), 7.08–7.06 (m, 1H), 6.78–6.74 (m, 1H), 5.24 (s, **2H**), 3.52 (s, **3H**) ppm. **$^{13}\text{C NMR}$** (126 MHz, CDCl_3): $\delta = 156.2$ (Cq), 139.7, 129.6, 123.8, 115.1, 95.1 (CH_2), 87.4 (Cq), 56.6 (CH_3) ppm. MS (ESI) m/z (rel intensity): 263 $[\text{M-H}]^-$ (100).

1,2,3,4-Tetrahydro-2-phenylisoquinoline (S.10a) (CAS: 3340-78-1)⁴⁶¹



Using the general procedure IX, the expected **S.10a** was isolated as a white solid. Yield: 47%. $R_f = 0.53$ (cyclohexane/EtOAc 9:1). **IR** (neat, cm^{-1}): 3060, 3024, 2922, 2815, 1599, 1503, 1462, 1388, 1225, 1034, 930, 752, 691. **$^1\text{H NMR}$** (500 MHz, CDCl_3): $\delta = 7.32\text{--}7.28$ (m, 2H), 7.21–7.16 (m, 4H), 7.02–6.99 (m, 2H), 6.85 (tt, $^3J = 7.3$ Hz, $^4J = 1.1$ Hz, 1H), 4.43 (s, **2H**), 3.58 (t, $J = 5.8$ Hz, **2H**), 3.01 (t, $J = 5.9$ Hz, **2H**) ppm. **$^{13}\text{C NMR}$** (126 MHz, CDCl_3): $\delta = 150.7$ (Cq), 135.0 (Cq), 134.6 (Cq), 129.3, 128.7, 126.7, 126.5, 126.2, 118.8, 115.3, 50.9, 46.7, 29.3 ppm. MS (ESI) m/z (rel intensity): 210 $[\text{M+H}]^+$ (100).

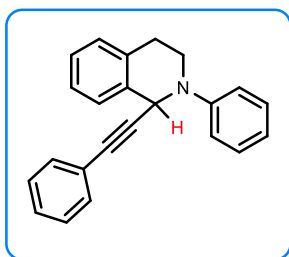
2-(2-(Methoxymethoxy)phenyl)-1,2,3,4-tetrahydroisoquinoline (S.10b)



Using the general procedure XI, the expected **S.10b** was isolated as a yellow liquid. Yield: 80%. $R_f = 0.35$ (cyclohexane/EtOAc 9:1). **IR** (neat, cm^{-1}): 3062, 3022, 2992, 2950, 2920, 2899, 2821, 2750, 2682, 1595, 1495, 1451, 1384, 1287, 1269, 1229, 1191, 1147, 1106, 1075, 1051, 992, 921, 741, 642, 431. **$^1\text{H NMR}$** (500 MHz, CDCl_3): $\delta = 7.17\text{--}7.09$ (m, 5H), 7.04–6.97 (m, 3H), 5.24 (s, **2H**), 4.30 (s, **2H**), 3.52 (s, **3H**), 3.44 (t, $J = 5.8$ Hz, **2H**), 2.99 (t, $J = 5.8$ Hz, **2H**) ppm. **$^{13}\text{C NMR}$** (126 MHz, CDCl_3): $\delta = 150.3$ (Cq), 142.4 (Cq), 135.3 (Cq), 134.7 (Cq), 129.0, 126.5, 126.3, 125.9, 123.0, 122.8, 119.37, 116.7, 95.4, 56.4, 53.2, 49.3, 29.2 ppm. MS (ESI) m/z (rel intensity): 270 $[\text{M+H}]^+$ (100).

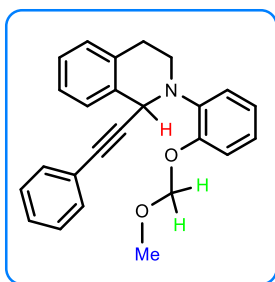
rac-2-Phenyl-1-phenylethynyl-1,2,3,4-tetrahydroisoquinoline (S.11a)

(CAS: 823814-00-2)⁴⁶¹



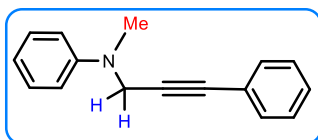
The expected **S.11a** was obtained using the general procedure XII. Yield: 98%. $R_f = 0.53$ (cyclohexane/EtOAc 9:1). $^1\text{H NMR}$ (500 MHz, CDCl_3): $\delta = 7.41\text{--}7.37$ (m, 1H), 7.35–7.28 (m, 5H), 7.25–7.20 (m, 6H), 7.15–7.12 (m, 2H), 6.90 (tt, $^3J = 7.3$ Hz, $^4J = 1.1$ Hz, 1H), 5.62 (s, **1H**), 3.79–3.75 (m, 1H), 3.71–3.66 (m, 1H), 3.19–3.12 (m, 1H), 3.00–2.97 (m, 1H) ppm. $^{13}\text{C NMR}$ (126 MHz, CDCl_3): 149.7, 135.6, 134.5, 132.0, 129.3, 129.1, 128.2, 128.1, 127.6, 127.4, 126.4, 123.1, 119.8, 116.8, 88.7, 84.9, 52.4, 43.6, 29.1.

2-(2-(Methoxymethoxy)phenyl)-1-(phenylethynyl)-1,2,3,4-tetrahydroisoquinoline (S.11b)



Using the general procedure XII, the expected **S.11b** was isolated as a yellow liquid. Yield: 86%. $R_f = 0.46$ (cyclohexane/EtOAc 9:1). **IR** (neat, cm^{-1}): 3060, 3022, 2953, 2921, 2825, 1595, 1490, 1452, 1442, 1373, 1272, 1253, 1230, 1192, 1153, 1135, 1102, 1075, 989, 967, 920, 746, 728, 690, 610, 546, 526, 449. $^1\text{H NMR}$ (500 MHz, CDCl_3): $\delta = 7.27\text{--}7.24$ (m, 1H), 7.18–7.10 (m, 9H), 7.06–7.04 (m, 1H), 6.99–6.94 (m, 2H), 5.67 (s, **1H**), 5.17 (d, $J = 6.6$ Hz, **1H**), 5.11 (d, $J = 6.5$ Hz, **1H**), 3.65–3.59 (m, 1H), 3.45–3.35 (m, 1H), 3.43 (s, **3H**), 3.17–3.10 (m, 1H), 2.85–2.81 (m, 1H) ppm. $^{13}\text{C NMR}$ (126 MHz, CDCl_3): $\delta = 150.5$ (Cq), 141.1 (Cq), 135.9 (Cq), 134.0 (Cq), 131.8, 129.3, 128.2, 128.0, 127.7, 127.1, 126.1, 123.7, 123.3, 122.7, 121.8, 116.8, 95.5, 88.9 (Cq), 85.7 (Cq), 56.4, 53.2, 44.2, 29.4 ppm. **MS** (ESI) m/z (rel intensity): 370 $[\text{M}+\text{H}]^+$ (100).

N-Methyl-*N*-(3-phenylprop-2-yn-1-yl)aniline (S.12) (CAS: 168074-12-2)⁵⁰¹



Using the general procedure XII, the expected **S.12** was isolated as a yellow liquid. Yield: 79%. $R_f = 0.40$ (cyclohexane/EtOAc 9.5:0.5). **IR** (neat, cm^{-1}): 3068, 3026, 2883, 2808, 1598, 1577, 1503, 1489, 1453, 1442, 1359, 1335, 1240, 1196, 1112, 1030, 995, 922, 750, 715, 688. $^1\text{H NMR}$ (500 MHz, CDCl_3): $\delta = 7.37\text{--}7.35$ (m, 2H), 7.30–7.24 (m, 5H), 6.92–6.90 (m, 2H), 6.82–6.79 (m, 1H), 4.26 (s, **2H**), 3.03 (s, **3H**) ppm. $^{13}\text{C NMR}$ (126 MHz, CDCl_3): $\delta = 149.5$ (Cq), 131.9 (Cq), 129.2, 128.3, 128.2, 123.2, 118.3, 114.5, 85.1 (Cq), 84.3 (Cq), 43.5 (CH_2), 38.8 (CH_3) ppm. **MS** (ESI) m/z (rel intensity): 222 $[\text{M}+\text{H}]^+$ (100).

References

1. Ullmann, F.; Bielecki, J. *Ber. Dtsch. Chem. Ges.* **1901**, 34(2), 2174-2185.
2. Miyaura, N.; Yanagi, T.; Suzuki, A. *Synth. Commun.* **1981**, 11(7), 513-519.
3. Glaser, C. *Ber. Dtsch. Chem. Ges.* **1869**, 2(1), 422-424.
4. Li, C. J. *Accounts Chem. Res.* **2009**, 42(2), 335-344.
5. Hartwig, J. F. *Nature* **2008**, 455(7211), 314-322.
6. Namsheer, K.; Rout, C. S. *RSC Adv.* **2021**, 11(10), 5659-5697.
7. Ullmann, F. *Ber. Dtsch. Chem. Ges.* **1903**, 36(2), 2382-2384.
8. Ullmann, F.; Sponagel, P. *Ber. Dtsch. Chem. Ges.* **1905**, 38(2), 2211-2212.
9. Evans, D. A.; Katz, J. L.; West, T. R. *Tetrahedron Lett.* **1998**, 39(19), 2937-2940.
10. Chan, D. M.; Monaco, K. L.; Wang, R. P.; Winters, M. P. *Tetrahedron Lett.* **1998**, 39(19), 2933-2936.
11. Lam, P. Y.; Clark, C. G.; Saubern, S.; Adams, J.; Winters, M. P.; Chan, D. M.; Combs, A. *Tetrahedron Lett.* **1998**, 39(19), 2941-2944.
12. Huisgen, R.; Szeimies, G.; Möbius, L. *Chem. Ber.* **1967**, 100(8), 2494-2507.
13. Anastas, P. T.; Warner, J. C. *Green Chemistry: Theory and Practice*. Oxford University Press, **2000**.
14. Dingerdissen, U.; Martin, A.; Herein, D.; Wernicke, H. J. *Handbook of Heterogeneous Catalysis: Online*. 2nd ed.; Wiley Online Library, **2008**.
15. Yu, J. H. In *Introduction to Zeolite Science Practice* (Eds.: Cejka, J.; Van Bekkum, H.; Corma, A.; Schueth, F.), Elsevier: Amsterdam, Netherlands, **2007**, Vol. 168, pp. 39-104.
16. Cruz Navarro, J. A.; Sánchez Mora, A.; Serrano García, J. S.; Amaya Flórez, A.; Colorado Peralta, R.; Reyes Márquez, V.; Morales Morales, D. *Catalysts* **2024**, 14(1), 69.
17. Tornøe, C. W.; Christensen, C.; Meldal, M. *J. Org. Chem.* **2002**, 67(9), 3057-3064.
18. Rostovtsev, V. V.; Green, L. G.; Fokin, V. V.; Sharpless, K. B. *Angew. Chem. Int. Ed.* **2002**, 41(14), 2708-2711.
19. Chassaing, S.; Kumarraja, M.; Sani Souna Sido, A.; Pale, P.; Sommer, J. *Org. Lett.* **2007**, 9(5), 883-886.
20. Chassaing, S.; Sani Souna Sido, A.; Alix, A.; Kumarraja, M.; Pale, P.; Sommer, J. *Chem. Eur. J.* **2008**, 14(22), 6713-6721.
21. Bringmann, G.; Günther, C.; Ochse, M.; Schupp, O.; Tasler, S.; Bringmann, G.; Günther, C.; Ochse, M.; Schupp, O.; Tasler, S. In *Fortschritte der Chemie organischer*

- Naturstoffe/Progress in the Chemistry of Organic Natural Products* (Ed.: Hunek, S.), Springer Science & Business Media: Berlin, Germany, **2001**, pp. 1-249.
22. Acharya, Y.; Dhanda, G.; Sarkar, P.; Haldar, J. *ChemComm.* **2022**, 58(12), 1881-1897.
 23. Manstein, D.; Preller, M.; Furch, M.; Kalesse, M.; Diaz Gomez, N. Biphenyl compounds for use in treating malaria and other parasitic disorders. EP 2753599 A1, September 8, **2016**.
 24. McGlacken, G. P.; Bateman, L. M. *Chem. Soc. Rev.* **2009**, 38(8), 2447-2464.
 25. Rappoport, Z. *The Chemistry of Phenols*. John Wiley & Sons, **2004**.
 26. Wang, H.; Zhao, Y. J.; Xu, H. R.; Wang, P.; Chen, S. M. *Arab. J. Chem.* **2023**, 16(11), 105204.
 27. Kamei, J. *Pulm. Pharmacol.* **1996**, 9(5-6), 349-356.
 28. Stanforth, S. P. *Tetrahedron* **1998**, 54(3-4), 263-303.
 29. Hassan, J.; Sévignon, M.; Gozzi, C.; Schulz, E.; Lemaire, M. *Chem. Rev.* **2002**, 102(5), 1359-1470.
 30. Negishi, E. I.; De Meijere, A. *Handbook of Organopalladium Chemistry for Organic Synthesis*. John Wiley & Sons, **2003**.
 31. Millini, R.; Bellussi, G. *Zeolite Science and Perspectives*. Royal Society of Chemistry: London, **2017**.
 32. Weitkamp, J.; Puppe, L. *Catalysis and Zeolites: Fundamentals and Applications*. Springer Science & Business Media, **2013**.
 33. Sartori, G.; Maggi, R. *Chem. Rev.* **2006**, 106(3), 1077-1104.
 34. Sheldon, R. A.; Van Bekkum, H. *Fine Chemicals through Heterogeneous Catalysis*. John Wiley & Sons, **2008**.
 35. Mallat, T.; Baiker, A. *Catal. Today* **2000**, 57(1-2), 1-2.
 36. Chassaing, S.; Beneteau, V.; Louis, B.; Pale, P. *Curr. Org. Chem.* **2017**, 21(9), 779-793.
 37. Chassaing, S.; Beneteau, V.; Pale, P. *Curr. Opin. Green Sustain. Chem.* **2018**, 10, 35-39.
 38. Kuhn, P.; Alix, A.; Kumarraja, M.; Louis, B.; Pale, P.; Sommer, J. *Eur. J. Org. Chem.* **2009**, (3), 423-429.
 39. Magné, V.; Garnier, T.; Danel, M.; Pale, P.; Chassaing, S. *Org. Lett.* **2015**, 17(18), 4494-4497.
 40. Garnier, T.; Danel, M.; Magné, V.; Pujol, A.; Beneteau, V.; Pale, P.; Chassaing, S. *J. Org. Chem.* **2018**, 83(12), 6408-6422.
 41. Clerc, A.; Bénéteau, V.; Pale, P.; Chassaing, S. *ChemCatChem* **2020**, 12(7), 2060-2065.
 42. Garnier, T.; Sakly, R.; Danel, M.; Chassaing, S.; Pale, P. *Synthesis* **2017**, 49(6), 1223-1230.
 43. Kulprathipanja, S. *Zeolites in Industrial Separation and Catalysis*. John Wiley & Sons, **2010**.

44. Loewenstein, W. *Am. Mineral.* **1954**, *39*(1-2), 92-96.
45. Chen, L.; Sun, M.; Wang, Z.; Yang, W.; Xie, Z.; Su, B. *Chem. Rev.* **2020**, *120*(20), 11194-11294.
46. Wei, Y.; Parmentier, T. E.; De Jong, K. P.; Zečević, J. *Chem. Soc. Rev.* **2015**, *44*(20), 7234-7261.
47. McDaniel, C.; Maher, P. In *Molecular Sieves* (Eds.: RL Mays; Pickert, P.), Society of the Chemical Industry: London, UK, **1968**, pp. 186-194.
48. Meng, X.; Jiang, D. *Acta Phys. -Chim. Sin.* **2006**, *22*(7), 891-894.
49. Taralkar, U.; Niphadkar, P.; Joshi, P. *J. Solgel. Sci. Technol.* **2009**, *51*, 244-250.
50. Qin, Z. W.; Shen, B. J.; Yu, Z. W.; Deng, F.; Zhao, L.; Zhou, S. H.; Yuan, D. L.; Gao, X. H.; Wang, B. J.; Zhao, H. J. *J. Catal.* **2013**, *298*, 102-111.
51. Ren, S.; Liu, G.; Wu, X.; Chen, X.; Wu, M.; Zeng, G.; Liu, Z.; Sun, Y. *Chinese J. Catal.* **2017**, *38*(1), 123-130.
52. Rezlerová, E.; Zukal, A.; Čejka, J.; Siperstein, F. R.; Brennan, J. K.; Lísal, M. *Langmuir* **2017**, *33*(42), 11126-11137.
53. González, M. D.; Cesteros, Y.; Salagre, P. *Micropor. Mesopor. Mat.* **2011**, *144*(1-3), 162-170.
54. Hua, Z. L.; Zhou, J.; Shi, J. L. *ChemComm.* **2011**, *47*(38), 10536-10547.
55. Verboekend, D.; Pérez Ramírez, J. *Catal. Sci. Technol.* **2011**, *1*(6), 879-890.
56. Verboekend, D.; Pérez Ramírez, J. *Chem. Eur. J.* **2011**, *17*(4), 1137-1147.
57. Verboekend, D.; Mitchell, S.; Milina, M.; Groen, J. C.; Pérez Ramírez, J. *J. Phys. Chem. C* **2011**, *115*(29), 14193-14203.
58. Fernandez, C.; Stan, I.; Gilson, J. P.; Thomas, K.; Vicente, A.; Bonilla, A.; Pérez Ramírez, J. *Chem. Eur. J.* **2010**, *16*(21), 6224-6233.
59. Caicedo Realpe, R.; Pérez Ramírez, J. *Micropor. Mesopor. Mat.* **2010**, *128*(1-3), 91-100.
60. Svelle, S.; Sommer, L.; Barbera, K.; Vennestrøm, P. N.; Olsbye, U.; Lillerud, K. P.; Bordiga, S.; Pan, Y.; Beato, P. *Catal. Today* **2011**, *168*(1), 38-47.
61. Valtchev, V.; Balanzat, E.; Mavrodinova, V.; Diaz, I.; El Fallah, J.; Goupil, J. M. *J. Am. Chem. Soc.* **2011**, *133*(46), 18950-18956.
62. Qin, Z.; Lakiss, L.; Gilson, J.; Thomas, K.; Goupil, J.; Fernandez, C.; Valtchev, V. *Chem. Mater.* **2013**, *25*(14), 2759-2766.
63. Valtchev, V.; Gilson, J. P.; Qin, Z. X. Method for the preparation of synthetic crystalline zeolite materials with enhanced pore volume. WO 2016005783 A1, January 14, **2020**.
64. Qin, Z. X.; Gilson, J. P.; Valtchev, V. *Curr. Opin. Chem. Eng.* **2015**, *8*, 1-6.

65. Cejka, J.; Bekkum, H. V.; Corma, A.; Schueth, F. *Introduction to Zeolite Molecular Sieves*. 3rd ed.; Elsevier, **2007**.
66. Teketel, S.; Erichsen, M. W.; Bleken, F. L.; Svelle, S.; Lillerud, K. P.; Olsbye, U. *Catalysis* **2014**, *26*, 179-217.
67. Corma, A. *J. Catal.* **2003**, *216*(1-2), 298-312.
68. Chen, N.; Kaeding, W.; Dwyer, F. *J. Am. Chem. Soc.* **1979**, *101*(22), 6783-6784.
69. Smit, B.; Maesen, T. L. *Nature* **2008**, *451*(7179), 671-678.
70. Csicsery, S. M. *Pure Appl. Chem.* **1986**, *58*(6), 841-856.
71. Bekkum, H. V.; Jansen, J.; Flanigen, E. *Introduction to Zeolite Science and Practice*. Elsevier, **1991**.
72. Haw, J. F. *Phys. Chem. Chem. Phys.* **2002**, *4*(22), 5431-5441.
73. Chizallet, C.; Raybaud, P. *Angew. Chem. Int. Ed.* **2009**, *121*(16), 2935-2937.
74. Mortier, W. J. *J. Catal.* **1978**, *55*(2), 138-145.
75. Krossing, I.; Raabe, I. *Angew. Chem. Int. Ed.* **2004**, *43*(16), 2066-2090.
76. Sastre, G.; Corma, A. *J. Mol. Catal. A Chem.* **2009**, *305*(1-2), 3-7.
77. Leydier, F.; Chizallet, C.; Costa, D.; Raybaud, P. *J. Catal.* **2015**, *325*, 35-47.
78. Dyer, A. *An Introduction to Zeolite Molecular Sieves*. Office of Scientific and Technical Information, **1988**.
79. Xu, T.; Munson, E. J.; Haw, J. F. *J. Am. Chem. Soc.* **1994**, *116*(5), 1962-1972.
80. Rhodes, C. *Sci. Prog.* **2010**, *93*(3), 223-284.
81. Li, Z.; Xie, K.; Slade, R. C. *Appl. Catal. A-Gen.* **2001**, *209*(1-2), 107-115.
82. Król, M. *Crystals* **2020**, *10*(7), 622.
83. Claire Deville, H. S. *Comptes Rendus* **1862**, *54*(1862), 324-327.
84. Barrer, R. M. *J. Chem. Soc.* **1948**, 127-132.
85. Milton, R. M. In *Zeolite Synthesis* (Eds.: Occelli, M. L.; Robson, H. E.), ACS Publications: Washington, USA, **1989**, pp. 1-10.
86. Cundy, C. S.; Cox, P. A. *Chem. Rev.* **2003**, *103*(3), 663-702.
87. Barrer, R.; Denny, P. *J. Chem. Soc.* **1961**, 971-982.
88. Asgar Pour, Z.; Sebakhy, K. O. *Chemistry* **2022**, *4*(2), 431-446.
89. Mintova, S.; Gilson, J. P.; Valtchev, V. *Nanoscale* **2013**, *5*(15), 6693-6703.
90. Alipour, S. M.; Halladj, R.; Askari, S. *Rev. Chem. Eng.* **2014**, *30*(3), 289-322.
91. Cejka, J.; Corma, A.; Zones, S. *Zeolites and Catalysis: Synthesis, Reactions and Applications*. John Wiley & Sons, **2010**.

92. Wadlinger, R. L.; Kerr, G. T.; Rosinski, E. J. Catalytic composition of a crystalline zeolite. US 3308069 A, March 7, **1967**.
93. Argauer, R. J.; Landolt, G. R. Crystalline zeolite ZSM-5 and method of preparing the same. US 3702886 A, November 14, **1972**.
94. Pophale, R.; Cheeseman, P. A.; Deem, M. W. *Phys. Chem. Chem. Phys.* **2011**, *13*(27), 12407-12412.
95. Flanigen, E. M.; Patton, R. L. Silica polymorph and process for preparing same. US 4073865 A, February 14, **1978**.
96. Shimizu, S.; Hamada, H. *Angew. Chem. Int. Ed.* **1999**, *38*(18), 2725-2727.
97. Mitsui, G.; Dote, T.; Adachi, K.; Dote, E.; Fujimoto, K.; Shimbo, Y.; Fujihara, M.; Shimizu, H.; Usuda, K.; Kono, K. *Toxicol. Ind. Health* **2007**, *23*(1), 5-12.
98. Woo, J.; Seo, J. Y.; Kim, H.; Lee, D.; Park, Y. C.; Yi, C.; Park, Y. S.; Moon, J. *Ultrason. Sonochem.* **2018**, *44*, 146-151.
99. Szostak, R. *Molecular Sieves: Principles of Synthesis and Identification*. Springer Dordrecht, **1988**.
100. Murakami, Y.; Iijima, A.; Ward, J. W. *J. Am. Chem. Soc.* **1982**, *104*(4), 1146-1147.
101. Flanigen, E. M.; Lok, B. M.; Patton, R. L.; Wilson, S. T. In *Studies in Surface Science and Catalysis* (Eds.: Murakami, Y.; Iijima, A.; Ward, J. W.), Elsevier: Amsterdam, Netherlands, **1986**, Vol. 28, pp. 103-112.
102. Jarupatrakorn, J.; Tilley, T. D. *J. Am. Chem. Soc.* **2002**, *124*(28), 8380-8388.
103. Bouh, A. O.; Rice, G. L.; Scott, S. L. *J. Am. Chem. Soc.* **1999**, *121*(31), 7201-7210.
104. Smeets, V.; Gaigneaux, E. M.; Debecker, D. P. *ChemCatChem* **2022**, *14*(1), e202101132.
105. Li, Y.; Li, L.; Yu, J. *Chem* **2017**, *3*(6), 928-949.
106. Ipaktschi, J. Z. *Naturforsch. B* **1986**, *41*(4), 496-498.
107. Rabo, J. A.; Poutsma M. L.; Skeels, G. W. Proceedings of the Fifth International Congress on Catalysis; Burwell Jr, R. L. Taylor & Francis Online, **1972**, 1353-1361.
108. Clearfield, A.; Saldarriaga, C.; Buckley, R. Proceedings of the 3rd International Conference on Molecular Sieves, Recent Progress Reports; Leuven University Press, **1973**.
109. Karge, H. G. *Stud. Surf. Sci. Catal.* **1997**, *105*, 1901-1948.
110. Townsend, R. P.; Coker, E. N. In *Studies in surface science and catalysis* (Eds.: Bekkum, H. V.; Flanigen, E.; Jacobs, P. A.; Jansen, J.), Elsevier: Amsterdam, Netherlands, **2001**, Vol. 137, pp. 467-524.
111. Chassaing, S.; Alix, A.; Boningari, T.; Sido, K. S. S.; Keller, M.; Kuhn, P.; Louis, B.; Sommer, J.; Pale, P. *Synthesis* **2010**, *2010*(9), 1557-1567.

112. Centi, G.; Wichterlová, B.; Bell, A. T. *Catalysis by Unique Metal Ion Structures in Solid Matrices: from Science to Application*. Springer Science & Business Media, **2001**.
113. Yousefzadeh, H.; Bozbag, S. E.; Erkey, C. *J. Supercrit Fluids* **2022**, *179*, 105417.
114. Li, P.; Liu, G.; Wu, H.; Liu, Y.; Jiang, J.; Wu, P. *J. Phys. Chem. C* **2011**, *115*(9), 3663-3670.
115. Zhang, J.; Tu, R.; Goto, T. *J. Ceram. Soc. JAPAN* **2013**, *121*(1410), 226-229.
116. Kusakari, T.; Sasaki, T.; Iwasawa, Y. *ChemComm.* **2004**, (8), 992-993.
117. Serna, P.; Yardimci, D.; Kistler, J. D.; Gates, B. C. *Phys. Chem. Chem. Phys.* **2014**, *16*(3), 1262-1270.
118. Lu, J.; Aydin, C.; Browning, N. D.; Wang, L.; Gates, B. C. *Catal. Letters* **2012**, *142*, 1445-1451.
119. Kistler, J. D.; Chotigkrai, N.; Xu, P.; Enderle, B.; Praserttham, P.; Chen, C. Y.; Browning, N. D.; Gates, B. C. *Angew. Chem. Int. Ed.* **2014**, *53*(34), 8904-8907.
120. Martinez Macias, C.; Xu, P.; Hwang, S. J.; Lu, J.; Chen, C. Y.; Browning, N. D.; Gates, B. C. *ACS Catalysis* **2014**, *4*(8), 2662-2666.
121. Wang, H.; Wang, L.; Xiao, F. *ACS Central Sci.* **2020**, *6*(10), 1685-1697.
122. Wu, S.; Yang, X.; Janiak, C. *Angew. Chem. Int. Ed.* **2019**, *131*(36), 12468-12482.
123. Wang, N.; Sun, Q.; Yu, J. *Adv. Mater.* **2019**, *31*(1), 1803966.
124. Kosinov, N.; Liu, C.; Hensen, E. J.; Pidko, E. A. *Chem. Mater.* **2018**, *30*(10), 3177-3198.
125. Wang, L.; Xu, S.; He, S.; Xiao, F. *Nano Today* **2018**, *20*, 74-83.
126. Sadjadi, S. *Encapsulated Catalysts*. Academic Press, **2017**.
127. Gallezot, P. In *Post-Synthesis Modification I* (Eds.: Karge, H. G.; Weitkamp, J.), Springer: Heidelberg, Germany, **2002**, pp. 257-305.
128. Liu, L.; Diaz, U.; Arenal, R.; Agostini, G.; Concepcion, P.; Corma, A. *Nat. Mater.* **2017**, *16*(1), 132-138.
129. Pala Rosas, I.; Contreras, J. L.; Salmones, J.; Tapia, C.; Zeifert, B.; Navarrete, J.; Vázquez, T.; García, D. C. *Catalysts* **2017**, *7*(3), 73.
130. Goel, S.; Wu, Z.; Zones, S. I.; Iglesia, E. *J. Am. Chem. Soc.* **2012**, *134*(42), 17688-17695.
131. Wang, N.; Sun, Q.; Bai, R.; Li, X.; Guo, G.; Yu, J. *J. Am. Chem. Soc.* **2016**, *138*(24), 7484-7487.
132. Shamzhy, M.; Opanasenko, M.; Concepción, P.; Martínez, A. *Chem. Soc. Rev.* **2019**, *48*(4), 1095-1149.
133. Corma, A.; Garcia, H. *Eur. J. Inorg. Chem.* **2004**, *2004*(6), 1143-1164.
134. Amooghin, A. E.; Sanaeepur, H.; Omidkhah, M.; Kargari, A. *J. Mater. Chem. A* **2018**, *6*(4), 1751-1771.

135. Herron, N. *Inorg. Chem.* **1986**, 25(26), 4714-4717.
136. Jafarian, M.; Etezadi, S.; Gopal, F.; Khakali, M.; Rayati, S.; Mahjani, M. G. *Talanta* **2013**, 108, 19-29.
137. Briot, E.; Bedioui, F.; Balkus Jr, K. J. *J. Electroanal. Chem.* **1998**, 454(1-2), 83-89.
138. Varkey, S. P.; Ratnasamy, C.; Ratnasamy, P. *J. Mol. Catal. A Chem.* **1998**, 135(3), 295-306.
139. Bardakçi, B.; Bahçeli, S. *Indian J. Pure Appl. Phys.* **2010**, 48, 615-620.
140. Nozue, Y.; Kodaira, T.; Goto, T. *Phys. Rev. Lett.* **1992**, 68(25), 3789.
141. Singh, J.; Im, J.; Whitten, J. E.; Soares, J. W.; Steeves, D. M. *Langmuir* **2009**, 25(17), 9947-9953.
142. Wu, C.; Bein, T. *Science* **1994**, 266(5187), 1013-1015.
143. Salavati-Niasari, M.; Bazarganipour, M. *Catal. Commun.* **2006**, 7(6), 336-343.
144. Salavati-Niasari, M. *Micropor. Mesopor. Mat.* **2006**, 95(1-3), 248-256.
145. Rolison, D. R. *Chem. Rev.* **1990**, 90(5), 867-878.
146. DeWilde, W.; Peeters, G.; Lunsford, J. H. *J. Phys. Chem.* **1980**, 84(18), 2306-2310.
147. Barton, D. H. R.; Doller, D. *Acc. Chem. Res.* **1992**, 25(11), 504-512.
148. Álvaro, M.; Ferrer, B.; García, H.; Sanjuán, A. *Tetrahedron* **1999**, 55(40), 11895-11902.
149. Kim, K.; Park, M.-H. *Biomedicines* **2024**, 12(2), 326.
150. Di Nunzio, M. R.; Agostoni, V.; Cohen, B.; Gref, R.; Douhal, A. *J. Med. Chem.* **2014**, 57(2), 411-420.
151. Yamane, I.; Nakazawa, T. *Pure Appl. Chem.* **1986**, 58(10), 1397-1404.
152. Bish, D. L.; Ming, D. W. *Natural Zeolites: Occurrence, Properties, Applications*. Walter de Gruyter GmbH & Co KG, **2018**.
153. Schneider, A. F.; Zimmermann, O. F.; Gewehr, C. E. *Ciênc. Rural* **2017**, 47(8), 1-8.
154. Karamanlis, X.; Fortomaris, P.; Arsenos, G.; Dosis, I.; Papaioannou, D.; Batzios, C.; Kamarianos, A. *Asian Austral. J. Anim.* **2008**, 21(11), 1642-1650.
155. Cabuk, M.; Alcicek, A.; Bozkurt, M.; Akkan, S. *Int. J. Poult. Sci.* **2004**, 3(10), 651-654.
156. Abusafa, A.; Yücel, H. *Sep. Purif. Technol.* **2002**, 28(2), 103-116.
157. McKetta Jr, J. J. *Petroleum Processing Handbook*. CRC press, **1992**.
158. Wang, S.; Peng, Y. *Chem. Eng. J.* **2010**, 156(1), 11-24.
159. Soltanian, S.; Lee, C. L.; Lam, S. S. *Biofuel Res. J.* **2020**, 7(3), 1217-1234.
160. Sánchez López, P.; Kotolevich, Y.; Yocupicio Gaxiola, R. I.; Antúnez García, J.; Chowdari, R. K.; Petranovskii, V.; Fuentes Moyado, S. *Front. Chem.* **2021**, 9, 716745.
161. Botella, P.; Corma, A.; López-Nieto, J.; Valencia, S.; Jacquot, R. *J. Catal.* **2000**, 195(1), 161-168.

162. Corma, A.; Climent, M. J.; Carcía, H.; Primo, J. *Appl. Catal.* **1990**, *59*(1), 333-340.
163. Ballini, R.; Bosica, G.; Frullanti, B.; Maggi, R.; Sartori, G.; Schroer, F. *Tetrahedron Lett.* **1998**, *39*(12), 1615-1618.
164. Rao, M. N.; Kumar, P.; Singh, A. P.; Reddy, R. S. *Synth. Commun.* **1992**, *22*(9), 1299-1305.
165. Choi, J.; Ko, K. Y. *Bull. Korean Chem. Soc.* **2001**, *22*(11), 1177-1178.
166. Ballini, R.; Bigi, F.; Carloni, S.; Maggi, R.; Sartori, G. *Tetrahedron Lett.* **1997**, *38*(23), 4169-4172.
167. Pilkington, L. I.; Barker, D. *Synlett* **2015**, *26*(17), 2425-2428.
168. Wimmer, E.; Borghèse, S.; Blanc, A.; Bénéteau, V.; Pale, P. *Chem. Eur. J.* **2017**, *23*(7), 1484-1489.
169. Srinivas, K.; Mahender, I.; Das, B. *Synlett* **2003**, *2003*(15), 2419-2421.
170. Chavan, S. P.; Anand, R.; Pasupathy, K.; Rao, B. *Green Chem.* **2001**, *3*(6), 320-322.
171. Pandey, R. K.; Kadam, V. S.; Upadhyay, R. K.; Dongare, M. K.; Kumar, P. *Synth. Commun.* **2003**, *33*(17), 3017-3024.
172. Losch, P.; Felten, A. S.; Pale, P. *Adv. Synth. Catal.* **2015**, *357*(13), 2931-2938.
173. Tang, B.; Lu, X.; Zhou, D.; Lei, J.; Niu, Z.; Fan, J.; Xia, Q. *Catal. Commun.* **2012**, *21*, 68-71.
174. Olmos, A.; Rigolet, S.; Louis, B.; Pale, P. *J. Phys. Chem. C* **2012**, *116*(25), 13661-13670.
175. Olmos, A.; Alix, A.; Sommer, J.; Pale, P. *Chem. Eur. J.* **2009**, *15*(42), 11229-11234.
176. Olmos, A.; Sommer, J.; Pale, P. *Chem. Eur. J.* **2011**, *17*(6), 1907-1914.
177. Olmos, A.; Louis, B.; Pale, P. *Chem. Eur. J.* **2012**, *18*(16), 4894-4901.
178. Baruah, M. J.; Dutta, A.; Biswas, S.; Gogoi, G.; Hoque, N.; Bhattacharyya, P. K.; Bania, K. K. *ACS Appl. Nano Mater.* **2022**, *5*(1), 1446-1459.
179. Bania, K. K.; Bharali, D.; Viswanathan, B.; Deka, R. C. *Inorg. Chem.* **2012**, *51*(3), 1657-1674.
180. Barton, D. H.; Li, T. *Tetrahedron* **1998**, *54*(9), 1735-1744.
181. Borghèse, S.; Drouhin, P.; Bénéteau, V.; Louis, B.; Pale, P. *Green Chem.* **2013**, *15*(6), 1496-1500.
182. Gillard, R. M.; Brimble, M. A. *Org. Biomol. Chem.* **2019**, *17*(36), 8272-8307.
183. Utimoto, K. *Pure Appl. Chem.* **1983**, *55*(11), 1845-1852.
184. Messerle, B. A.; Vuong, K. Q. *Pure Appl. Chem.* **2006**, *78*(2), 385-390.
185. Messerle, B. A.; Vuong, K. Q. *Organometallics* **2007**, *26*(12), 3031-3040.
186. Selvaratnam, S.; Ho, J. H.; Huleatt, P. B.; Messerle, B. A.; Chai, C. L. *Tetrahedron Lett.* **2009**, *50*(10), 1125-1127.

187. Ravindar, K.; Sridhar Reddy, M.; Deslongchamps, P. *Org. Lett.* **2011**, *13*(12), 3178-3181.
188. Liu, B.; De Brabander, J. K. *Org. Lett.* **2006**, *8*(21), 4907-4910.
189. Aponick, A.; Li, C.; Palmes, J. A. *Org. Lett.* **2009**, *11*(1), 121-124.
190. Tlais, S. F.; Dudley, G. B. *Beilstein J. Org. Chem.* **2011**, *7*(1), 570-577.
191. Hampton, C. S.; Harmata, M. *Adv. Synth. Catal.* **2015**, *357*(2-3), 549-552.
192. Harmata, M.; Huang, C. *Adv. Synth. Catal.* **2008**, *350*(7-8), 972-974.
193. Emayavaramban, P.; Kadirvelu, K.; Dharmaraj, N. *J. Nanosci. Nanotechnol.* **2016**, *16*(9), 9093-9103.
194. Ali, Z.; Ferreira, D.; Carvalho, P.; Avery, M. A.; Khan, I. A. *J. Nat. Prod.* **2008**, *71*(6), 1111-1112.
195. Ghosh, S.; Mondal, S.; Hajra, A. *Adv. Synth. Catal.* **2020**, *362*(18), 3768-3794.
196. Kowalak, S.; Weiss, R. C.; Balkus, K. J. *J. Chem. Soc., Chem. Commun.* **1991**, (1), 57-58.
197. Djakovitch, L.; Heise, H.; Köhler, K. *J. Organomet. Chem.* **1999**, *584*(1), 16-26.
198. Michalik, J.; Narayana, M.; Kevan, L. *J. Phys. Chem. C* **1985**, *89*(21), 4553-4560.
199. Sachtler, W. M.; Cavalcanti, F. A.; Zhang, Z. *Catal. Letters* **1991**, *9*, 261-271.
200. Djakovitch, L.; Koehler, K. *J. Am. Chem. Soc.* **2001**, *123*(25), 5990-5999.
201. Köhler, K.; Wagner, M.; Djakovitch, L. *Catal. Today* **2001**, *66*(1), 105-114.
202. Djakovitch, L.; Koehler, K. *J. Mol. Catal. A Chem.* **1999**, *142*(2), 275-284.
203. Tarabay, J.; Al Maksoud, W.; Jaber, F.; Pinel, C.; Prakash, S.; Djakovitch, L. *Appl. Catal. A-Gen.* **2010**, *388*(1-2), 124-133.
204. Raboisson, P.; Baurand, A.; Cazenave, J. P.; Gachet, C.; Schultz, D.; Spiess, B.; Bourguignon, J. J. *J. Org. Chem.* **2002**, *67*(23), 8063-8071.
205. Marcel, R.; Durillon, T.; Djakovitch, L.; Fache, F.; Rataboul, F. *ChemistrySelect* **2019**, *4*(12), 3329-3333.
206. Djakovitch, L.; Wagner, M.; Hartung, C.; Beller, M.; Koehler, K. *J. Mol. Catal. A Chem.* **2004**, *219*(1), 121-130.
207. Astruc, D. *Nanoparticles and Catalysis*. John Wiley & Sons, **2008**.
208. Djakovitch, L.; Rollet, P. *Adv. Synth. Catal.* **2004**, *346*(13-15), 1782-1792.
209. Djakovitch, L.; Rollet, P. *Tetrahedron Lett.* **2004**, *45*(7), 1367-1370.
210. Sonogashira, K. In *Comprehensive Organic Synthesis: Selectivity, Strategy, and Efficiency in Modern Organic Chemistry* (Eds.: Trost, B. M.; Fleming, I.), Elsevier: Amsterdam, Netherlands, **1991**, Vol. 3, pp. 521-549.
211. Rollet, P.; Kleist, W.; Dufaud, V.; Djakovitch, L. *J. Mol. Catal. A Chem.* **2005**, *241*(1-2), 39-51.

212. Baghbanian, S. M.; Yadollahy, H.; Tajbakhsh, M.; Farhang, M.; Biparva, P. *RSC Adv.* **2014**, 4(107), 62532-62543.
213. Kumbhar, A.; Kamble, S.; Mane, A.; Jha, R.; Salunkhe, R. *J. Organomet. Chem.* **2013**, 738, 29-34.
214. Tadjarodi, A.; Dehghani, M.; Imani, M. *Appl. Organomet. Chem.* **2018**, 32(12), e4594.
215. Mohan, S.; Dinesha, P.; Kumar, S. *Chem. Eng. J.* **2020**, 384, 123253.
216. Evano, G.; Blanchard, N.; Toumi, M. *Chem. Rev.* **2008**, 108(8), 3054-3131.
217. Krause, N. *Modern Organocopper Chemistry*. John Wiley & Sons, **2002**.
218. Crabtree, R.; Mingos, M. *Comprehensive Organometallic Chemistry III: from Fundamentals to Applications*. Elsevier Science, **2006**.
219. Trammell, R.; Rajabimoghadam, K.; Garcia Bosch, I. *Chem. Rev.* **2019**, 119(4), 2954-3031.
220. Innocenti, R.; Lenci, E.; Trabocchi, A. *Tetrahedron Lett.* **2020**, 61(29), 152083.
221. Anilkumar, G.; Saranya, S. *Copper Catalysis in Organic Synthesis*. John Wiley & Sons, **2020**.
222. Yamamoto, Y. *J. Org. Chem.* **2007**, 72(21), 7817-7831.
223. Dauben, W. G.; Krabbenhoft, H. O. *J. Am. Chem. Soc.* **1976**, 98(7), 1992-1993.
224. Langham, C.; Taylor, S.; Bethell, D.; McMorn, P.; Page, P. C. B.; Willock, D. J.; Sly, C.; Hancock, F. E.; King, F.; Hutchings, G. J. *J. Chem. Soc. Perkin trans. II* **1999**, (5), 1043-1050.
225. Evans, D. A.; Bilodeau, M. T.; Faul, M. M. *J. Am. Chem. Soc.* **1994**, 116(7), 2742-2753.
226. Taylor, S.; Gullick, J.; McMorn, P.; Bethell, D.; Page, P. C. B.; Hancock, F. E.; King, F.; Hutchings, G. J. *J. Chem. Soc. Perkin trans. II* **2001**, (9), 1724-1728.
227. Alix, A.; Chassaing, S.; Pale, P.; Sommer, J. *Tetrahedron* **2008**, 64(37), 8922-8929.
228. Bénéteau, V.; Olmos, A.; Boningari, T.; Sommer, J.; Pale, P. *Tetrahedron Lett.* **2010**, 51(28), 3673-3677.
229. Boningari, T.; Olmos, A.; Reddy, B. M.; Sommer, J.; Pale, P. *Eur. J. Org. Chem.* **2010**, 2010(33), 6338-6347.
230. Sarmah, B.; Satpati, B.; Srivastava, R. *RSC Adv.* **2016**, 6(90), 87066-87081.
231. Costa, E. R.; Andrade, F. C.; de Albuquerque, D. Y.; Ferreira, L. E.; Lima, T. M.; Lima, C. G.; Silva, D. S.; Urquieta González, E. A.; Paixao, M. W.; Schwab, R. S. *New J. Chem.* **2020**, 44(35), 15046-15053.
232. Goldberg, I. *Ber. Dtsch. Chem. Ges.* **1906**, 39(2), 1691-1692.
233. Harkat, H.; Borghese, S.; Nigris, M. D.; Kiselev, S.; Beneteau, V.; Pale, P. *Adv. Synth. Catal.* **2014**, 356(18), 3842-3848.

234. Frederick, M. O.; Mulder, J. A.; Tracey, M. R.; Hsung, R. P.; Huang, J.; Kurtz, K. C.; Shen, L.; Douglas, C. J. *J. Am. Chem. Soc.* **2003**, *125*(9), 2368-2369.
235. Zhang, Y.; Hsung, R. P.; Tracey, M. R.; Kurtz, K. C.; Vera, E. L. *Org. Lett.* **2004**, *6*(7), 1151-1154.
236. Henrion, M.; Smolders, S.; De Vos, D. E. *Catal. Sci. Technol.* **2020**, *10*(4), 940-943.
237. Astruc, D. *Modern Arene Chemistry*. Wiley Online Library, **2002**.
238. Miyaura, N.; Yamada, K.; Suzuki, A. *Tetrahedron Lett.* **1979**, *20*(36), 3437-3440.
239. Miyaura, N.; Suzuki, A. *J. Chem. Soc. Chem. Commun.* **1979**, (19), 866-867.
240. Shi, F.; Tse, M. K.; Pohl, M.; Brückner, A.; Zhang, S.; Beller, M. *Angew. Chem. Int. Ed.* **2007**, *46*(46), 8866-8868.
241. Guérinot, A.; Reymond, S.; Cossy, J. *Angew. Chem. Int. Ed.* **2007**, *46*(34), 6521-6524.
242. Fürstner, A.; Leitner, A.; Méndez, M.; Krause, H. *J. Am. Chem. Soc.* **2002**, *124*(46), 13856-13863.
243. Hatakeyama, T.; Nakamura, M. *J. Am. Chem. Soc.* **2007**, *129*(32), 9844-9845.
244. Nakamura, E.; Yoshikai, N. *J. Org. Chem.* **2010**, *75*(18), 6061-6067.
245. Monnier, F.; Taillefer, M. *Angew. Chem. Int. Ed.* **2009**, *48*(38), 6954-6971.
246. West, M. J.; Fyfe, J. W.; Vantourout, J. C.; Watson, A. J. *Chem. Rev.* **2019**, *119*(24), 12491-12523.
247. Weingarten, H. *J. Org. Chem.* **1964**, *29*(12), 3624-3626.
248. Couture, C.; Paine, A. J. *Can. J. Chem.* **1985**, *63*(1), 111-120.
249. OI, R.; Shimakawa, C.; Takenaka, S. *Chem. Lett.* **1988**, *17*(5), 899-900.
250. Marcoux, J. F.; Doye, S.; Buchwald, S. L. *J. Am. Chem. Soc.* **1997**, *119*(43), 10539-10540.
251. Ma, D.; Zhang, Y.; Yao, J.; Wu, S.; Tao, F. *J. Am. Chem. Soc.* **1998**, *120*(48), 12459-12467.
252. Kiyomori, A.; Marcoux, J. F.; Buchwald, S. L. *Tetrahedron Lett.* **1999**, *40*(14), 2657-2660.
253. Goodbrand, H. B.; Hu, N. X. *J. Org. Chem.* **1999**, *64*(2), 670-674.
254. Fagan, P. J.; Hauptman, E.; Shapiro, R.; Casalnuovo, A. *J. Am. Chem. Soc.* **2000**, *122*(21), 5043-5051.
255. Vasconcelos, S. N.; Reis, J. S.; De Oliveira, I. M.; Balfour, M. N.; Stefani, H. A. *Tetrahedron* **2019**, *75*(13), 1865-1959.
256. Hennings, D. D.; Iwama, T.; Rawal, V. H. *Org. Lett.* **1999**, *1*(8), 1205-1208.
257. Qi, C.; Sun, X.; Lu, C.; Yang, J.; Du, Y.; Wu, H.; Zhang, X. M. *J. Organomet. Chem.* **2009**, *694*(18), 2912-2916.
258. Huang, Y.; Liu, L.; Feng, W. *ChemistrySelect* **2016**, *1*(3), 630-634.

259. Shao, L.; Du, Y.; Zeng, M.; Li, X.; Shen, W.; Zuo, S.; Lu, Y.; Zhang, X. M.; Qi, C. *Appl. Organomet. Chem.* **2010**, *24*(5), 421-425.
260. Shen, G.; Wang, Y.; Zhao, X.; Huangfu, X.; Tian, Y.; Zhang, T.; Yang, B. *Synlett* **2017**, *28*(15), 2030-2035.
261. Cheng, J.; Zhang, G.; Du, J.; Tang, L.; Xu, J.; Li, J. *J. Mater. Chem.* **2011**, *21*(10), 3485-3494.
262. Dhital, R. N.; Kamonsatikul, C.; Somsook, E.; Bobuatong, K.; Ehara, M.; Karanjit, S.; Sakurai, H. *J. Am. Chem. Soc.* **2012**, *134*(50), 20250-20253.
263. Hu, Y.; Li, F.; Gu, G.; Lu, M. *Catal. Letters* **2011**, *141*, 467-473.
264. Narasimharao, K.; Al Sabban, E.; Saleh, T. S.; Gallastegui, A. G.; Sanfiz, A. C.; Basahel, S.; Al Thabaiti, S.; Alyoubi, A.; Obaid, A.; Mokhtar, M. *J. Mol. Catal. A Chem.* **2013**, *379*, 152-162.
265. Gao, A.; Zhang, H.; Hu, L.; Hou, A.; Xie, K. *Catal. Commun.* **2017**, *102*, 118-122.
266. Primo, A.; Esteve Adell, I.; Blandez, J. F.; Dhakshinamoorthy, A.; Álvaro, M.; Candu, N.; Coman, S. M.; Parvulescu, V. I.; García, H. *Nat. Commun.* **2015**, *6*(1), 8561.
267. Dumbre, D.; Choudhary, V. R.; Selvakannan, P. *Polyhedron* **2016**, *120*, 180-184.
268. Agrawal, A.; Goyal, R.; Abraham, B. M.; Singh, O.; Tripathi, S.; Poddar, M. K.; Bal, R.; Sarkar, B. *React. Chem. Eng.* **2021**, *6*(5), 929-936.
269. Karimi, B.; Esfahani, F. K. *ChemComm.* **2011**, *47*(37), 10452-10454.
270. Layek, K.; Maheswaran, H.; Kantam, M. L. *Catal. Sci. Technol.* **2013**, *3*(4), 1147-1150.
271. Movahed, S. K.; Fakharian, M.; Dabiri, M.; Bazgir, A. *RSC Adv.* **2014**, *4*(10), 5243-5247.
272. Yuan, Y.; Bian, Y. *Appl. Organomet. Chem.* **2008**, *22*(1), 15-18.
273. Lv, D.; Zhang, Y.; Li, J. *J. Chem. Res.* **2009**, *2009*(6), 397-399.
274. Yurino, T.; Ueda, Y.; Shimizu, Y.; Tanaka, S.; Nishiyama, H.; Tsurugi, H.; Sato, K.; Mashima, K. *Angew. Chem. Int. Ed.* **2015**, *127*(48), 14645-14649.
275. Moncomble, A.; Le Floch, P.; Gosmini, C. *Chem. Eur. J.* **2009**, *15*(19), 4770-4774.
276. Kazmierski, I.; Gosmini, C.; Paris, J. M.; Périchon, J. *Tetrahedron Lett.* **2003**, *44*(34), 6417-6420.
277. Zhang, Y. Y.; Lin, J. D.; Xu, X. L.; Li, J. H. *Synth. Commun.* **2010**, *40*(17), 2556-2563.
278. Suzuki, A. *Angew. Chem. Int. Ed.* **2011**, *50*(30), 6722-6737.
279. Hall, D. G. *Boronic Acids: Preparation, Applications in Organic Synthesis and Medicine*. John Wiley & Sons, **2006**.
280. Levitskiy, O. A.; Grishin, Y. K.; Sentyurin, V. V.; Magdesieva, T. V. *Chem. Eur. J.* **2017**, *23*(51), 12575-12584.

281. Moon, S.; Nam, J.; Rathwell, K.; Kim, W. *Org. Lett.* **2014**, *16*(2), 338-341.
282. Dhital, R. N.; Murugadoss, A.; Sakurai, H. *Chem. Asian J.* **2012**, *7*(1), 55-59.
283. Wang, L.; Wang, H.; Zhang, W.; Zhang, J.; Lewis, J. P.; Meng, X.; Xiao, F. S. *J. Catal.* **2013**, *298*, 186-197.
284. Zheng, J.; Lin, S.; Zhu, X.; Jiang, B.; Yang, Z.; Pan, Z. *ChemComm.* **2012**, *48*(50), 6235-6237.
285. Matsuda, T.; Asai, T.; Shiose, S.; Kato, K. *Tetrahedron Lett.* **2011**, *52*(37), 4779-4781.
286. Luque, R.; Baruwati, B.; Varma, R. S. *Green Chem.* **2010**, *12*(9), 1540-1543.
287. Vogler, T.; Studer, A. *Adv. Synth. Catal.* **2008**, *350*(13), 1963-1967.
288. Wong, M. S.; Zhang, X. L. *Tetrahedron Lett.* **2001**, *42*(24), 4087-4089.
289. Kabalka, G. W.; Wang, L. *Tetrahedron Lett.* **2002**, *43*(16), 3067-3068.
290. Wu, N.; Li, X.; Xu, X.; Wang, Y.; Xu, Y.; Chen, X. *Lett. Org. Chem.* **2010**, *7*(1), 11-14.
291. Dwivedi, S.; Bardhan, S.; Ghosh, P.; Das, S. *RSC Adv.* **2014**, *4*(77), 41045-41050.
292. Xu, X.; Gao, S.; Chen, W.; Gao, Z.; Luo, J. *ChemistrySelect* **2018**, *3*(31), 8863-8866.
293. Cravotto, G.; Beggiato, M.; Penoni, A.; Palmisano, G.; Tollari, S.; Lévêque, J. M.; Bonrath, W. *Tetrahedron Lett.* **2005**, *46*(13), 2267-2271.
294. Chen, J. S.; Krogh Jespersen, K.; Khinast, J. G. *J. Mol. Catal. A Chem.* **2008**, *285*(1-2), 14-19.
295. Prastaro, A.; Ceci, P.; Chiancone, E.; Boffi, A.; Fabrizi, G.; Cacchi, S. *Tetrahedron Lett.* **2010**, *51*(18), 2550-2552.
296. Demir, A. S.; Reis, Ö.; Emrullahoglu, M. *J. Org. Chem.* **2003**, *68*(26), 10130-10134.
297. Kirai, N.; Yamamoto, Y. *Eur. J. Org. Chem.* **2009**, (12), 1864-1867.
298. Kaboudin, B.; Haruki, T.; Yokomatsu, T. *Synthesis* **2011**, *2011*(1), 91-96.
299. Cheng, G.; Luo, M. *Eur. J. Org. Chem.* **2011**, *2011*(13), 2519-2523.
300. Cao, Y. N.; Tian, X. C.; Chen, X. X.; Yao, Y. X.; Gao, F.; Zhou, X. L. *Synlett* **2017**, *28*(5), 601-606.
301. Dar, B. A.; Singh, S.; Pandey, N.; Singh, A.; Sharma, P.; Lazar, A.; Sharma, M.; Vishwakarma, R. A.; Singh, B. *Appl. Catal. A-Gen.* **2014**, *470*, 232-238.
302. Puthiaraj, P.; Suresh, P.; Pitchumani, K. *Green Chem.* **2014**, *16*(5), 2865-2875.
303. Shafeek, A.; Taufeeqaslam, M. *RSC Adv.* **2015**, *5*(31), 24675-24680.
304. Hussain, N.; Gogoi, P.; Azhaganand, V. K.; Shelke, M. V.; Das, M. R. *Catal. Sci. Technol.* **2015**, *5*(2), 1251-1260.
305. Lin, C.; Huang, C.; Yu, C.; Chen, Y.; Ke, W.; Wang, G.; Lee, G.; Shieh, M. *Dalton Trans.* **2015**, *44*(38), 16675-16679.

306. Das, S. K.; Chandra, B. K.; Molla, R. A.; Sengupta, M.; Islam, S. M.; Majee, A.; Bhaumik, A. *Mol. Catal.* **2020**, *480*, 110650.
307. Mo, F.; Qiu, D.; Zhang, L.; Wang, J. *Chem. Rev.* **2021**, *121*(10), 5741-5829.
308. Ding, Y. Y.; Cheng, K.; Qi, C. Z.; Song, Q. B. *Tetrahedron Lett.* **2012**, *53*(46), 6269-6272.
309. Savanur, H. M.; Kalkhambkar, R. G.; Laali, K. K. *Tetrahedron Lett.* **2016**, *57*(6), 663-667.
310. Atkinson, E. R.; Lawler, H.; Heath, J.; Kimball, E.; Read, E. *J. Am. Chem. Soc.* **1941**, *63*(3), 730-733.
311. Atkinson, E. R.; Morgan, C.; Warren, H.; Manning, T. *J. Am. Chem. Soc.* **1945**, *67*(9), 1513-1515.
312. Cohen, T.; Lewarchik, R. J.; Tarino, J. Z. *J. Am. Chem. Soc.* **1974**, *96*(25), 7753-7760.
313. Capanec, I.; Litvić, M.; Udiković, J.; Pogorelić, I.; Lovrić, M. *Tetrahedron* **2007**, *63*(25), 5614-5621.
314. Robinson, M. K.; Kochurina, V. S.; Hanna Jr, J. M. *Tetrahedron Lett.* **2007**, *48*(43), 7687-7690.
315. Vajpayee, V.; Song, Y.; Ahn, J.; Chi, K. *Bull. Korean Chem. Soc.* **2011**, *32*(8), 2970-2972.
316. Zhou, J.; Yu, S.; Cheng, K.; Qi, C. *J. Chem. Res.* **2012**, *36*(11), 672-674.
317. Ghigo, G.; Bonomo, M.; Antenucci, A.; Damin, A.; Dughera, S. *RSC Adv.* **2022**, *12*(41), 26640-26647.
318. Kuhn, P.; Pale, P.; Sommer, J.; Louis, B. *J. Phys. Chem. C* **2009**, *113*(7), 2903-2910.
319. Qiao, J. X.; Lam, P. Y. *Synthesis* **2011**, *2011*(6), 829-856.
320. Keller, M.; Sido, A. S. S.; Pale, P.; Sommer, J. *Chem. Eur. J.* **2009**, *15*(12), 2810-2817.
321. Patil, M. K.; Keller, M.; Reddy, B. M.; Pale, P.; Sommer, J. *Eur. J. Org. Chem.* **2008**, *4440*, 4440-4445.
322. Liotta, L.; Gruttadauria, M.; Di Carlo, G.; Perrini, G.; Librando, V. *J. Hazard. Mater.* **2009**, *162*(2-3), 588-606.
323. Yuan, C.; Zheng, L.; Zhao, Y. *Molecules* **2019**, *24*(20), 3678.
324. Agrahari, B.; Layek, S.; Kumari, S.; Ganguly, R.; Pathak, D. D. *J. Mol. Struct.* **2017**, *1134*, 85-90.
325. Salamé, A.; Rio, J.; Ciofini, I.; Perrin, L.; Grimaud, L.; Payard, P. A. *Molecules* **2022**, *27*(21), 7517.
326. Vilella, L.; Studt, F. *Eur. J. Inorg. Chem.* **2016**, *2016*(10), 1514-1520.
327. Xie, P.; Pu, T.; Aranovich, G.; Guo, J.; Donohue, M.; Kulkarni, A.; Wang, C. *Nat. Catal.* **2021**, *4*(2), 144-156.

328. Drake, I. J.; Zhang, Y.; Briggs, D.; Lim, B.; Chau, T.; Bell, A. T. *J. Phys. Chem. B* **2006**, *110*(24), 11654-11664.
329. Phan, T. B.; Breugst, M.; Mayr, H. *Angew. Chem. Int. Ed.* **2006**, *45*(23), 3869-3874.
330. Antenucci, A.; Bonomo, M.; Ghigo, G.; Gontrani, L.; Barolo, C.; Dughera, S. *J. Mol. Liq.* **2021**, *339*, 116743.
331. Bihelovic, F.; Ferjancic, Z. *Angew. Chem. Int. Ed.* **2016**, *128*(7), 2615-2618.
332. Goldberg, I. *Ber. Dtsch. Chem. Ges.* **1907**, *40*(4), 4541-4546.
333. Hurltley, W. R. H. *J. Chem. Soc.* **1929**, 1870-1873.
334. Chen, J.; Li, J.; Dong, Z. *Adv. Synth. Catal.* **2020**, *362*(16), 3311-3331.
335. Soto Hernández, M.; Tenango, M. P.; García Mateos, R. *Phenolic Compounds: Natural Sources, Importance and Applications*. BoD—Books on Demand, **2017**.
336. Huang, W.; Cai, Y.; Zhang, Y. *Nutr. Cancer* **2009**, *62*(1), 1-20.
337. Scott, K. A.; Cox, P. B.; Njardarson, J. T. *J. Med. Chem.* **2022**, *65*(10), 7044-7072.
338. Anderson, K. W.; Ikawa, T.; Tundel, R. E.; Buchwald, S. L. *J. Am. Chem. Soc.* **2006**, *128*(33), 10694-10695.
339. Tlili, A.; Xia, N.; Monnier, F.; Taillefer, M. *Angew. Chem. Int. Ed.* **2009**, *121*(46), 8881-8884.
340. Burgos, C. H.; Barder, T. E.; Huang, X.; Buchwald, S. L. *Angew. Chem. Int. Ed.* **2006**, *118*(26), 4427-4432.
341. Vorogushin, A. V.; Huang, X.; Buchwald, S. L. *J. Am. Chem. Soc.* **2005**, *127*(22), 8146-8149.
342. Kataoka, N.; Shelby, Q.; Stambuli, J. P.; Hartwig, J. F. *J. Org. Chem.* **2002**, *67*(16), 5553-5566.
343. Torraca, K. E.; Huang, X.; Parrish, C. A.; Buchwald, S. L. *J. Am. Chem. Soc.* **2001**, *123*(43), 10770-10771.
344. Shelby, Q.; Kataoka, N.; Mann, G.; Hartwig, J. *J. Am. Chem. Soc.* **2000**, *122*(43), 10718-10719.
345. Hao, L.; Ding, G.; Deming, D. A.; Zhang, Q. *Eur. J. Org. Chem.* **2019**, *2019*(44), 7307-7321.
346. Johansson Seechurn, C. C.; Kitching, M. O.; Colacot, T. J.; Snieckus, V. *Angew. Chem. Int. Ed.* **2012**, *51*(21), 5062-5085.
347. Guram, A. S.; Rennels, R. A.; Buchwald, S. L. *Angew. Chem. Int. Ed.* **1995**, *34*(12), 1348-1350.
348. Wolfe, J. P.; Wagaw, S.; Buchwald, S. L. *J. Am. Chem. Soc.* **1996**, *118*(30), 7215-7216.

349. Driver, M. S.; Hartwig, J. F. *J. Am. Chem. Soc.* **1996**, *118*(30), 7217-7218.
350. Prim, D.; Campagne, J. M.; Joseph, D.; Andrioletti, B. *Tetrahedron* **2002**, *58*(11), 2041-2075.
351. Palucki, M.; Wolfe, J. P.; Buchwald, S. L. *J. Am. Chem. Soc.* **1997**, *119*(14), 3395-3396.
352. Chen, G. S.; Chan, A. S.; Kwong, F. Y. *Tetrahedron Lett.* **2007**, *48*(3), 473-476.
353. Louie, J.; Hartwig, J. F. *Tetrahedron Lett.* **1995**, *36*(21), 3609-3612.
354. Guram, A. S.; Buchwald, S. L. *J. Am. Chem. Soc.* **1994**, *116*(17), 7901-7902.
355. Reddy, N. P.; Tanaka, M. *Tetrahedron Lett.* **1997**, *38*(27), 4807-4810.
356. Marcoux, J. F.; Wagaw, S.; Buchwald, S. L. *J. Org. Chem.* **1997**, *62*(6), 1568-1569.
357. Barder, T. E.; Biscoe, M. R.; Buchwald, S. L. *Organometallics* **2007**, *26*(9), 2183-2192.
358. Old, D. W.; Wolfe, J. P.; Buchwald, S. L. *J. Am. Chem. Soc.* **1998**, *120*(37), 9722-9723.
359. Wolfe, J. P.; Buchwald, S. L. *Angew. Chem. Int. Ed.* **1999**, *38*(16), 2413-2416.
360. Wolfe, J. P.; Tomori, H.; Sadighi, J. P.; Yin, J.; Buchwald, S. L. *J. Org. Chem.* **2000**, *65*(4), 1158-1174.
361. Charles, M. D.; Schultz, P.; Buchwald, S. L. *Org. Lett.* **2005**, *7*(18), 3965-3968.
362. Ehrentraut, A.; Zapf, A.; Beller, M. *J. Mol. Catal. A Chem.* **2002**, *182*, 515-523.
363. Zapf, A.; Jackstell, R.; Rataboul, F.; Riermeier, T.; Monsees, A.; Fuhrmann, C.; Shaikh, N.; Dingerdissen, U.; Beller, M. *ChemComm.* **2004**, (1), 38-39.
364. Rataboul, F.; Zapf, A.; Jackstell, R.; Harkal, S.; Riermeier, T.; Monsees, A.; Dingerdissen, U.; Beller, M. *Chem. Eur. J.* **2004**, *10*(12), 2983-2990.
365. Dai, Q.; Gao, W.; Liu, D.; Kapes, L. M.; Zhang, X. *J. Org. Chem.* **2006**, *71*(10), 3928-3934.
366. Murthy Bandaru, S. S.; Bhilare, S.; Chrysochos, N.; Gayakhe, V.; Trentin, I.; Schulzke, C.; Kapdi, A. R. *Org. Lett.* **2018**, *20*(2), 473-476.
367. Lai, W. I.; Leung, M. P.; Choy, P. Y.; Kwong, F. Y. *Synthesis* **2019**, *51*(13), 2678-2686.
368. Sarvestani, M.; Azadi, R. *Appl. Organomet. Chem.* **2018**, *32*(1), e3906.
369. Veisi, H.; Safarimehr, P.; Hemmati, S. *Mater. Sci. Eng. C* **2019**, *96*, 310-318.
370. Fareghi Alamdari, R.; Haqiqi, M. G.; Zekri, N. *New J. Chem.* **2016**, *40*(2), 1287-1296.
371. Heshmatpour, F.; Abazari, R. *RSC Adv.* **2014**, *4*(99), 55815-55826.
372. Sobhani, S.; Zarei, H.; Sansano, J. M. *Sci. Rep.* **2021**, *11*(1), 17025.
373. Cheung, C. W.; Buchwald, S. L. *J. Org. Chem.* **2014**, *79*(11), 5351-5358.
374. Lavery, C. B.; Rotta Loria, N. L.; McDonald, R.; Stradiotto, M. *Adv. Synth. Catal.* **2013**, *355*(5), 981-987.

375. Schulz, T.; Torborg, C.; Schäffner, B.; Huang, J.; Zapf, A.; Kadyrov, R.; Börner, A.; Beller, M. *Angew. Chem. Int. Ed.* **2009**, *48*(5), 918-921.
376. Sergeev, A. G.; Schulz, T.; Torborg, C.; Spannenberg, A.; Neumann, H.; Beller, M. *Angew. Chem. Int. Ed.* **2009**, *48*(41), 7595-7599.
377. Buchwald, S.; Klapars, A.; Antilla, J.; Job, G.; Wolter, M.; Kwong, F.; Nordmann, G.; Hennessy, E. Copper-catalyzed formation of carbon-heteroatom and carbon-carbon bonds. WO 2002085838 A1, October 31, **2002**.
378. Taillefer, M.; Cristau, H. J.; Cellier, P. P.; Spindler, J. F. Process for arylation or vinylation or alkylation of a nucleophilic compound. US 7202367 B2, May 31, **2002**.
379. Ma, D.; Cai, Q. *Org. Lett.* **2003**, *5*(21), 3799-3802.
380. Cristau, H. J.; Cellier, P. P.; Hamada, S.; Spindler, J. F.; Taillefer, M. *Org. Lett.* **2004**, *6*(6), 913-916.
381. Huang, L.; Yu, R.; Zhu, X.; Wan, Y. *Tetrahedron* **2013**, *69*(42), 8974-8977.
382. Yang, B.; Mao, Z.; Zhu, X.; Wan, Y. *Catal. Commun.* **2015**, *60*, 92-95.
383. Xia, S.; Gan, L.; Wang, K.; Li, Z.; Ma, D. *J. Am. Chem. Soc.* **2016**, *138*(41), 13493-13496.
384. Maurer, S.; Liu, W.; Zhang, X.; Jiang, Y.; Ma, D. *Synlett* **2010**, *2010*(6), 976-978.
385. Song, G. L.; Zhang, Z.; Da, Y. X.; Wang, X. C. *Tetrahedron* **2015**, *71*(46), 8823-8829.
386. Wang, D.; Kuang, D.; Zhang, F.; Tang, S.; Jiang, W. *Eur. J. Org. Chem.* **2014**, *2014*(2), 315-318.
387. Chen, J.; Yuan, T.; Hao, W.; Cai, M. *Catal. Commun.* **2011**, *12*(15), 1463-1465.
388. Thakur, K. G.; Sekar, G. *ChemComm.* **2011**, *47*(23), 6692-6694.
389. Ding, G.; Han, H.; Jiang, T.; Wu, T.; Han, B. *ChemComm.* **2014**, *50*(65), 9072-9075.
390. Chan, C. C.; Chen, Y. W.; Su, C. S.; Lin, H. P.; Lee, C. F. *Eur. J. Org. Chem.* **2011**, (36), 7288-7293.
391. Chen, J. B.; Natte, K.; Man, N. Y.; Stewart, S. G.; Wu, X. F. *Tetrahedron Lett.* **2015**, *56*(33), 4843-4847.
392. Rao, D. N.; Rasheed, S.; Kumar, K. A.; Reddy, A. S.; Das, P. *Adv. Synth. Catal.* **2016**, *358*(13), 2126-2133.
393. Rasheed, S.; Rao, D. N.; Das, P. *J. Org. Chem.* **2015**, *80*(18), 9321-9327.
394. Duan, X. Y.; Liu, N.; Liu, K.; Song, Y. K.; Wang, J.; Mao, X. H.; Xu, W. D.; Yang, S. J.; Li, H. X.; Ma, J. Y. *Tetrahedron Lett.* **2018**, *59*(47), 4187-4190.
395. Khosravi, A.; Mokhtari, J.; Naimi Jamal, M. R.; Tahmasebi, S.; Panahi, L. *RSC Adv.* **2017**, *7*(73), 46022-46027.

396. Seyedi, N.; Shahabi Nejad, M.; Saidi, K.; Sheibani, H. *Appl. Organomet. Chem.* **2020**, *34*(1), e5307.
397. Mittal, A.; Kumari, S.; Parmanand; Yadav, D.; Sharma, S. K. *Appl. Organomet. Chem.* **2020**, *34*(2), e5362.
398. Sarmah, M.; Dewan, A.; Boruah, P. K.; Das, M. R.; Bora, U. *Appl. Organomet. Chem.* **2020**, *34*(4), e5554.
399. Sharma, H.; Mahajan, H.; Jamwal, B.; Paul, S. *Catal. Commun.* **2018**, *107*, 68-73.
400. Xu, J.; Wang, X.; Shao, C.; Su, D.; Cheng, G.; Hu, Y. *Org. Lett.* **2010**, *12*(9), 1964-1967.
401. Yang, H.; Li, Y.; Jiang, M.; Wang, J.; Fu, H. *Chem. Eur. J.* **2011**, *17*(20), 5652-5660.
402. Yang, D.; An, B.; Wei, W.; Jiang, M.; You, J.; Wang, H. *Tetrahedron* **2014**, *70*(22), 3630-3634.
403. Han Sem, K.; Sung Ryu, J.; Ueon Sang, S.; Seung Hoi, K. *Tetrahedron Lett.* **2018**, *59*(52), 4597-4601.
404. Joo, S. R.; Kwon, G. T.; Park, S. Y.; Kim, S. H. *Bull. Korean Chem. Soc.* **2019**, *40*(5), 465-468.
405. Cheng, Y.; Xu, Q.; Liu, J.; Zhao, C.; Xue, F.; Zhao, Y. *J. Braz. Chem. Soc.* **2014**, *25*, 2102-2107.
406. Minatel, I. O.; Borges, C. V.; Ferreira, M. I.; Gomez, H. A.; Gomez; Chen, C. O.; Lima, G. P. P. In *Phenolic Compounds: Biological Activity* (Eds.: Soto Hernández, M.; Palma Tenango, M.; Garcia Mateos, M. D. R.), Books on Demand: Rijeka, Croacia, **2017**, Vol. 8, pp. 1-24.
407. Wang, Y. Y.; Xu, F. Z.; Yu, G.; Shi, J.; Li, C. H.; Dai, A. L.; Liu, Z. Q.; Xu, J. H.; Wang, F. H.; Wu, J. *Chem. Cent. J.* **2017**, *11*(1), 1-11.
408. Kuivila, H. G.; Reuwer Jr, J. F.; Mangravite, J. A. *Can. J. Chem.* **1963**, *41*(12), 3081-3090.
409. Kuivila, H. G.; Reuwer Jr, J. F.; Mangravite, J. A. *J. Am. Chem. Soc.* **1964**, *86*(13), 2666-2670.
410. Bosebabu, B.; Cheruku, S. P.; Chamallamudi, M. R.; Nampoothiri, M.; Shenoy, R. R.; Nandakumar, K.; Parihar, V. K.; Kumar, N. *Mini. Rev. Med. Chem.* **2020**, *20*(11), 988-1000.
411. Groen, J. C.; Bach, T.; Ziese, U.; Paulaime Van Donk, A. M.; De Jong, K. P.; Moulijn, J. A.; Pérez Ramírez, J. *J. Am. Chem. Soc.* **2005**, *127*(31), 10792-10793.
412. Verboekend, D.; Vilé, G.; Pérez Ramírez, J. *Cryst. Growth Des.* **2012**, *12*(6), 3123-3132.
413. Ates, A. *J. Colloid Interface Sci.* **2018**, *523*, 266-281.
414. Casitas Montero, A.; Ribas Salamaña, X. *Chem. Sci.* **2013**, *4*(6), 2301-2318.

415. Moon, P. J.; Halperin, H. M.; Lundgren, R. J. *Angew. Chem. Int. Ed.* **2016**, *55*(5), 1894-1898.
416. Sun, C. L.; Li, B. J.; Shi, Z. J. *Chem. Rev.* **2011**, *111*(3), 1293-1314.
417. Sun, C.; Li, B.; Shi, Z. *ChemComm.* **2010**, *46*(5), 677-685.
418. Ackermann, L.; Vicente, R.; Kapdi, A. R. *Angew. Chem. Int. Ed.* **2009**, *48*(52), 9792-9826.
419. Tian, T.; Li, Z. P.; Li, C. J. *Green Chem.* **2021**, *23*(18), 6789-6862.
420. Ackermann, L. *Modern Arylation Methods*. Wiley Online Library, **2009**.
421. Yeung, C. S.; Dong, V. M. *Chem. Rev.* **2011**, *111*(3), 1215-1292.
422. Zhuang, W. H.; Zhang, X. F.; Huang, Q. F. *Chinese J. Org. Chem.* **2020**, *41*(2), 529.
423. Kuhl, N.; Hopkinson, M. N.; Glorius, F. *Angew. Chem. Int. Ed.* **2012**, *51*(33), 8230-8234.
424. Ackerman, L. J.; Sadighi, J. P.; Kurtz, D. M.; Labinger, J. A.; Bercaw, J. E. *Organometallics* **2003**, *22*(19), 3884-3890.
425. Izawa, Y.; Stahl, S. S. *Adv. Synth. Catal.* **2010**, *352*(18), 3223-3229.
426. Li, Z. P.; Cao, L.; Li, C. J. *Angew. Chem. Int. Ed.* **2007**, *119*(34), 6625-6627.
427. Wu, H. R.; Huang, H. Y.; Ren, C. L.; Liu, L.; Wang, D.; Li, C. J. *Chem. Eur. J.* **2015**, *21*(47), 16744-16748.
428. Li, Q.; Hu, W.; Hu, R.; Lu, H.; Li, G. *Org. Lett.* **2017**, *19*(17), 4676-4679.
429. Kitahara, M.; Umeda, N.; Hirano, K.; Satoh, T.; Miura, M. *J. Am. Chem. Soc.* **2011**, *133*(7), 2160-2162.
430. Huang, C. Y.; Kang, H.; Li, J. B.; Li, C. J. *J. Org. Chem.* **2019**, *84*(20), 12705-12721.
431. Siemsen, P.; Livingston, R. C.; Diederich, F. *Angew. Chem. Int. Ed.* **2000**, *112*(15), 2740-2767.
432. Kozhushkov, S. I.; Ackermann, L. *Chem. Sci.* **2013**, *4*(3), 886-896.
433. Girard, S. A.; Knauber, T.; Li, C. J. *Angew. Chem. Int. Ed.* **2014**, *53*(1), 74-100.
434. Murahashi, S. I.; Zhang, D. *Chem. Soc. Rev.* **2008**, *37*(8), 1490-1501.
435. Murahashi, S.; Komiya, N.; Terai, H.; Nakae, T. *J. Am. Chem. Soc.* **2003**, *125*(50), 15312-15313.
436. Dewick, P. M. *Medicinal Natural Products: A Biosynthetic Approach*. John Wiley & Sons, **2002**.
437. Amat Tusón, M.; Elias, V.; Llor Brunés, N.; Subrizi, F.; Molins i Grau, E.; Bosch Cartes, J. *Eur. J. Org. Chem.* **2010**, *2010*(21), 4017-4026.
438. Kaufman, T. S. *Tetrahedron: Asymmetry* **2004**, *15*(8), 1203-1237.
439. Chuliá, S.; Ivorra, M. D.; Lugnier, C.; Vila, E.; Noguera, M. A.; D'Ocon, P. *Brit. J. Pharmacol.* **1994**, *113*(4), 1377-1385.

440. Manske, R. H. F.; Holmes, H. L. *The Alkaloids: Chemistry and Physiology*. Elsevier, **2014**.
441. Charifson, P. S.; Wyrick, S. D.; Hoffman, A. J.; Simmons, R. M. A.; Bowen, J. P.; McDougald, D. L.; Mailman, R. B. *J. Med. Chem.* **1988**, *31*(10), 1941-1946.
442. Konkala, A.; Sabita Raja, S.; Kaur, A. *Pharm. Bio. Sci.* **2012**, *2*, 25-29.
443. Yadav, D. K.; Singh, N.; Dev, K.; Sharma, R.; Sahai, M.; Palit, G.; Maurya, R. *Fitoterapia* **2011**, *82*(4), 666-675.
444. Kim, A. N.; Ngamnithiporn, A.; Du, E.; Stoltz, B. M. *Chem. Rev.* **2023**, *123*(15), 9447-9496.
445. Chrzanowska, M.; Rozwadowska, M. D. *Chem. Rev.* **2004**, *104*(7), 3341-3370.
446. Ma, L.; Chen, W.; Seidel, D. *J. Am. Chem. Soc.* **2012**, *134*(37), 15305-15308.
447. Das, D.; Seidel, D. *Org. Lett.* **2013**, *15*(17), 4358-4361.
448. Seidel, D. *Org. Chem. Front.* **2014**, *1*(4), 426-429.
449. Lin, W.; Ma, S. *Org. Chem. Front.* **2014**, *1*(4), 338-346.
450. Mons, E.; Wanner, M. J.; Ingemann, S.; Van Maarseveen, J. H.; Hiemstra, H. *J. Org. Chem.* **2014**, *79*(16), 7380-7390.
451. Ruiz Olalla, A.; Wurdemann, M. A.; Wanner, M. J.; Ingemann, S.; Van Maarseveen, J. H.; Hiemstra, H. *J. Org. Chem.* **2015**, *80*(10), 5125-5132.
452. Werner, F.; Blank, N.; Opatz, T. *Eur. J. Org. Chem.* **2007**, *2007*(23), 3911-3915.
453. Chrzanowska, M.; Grajewska, A.; Rozwadowska, M. D. *Chem. Rev.* **2016**, *116*(19), 12369-12465.
454. Li, Z. P.; Li, C. J. *J. Am. Chem. Soc.* **2004**, *126*(38), 11810-11811.
455. Li, Z. P.; Li, C. J. *Eur. J. Org. Chem.* **2005**, *2005*(15), 3173-3176.
456. Li, Z. P.; Li, C. J. *J. Am. Chem. Soc.* **2005**, *127*(11), 3672-3673.
457. Basle, O.; Li, C. J. *Org. Lett.* **2008**, *10*(17), 3661-3663.
458. Chu, L.; Zhang, X.; Qing, F. *Org. Lett.* **2009**, *11*(10), 2197-2200.
459. Zhang, Y.; Fu, H.; Jiang, Y.; Zhao, Y. *Org. Lett.* **2007**, *9*(19), 3813-3816.
460. Li, Z. P.; Li, C. J. *Org. Lett.* **2004**, *6*(26), 4997-4999.
461. Li, Z. P.; MacLeod, P. D.; Li, C. J. *Tetrahedron: Asymmetry* **2006**, *17*(4), 590-597.
462. Su, W.; Yu, J.; Li, Z.; Jiang, Z. *J. Org. Chem.* **2011**, *76*(21), 9144-9150.
463. Yu, J.; Li, Z.; Jia, K.; Jiang, Z.; Liu, M.; Su, W. *Tetrahedron Lett.* **2013**, *54*(15), 2006-2009.
464. Boess, E.; Sureshkumar, D.; Sud, A.; Wirtz, C.; Farès, C.; Klussmann, M. *J. Am. Chem. Soc.* **2011**, *133*(21), 8106-8109.
465. Boess, E.; Schmitz, C.; Klussmann, M. *J. Am. Chem. Soc.* **2012**, *134*(11), 5317-5325.
466. Ratnikov, M. O.; Doyle, M. P. *J. Am. Chem. Soc.* **2013**, *135*(4), 1549-1557.

467. Sun, S. T.; Li, C. K.; Floreancig, P. E.; Lou, H. X.; Liu, L. *Org. Lett.* **2015**, *17*(7), 1684-1687.
468. Perepichka, I.; Kundu, S.; Hearne, Z.; Li, C. J. *Org. Biomol. Chem.* **2015**, *13*(2), 447-451.
469. Rueping, M.; Koenigs, R. M.; Poscharny, K.; Fabry, D. C.; Leonori, D.; Vila, C. *Chem. Eur. J.* **2012**, *18*(17), 5170-5174.
470. Alonso, F.; Arroyo, A.; Martín García, I.; Moglie, Y. *Adv. Synth. Catal.* **2015**, *357*(16-17), 3549-3561.
471. Alonso, F.; Calvino, J. J.; Osante, I.; Yus, M. *Chem. Lett.* **2005**, *34*(9), 1262-1263.
472. Alonso, F.; Calvino, J. J.; Osante, I.; Yus, M. *J. Exp. Nanosci.* **2006**, *1*(4), 419-433.
473. Yang, H.; Sun, Z.; Chen, H.; Mao, F.; Li, X.; Xu, X. *Tetrahedron Lett.* **2022**, *109*, 154136.
474. Kwong, F. Y.; Klapars, A.; Buchwald, S. L. *Org. Lett.* **2002**, *4*(4), 581-584.
475. Cao, W.; Chen, P.; Tang, Y. *J. Nat. Prod.* **2020**, *83*(5), 1701-1705.
476. Kawamoto, Y.; Kobayashi, T.; Ito, H. *Tetrahedron Lett.* **2022**, *103*, 153975.
477. Bhunia, S.; Pawar, G. G.; Kumar, S. V.; Jiang, Y.; Ma, D. *Angew. Chem. Int. Ed.* **2017**, *56*(51), 16136-16179.
478. Gao, J.; Bhunia, S.; Wang, K.; Gan, L.; Xia, S.; Ma, D. *Org. Lett.* **2017**, *19*(11), 2809-2812.
479. De, S.; Yin, J.; Ma, D. *Org. Lett.* **2017**, *19*(18), 4864-4867.
480. Job, G. E.; Buchwald, S. L. *Org. Lett.* **2002**, *4*(21), 3703-3706.
481. Antilla, J. C.; Klapars, A.; Buchwald, S. L. *J. Am. Chem. Soc.* **2002**, *124*(39), 11684-11688.
482. Antilla, J. C.; Baskin, J. M.; Barder, T. E.; Buchwald, S. L. *J. Org. Chem.* **2004**, *69*(17), 5578-5587.
483. Altman, R. A.; Anderson, K. W.; Buchwald, S. L. *J. Org. Chem.* **2008**, *73*(13), 5167-5169.
484. Altman, R. A.; Buchwald, S. L. *Org. Lett.* **2006**, *8*(13), 2779-2782.
485. Modak, A.; Nett, A. J.; Swift, E. C.; Haibach, M. C.; Chan, V. S.; Franczyk, T. S.; Shekhar, S.; Cook, S. P. *ACS Catal.* **2020**, *10*(18), 10495-10499.
486. Appa, R. M.; Lakshmidēvi, J.; Naidu, B. R.; Venkateswarlu, K. *Mol. Catal.* **2021**, *501*, 111366.
487. Minus, M. B.; Moor, S. R.; Pary, F. F.; Nirmani, L. P. T.; Chwatko, M.; Okeke, B.; Singleton, J. E.; Nelson, T. L.; Lynd, N. A.; Anslyn, E. V. *Org. Lett.* **2021**, *23*(8), 2873-2877.
488. Kaboudin, B.; Mostafalu, R.; Yokomatsu, T. *Green Chem.* **2013**, *15*(8), 2266-2274.
489. Ostrowska, S.; Rogalski, S.; Lorkowski, J.; Walkowiak, J.; Pietraszuk, C. *Synlett* **2018**, *29*(13), 1735-1740.
490. Iosub, A. V.; Stahl, S. S. *J. Am. Chem. Soc.* **2015**, *137*(10), 3454-3457.

491. Thirion, D.; Poriel, C.; Rault Berthelot, J.; Barrière, F.; Jeannin, O. *Chem. Eur. J.* **2010**, *16*(46), 13646-13658.
492. Das, D.; Rajkumari, K.; Rokhum, L. *Curr. Org. Synth.* **2019**, *16*(7), 1024-1031.
493. Luo, D. P.; Huang, Y. F.; Hong, X. Y.; Chen, D.; Li, G. X.; Huang, X. B.; Gao, W. X.; Liu, M. C.; Zhou, Y. B.; Wu, H. Y. *Adv. Synth. Catal.* **2019**, *361*(5), 961-964.
494. Schmidt, B.; Riemer, M. *Synthesis* **2016**, 1399-1406.
495. Elumalai, V.; Hansen, J. H. *RSC Adv.* **2020**, *10*(66), 40582-40587.
496. Jiang, M.; Yang, H.; Li, Y.; Jia, Z.; Fu, H. *Chinese Chem. Lett.* **2014**, *25*(5), 715-719.
497. Bomme Gowda, Y. K.; Mallesha, N.; Vinayaka, A. C.; Sadashiva, M. P. *Chem. Lett.* **2016**, *45*(3), 268-270.
498. Maleczka, R. E.; Shi, F.; Holmes, D.; Smith, M. R. *J. Am. Chem. Soc.* **2003**, *125*(26), 7792-7793.
499. Casado Sánchez, A.; Uygur, M.; González Muñoz, D.; Aguilar Galindo, F.; Nova Fernández, J. L.; Arranz Plaza, J.; Díaz Tendero, S.; Cabrera, S.; Mancheño, O. G.; Alemán, J. *J. Org. Chem.* **2019**, *84*(10), 6437-6447.
500. Liu, Y.; Lu, T.; Tang, W.; Gao, J. *RSC Adv.* **2018**, *8*(50), 28637-28641.
501. Li, Z.; Li, C.-J. *J. Am. Chem. Soc.* **2004**, *126*(38), 11810-11811.

Zéolithes dopées au cuivre(I) comme catalyseurs verts pour la synthèse organique

Résumé

Les motifs aryliques sont présents dans de nombreux composés biologiquement actifs. Nombre d'entre eux se retrouvent sous forme de biaryles, de phénols et de tétrahydroisoquinoléines, systèmes que l'on trouve dans de nombreux produits naturels et certains intermédiaires synthétiques importants. Au cours des dernières décennies, diverses réactions de couplage catalysées par des métaux (de transition) ont émergé pour synthétiser de tels motifs ou molécules en formant des liaisons carbone-carbone ou des liaisons carbone-hétéroatome. Cependant, la plupart de ces réactions ont été réalisées dans des conditions homogènes avec des conditions de réaction non satisfaisantes, telles que des températures élevées, des solvants toxiques et des bases et ligands supplémentaires. Afin de rendre ces conditions plus vertes et plus durables, le potentiel des zéolithes dopées au cuivre en tant que catalyseurs hétérogènes et recyclables a été évalué pour la synthèse de biaryles, de phénols et de dérivés de tétrahydroisoquinoléine au travers de plusieurs réactions de couplage, telles que les réactions de type homocouplage, les réactions de couplage croisé de type Chan-Lam-Evans et les réactions de couplage déhydrogénatif croisé. Plusieurs procédés catalytiques efficaces et économiques ont été développés dans des conditions plus vertes et plus douces, sans avoir besoin d'un ligand ni d'une base supplémentaire.

De plus, l'application des motifs biaryles ainsi obtenus a également été explorée dans des réactions de Diels-Alder pour la construction d'hétérocycles d'intérêt avec des économies d'atomes élevées.

Mots clés: zéolithe, cuivre, composés biarylés, phénols, tétrahydroisoquinoléines, réactions de couplage, catalyseur hétérogène, chimie verte

Résumé en anglais

Aryl rings are a predominant feature in numerous biologically active compounds. Most of them can exist as biaryl, phenol, and tetrahydroisoquinoline moieties, which are encountered in many natural products and in various important synthetic intermediates. In the last few decades, various (transition) metal-catalyzed coupling reactions have emerged to synthesize such motifs or molecules via the formation of carbon-carbon bonds or carbon-heteroatom bonds. However, most of them were performed under homogeneous conditions with unsatisfactory reaction conditions, such as high temperatures, toxic solvents, and additional bases and ligands. To improve the greenness and sustainability of these processes, the potential of copper-doped zeolites as heterogeneous and recyclable catalysts was evaluated for the synthesis of biaryls, phenols, and tetrahydroisoquinoline derivatives through the study of several coupling reactions, such as homocoupling-type reactions, Chan-Lam-Evans-type cross-coupling and cross-dehydrogenative coupling reactions. Several efficient and economical catalytic procedures were developed under greener and milder conditions without the need for any additional ligand and base.

Furthermore, the application of the so-obtained important biaryl motifs has also been explored in Diels-Alder reactions for the construction of heterocycles of interest with high atom economies.

Keywords: zeolite, copper, biaryl compounds, phenols, tetrahydroisoquinolines, coupling reactions, heterogeneous catalyst, green chemistry